

---

Christoph Herwig



TECHNISCHE  
UNIVERSITÄT  
WIEN

Vienna University of Technology

DIPLOMARBEIT

# Enzymes in medical applications: Investigating the enzyme horseradish peroxidase

Ausgeführt am Institut für

**Biochemical Engineering**

der Technischen Universität Wien

unter der Anleitung von

Univ.Prof. Dipl.-Ing. Dr. Christoph Herwig

Univ.Ass. Dipl.-Ing. Dr. Oliver Spadiut

durch

**Pletzenauer Robert**

Dr. Thomas Klestil Str. 1/7

2231 Strasshof an der Nordbahn

---

Datum

---

Unterschrift (Student)

# I. Table of Contents

<b>PREFACE</b> .....	<b>1</b>
1 Introduction .....	2
2 Aim of the project and scientific questions .....	9
3 Scientific Contributions .....	11
4 References .....	12
<b>CHAPTER I: Development of an efficient Downstream Process for recombinant HRP from <i>P. pastoris</i> and search for novel potentially useful isoenzymes</b> .....	<b>15</b>
1 Abstract .....	17
2 Introduction .....	17
3 Materials and Methods .....	20
4 Results and Discussion .....	25
5 Conclusions .....	36
6 Acknowledgements .....	38
7 References .....	38
8 Supplementary Figures .....	42
<b>CHAPTER II: Can glycoengineering help in tailoring HRP for medical applications, especially in terms of reducing hyperglycosylation?</b> .....	<b>48</b>
1 Abstract .....	50
2 Introduction .....	50
3 Results and Discussion .....	53
4 Material and Methods .....	66
5 Abbreviations .....	74
6 Acknowledgments .....	74
7 References .....	74
8 Supplementary Figures .....	78
<b>CHAPTER III Expression of HRP C1A in glyco-engineered <i>P. pastoris</i></b> .....	<b>85</b>
1 Abstract .....	87

2	Introduction .....	87
3	Results .....	90
4	Discussion .....	101
5	Methods .....	109
6	References .....	119
7	Acknowledgments .....	122
8	Author Contributions Statement .....	122
9	Supplementary Figures .....	123
	<b>OVERALL CONCLUSIONS.....</b>	<b>129</b>
	<b>APPENDIX.....</b>	<b>132</b>

## **II. Acknowledgements**

Foremost, I want to thank Professor Christoph Herwig for providing me the opportunity of being part of his team and supervising me through my master thesis. I would like to thank him for his valuable feedback and allowing me to develop my scientific abilities.

Furthermore, I would like to express my sincere gratefulness to my advisor Oliver Spadiut, for his continuous support during my master thesis, for his patience, motivation, enthusiasm and huge knowledge. He has always guided me perfectly through my work and has also become a very good friend.

Moreover I want to thank all colleagues I got to know during this time, especially my mates of the “HRP team”, for their valuable assistance during my master thesis.

Finally, I would like to thank my beloved girlfriend Simone Brunnhuber who always was a great support in these moments when there was no one to answer my queries and also to our daughter Katja. Although she is not yet able to speak she is definitely able to enlighten one's life.

### III. Abstract

This diploma thesis focuses on the plant enzyme horseradish peroxidase (HRP) and its application in medical diagnostics and targeted cancer treatment. Currently, HRP is isolated from plant, resulting in low yields and a mixture of different HRP isoenzymes with varying biochemical properties as final enzyme preparation. This strongly contradicts Quality by Design guidelines and FDA regulations. Another major drawback lies in the foreign glycosylation of the plant enzyme leading to a rapid clearance from the human body.

The objective of the present work was the recombinant production, purification and characterization of a specifically tailored HRP enzyme. Because this was a rather versatile task, the thesis was divided into three parts.

1. Until now, the majority of studies only dealt with isoenzyme HRP C1A. Therefore, we recombinantly produced **18 novel HRP isoenzymes** and performed subsequent biochemical characterization as well as an optimization of the existing downstream procedure for hyperglycosylated HRP derived from yeast. We were able to identify potential candidates for specific diagnostic applications and to optimize the present **downstream procedure**.
2. In order to handle the tendency of yeasts for hypermannosylating glyco-proteins we tested a **glycoengineering approach**. Thus, all 8 N-glycosylation sites of HRP C1A were mutated and the most suitable mutation was determined. Afterwards we combined the 8 most promising mutations in order to produce active HRP C1A without N-glycosylation. Although this mutant hardly showed catalytic activity the overall outcome described a useful basis for further enzyme engineering approaches.
3. The third project dealt with the production of HRP in a **modified *P. pastoris* strain**. Therefore, the mannosyltransferase OCH1, which triggers hypermannosylation, was knocked out. Although this strain was hard to cultivate and showed a growth-impaired phenotype, more homogeneously glycosylated protein could be produced at an adequate production rate.

## IV. Zusammenfassung

Im Zentrum dieser Diplomarbeit stand das Pflanzenenzym Meerrettich-Peroxidase (MRP) sowie dessen Verwendungen in der medizinischen Diagnostik und gezielten Krebs Therapie. Aktuell wird dieses Enzym aus der Pflanze extrahiert, allerdings erhält man nur geringe Ausbeuten sowie eine Mischung aus verschiedenen Isoenzymen mit unterschiedlichen biochemischen Eigenschaften. Dies ist aber widersprüchlich zu Quality by Design sowie FDA Richtlinien. Ein weiterer Nachteil liegt in der pflanzlichen Glykosylierung des Enzyms, welche zu einem raschen Abbau im menschlichen Körper führt.

Das Ziel dieser Arbeit war die rekombinante Produktion, Reinigung und Charakterisierung eines maßgeschneiderten MRP Enzyms. Da dies eine sehr vielfältige Aufgabe war, wurde die Diplomarbeit in drei Teile aufgeteilt.

1. Bis jetzt wurde ein Großteil der Studien nur am MRP Isoenzym C1A durchgeführt. Wir produzierten daher **18 neuartige MRP Isoenzyme** rekombinant, charakterisierten diese und versuchten eine vorhandene **Reinigungsstrategie zu optimieren**. Es war möglich neue potentielle Kandidaten für spezifische Diagnose Kits zu finden und die Reinigungsstrategie zu optimieren.
2. Um die von Hefen durchgeführte Hypermannosylierung von Glykoproteinen in den Griff zu bekommen, wurde ein **Glycoengineering Ansatz** getestet. Hierfür wurden alle 8 N-Glykosylierungsstellen der MRP C1A einzeln mutiert und jeweils die am besten geeignetste Mutation ermittelt. Anschließend wurden alle 8 Stellen mutiert, um MRP C1A ohne N-Glykosylierung herzustellen. Obwohl dieser Mutant kaum katalytische Aktivität zeigte, stellt das Gesamtergebnis eine solide Basis für zukünftige Enzymmodifikationen dar.
3. Das dritte Projekt befasste sich mit der Herstellung von MRP in einem **modifizierten *P. pastoris*** Stamm. Hierfür wurde die Mannosyltransferase OCH1, welche Hypermannosylierung initiiert, inaktiviert. Obwohl dieser Stamm sehr schwer zu kultivieren war und einen im Wachstum gehemmten Phänotyp zeigte, war es möglich, ein homogener glykosyliertes Protein zu erzeugen.

## **PREFACE**

# 1 Introduction

## 1.1 Peroxidases

Peroxidases are a group of enzymes which are catalysing an oxidoreduction of various reductants utilizing hydrogen peroxide. Peroxidases can be found in animals, microorganisms and plants. Based on their origin, their structure and the catalytic properties they are divided in three superfamilies, namely animal peroxidases, catalases and plant peroxidases [1]. An overview of the peroxidase classification is given in Table 1.

**Table 1: Classification of peroxidases**

Superfamily	Class <sup>1</sup>	Member (EC number)	Origin
Animal peroxidase		Eosinophill peroxidase (EC 1.11.1.7)	Animal
		Lactoperoxidase (EC 1.11.1.7)	Animal
		Myeloperoxidase (EC 1.11.1.7)	Animal
		Thyroid peroxidase (EC 1.11.1.7)	Animal and plant
		Glutathione peroxidase (EC 1.11.1.9)	Animal
		Prostaglandin endoperoxide synthase (EC 1.14.99.1, partial) <sup>2</sup>	Animal
Catalase		Catalase (EC 1.11.1.6)	Animal, plant, fungus and yeast
Plant peroxidase		Cytochrome c peroxidase (EC 1.11.1.5)	Yeast and bacterium
	I	Catalase-peroxidase (EC 1.11.1.6)	Bacterium and fungus
		Ascorbate peroxidase (EC 1.11.1.11)	Plant
	II	Manganese-dependent peroxidase (EC 1.11.1.13)	Fungus
		Ligninase (EC 1.11.1.14)	Fungus
	III	Peroxidase (EC 1.11.1.7)	Plant

<sup>1</sup> Established only for the plant peroxidase superfamily.

<sup>2</sup> Homology was observed in the central region (approximately 180 residues) with other animal peroxidases.

Source: Hiraga, Sasaki (2001)

This project focuses on the enzyme horseradish peroxidase (EC 1.11.17), which is an extremely versatile member of the class III plant peroxidases. This class of enzymes can be found in all land plants [3].

## 1.2 Horseradish peroxidase (HRP)

Horseradish peroxidase originates from the perennial herb *Armoracia rusticana*



**Figure 1: *Armoracia rusticana***  
Source: Kops (1822)

(Figure 1) also known as horseradish. The enzyme is able to oxidise various substrates (Figure 2) *i.e.*: aromatic phenols, indoles, phenolic acids, amines or sulfonates [4-6]. HRP is participating in a plenty of physiological processes during the plants lifecycle such as crosslinking of phenolic molecules, the regulation of H<sub>2</sub>O<sub>2</sub> levels, cell wall networking and auxin catabolism [3, 7, 8]. That huge variety of functions is not achieved via one distinct enzyme, rather are there several different isoenzymes involved. Additionally, a seasonal variation of the relative amounts as well as differences in their substrate affinities could be shown [9]. Several different proteins with

peroxidase activity were identified in the horseradish root. In fact, up to 42 different isoenzymes have been identified via isoelectric focusing of three different commercial HRP preparations [10]. A recent next generation sequencing approach of the horseradish transcriptome led to the discovery of 28 secretory peroxidases, 23 of them were previously unknown [11].

Nevertheless, only little is known about the majority of these enzymes. Until now, most studies have only focused on the isoenzyme C1A [12].

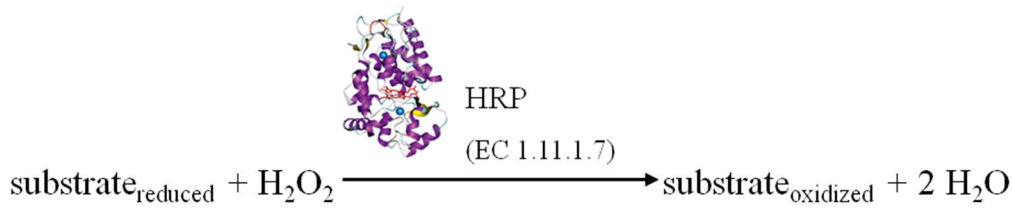


**Figure 2: Catalytic reaction of the enzyme horseradish peroxidase.**

Source: Spadiut and Herwig (2013)

### 1.3 Horseradish peroxidase C1A

The isoenzyme C1A is a monomeric oxidoreductase, 34 kDa in size, consisting of

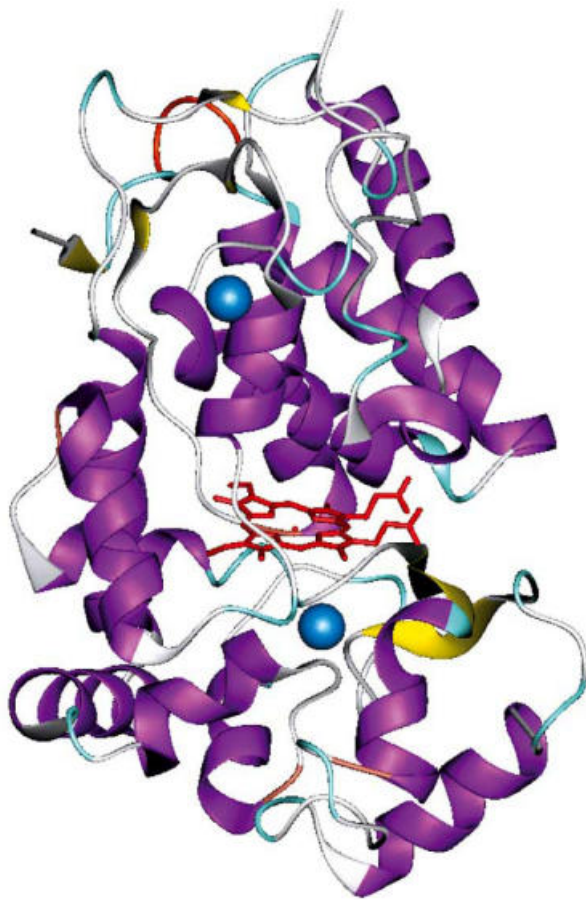


**Figure 3: X-ray crystal structure of the HRP isoenzyme C.** The red group in the center of the enzyme represents the heme group. The blue spheres show the two calcium atoms.  $\alpha$ -Helical regions are shown in purple and  $\beta$ -sheets in yellow. Source: Veitch (2004)

308 aminoacids. It contains a heme-group as well as two calcium-ions as prosthetic groups (Figure 3). Furthermore, four disulphide bridges are present. The enzyme consists of a distal and a proximal domain, between which the heme group is positioned [13, 14]. HRP C1A provides nine N-glycosylation sites of the Asn–X–Ser/Thr type with X standing for any amino acid [15, 16]. Eight of these are occupied when the enzyme is expressed in plant. Thus, the molecular mass of HRP expressed in plant increases from 34 kDa to approximately 44 kDa. The typical glycan structure of HRP from plant is a branched heptasaccharide, shown in Figure 4. This characteristic heptasaccharide accounts for up to 80 % of the total glycan pattern [14].



decreases cell viability of carcinoma cells by activating apoptotic pathways [29, 32, 34, 36-39]. One of the main tasks in antitumor therapy is the problem to target only the tumour cells and not to harm healthy tissue. According to Folkes and Wardman (2001), three possible ways to direct the enzyme/prodrug couple HRP C1A/IAA to the tumour cells exist (Figure 5):

- antibody-directed enzyme-prodrug therapy (ADEPT)
- polymer-directed enzyme-prodrug therapy (PDEPT)
- gene-directed enzyme-prodrug therapy (GDEPT)

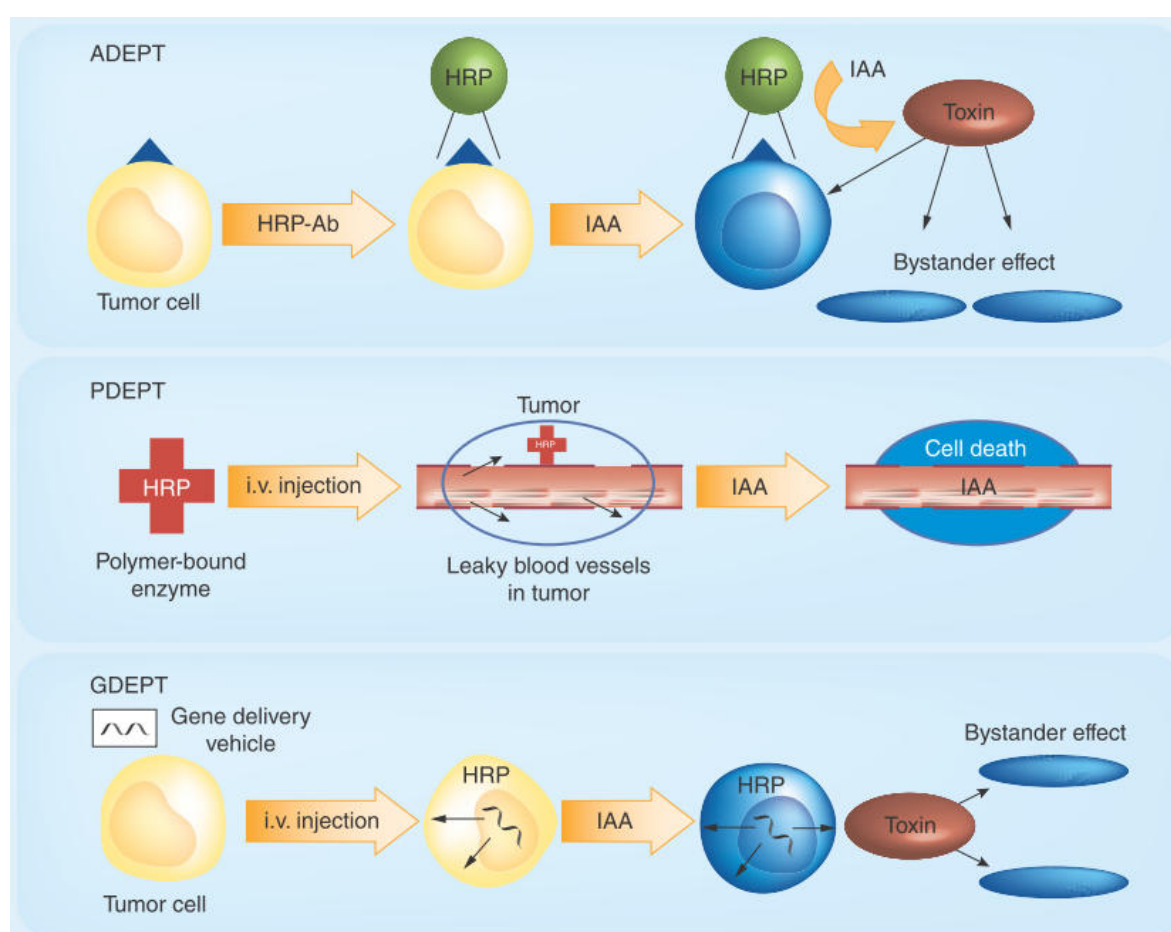


**Figure 5: Main targeting strategies for HRP C1A/IAA in anti-tumour therapy**

Source: Spadiut and Herwig (2013)

Although these strategies could be successful, there exist some major drawbacks [40]:

- Purified HRP from plant is quite expensive (100 mg cost around 360 Euro; P6782-100MG, Sigma)

- HRP preparations originating from plant consist of a variety of different isoenzymes instead of one defined enzyme species
- The enzymes glycosylation pattern is heterogeneous
- HRP-conjugates are rapidly cleared from the blood due to the foreign glycosylation pattern of the plant enzyme.

Due to these hurdles, HRP has not been tested in the clinic yet [40]. A simple solution to these problems would be a straight forward recombinant production of a specifically tailored enzyme followed by an efficient downstream process.

## 1.5 Recombinant production and purification of HRP C1A

### 1.5.1 Recombinant production

The most important recombinant host organisms for the production of biopharmaceuticals today are:

- *E. coli*
- Yeast cells (e.g. *S. cerevisiae* and *P. pastoris*)
- Mammalian cells

HRP C1A could be expressed in a non-glycosylated and inactive form as cytoplasmic inclusion bodies in *E. coli*. Refolding attempts in the presence of calcium-ions and heme partly worked, showing that glycosylation on the surface was not required to obtain active enzyme. Nevertheless, due to the overall yield of only 3 % [16], this strategy is not attractive for commercial production. Thus HRP C1A was also produced in **mammalian cells** [39], **baculovirus and insect cells** [41], but yields were low and the production costs were high, making the recombinant production of this enzyme in these host organisms not competitive to its isolation from plant. The last resort to potentially solve the production issue were **yeast cells**. HRP C1A was successfully produced in *P. pastoris* and *S. cerevisiae* [42]. However, yeasts have the tendency for hypermannosylating glyco-proteins [40] resulting in recombinant enzyme preparations which are basically wrapped in glycan chains. In the case of HRP C1A the additional glycans increase the molecular weight of more than 20 kDa compared to the enzyme isolated from plant (Figure 6). In general, *P. pastoris* attaches shorter glycans to recombinant glycoproteins than

*S. cerevisiae* [43], which is advantageous for following deglycosylation and purification steps. Therefore, *P. pastoris* as a recombinant expression platform for HRP C1A was used in this Master Thesis.

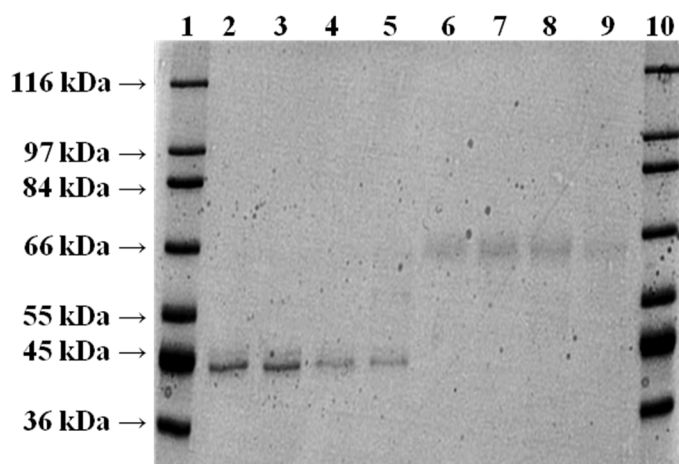


**Figure 6: SDS-PAGE analysis of HRP isolated from plant and HRP expressed in *P. pastoris*.** Lanes 1 and 10, molecular weight standard (Sigma S8445); lanes 2-4, different concentrations of HRP isolated from plant (Sigma Type VI-A, P6782); lanes 5-9, different concentrations of HRP C1A produced in *P. pastoris*.

Source: Spadiut and Herwig (2013)

### 1.5.2 Downstream Process

Although HRP C1A can be expressed in the yeast *P. pastoris* in acceptable amounts nowadays [44-47], the extensive glycosylation pattern of the recombinant product masks the physico-chemical properties and thus impedes a satisfying downstream process [42]. Due to the fact that, according to Tams and Welinder [48], a simple enzymatic deglycosylation is not possible, the state of the art processes for the purification of recombinant HRP from *P. pastoris* are cumbersome comprising several steps [40, 42].

Recently, Spadiut *et al.* [49] produced the isoenzyme HRP C1A recombinant in *P. pastoris* in the controlled environment of a bioreactor and tested a variety of different common protein purification techniques.

They developed a fast and efficient 2-step purification strategy for recombinant HRP C1A comprising a hydrophobic charge induction chromatography (HCIC) step operated in flowthrough mode followed by a size exclusion chromatography (SEC) step. SEC bears several disadvantages like long process times and small sample volumes, making this 2-step strategy still not acceptable for commercial purposes.

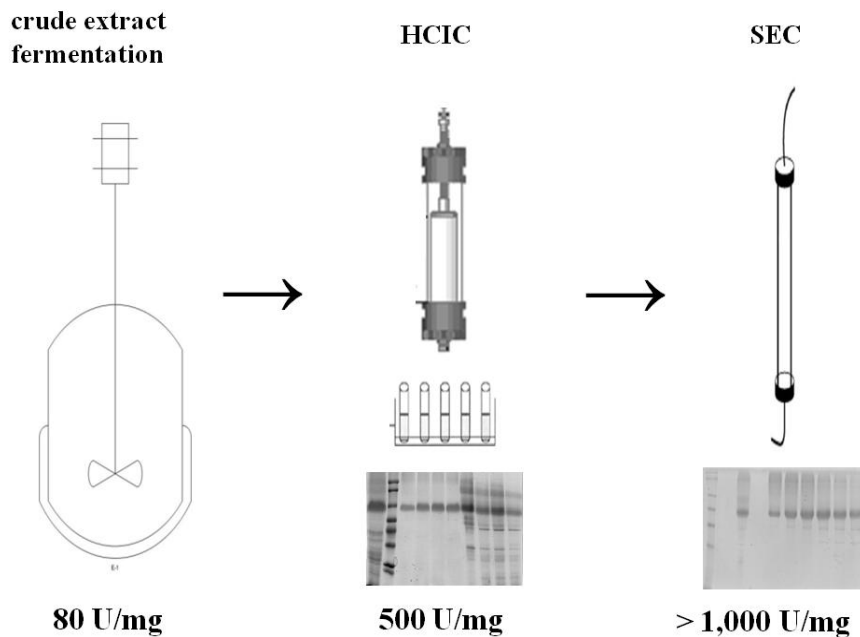


**Figure 7: 2-step strategy for the purification of hyperglycosylated HRP C1A from a cell-free fermentation broth of *P. pastoris*.** Using a strategy combining a HCIC step in flowthrough mode and a subsequent SEC step, HRP C1A could be enriched more than 12-fold from 80 U/mg to more than 1,000 U/mg. Source: Spadiut and Herwig (2013)

In a recent article, published by the group where I did my Master Thesis, the applications of HRP C1A, its recombinant production as well as downstream procedures for this versatile enzyme have also been nicely reviewed and discussed [40].

## 2 Aim of the project and scientific questions

The present Master Thesis focused on the versatile enzyme horseradish peroxidase and its applications in medical diagnostics and targeted cancer treatment. Basically, I wanted to answer the following scientific questions:

1. Are there any other HRP isoenzymes useful for medical applications?
2. Is it possible to develop a more efficient downstream process for hyperglycosylated enzyme preparations recombinantly produced in *P. pastoris*?
3. Can glyco-engineering help in tailoring HRP for medical applications, especially in terms of reducing hyperglycosylation?
4. Can we produce HRP in a humanized, glyco-engineered *P. pastoris* strain?

Obviously, the scientific questions of my Master Thesis were quite diverse which is why I structured the Thesis in 3 Parts:

1. Development of an efficient Downstream Process for recombinant HRP from *P. pastoris* and search for novel potentially useful isoenzymes
2. Glyco-engineering of HRP C1A
3. Expression of HRP C1A in glyco-engineered *P. pastoris*

All these three parts resulted in peer-reviewed scientific publications, which are attached in their final form in the Appendix.

Paper I entitled **“Purification and basic biochemical characterization of 19 recombinant plant peroxidase isoenzymes produced in *Pichia pastoris*”** deals with the first 2 scientific questions. I am 1<sup>st</sup> author of this publication.

Paper II deals with rational protein design of HRP C1A and its glyco-engineering and is entitled **“Glyco-variant library of the versatile enzyme horseradish peroxidase”**. I am 2<sup>nd</sup> author of this publication.

Paper III which is entitled **“Knockout of an endogenous mannosyltransferase increases the homogeneity of glycoproteins produced in *Pichia pastoris*”** deals with the expression of HRP C1A in a glyco-engineered *P. pastoris* strain. I am co-author of this paper.

### **3 Scientific Contributions**

In this section, my contributions to each enclosed publication are explained.

#### **Purification and basic biochemical characterization of 19 recombinant plant peroxidase isoenzymes produced in *Pichia pastoris***

I contributed to the design and conduction of the experiments mentioned. I produced one half of the isoenzymes, purified these portion and biochemically characterized all mentioned isoenzymes. Finally I contributed to the draft of this manuscript.

#### **Glyco-variant library of the versatile enzyme horseradish peroxidase**

My contributions to this project were the combination of the single mutations and the production, purification and characterisation of the respective enzyme.

#### **Knockout of an endogenous mannosyltransferase increases the homogeneity of glycoproteins produced in *Pichia pastoris***

In this project I performed fermentations and I was involved in the strain characterization.

## 4 References

1. Hiraga, S., et al., *A large family of class III plant peroxidases*. Plant Cell Physiol, 2001. **42**(5): p. 462-8.
2. Kops, J., *Flora batava*. 1822.
3. Passardi, F., et al., *Peroxidases have more functions than a Swiss army knife*. Plant Cell Rep, 2005. **24**(5): p. 255-65.
4. Chance, B., *The kinetics and stoichiometry of the transition from the primary to the secondary peroxidase peroxide complexes*. Arch Biochem Biophys, 1952. **41**(2): p. 416-24.
5. George, P., *Chemical nature of the secondary hydrogen peroxide compound formed by cytochrome-c peroxidase and horseradish peroxidase*. Nature, 1952. **169**(4302): p. 612-3.
6. George, P., *The chemical nature of the second hydrogen peroxide compound formed by cytochrome c peroxidase and horseradish peroxidase. I. Titration with reducing agents*. Biochem J, 1953. **54**(2): p. 267-76.
7. Gross, A.J. and I.W. Sizer, *The oxidation of tyramine, tyrosine, and related compounds by peroxidase*. J Biol Chem, 1959. **234**(6): p. 1611-4.
8. Passardi, F., C. Penel, and C. Dunand, *Performing the paradoxical: how plant peroxidases modify the cell wall*. Trends Plant Sci, 2004. **9**(11): p. 534-40.
9. Jermyn, M.A. and R. Thomas, *Multiple components in horse-radish peroxidase*. Biochem J, 1954. **56**(4): p. 631-9.
10. Hoyle, M.C., *High resolution of peroxidase-indoleacetic Acid oxidase isoenzymes from horseradish by isoelectric focusing*. Plant Physiol, 1977. **60**(5): p. 787-93.
11. Naatsaari, L., et al., *Peroxidase gene discovery from the horseradish transcriptome*. BMC Genomics, 2014. **15**: p. 227.
12. Fujiyama, K., et al., *Structure of the horseradish peroxidase isozyme C genes*. Eur J Biochem, 1988. **173**(3): p. 681-7.
13. Carlsson, G.H., et al., *Complexes of horseradish peroxidase with formate, acetate, and carbon monoxide*. Biochemistry, 2005. **44**(2): p. 635-42.
14. Veitch, N.C., *Horseradish peroxidase: a modern view of a classic enzyme*. Phytochemistry, 2004. **65**(3): p. 249-59.
15. Gajhede, M., et al., *Crystal structure of horseradish peroxidase C at 2.15 Å resolution*. Nat Struct Biol, 1997. **4**(12): p. 1032-8.
16. Smith, A.T., et al., *Expression of a synthetic gene for horseradish peroxidase C in Escherichia coli and folding and activation of the recombinant enzyme with Ca<sup>2+</sup> and heme*. J Biol Chem, 1990. **265**(22): p. 13335-43.
17. Gholami-Borujeni, F., et al., *Enzymatic treatment and detoxification of acid orange 7 from textile wastewater*. Appl Biochem Biotechnol, 2011. **165**(5-6): p. 1274-84.
18. Vasileva, N., et al., *Application of immobilized horseradish peroxidase onto modified acrylonitrile copolymer membrane in removing of phenol from water*. Int J Biol Macromol, 2009. **44**(2): p. 190-4.
19. Litescu, S.C., S. Eremia, and G.L. Radu, *Biosensors for the determination of phenolic metabolites*. Adv Exp Med Biol, 2010. **698**: p. 234-40.
20. Yang, H., *Enzyme-based ultrasensitive electrochemical biosensors*. Curr Opin Chem Biol, 2012. **16**(3-4): p. 422-8.

21. Dhore, C.R., et al., *Differential expression of bone matrix regulatory proteins in human atherosclerotic plaques*. *Arterioscler Thromb Vasc Biol*, 2001. **21**(12): p. 1998-2003.
22. McDermott, J.R., et al., *Mast cells disrupt epithelial barrier function during enteric nematode infection*. *Proc Natl Acad Sci U S A*, 2003. **100**(13): p. 7761-6.
23. Krieg, R. and K.J. Halhuber, *Recent advances in catalytic peroxidase histochemistry*. *Cell Mol Biol (Noisy-le-grand)*, 2003. **49**(4): p. 547-63.
24. Marquette, C.A. and L.J. Blum, *Chemiluminescent enzyme immunoassays: a review of bioanalytical applications*. *Bioanalysis*, 2009. **1**(7): p. 1259-69.
25. Dotsikas, Y. and Y.L. Loukas, *Improved performance of antigen-HRP conjugate-based immunoassays after the addition of anti-HRP antibody and application of a liposomal chemiluminescence marker*. *Anal Sci*, 2012. **28**(8): p. 753-7.
26. Huang, R.P., *Detection of multiple proteins in an antibody-based protein microarray system*. *J Immunol Methods*, 2001. **255**(1-2): p. 1-13.
27. Palmgren, B., et al., *Horseradish peroxidase dye tracing and embryonic statoacoustic ganglion cell transplantation in the rat auditory nerve trunk*. *Brain Res*, 2011. **1377**: p. 41-9.
28. Romero, M.I., M.A. Romero, and G.M. Smith, *Visualization of axonally transported horseradish peroxidase using enhanced immunocytochemical detection: a direct comparison with the tetramethylbenzidine method*. *J Histochem Cytochem*, 1999. **47**(2): p. 265-72.
29. Folkes, L.K. and P. Wardman, *Oxidative activation of indole-3-acetic acids to cytotoxic species- a potential new role for plant auxins in cancer therapy*. *Biochem Pharmacol*, 2001. **61**(2): p. 129-36.
30. Bruck, T.B. and D.W. Bruck, *Oxidative metabolism of the anti-cancer agent mitoxantrone by horseradish, lacto-and lignin peroxidase*. *Biochimie*, 2011. **93**(2): p. 217-26.
31. Wardman, P., *Indole-3-acetic acids and horseradish peroxidase: a new prodrug/enzyme combination for targeted cancer therapy*. *Curr Pharm Des*, 2002. **8**(15): p. 1363-74.
32. Huang, C., et al., *Apoptosis of pancreatic cancer BXPc-3 cells induced by indole-3-acetic acid in combination with horseradish peroxidase*. *World J Gastroenterol*, 2005. **11**(29): p. 4519-23.
33. Jeong, Y.M., et al., *Indole-3-acetic acid/horseradish peroxidase induces apoptosis in TCCSUP human urinary bladder carcinoma cells*. *Pharmazie*, 2010. **65**(2): p. 122-6.
34. Tupper, J., et al., *In vivo characterization of horseradish peroxidase with indole-3-acetic acid and 5-bromoindole-3-acetic acid for gene therapy of cancer*. *Cancer Gene Ther*, 2010. **17**(6): p. 420-8.
35. Diengott, D. and I.A. Mirsky, *Hypoglycemic action of indole-3-acetic acid by mouth in patients with diabetes mellitus*. *Proc Soc Exp Biol Med*, 1956. **93**(1): p. 109-10.
36. Folkes, L.K., L.P. Candeias, and P. Wardman, *Toward targeted "oxidation therapy" of cancer: peroxidase-catalysed cytotoxicity of indole-3-acetic acids*. *Int J Radiat Oncol Biol Phys*, 1998. **42**(4): p. 917-20.
37. Folkes, L.K., S. Rossiter, and P. Wardman, *Reactivity toward thiols and cytotoxicity of 3-methylene-2-oxindoles, cytotoxins from indole-3-acetic*

- acids, on activation by peroxidases. *Chem Res Toxicol*, 2002. **15**(6): p. 877-82.
38. Greco, O., et al., *Mechanisms of cytotoxicity induced by horseradish peroxidase/indole-3-acetic acid gene therapy*. *J Cell Biochem*, 2002. **87**(2): p. 221-32.
  39. Greco, O., et al., *Development of a novel enzyme/prodrug combination for gene therapy of cancer: horseradish peroxidase/indole-3-acetic acid*. *Cancer Gene Ther*, 2000. **7**(11): p. 1414-20.
  40. Spadiut, O. and C. Herwig, *Production and purification of the multifunctional enzyme horseradish peroxidase*. *Pharm Bioprocess*, 2013. **1**(3): p. 283-295.
  41. Hartmann, C. and P.R. Ortiz de Montellano, *Baculovirus expression and characterization of catalytically active horseradish peroxidase*. *Arch Biochem Biophys*, 1992. **297**(1): p. 61-72.
  42. Morawski, B., et al., *Functional expression of horseradish peroxidase in Saccharomyces cerevisiae and Pichia pastoris*. *Protein Eng*, 2000. **13**(5): p. 377-84.
  43. Romanos, M.A., C.A. Scorer, and J.J. Clare, *Foreign gene expression in yeast: a review*. *Yeast*, 1992. **8**(6): p. 423-88.
  44. Dietzsch, C., O. Spadiut, and C. Herwig, *A dynamic method based on the specific substrate uptake rate to set up a feeding strategy for Pichia pastoris*. *Microb Cell Fact*, 2011. **10**: p. 14.
  45. Dietzsch, C., O. Spadiut, and C. Herwig, *A fast approach to determine a fed batch feeding profile for recombinant Pichia pastoris strains*. *Microb Cell Fact*, 2011. **10**: p. 85.
  46. Krainer, F.W., et al., *Recombinant protein expression in Pichia pastoris strains with an engineered methanol utilization pathway*. *Microb Cell Fact*, 2012. **11**: p. 22.
  47. Zalai, D., et al., *A dynamic fed batch strategy for a Pichia pastoris mixed feed system to increase process understanding*. *Biotechnol Prog*, 2012. **28**(3): p. 878-86.
  48. Tams, J.W. and K.G. Welinder, *Mild chemical deglycosylation of horseradish peroxidase yields a fully active, homogeneous enzyme*. *Anal Biochem*, 1995. **228**(1): p. 48-55.
  49. Spadiut, O., et al., *Purification of a recombinant plant peroxidase produced in Pichia pastoris by a simple 2-step strategy*. *Protein Expr Purif*, 2012. **86**(2): p. 89-97.

## **CHAPTER I:**

**Development of an efficient Downstream Process for  
recombinant HRP from *P. pastoris* and search for  
novel potentially useful isoenzymes**

# Purification and basic biochemical characterization of 19 recombinant plant peroxidase isoenzymes produced in *Pichia pastoris*

Published in the journal Protein Expression and Purification Volume 95, March 2014  
DOI: 10.1016/j.pep.2013.12.003

**Robert Pletzenauer**<sup>1\*</sup>, Florian W. Krainer<sup>2\*</sup>, Laura Rossetti<sup>1</sup>, Christoph Herwig<sup>1</sup>, Anton Glieder<sup>3</sup> and Oliver Spadiut<sup>1§</sup>

<sup>1</sup> Vienna University of Technology, Institute of Chemical Engineering, Research Area Biochemical Engineering, Vienna, Austria

<sup>2</sup> Graz University of Technology, Institute of Molecular Biotechnology, Graz, Austria

<sup>3</sup> Austrian Centre of Industrial Biotechnology (ACIB GmbH), Graz, Austria

\* these authors contributed equally

§ corresponding author

Corresponding author: Oliver Spadiut, Vienna University of Technology, Institute of Chemical Engineering, Research Area Biochemical Engineering, Gumpendorfer Strasse 1a, A-1060 Vienna, Austria; oliver.spadiut@tuwien.ac.at; Tel: +43 (0)1 58801 166473

## **Keywords:**

horseradish peroxidase, *Pichia pastoris*, glycosylation, protein purification, negative chromatography, monolith

## 1 Abstract

The plant enzyme horseradish peroxidase (HRP) is used in several important industrial and medical applications, of which especially biosensors and diagnostic kits describe an emerging field. Although there is an increasing demand for high amounts of pure enzyme preparations, HRP is still isolated from the plant as a mixture of different isoenzymes with different biochemical properties.

Based on a recent next generation sequencing approach of the horseradish transcriptome, we produced 19 individual HRP isoenzymes recombinantly in the yeast *Pichia pastoris*. After optimizing a previously reported 2-step purification strategy for the recombinant isoenzyme HRP C1A by substituting an unfavorable size exclusion chromatography step with an anion exchange step using a monolithic column, we purified the 19 HRP isoenzymes with varying success. Subsequent basic biochemical characterization revealed differences in catalytic activity, substrate specificity and thermal stability of the purified HRP preparations. The preparations of the isoenzymes HRP A2A and HRP A2B were found to be highly interesting candidates for future applications in diagnostic kits with increased sensitivity.

## 2 Introduction

Horseradish peroxidase (HRP; EC 1.11.1.7) is a class III peroxidase or classical secretory plant peroxidase which oxidizes different substrates (*e.g.* aromatic phenols, indoles, phenolic acids, amines, sulfonates) using peroxides, commonly H<sub>2</sub>O<sub>2</sub>, as initial electron acceptors [1–3]. This enzyme has been studied for more than 200 years. Already in 1810, horseradish roots were observed to cause a color reaction when mixed with the resin of *Guaiacum* plants [4], probably the oxidation of  $\alpha$ -guaiaconic acid to guaiacum blue by HRP [5]. In plants, HRP is involved in numerous reactions, such as the crosslinking of phenolic molecules and the regulation of H<sub>2</sub>O<sub>2</sub> levels, the cell wall network and auxin catabolism [6–8]. Correlating with the large number of different *in vivo* functions, horseradish was found to contain a multitude of different HRP isoenzymes. Up to 42 isoenzymes were detected by isoelectric focusing of commercial HRP preparations [9]. Jermyn *et al.* observed multiple proteins in the horseradish plant with peroxidase activity and

found seasonal variation in their relative amounts as well as differences in substrate affinity [10,11]. This biochemical versatility of HRP isoenzymes was further demonstrated in several subsequent studies (e.g. [12–16]).

Until now, however, most studies have focused on the isoenzyme C1A [17], which is the only isoenzyme with a solved structure [18]. HRP C1A contains nine potential N-glycosylation sites, defined by the N-X-S/T motif, with X being any amino acid but proline, of which eight are glycosylated when isolated from plant [19]. Plant-derived HRP C1A has a total carbohydrate content of 21.8 % [20]. Interestingly, plant-derived HRP isoenzymes with a basic isoelectric point (pI) of >12 were found to be less glycosylated, e.g. only 0.8-4.2 % carbohydrate content for isoenzymes E3-E6 [15]. Tams *et al.* studied the effect of the N-glycans on the biochemical properties of HRP C1A and found that pI, absorption spectrum, peroxidase activity towards *o*-dianisidine and thermal stability remained the same, whereas the kinetic stability and the solubility in ammonium sulfate were decreased upon deglycosylation [21,22]. Thus, the presence of glycan structures on the enzyme surface has a considerable impact on HRP.

Today, the roots of the horseradish plant are the main source for commercially available HRP preparations. These preparations commonly describe mixtures of isoenzymes whose expression patterns change seasonally and in response to uncontrollable environmental factors [8]. The yields of HRP are rather low with less than 10 mg of total HRP protein, which presents a mixture of different isoenzymes, from 100 g of horseradish roots [23]. Thus, the yield of specific isoenzymes purified from such a mixture is extremely low, e.g. Aibara *et al.* reported as little as 40 mg of isoenzyme E1 from 200 kg of horseradish roots [15]. Unfortunately, due to intrinsic enzyme properties such as intramolecular disulfide bridges [18], the recombinant production of HRP is challenging. Recombinant production as inclusion bodies in *E. coli* is possible (e.g. [24,25]), but refolding yields are as low as 10 mg·L<sup>-1</sup> [25]. Beside the recombinant production of HRP in insect cell cultures (e.g. [26,27]), the currently most promising production systems are yeasts such as *Saccharomyces cerevisiae* [28–30] and *Pichia pastoris* [29,31]. However, HRP produced in *P. pastoris* is heterogeneously hyperglycosylated, causing the enzyme to appear as a smear on a SDS polyacrylamide gel at a size of approximately 65 kDa instead of its unglycosylated size of 35 kDa [29,32,33]. These excessive yeast-type glycans

considerably impede classical downstream processing approaches. Whereas plant-derived HRP can be purified either by several consecutive steps of column chromatography (e.g. [12,15,16]) or by affinity chromatography using the lectin concanavalin A (e.g. [34–37]) as an isoenzyme mixture in a quite simple way, yeast-derived HRP cannot be purified by these strategies [33].

One obvious advantage of the recombinant production of single HRP isoenzymes in *P. pastoris* is the fact that this isoenzyme does not need to be isolated from an isoenzyme mixture, an otherwise time-intensive and tedious purification effort. Consequently, all HRP activity can be ascribed to the produced individual isoenzyme, allowing its specific enzymatic characterization. However, for that purpose, the HRP isoenzyme still has to be purified from yeast proteins. Hyperglycosylated HRP isoenzyme C1A from *P. pastoris* was previously purified by subsequent steps of hydrophobic interaction chromatography (HIC), size exclusion chromatography (SEC) and anion exchange chromatography (AEC) [29,30]. Recently, we addressed the issue of this cumbersome purification strategy by even making use of the high carbohydrate content of recombinant HRP C1A. We applied hydrophobic charge induction chromatography (HCIC) operated in flowthrough mode to remove contaminating proteins that bound to the resin, whereas the hyperglycosylated HRP eluted in the flowthrough. The glycan coat surrounding HRP C1A seemed to mask the physicochemical properties of the enzyme, allowing this rather unconventional, negative chromatography approach. An additional polishing step by SEC gave a preparation of HRP C1A with a specific activity comparable to the purest commercially available HRP preparation from plant [33].

Recently, we performed a next generation sequencing approach of the horseradish transcriptome which greatly increased the amount of available HRP isoenzyme sequences [38], and thus allowed more detailed studies of single isoenzymes. Considering the numerous applications of HRP as a reporter enzyme in diagnostic assays and histochemical staining as well as in strain engineering studies (e.g. [31,39,40]), biocatalysis (e.g. [41]), wastewater cleanup systems (e.g. [42]) and antibody-directed enzyme-prodrug cancer therapy (e.g. [43]), it is highly interesting to biochemically characterize the different HRP isoenzymes to find the most suitable one for a certain application.

Here, we report the production, purification and basic biochemical characterization of 19 individual HRP isoenzyme preparations. We significantly improved our recently reported 2-step purification procedure [33], replacing the rather inefficient and slow SEC polishing step by using a tube monolithic AEC column. Finally, we performed a basic enzymatic characterization of the final HRP preparations to determine potential differences in their catalytic activities, substrate specificities and thermal stabilities.

### **3 Materials and Methods**

#### **3.1 Chemicals**

Enzymes were obtained from Thermo Scientific (formerly Fermentas, Germany). 2,2'-azino-bis(3-ethylbenzthiazoline-6-sulfonic acid) diammonium salt (ABTS), 3,3',5,5'-tetramethylbenzidine·HCl (TMB) and D(+)-biotin were purchased from Sigma-Aldrich (Austria). Difco™ yeast nitrogen base w/o amino acids (YNB), Bacto™ tryptone and Bacto™ yeast extract were obtained from Becton Dickinson (Austria). Zeocin™ was obtained from InvivoGen (France). Other chemicals were obtained from Carl Roth (Germany).

#### **3.2 *P. pastoris* strains for HRP production**

All *P. pastoris* strains in this study were based on the *P. pastoris* wildtype strain CBS 7435 (identical to NRRL Y-11430 and ATCC 76273). The Mut<sup>S</sup> (methanol utilization slow) phenotype of *P. pastoris* was shown to be superior over the Mut<sup>+</sup> phenotype in terms of volumetric productivity and production efficiency of HRP [31]. Thus, all HRP production strains in this study were strains with Mut<sup>S</sup> phenotype [44]. A detailed description of the identification of new HRP isoenzyme sequences and the generation of the *P. pastoris* strains producing the various HRP isoenzymes was given elsewhere [38]. Calculated basic protein parameters and the corresponding database accession codes are shown in Table 1.

**Table 1: Calculated basic characteristics of HRP isoenzymes.** The isoelectric point (pI) and the molecular weight (MW) were calculated using the Compute pI/Mw tool of the ExPASy server [55,56] and the number of potential N-glycosylation sites (N-X-S/T) was deduced from the NetNGlyc 1.0 Server [57]. All calculations were based on a cleavage of the prepro signal peptide of the *S. cerevisiae* mating factor alpha between A87 and E88, upstream of the mature HRP peptide.

HRP isoenzyme	pI	MW [kDa]	N-X-S/T	GenBank	UniProt
C1A	5.41	35.82	9	HE963800.1	K7ZWW6
25148.1 (C1C)	6.13	35.86	7	HE963802.1	K7ZWQ1
25148.2 (C1D)	6.50	35.89	7	HE963803.1	K7ZW56
04627 (C2)	8.38	35.67	4	HE963804.1	K7ZW02
C3	7.05	35.48	3	HE963805.1	K7ZWW7
A2A	4.84	32.09	9	HE963806.1	K7ZW28
A2B	4.84	32.12	9	HE963807.1	K7ZWQ2
E5	8.99	33.92	3	HE963808.1	K7ZW57
1805	5.75	35.96	5	HE963809.1	K7ZW05
22684.1	6.39	35.06	4	HE963810.1	K7ZWW8
22684.2	6.00	35.15	4	HE963811.1	K7ZW29
1350	8.47	31.42	3	HE963812.1	K7ZWQ3
5508	8.22	31.35	3	HE963815.1	K7ZWW9
6351	5.99	32.89	2	HE963816.1	K7ZW31
22489.1	8.24	31.37	2	HE963818.1	K7ZW59
22489.2	8.24	31.39	2	HE963819.1	K7ZW11
17517.2	9.30	32.69	4	HE963823.1	K7ZW60
08562.4	8.91	33.26	3	HE963825.1	K7ZWX1
08562.1	8.89	33.81	3	HE963824.1	K7ZW15

Synthetic codon-optimized genes encoding mature HRP isoenzymes were N-terminally fused to the prepro signal peptide of the *S. cerevisiae* mating factor alpha to facilitate efficient secretion of the recombinant HRP to the cultivation supernatant. The expression of the HRP encoding genes was regulated by the methanol-inducible promoter of the *P. pastoris* *AOX1* gene.

### 3.3 Production of recombinant HRP isoenzymes

Recombinant production of 19 different HRP isoenzymes in *P. pastoris* was performed in 2.5 L Ultra Yield Flasks from BioSilta (Finland), applying a protocol based on [45] with the following modifications: An overnight culture (ONC) of 30 mL YPD (yeast extract-peptone-dextrose) in 250 mL baffled shake flasks was inoculated with a single colony of a *P. pastoris* strain producing a specific HRP isoenzyme and incubated at 28 °C, 90 rpm and approximately 50 % humidity for at least 12 h. 1.5 mL of this ONC were transferred to 270 mL of iron-supplemented BMD1% (11 g·L<sup>-1</sup> α-D(+)-glucose monohydrate, 13.4 g·L<sup>-1</sup> YNB, 0.4 mg·L<sup>-1</sup> D(+)-

biotin, 278 mg·L<sup>-1</sup> FeSO<sub>4</sub>·7H<sub>2</sub>O, 0.1 M potassium phosphate buffer, pH 6.0) per Ultra Yield Flask and cultivated under the same conditions for approximately 60 h. A first induction pulse was performed by addition of 30 mL BMM10 (5 % (v/v) methanol, 13.4 g·L<sup>-1</sup> YNB, 0.4 mg·L<sup>-1</sup> D(+)-biotin, 0.1 M potassium phosphate buffer, pH 6.0). 3.0 mL of pure methanol were added approximately 12 h and 36 h after the first induction pulse, 1.5 mL of pure methanol were added approximately 24 h and 48 h after the first induction pulse. 72 h after the first induction pulse, the culture broth was centrifuged (15,000 xg, 30 min, 4 °C) and the supernatant was filtered through a 0.2 µm cellulose acetate filter (Sartorius Stedim Biotech, Germany).

### **3.4 Purification of recombinant HRP isoenzymes**

In accordance to our previous study, the supernatant was concentrated using the Vivaflow 50 system (Sartorius Stedim Biotech, Germany) with a 10 kDa MWCO membrane prior to hydrophobic charge induction chromatography (HCIC; [33]). The buffer was changed to HCIC-A (500 mM NaCl, 20 mM NaOAc, pH 6.0) and concentrated to a final volume of 10-15 mL. All further steps of concentration and buffer change were performed using Vivaspin 20 tubes (Sartorius Stedim Biotech, Germany) with 10 kDa MWCO. The HCIC resin MEP HyperCel™ was obtained from Pall (Austria), and HCIC was performed in flowthrough mode based on [33]: A column containing approximately 25 mL of MEP HyperCel™ resin was equilibrated with at least 4 column volumes (CV) of buffer HCIC-A. 10-15 mL concentrated HRP solution in HCIC-A were loaded onto the column and washed with at least 220 mL of HCIC-A at a flow rate of approximately 55 cm·h<sup>-1</sup>. Fractions of 10 mL were collected. Fractions containing HRP activity were pooled and concentrated to 500-1000 µL. The column was washed with 5 CV of 800 mM NaOH, then re-equilibrated with HCIC-A for subsequent runs.

Univariate screenings for a potential application of CIM® tube monolithic columns (BIA separations, Slovenia) as a second chromatographic purification step were performed with the partially purified isoenzyme C1A after HCIC. Flowthrough fractions from HCIC purifications were pooled, concentrated and rebuffed in either of the loading buffers: 50 mM Tris-HCl, pH 7.4, 50 mM Tris-HCl, pH 8.0 or 50 mM potassium phosphate, pH 6.0. The respective elution buffers contained 1 M NaCl. The tube monolithic columns tested were 1 mL CIM®-DEAE, 1 mL CIM®-QA and 1

mL CIM<sup>®</sup>-OH (BIA separations, Slovenia), which were equilibrated in the respective loading buffer at a flow rate of 156 cm·h<sup>-1</sup>. A post-load wash of 4 CV binding buffer was performed before elution was conducted by either increasing the elution buffer in a single step to 100 % or in a linear gradient to 100 % over 30 CV.

Ultimately, anion exchange chromatography (AEC) with an 8 mL CIM<sup>®</sup>-DEAE tube monolithic column was performed as a second purification step for all the HRP isoenzymes. The column was equilibrated in loading buffer AEC-A (50 mM Tris-HCl, pH 8.0) at a flow rate of 16.8 cm·h<sup>-1</sup>. Post-HCIC pools of each HRP isoenzyme were subjected to diafiltration in AEC-A and were subsequently loaded onto the AEC column at an average linear flow rate of 16.8 cm·h<sup>-1</sup>. Elution was performed in a single step from 0 % to 100 % AEC-B (50 mM Tris-HCl, 1 M NaCl, pH 8.0). For column recovery the column was washed with 5 CV of a 1 M NaOH/1 M NaCl solution at an average linear flow rate of 33.6 cm·h<sup>-1</sup>.

### **3.5 Electrophoresis**

To check the electrophoretic purity of HRP isoenzyme preparations SDS-PAGE was performed using a 5 % stacking gel and a 10 % separating gel in 1x Tris-glycine buffer. Unless otherwise stated, samples were diluted to a protein concentration between 0.1-0.5 mg·mL<sup>-1</sup> before loading. Gels were run in a vertical electrophoresis Mini-PROTEAN Tetra Cell apparatus (Biorad, Austria) and stained with Coomassie blue. The protein mass standard used was the PageRuler Prestained Ladder (Fermentas, Austria).

### **3.6 Data analysis and basic enzymatic characterization of purified recombinant HRP isoenzymes**

Protein concentrations were determined at 595 nm by the Bradford assay using the Sigma-Aldrich (Austria) Protein Assay Kit with bovine serum albumin as standard in the range of 0.2-1.2 mg·mL<sup>-1</sup>.

The enzymatic activity of HRP was measured using an ABTS assay in a CuBiAn XC enzymatic robot (Innovatis, Germany). 10 µL of sample were mixed with 140 µL 1 mM ABTS solution (50 mM potassium phosphate buffer, pH 6.5). The reaction mixture was incubated at 37 °C for 5 min before the reaction was started by the addition of 20 µL 0.078 % (w/w) H<sub>2</sub>O<sub>2</sub>. Changes in absorption at 415 nm were

measured for 80 s and rates were calculated. The standard curve was prepared using a commercially available HRP preparation (Type VI-A, Sigma-Aldrich, Austria) in the range from 0.02-2.0 U·mL<sup>-1</sup>.

The efficiency of the applied purification approach was evaluated by determining the purification factor (PF) and the recovery yield of HRP activity in percentage (R%). PF and R% were calculated by equations 1 and 2.

$$PF = \frac{\text{specific activity}_{\text{post}}}{\text{specific activity}_{\text{pre}}} \quad \text{Equation 1}$$

$$R\% = 100 * \frac{\text{volumetric activity}_{\text{post}} * \text{volume}_{\text{post}}}{\text{volumetric activity}_{\text{pre}} * \text{volume}_{\text{pre}}} \quad \text{Equation 2}$$

The suffixes “pre” and “post” indicate the respective values before and after a purification step. To obtain an overall PF and R% for the 2-step purification approach, we combined the values we determined for the single purification steps (Table 2). In case one purification step did not work or could not be evaluated, e.g. due to too low HRP activity, we only presented the successful purification step. The pooled active fractions after AEC were concentrated using Amicon Ultra-15 Centrifugal Filter Units with 10 kDa MWCO (Merck-Millipore, Austria) to the final enzyme preparation of a volume of approximately 1.5 mL.

Characterization of the purified HRP isoenzyme preparations included the determination of the basic kinetic parameters,  $V_{\text{max}}$  and  $K_M$ , for the electron acceptors ABTS and TMB in a spectrophotometer UV-1601 from Shimadzu (Austria). These peroxidase substrates are commonly used in enzyme-linked immunosorbent assays (ELISA), The reaction mixture with a final volume of 1.0 mL contained a concentration of 1 mM H<sub>2</sub>O<sub>2</sub>, 10 μL of HRP isoenzyme preparation and varying concentrations of ABTS (0.05-10 mM) or TMB (0.005-0.5 mM) in 50 mM potassium phosphate buffer, pH 6.5. The increase in absorption was followed at 420 nm for ABTS and at 653 nm for TMB at 30 °C for 180 s, respectively. Absorption curves were recorded with an adapted software program (UVPC Optional Kinetics software, Shimadzu). The maximum reaction rate ( $V_{\text{max}}$ ) and the Michaelis constant ( $K_M$ ) were calculated with the Sigma Plot software (Version 11.0, Systat Software Inc., USA).

**Table 2: Summary of the 2-step purification approach of 19 recombinant HRP isoenzymes.** The purification factor (PF) and the recovery of HRP activity in percentage (R%) of the applied HCIC and AEC flowthrough steps, as well as the combined purification results are shown. Some isoenzymes did not show any detectable peroxidase activity. In these cases, no values for PF or R% are available (n/a). The combined PF value is a product of the PFs of the HCIC and AEC step; in case no values were available for one purification step (n/a), the combined value only describes the working step.

HRP isoenzyme	HCIC		AEC		combined	
	PF	R%	PF	R%	PF	R%
C1A	7.02	95.4	10.92	58.5	76.66	55.8
25148.1 (C1C)	6.80	95.5	2.28	66.4	15.50	63.4
25148.2 (C1D)	8.96	32.9	2.42	66.5	21.68	21.9
04627 (C2)	10.08	100.0	6.17	45.7	62.19	45.7
C3	2.17	17.6	2.50	100.0	5.43	17.6
A2A	15.85	100.0	43.18	15.6	684.40	15.6
A2B	5.82	92.0	6.64	80.0	38.64	73.6
E5	3.89	33.1	0.54	81.0	2.10	26.8
1805	n/a	n/a	15.68	38.4	15.68	38.4
22684.1	0.11	1.4	n/a	n/a	n/a	n/a
22684.2	n/a	n/a	n/a	n/a	n/a	n/a
1350	n/a	n/a	n/a	n/a	n/a	n/a
5508	2.18	33.2	66.25	31.5	144.43	10.5
6351	3.01	32.6	n/a	n/a	n/a	n/a
22489.1	0.42	3.8	n/a	n/a	n/a	n/a
22489.2	0.02	0.3	2.09	74.6	0.04	0.2
17517.2	3.48	38.9	0.98	75.0	3.41	29.2
08562.4	n/a	n/a	0.89	32.6	0.89	32.6
08562.1	1.18	16.5	0.27	45.5	0.32	7.5

The thermal stability of individual HRP isoenzyme preparations was tested at 60 °C. The residual activity towards ABTS was measured after 5, 10, 15, 20, 30 and 60 min of incubation at 60 °C. The residual activities were plotted versus the incubation time and the half life times of thermal inactivation at 60 °C ( $\tau_{1/2}$ ) were calculated using equation 3 [46]:

$$\tau_{1/2} = \frac{\ln 2}{k_{in}} \quad \text{Equation 3}$$

$k_{in}$  rate of inactivation (slope of the logarithmic residual activity)

## 4 Results and Discussion

HRP is a well-studied enzyme which is used in numerous industrial and medical applications (e.g. [31,39–43]). Due to certain intrinsic enzyme features, the recombinant production and purification of this important enzyme is quite cumbersome, and HRP is still isolated from horseradish roots as a mixture of

isoenzymes at low yields. A recombinant production process in combination with an efficient purification strategy would allow the reliable production of individual HRP isoenzymes for the various applications in large amounts.

#### **4.1 HRP production**

In this study, 19 HRP isoenzymes were recombinantly produced in the methylotrophic yeast *P. pastoris* in shake flask cultivations. By fusing the genes to the prepro signal sequence of the *S. cerevisiae* mating factor alpha, the HRP isoenzymes were secreted to the cultivation broth. Due to the fact that *P. pastoris* actively secretes only few endogenous proteins [47,48], the subsequent downstream process was thereby considerably facilitated already. After centrifugation and diafiltration, the HRP isoenzymes could already be subjected to chromatography. Typical total protein concentrations in the cultivation broth at the time of harvesting were in the range of 200-500 mg·L<sup>-1</sup>. The amount of obtainable purified HRP isoenzyme preparation differed vastly; for the isoenzymes which could be purified best using the here presented 2-step strategy the following protein contents per liter cultivation broth were obtained: 1.0 mg C1A, 0.6 mg C2, 0.1 mg A2A and 0.15 mg 5508. Also volumetric HRP activities with ABTS as reducing substrate varied considerably from isoenzyme to isoenzyme. For instance, the HRP isoenzymes 8562.1, 22489.1, A2A, C1A and E5 gave approximately 3, 70, 220, 440 and 670 U·L<sup>-1</sup>, respectively.

#### **4.2 Hydrophobic charge induction chromatography (HCIC)**

In a recent multivariate Design of Experiments screening study, we found HCIC operated in the flowthrough mode to be very effective for the purification of the hyperglycosylated recombinant HRP C1A, allowing a 5-fold purification at almost 100 % recovery [33]. However, in the present study the application of this flowthrough purification step to the 19 different HRP isoenzymes produced in *P. pastoris* led to quite diverse results in terms of purification factor (PF) and recovery yield (R%; Table 2), indicating significant differences in the physicochemical properties, to some extent probably caused by the different degrees of glycosylation of the individual HRP isoenzymes. However, the HCIC elution profile of the HRP isoenzyme C1A that was shown previously [33], could be reproduced under the

conditions applied in the present study as the whole HRP activity was found in the flowthrough (Figure 1). The higher PF for HRP C1A in this study compared to our previous results [33] (*i.e.* 7-fold versus 5-fold, respectively) might be explained by the different cultivation approaches. In the present study, we produced HRP C1A in shake flask cultivations, whereas previous cultivations were done in the controlled environment of a bioreactor [33]. The latter allowed cultivation under optimized conditions, thus limiting cell lysis and contamination of the cultivation broth by intracellular proteins. Presumably, the amount of contaminating proteins in the starting solution was therefore lower, causing an overall lower PF for the C1A preparation from the bioreactor.

Elution profiles similar to the one shown in Figure 1 were found for ten other HRP isoenzymes (graphs not shown), indicating the applicability of the HCIC flowthrough purification for these isoenzymes (Table 2). Remarkably, a 16-fold purification at 100 % recovery was achieved for isoenzyme HRP A2A (Table 2). However, for some isoenzymes the flowthrough based HCIC step could not be applied successfully as no purification was achieved (*e.g.* HRP 22489.1; Table 2).

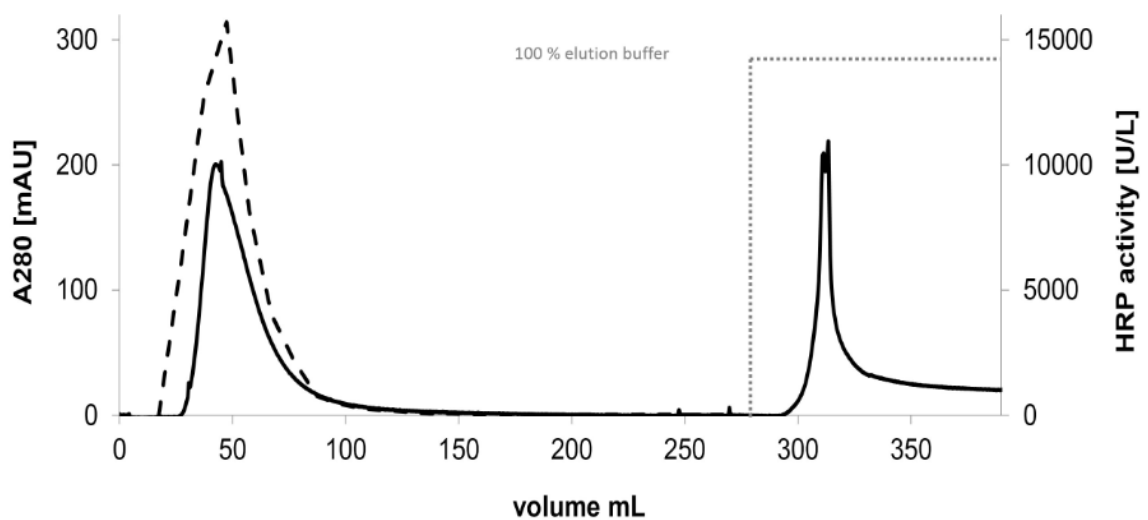


**Figure 1: HCIC chromatogram of the recombinant HRP isoenzyme C1A.** The HRP activity (dashed line) was determined by using ABTS as reducing substrate. Protein content was followed throughout the run by recording the absorption at 280 nm (solid line).

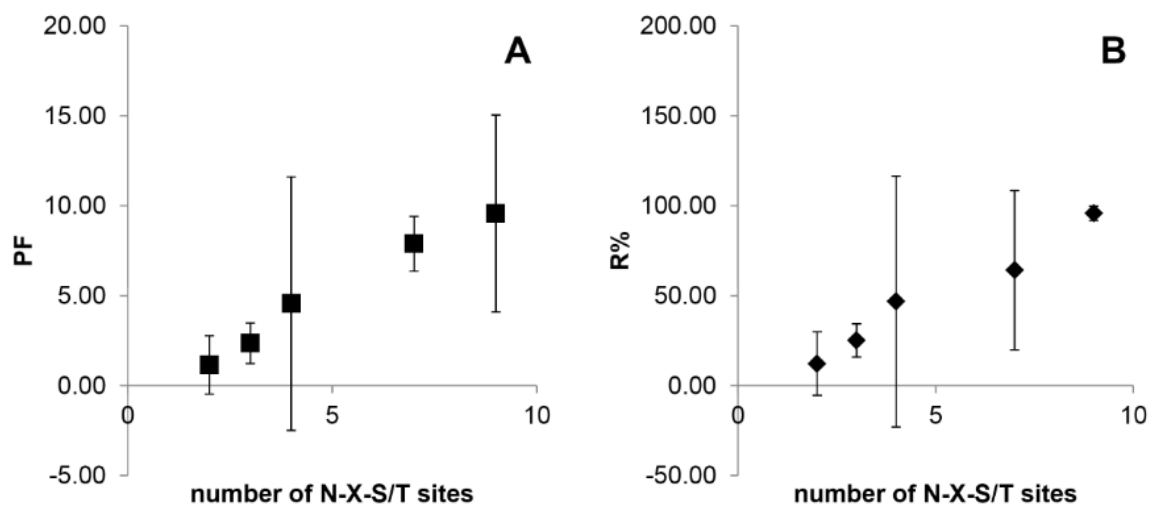


**Figure 2: Correlation of the number of N-glycosylation sites and HCIC purification parameters.** A, purification factor (PF); B, recovery yield of HRP activity in percentage (R%). The average PF and R% for HRPs with n N-X-S/T sites are shown with the corresponding calculated standard deviations;  $n_2=3$ ,  $n_3=4$ ,  $n_4=3$ ,  $n_7=2$ ,  $n_9=3$ .

To find an explanation for that phenomenon, we looked at the single isoenzymes in more detail. Predictions of potential N-glycosylation sites, based on the identification of the conserved N-X-S/T motif, were performed using the NetNGlyc 1.0 Server (Table 1). Interestingly, the number of predicted potential N-glycosylation sites correlated well with both the PF and the recovery yield (R%; Figure 2). This observation strongly underlines our previous hypothesis that extensive glycosylation prevents the interaction of recombinant HRP from *P. pastoris* with the HCIC material, hence allowing the negative chromatography purification step [33]. For example, HRP C1A and HRP A2A each contain nine N-X-S/T motifs and could be purified 7.0- and 15.9-fold at 95.4 and 100.0 % recovery, respectively. HRP 6351 and HRP C3, on the other hand, contain only 2 and 3 N-X-S/T motifs and could only be purified 3.0- and 2.2-fold at 32.6 and 17.6 % recovery, respectively (Tables 1 and 2). Outliers from that correlation, e.g. HRP 22684.1, which could not be purified via HCIC (PF of 0.1; Table 2) despite containing four N-X-S/T motifs, might be explained by varying degrees in glycosylation due to steric hindrance at certain N-glycosylation sites. However, the generally high correlation between the number of glycosylation sites and both the PF and the R%, as evident in Figure 2, allows the design of an appropriate purification strategy for extensively glycosylated enzymes produced in *P. pastoris*.

### 4.3 Anion exchange chromatography (AEC)

Recently, monolithic columns were discovered as a powerful tool for both analytical purposes and preparative protein purification [49–51]. The solid support, a uniform monolithic porous material (*e.g.* glycidyl methacrylate-based materials), is simple to handle and to scale up, allows elevated operating flow rates and pressures (*e.g.* flow rates of up to 336 cm·h<sup>-1</sup> and a back pressure of up to 20 bar for an 8 mL tube monolithic column from BIA separations), and provides high binding capacity (> 20 mg·mL<sup>-1</sup>). These beneficial features are mainly enabled by the convective mass transfer of the target molecule through the highly interconnected channel structure of the porous polymer block. In convective processes, both resolution and binding capacity are not affected by the flow rate, an effect that is emphasized when large biomolecules such as proteins are separated due to their high diffusion coefficients [49]. On the other hand, porous particles which are applied in conventional chromatographic media require diffusive transport of the molecules which have to enter the pores to get in contact with the active surface. This diffusive transport results in increased separation times and void volumes.

In our previous study, we polished partially purified recombinant HRP C1A after HCIC by SEC [33]. Although this strategy gave a good PF of >2.0 and a recovery yield of 100 %, SEC has several uneconomical disadvantages such as low flow rates, sample dilution, temperature effects due to long process times, limited sample volumes and limited scalability. Thus, we tested monolithic columns as an alternative to SEC. A wide range of monolithic formats and ligands is available today [52]. In this study, we tested two AEC resins and a HIC resin, since these two purification principles had shown promising results using particle-based resins for recombinant HRP C1A before [33]. We used different buffer systems and elution profiles for the potential application of CIM<sup>®</sup> tube monolithic columns as polishing step for recombinant HRP C1A, partially purified after HCIC. Active flowthrough fractions from HCIC purifications were pooled, concentrated via diafiltration and loaded on the different CIM<sup>®</sup> tube columns. The HIC resin CIM<sup>®</sup>-OH was not able to purify recombinant HRP C1A after HCIC any further, regardless of the buffers applied. We believe that this was due to the fact that the vast majority of hydrophobic proteins had already been retained on the HCIC resin. Using the strong AEC resin CIM<sup>®</sup>-QA, the enzyme preparation could not be purified more than 1.3-fold

regardless of the buffer, a phenomenon which we also observed with particle-based strong AEC materials before [33]. However, the weak AEC tube monolithic column CIM<sup>®</sup>-DEAE gave satisfactory results. Using Tris-HCl (50 mM, pH 8.0) as loading buffer, a PF of nearly 11.0 was obtained for recombinant HRP C1A when the negative chromatography approach was applied.

Interestingly, similar to the HCIC flowthrough step, operation of AEC in the flowthrough mode also gave diverse results in terms of PF and R% for the different recombinant HRP isoenzymes (Table 2). Some isoenzymes could not be purified by this strategy, whereas other isoenzymes were purified up to 66-fold. Remarkably, for isoenzymes 1805, 5508 and 22489.2 only the second purification step via the CIM<sup>®</sup>-DEAE monolithic column worked, whereas HCIC could not improve the preparations in terms of enzyme purity; in fact, PFs of more than 30 showed that for some HRP isoenzymes the AEC step alone already described an efficient purification strategy (Table 2). The HRP isoenzymes 22684.1, 6351 and 22489.1 did not show any detectable peroxidase activity after diafiltration indicating instability under the conditions applied. Furthermore, no HRP activity was detected prior to AEC for 22684.2 and 1350 due to the high dilution of the enzyme at that stage (Table 2). Therefore, we cannot comment on the applicability of the AEC strategy for these five isoenzymes.

Summarizing, the CIM<sup>®</sup>-DEAE tube monolith describes a highly interesting alternative to SEC as a polishing step for partially purified recombinant HRP isoenzymes. Compared to the PF of around 2.0 which we achieved for the recombinant HRP isoenzyme C1A using SEC before [33], the flowthrough step applying an anion exchange monolith presented here is not only advantageous in terms of flow rates, sample volumes and thus process time, but also gave a 5-fold higher PF of nearly 11.0. In Figure 3 we exemplarily show a SDS gel of the different steps during AEC purification of the HRP isoenzyme C1A. Although there are no striking bands indicating contaminant proteins in the flowthrough fraction of AEC, the specific activity of the purified HRP C1A preparation in this study was remarkably lower than in our previous study [33]:

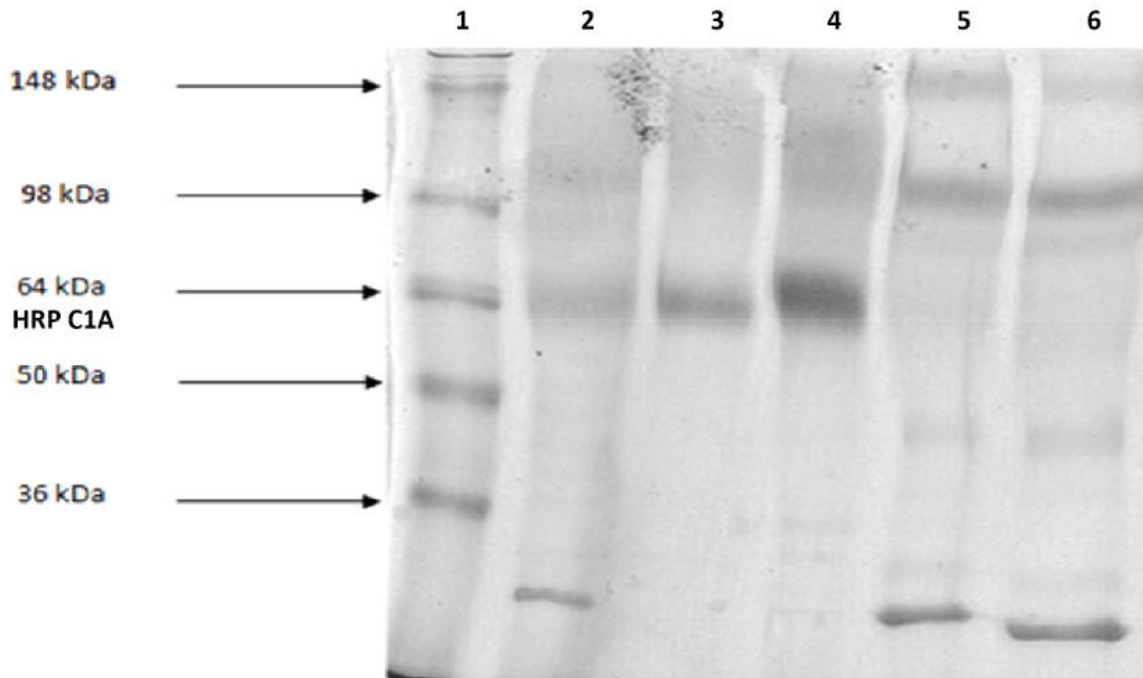


**Figure 3: SDS-PAGE of fractions from AEC with HRP C1A.** Lane 1, molecular mass standard; lane 2, cell-free cultivation supernatant (5 µg); lane 3, flowthrough (5 µg); lane 4, flowthrough (10 µg); lane 5 and 6, fractions eluted with buffer AEC-B (5 µg).

The preparation of HRP C1A in this study yielded a specific activity of only approximately 100 U·mg<sup>-1</sup>, whereas the C1A preparation in our previous study yielded a specific activity of approximately 1000 U·mg<sup>-1</sup> [33]. We ascribe this phenomenon to the different cultivation procedures. Whereas HRP C1A was produced in the controlled environment of a bioreactor constantly providing optimal conditions for *P. pastoris* in our previous work [33], in the present study the HRP isoenzymes, including HRP C1A, were produced in shake flasks where conditions were not controlled. Limitations in oxygen and nutrients as well as gradients, which can occur in shake flasks, apparently influence the physiology of the cells and hence their ability to produce catalytically active enzyme. In fact, this is a very good example how the upstream process might influence the downstream process and the final product quality.

#### 4.4 Basic biochemical characterization of HRP isoenzyme preparations

After the chromatographic 2-step purification procedure, the flowthrough fractions of the single HRP isoenzymes were pooled and concentrated by ultrafiltration before basic biochemical characterization was done. Especially, for HRP isoenzymes 22684.2 and 1350, where the concentration of HRP in the collected fractions was very low, this step was essential to be able to obtain reliable kinetic data.

As anticipated from our preliminary data [38], the preparations of the recombinant HRP isoenzymes featured significantly different biochemical properties. Not only physicochemical parameters, such as the predicted pI (Table 1), covered a broad range, but also the enzymatic activity towards the two tested electron donors ABTS and TMB were found to be highly versatile (Table 3; examples for Michaelis Menten plots shown in Figure 4).

For the oxidation of ABTS, the highest  $V_{max}$  values were obtained for the preparations of the isoenzymes A2A and A2B. These two isoenzyme preparations were able to oxidize ABTS 4- to 5-fold better than the preparation of the well-studied isoenzyme C1A (Table 3), rendering our preparations of HRP A2A and A2B particularly interesting for diagnostic bioassays with increased sensitivity. In a previous study on commercial preparations of acidic HRP isoenzymes from the plant, a comparatively high  $K_M$  value of 4.0 mM was reported for ABTS as the reducing substrate [53]. In contrast, the here reported  $K_M$  values of recombinant preparations of the acidic isoenzymes A2A and A2B were significantly lower with 1.95 and 1.73 mM, respectively.

An explanation for this difference in substrate affinity remains speculative, but might be ascribed to the slightly different amino acid sequences of isoenzymes A2A and A2B used in this study compared to the commercial isoenzymes.

The here presented apparent  $K_M$  of 1.01 mM for ABTS for the HRP C1A preparation was higher than the previously published  $K_M$  values of 0.27 mM and 0.18 mM for C1A preparations from plant and *E. coli*, respectively [54]. In a previous study on recombinant HRP C1A from *P. pastoris* a  $K_M$  of 0.68 mM was reported [30]. Apparently, yeast-derived HRP C1A preparations generally have a tendency for a lowered affinity for ABTS, probably related to the yeast-type hyperglycosylation compared to preparations from plant and *E. coli*.

**Table 3: Kinetic parameters of recombinant HRP isoenzyme preparations after 2-step flowthrough purification.** Kinetic data of the purified HRP isoenzyme preparations were recorded for the electron donors ABTS and TMB at a concentration of 1.0 mM H<sub>2</sub>O<sub>2</sub>. In some preparations, no peroxidase activity could be detected. In these cases, no values for V<sub>max</sub> or K<sub>M</sub> are available (n/a).

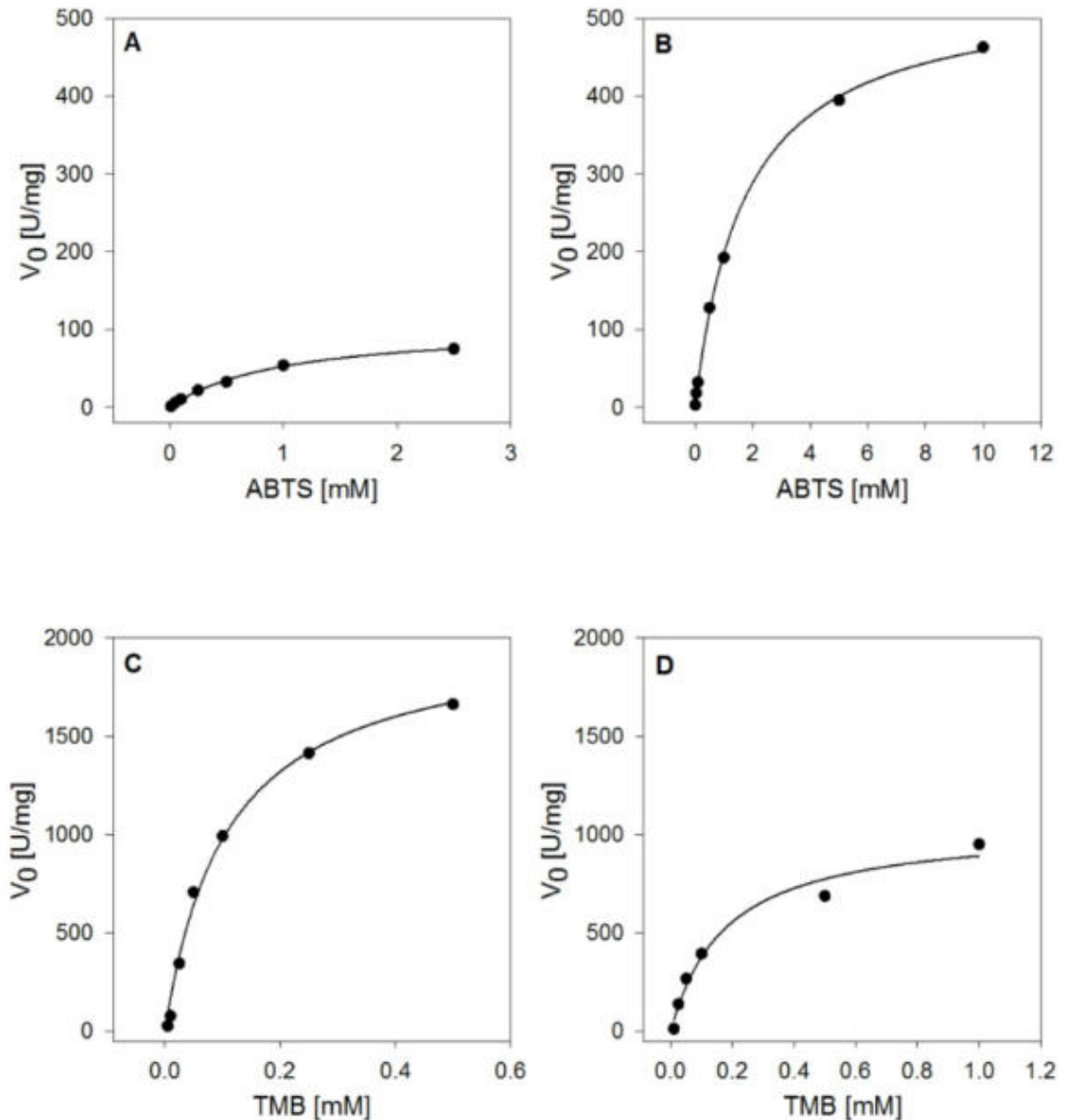
HRP isoenzyme	ABTS		TMB	
	V <sub>max</sub> [U·mg <sup>-1</sup> ]	K <sub>M</sub> [mM]	V <sub>max</sub> [U·mg <sup>-1</sup> ]	K <sub>M</sub> [mM]
C1A	105.54	1.01	2031.50	0.11
25148.1 (C1C)	8.13	4.02	243.14	0.16
25148.2 (C1D)	9.94	3.55	139.77	0.13
04627 (C2)	5.52	4.49	82.34	0.15
C3	0.31	12.5	2.60	0.08
A2A	483.02	1.95	397.99	0.12
A2B	538.40	1.73	1049.11	0.18
E5	33.15	3.51	14.38	0.06
1805	2.95	2.36	39.02	0.11
22684.1	n/a	n/a	n/a	n/a
22684.2	1.08	3.36	11.02	0.07
1350	2.64	2.62	23.62	0.06
5508	42.40	0.46	9.89	0.10
6351	n/a	n/a	n/a	n/a
22489.1	0.17	3.03	n/a	n/a
22489.2	2.42	2.70	1.89	0.16
17517.2	0.11	0.39	0.24	0.32
08562.4	0.05	0.31	0.10	0.20
08562.1	0.10	0.18	0.06	0.11

Interestingly, some HRP isoenzyme preparations did not show any (e.g. 22684.1) or only very low (e.g. 08562.4) catalytic activity with H<sub>2</sub>O<sub>2</sub> and ABTS. Nevertheless, bearing the biochemical diversity of HRP isoenzymes in mind, these isoenzymes might be more active towards other substrates that were not tested in this study.

The oxidation of TMB was catalyzed best by the HRP C1A preparation, followed by HRP A2A and A2B (Table 3). Interestingly, HRP A2A oxidized TMB slower than ABTS, whereas most other isoenzymes - including C1A and A2B - oxidized TMB faster than ABTS (Table 3).

Once more, these kinetic differences demonstrate the diverse substrate affinities and biochemical properties of the individual HRP isoenzymes. Keeping this variance in mind, it is of considerable importance to choose the most suitable isoenzyme for a certain application in the future, e.g. to use a HRP A2B preparation for a diagnostic kit with ABTS as substrate, but a HRP C1A preparation for diagnostics with TMB as substrate, to achieve optimal assay sensitivity.

**Figure 4. Michaelis Menten plots for preparations of recombinant HRP C1A and A2B.** A, HRP C1A with ABTS; B, HRP A2B with ABTS; C, HRP C1A with TMB; D, HRP A2B with TMB. The Michaelis Menten plots for all HRP isoenzyme preparations of this study are shown in Supplementary Figures 1-6.



On that note, the here described efficient purification strategy is a prerequisite for the application of specific HRP isoenzyme preparations. Also, the possibility for the recombinant production of a certain HRP isoenzyme with favourable characteristics for a given application in *P. pastoris* is superior to the currently applied, but unpredictable and irreproducible isolation of a mixture of HRP isoenzymes from horseradish roots.

## 4.5 Thermostability of HRP isoenzyme preparations

The HRP isoenzyme preparations did not only differ in terms of enzymatic activity and substrate specificity, but also in thermal stability (Table 4). The preparations of HRP C1A and HRP 1805 did not show a detectable decrease in catalytic activity after 60 min of incubation at 60 °C, whereas the activity of HRP 22489.2 was already below 20 % of the initial activity after 30 min.

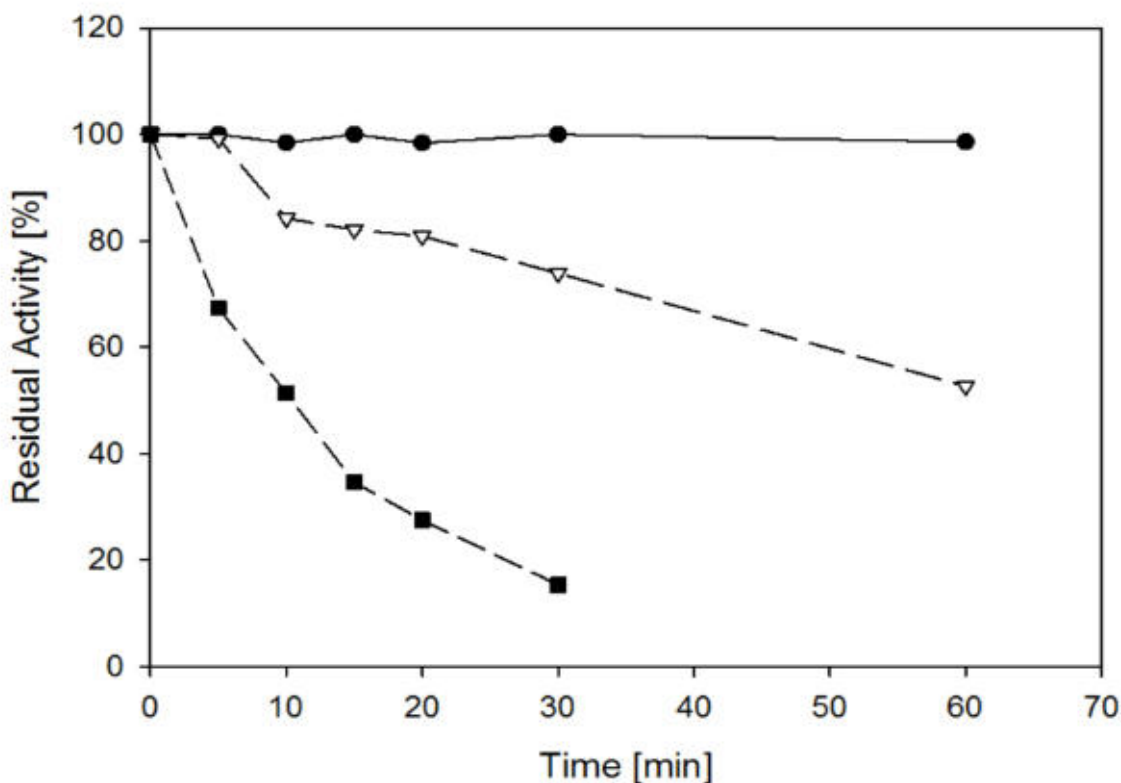


**Figure 5. Thermal stability profiles of selected recombinant HRP preparations.** Filled circles, HRP C1A; open triangles, HRP A2A; filled squares, HRP 22489.2. Residual HRP activity was determined over 60 min of incubation at 60 °C.

A summary of all the calculated thermal half-life times ( $\tau_{1/2}$ ) is given in Table 4. The thermal stability profiles of the stable HRP C1A preparation, the moderately stable HRP A2A and the quite unstable HRP 22489.2 at 60 °C over time are exemplarily shown in Figure 5. As shown in Table 4, the most thermostable HRP preparations of this study were HRP C1A and HRP 1805, which both did not show any detectable loss in catalytic activity at 60 °C after 60 min. HRP A2A and A2B, which are highly interesting in terms of catalytic activity with ABTS and TMB (Table 3), showed a significantly lower thermal stability (Table 4, Figure 5). However, for possible future applications of these isoenzymes in sensitive bioassays, their stability is supposedly

sufficient. In addition, no significant loss of peroxidase activity of these two isoenzymes could be detected over weeks when stored at 4 °C.

**Table 4. Calculated half life times at 60 °C ( $\tau_{1/2}$ ) of recombinant HRP isoenzyme preparations.** Some isoenzymes did not show any detectable loss in HRP activity after 60 min. The thermal stability of recombinant HRP preparations with an initial  $V_{max}$  lower than 0.5 U·mg<sup>-1</sup> for ABTS were not determined (n.d.). Due to a limited amount of purified enzyme, HRP 04627 (C2) and HRP E5 were not included in this study (n.i.).

HRP isoenzyme	$\tau_{1/2}$ [min]
C1A	stable for 60 min
25148.1 (C1C)	159
25148.2 (C1D)	21
04627 (C2)	n.i.
C3	n.d.
A2A	64
A2B	55
E5	n.i.
1805	stable for 60 min
22684.1	n.d.
22684.2	46
1350	62
5508	17
6351	n.d.
22489.1	n.d.
22489.2	11
17517.2	n.d.
08562.4	n.d.
08562.1	n.d.

## 5 Conclusions

In the present study, we recombinantly produced 19 single HRP isoenzymes in *P. pastoris* in shake flask cultivations. We optimized our recently reported 2-step purification approach for recombinant hyperglycosylated HRP replacing the tedious SEC step with an AEC step using a tube monolithic column. After purification, we biochemically characterized the individual HRP isoenzyme preparations with different substrates and evaluated their thermal stability.

The main outcomes of this study can be summarized as:

- The novel 2-step flowthrough purification strategy gave a recovery yield of 55 % and a PF of approximately 77 for the recombinant HRP isoenzyme C1A. Although the recovery yield was lower, the PF was more than 7-fold higher compared to our previous study, where we achieved a recovery yield of 93 % but only a PF of 10. Despite the lower recovery, the here presented strategy is superior, since the second purification step can be run in flowthrough mode, thus allowing both high sample volumes and flow rates.
- Regarding the other isoenzymes especially HRP 04627 (C2), A2A and 5508 could be purified very efficiently with PFs of 62, 684 and 144, respectively. HRP 25148.1 (C1C), 25148.2 (C1D), 04627 (C2), A2B and 1805 were purified 15- to 38-fold.
- The correlation between the amount of potential N-glycosylation sites and the success in flowthrough purification can be used to design an efficient purification strategy for glycosylated proteins expressed in *P. pastoris* in general.
- Basic biochemical characterization using ABTS and TMB revealed significant differences of the individual isoenzyme preparations. The preparations of HRP A2A and HRP A2B turned out to be highly active with H<sub>2</sub>O<sub>2</sub> and ABTS and hence are especially interesting for applications in diagnostic assays with high sensitivity.

The data provided in this study pave the way for cost-effective recombinant production of HRP isoenzymes in *P. pastoris*. Current efforts are made in our lab to provide detailed information on the identification of new HRP isoenzymes from a next generation sequencing of the horseradish transcriptome and to show classifying data on the new HRP isoenzyme sequences (Näätsaari *et al.*, manuscript in preparation). Future in-depth studies will provide information on the molecular mechanisms underlying the differences in activity and stability of the various interesting HRP isoenzymes.

## 6 Acknowledgements

The authors are very grateful to the Austrian Science Fund FWF: project P24861-B19 and FWF: W901 DK Molecular Enzymology for financial support. We further thank the company BIA separations (Slovenia) for providing the monolithic columns and Ms. Astrid Weninger for excellent technical assistance in the lab.

## 7 References

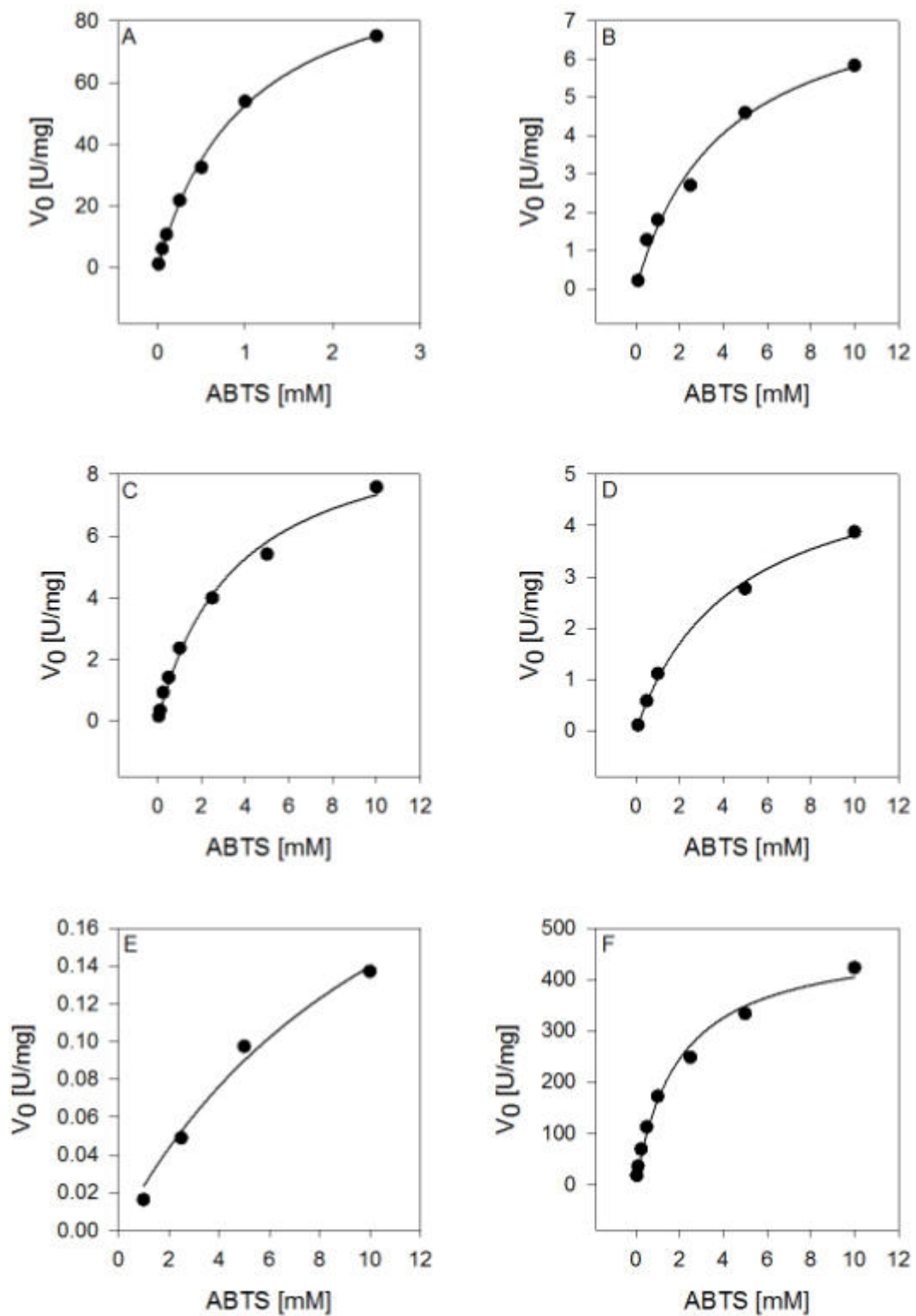
- [1] B. Chance, The kinetics and stoichiometry of the transition from the primary to the secondary peroxidase peroxide complexes., *Arch. Biochem. Biophys.* 41 (1952) 416–24.
- [2] P. George, Chemical nature of the secondary hydrogen peroxide compound formed by cytochrome-c peroxidase and horseradish peroxidase., *Nature.* 169 (1952) 612–3.
- [3] P. George, The chemical nature of the second hydrogen peroxide compound formed by cytochrome c peroxidase and horseradish peroxidase. I. Titration with reducing agents., *Biochem. J.* 54 (1953) 267–76.
- [4] L.A. Planche, Note sur la sophistication de la résine de jalap et sur les moyens de la reconnaître, *Bull. Pharm.* 2 (1810) 578–580.
- [5] J.F. Kratochvil, R.H. Burris, M.K. Seikel, J.M. Harkin, Isolation and characterization of  $\alpha$ -guaiaconic acid and the nature of guaiacum blue, *Phytochemistry.* 10 (1971) 2529–2531.
- [6] A.J. Gross, I.W. Sizer, The oxidation of tyramine, tyrosine, and related compounds by peroxidase., *J. Biol. Chem.* 234 (1959) 1611–4.
- [7] F. Passardi, C. Penel, C. Dunand, Performing the paradoxical: how plant peroxidases modify the cell wall., *Trends Plant Sci.* 9 (2004) 534–40.
- [8] F. Passardi, C. Cosio, C. Penel, C. Dunand, Peroxidases have more functions than a Swiss army knife., *Plant Cell Rep.* 24 (2005) 255–65.
- [9] M.C. Hoyle, High resolution of peroxidase-indoleacetic acid oxidase isoenzymes from horseradish by isoelectric focusing, *Plant Physiol.* 60 (1977) 787–93.
- [10] M.A. Jermyn, Horseradish peroxidase., *Nature.* 169 (1952) 488–9.
- [11] M.A. Jermyn, R. Thomas, Multiple components in horseradish peroxidase, *Biochem. J.* 56 (1954) 631–9.
- [12] L.M. Shannon, E. Kay, J.Y. Lew, Peroxidase isozymes from horseradish roots. I. Isolation and physical properties., *J. Biol. Chem.* 241 (1966) 2166–72.
- [13] E. Kay, L.M. Shannon, J.Y. Lew, Peroxidase isozymes from horseradish roots. II. Catalytic properties., *J. Biol. Chem.* 242 (1967) 2470–3.
- [14] S. Marklund, P.I. Ohlsson, A. Opara, K.G. Paul, The substrate profiles of the acidic and slightly basic horseradish peroxidases., *Biochim. Biophys. Acta.* 350 (1974) 304–13.
- [15] S. Aibara, T. Kobayashi, Y. Morita, Isolation and properties of basic isoenzymes of horseradish peroxidase., *J. Biochem.* 90 (1981) 489–96.

- [16] S. Aibara, H. Yamashita, E. Mori, M. Kato, Y. Morita, Isolation and characterization of five neutral isoenzymes of horseradish peroxidase., *J. Biochem.* 92 (1982) 531–9.
- [17] K. Fujiyama, H. Takemura, S. Shibayama, K. Kobayashi, J.K. Choi, A. Shinmyo, et al., Structure of the horseradish peroxidase isozyme C genes., *Eur. J. Biochem.* 173 (1988) 681–7.
- [18] M. Gajhede, D.J. Schuller, A. Henriksen, A.T. Smith, T.L. Poulos, Crystal structure of horseradish peroxidase C at 2.15 Å resolution., *Nat. Struct. Biol.* 4 (1997) 1032–8.
- [19] K.G. Welinder, Amino acid sequence studies of horseradish peroxidase. Amino and carboxyl termini, cyanogen bromide and tryptic fragments, the complete sequence, and some structural characteristics of horseradish peroxidase C., *Eur. J. Biochem.* 96 (1979) 483–502.
- [20] B.Y. Yang, J.S. Gray, R. Montgomery, The glycans of horseradish peroxidase., *Carbohydr. Res.* 287 (1996) 203–12.
- [21] J.W. Tams, K.G. Welinder, Mild chemical deglycosylation of horseradish peroxidase yields a fully active, homogeneous enzyme., *Anal. Biochem.* 228 (1995) 48–55.
- [22] J.W. Tams, K.G. Welinder, Glycosylation and thermodynamic versus kinetic stability of horseradish peroxidase., *FEBS Lett.* 421 (1998) 234–6.
- [23] C.B. Lavery, M.C. Macinnis, M.J. Macdonald, J.B. Williams, C.A. Spencer, A.A. Burke, et al., Purification of peroxidase from Horseradish (*Armoracia rusticana*) roots., *J. Agric. Food Chem.* 58 (2010) 8471–6.
- [24] A.T. Smith, N. Santama, S. Dacey, M. Edwards, R.C. Bray, R.N. Thorneley, et al., Expression of a synthetic gene for horseradish peroxidase C in *Escherichia coli* and folding and activation of the recombinant enzyme with Ca<sup>2+</sup> and heme., *J. Biol. Chem.* 265 (1990) 13335–43.
- [25] V. Grigorenko, T. Chubar, Y. Kapeliuch, T. Borchers, F. Spener, A. Egorov, New approaches for functional expression of recombinant horseradish peroxidase C in *Escherichia coli*, *Biocatal. Biotransformation.* 17 (1999) 359–379.
- [26] C. Hartmann, P.R. Ortiz de Montellano, Baculovirus expression and characterization of catalytically active horseradish peroxidase., *Arch. Biochem. Biophys.* 297 (1992) 61–72.
- [27] M. de las M. Segura, G. Levin, M. V Miranda, F.M. Mendive, H.M. Targovnik, O. Cascone, High-level expression and purification of recombinant horseradish peroxidase isozyme C in SF-9 insect cell culture, *Process Biochem.* 40 (2005) 795–800.
- [28] A. Vlamis-Gardikas, A.T. Smith, J.M. Clements, J.F. Burke, Expression of active horseradish peroxidase in *Saccharomyces cerevisiae*., *Biochem. Soc. Trans.* 20 (1992) 111S.
- [29] B. Morawski, Z. Lin, P. Cirino, H. Joo, G. Bandara, F.H. Arnold, Functional expression of horseradish peroxidase in *Saccharomyces cerevisiae* and *Pichia pastoris*., *Protein Eng.* 13 (2000) 377–84.
- [30] B. Morawski, S. Quan, F.H. Arnold, Functional expression and stabilization of horseradish peroxidase by directed evolution in *Saccharomyces cerevisiae*., *Biotechnol. Bioeng.* 76 (2001) 99–107.

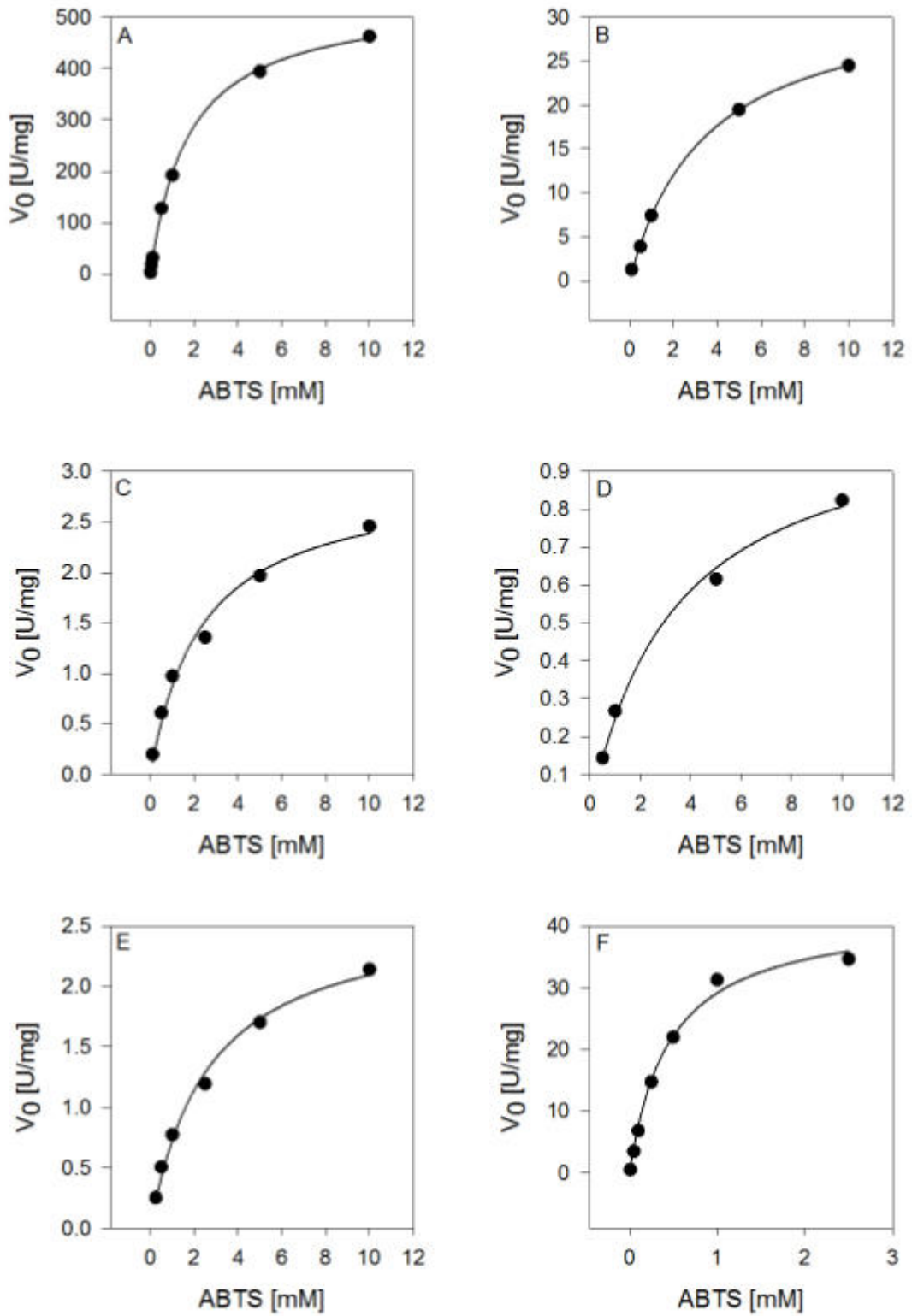
- [31] F.W. Krainer, C. Dietzsch, T. Hajek, C. Herwig, O. Spadiut, A. Glieder, Recombinant protein expression in *Pichia pastoris* strains with an engineered methanol utilization pathway., *Microb. Cell Fact.* 11 (2012) 22–35.
- [32] C. Dietzsch, O. Spadiut, C. Herwig, A dynamic method based on the specific substrate uptake rate to set up a feeding strategy for *Pichia pastoris*., *Microb. Cell Fact.* 10 (2011) 14–22.
- [33] O. Spadiut, L. Rossetti, C. Dietzsch, C. Herwig, Purification of a recombinant plant peroxidase produced in *Pichia pastoris* by a simple 2-step strategy., *Protein Expr. Purif.* 86 (2012) 89–97.
- [34] M.G. Brattain, M.E. Marks, T.G. Pretlow, The purification of horseradish peroxidase by affinity chromatography on Sepharose-bound concanavalin A1,2., *Anal. Biochem.* 72 (1976) 346–52.
- [35] M. V. Miranda, H.M. Fernández-Lahore, J. Dobrecky, O. Cascone, The extractive purification of peroxidase from plant raw materials in aqueous two-phase systems, *Acta Biotechnol.* 18 (1998) 179–188.
- [36] W. Guo, E. Ruckenstein, Separation and purification of horseradish peroxidase by membrane affinity chromatography, *J. Memb. Sci.* 211 (2003) 101–111.
- [37] L.F. Fraguas, F. Batista-Viera, J. Carlsson, Preparation of high-density Concanavalin A adsorbent and its use for rapid, high-yield purification of peroxidase from horseradish roots., *J. Chromatogr. B. Analyt. Technol. Biomed. Life Sci.* 803 (2004) 237–41.
- [38] A. Glieder, F.W. Krainer, M. Kulterer, L. Näätsaari, V. Reichel, Horseradish peroxidase isoenzymes, *Pat. No.* 11185833.8-2403.
- [39] S.K. Sharma, N. Sehgal, A. Kumar, A quick and simple biostrip technique for detection of lactose, *Biotechnol. Lett.* 24 (2002) 1737–1739.
- [40] C.C. Chiou, P.Y. Chang, E.C. Chan, T.L. Wu, K.C. Tsao, J.T. Wu, Urinary 8-hydroxydeoxyguanosine and its analogs as DNA marker of oxidative stress: development of an ELISA and measurement in both bladder and prostate cancers., *Clin. Chim. Acta.* 334 (2003) 87–94.
- [41] A. Singh, D. Ma, D.L. Kaplan, Enzyme-mediated free radical polymerization of styrene., *Biomacromolecules.* 1 (2000) 592–6.
- [42] N. Vasileva, T. Godjevargova, D. Ivanova, K. Gabrovska, Application of immobilized horseradish peroxidase onto modified acrylonitrile copolymer membrane in removing of phenol from water., *Int. J. Biol. Macromol.* 44 (2009) 190–4.
- [43] O. Greco, S. Rossiter, C. Kanthou, L.K. Folkes, P. Wardman, G.M. Tozer, et al., Horseradish peroxidase-mediated gene therapy: choice of prodrugs in oxic and anoxic tumor conditions., *Mol. Cancer Ther.* 1 (2001) 151–60.
- [44] L. Näätsaari, B. Mistlberger, C. Ruth, T. Hajek, F.S. Hartner, A. Glieder, Deletion of the *Pichia pastoris* KU70 Homologue Facilitates Platform Strain Generation for Gene Expression and Synthetic Biology., *PLoS One.* 7 (2012) e39720.
- [45] R. Weis, R. Luiten, W. Skranc, H. Schwab, M. Wubbolts, A. Glieder, Reliable high-throughput screening with *Pichia pastoris* by limiting yeast cell death phenomena., *FEMS Yeast Res.* 5 (2004) 179–89.
- [46] O. Spadiut, C. Leitner, C. Salaheddin, B. Varga, B.G. Vertessy, T.-C. Tan, et al., Improving thermostability and catalytic activity of pyranose 2-oxidase

- from *Trametes multicolor* by rational and semi-rational design., *FEBS J.* 276 (2009) 776–792.
- [47] D. Mattanovich, A. Graf, J. Stadlmann, M. Dragosits, A. Redl, M. Maurer, et al., Genome, secretome and glucose transport highlight unique features of the protein production host *Pichia pastoris*., *Microb. Cell Fact.* 8 (2009) 29.
- [48] C.-J. Huang, L.M. Damasceno, K.A. Anderson, S. Zhang, L.J. Old, C.A. Batt, A proteomic analysis of the *Pichia pastoris* secretome in methanol-induced cultures., *Appl. Microbiol. Biotechnol.* 90 (2011) 235–47.
- [49] H. Podgornik, A. Podgornik, A. Perdih, A method of fast separation of lignin peroxidases using convective interaction media disks., *Anal. Biochem.* 272 (1999) 43–7.
- [50] H. Podgornik, A. Podgornik, P. Milavec, A. Perdih, The effect of agitation and nitrogen concentration on lignin peroxidase (LiP) isoform composition during fermentation of *Phanerochaete chrysosporium*., *J. Biotechnol.* 88 (2001) 173–6.
- [51] H. Podgornik, A. Podgornik, Separation of manganese peroxidase isoenzymes on strong anion-exchange monolithic column using pH-salt gradient., *J. Chromatogr. B. Analyt. Technol. Biomed. Life Sci.* 799 (2004) 343–7.
- [52] M. Barut, A. Podgornik, P. Brne, A. Strancar, Convective interaction media short monolithic columns: enabling chromatographic supports for the separation and purification of large biomolecules., *J. Sep. Sci.* 28 (2005) 1876–92.
- [53] A.N. Hiner, J. Hernández-Ruíz, M.B. Arnao, F. García-Cánovas, M. Acosta, A comparative study of the purity, enzyme activity, and inactivation by hydrogen peroxide of commercially available horseradish peroxidase isoenzymes A and C., *Biotechnol. Bioeng.* 50 (1996) 655–62.
- [54] D.J. Gilfoyle, J.N. Rodriguez-Lopez, A.T. Smith, Probing the aromatic-donor-binding site of horseradish peroxidase using site-directed mutagenesis and the suicide substrate phenylhydrazine., *Eur. J. Biochem.* 236 (1996) 714–22.
- [55] B. Bjellqvist, G.J. Hughes, C. Pasquali, N. Paquet, F. Ravier, J.C. Sanchez, et al., The focusing positions of polypeptides in immobilized pH gradients can be predicted from their amino acid sequences., *Electrophoresis.* 14 (1993) 1023–31.
- [56] B. Bjellqvist, B. Basse, E. Olsen, J.E. Celis, Reference points for comparisons of two-dimensional maps of proteins from different human cell types defined in a pH scale where isoelectric points correlate with polypeptide compositions., *Electrophoresis.* 15 (1994) 529–39.
- [57] R. Gupta, E. Jung, S. Brunak, Prediction of N-glycosylation sites in human proteins, In prepara (2004).

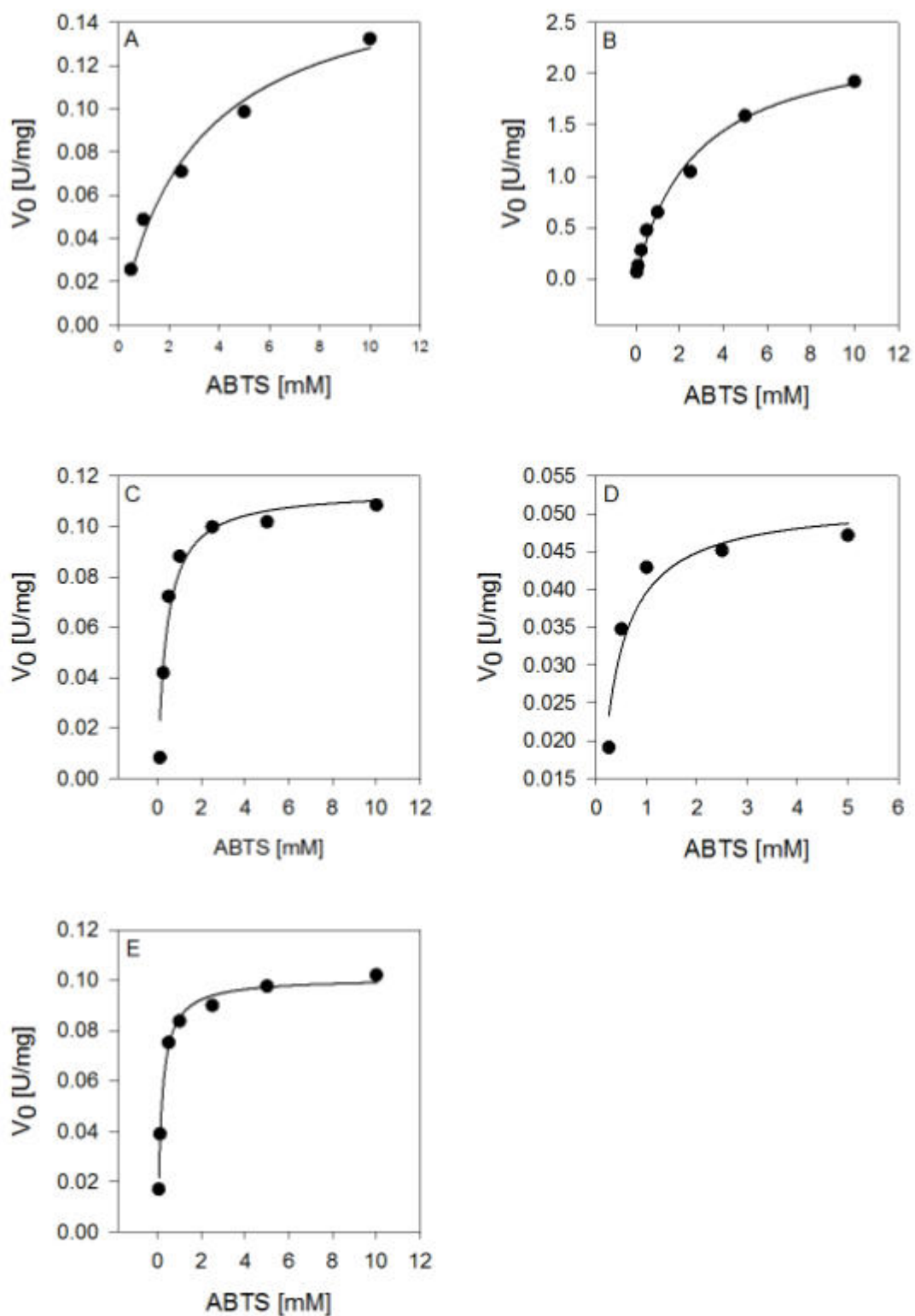
## 8 Supplementary Figures



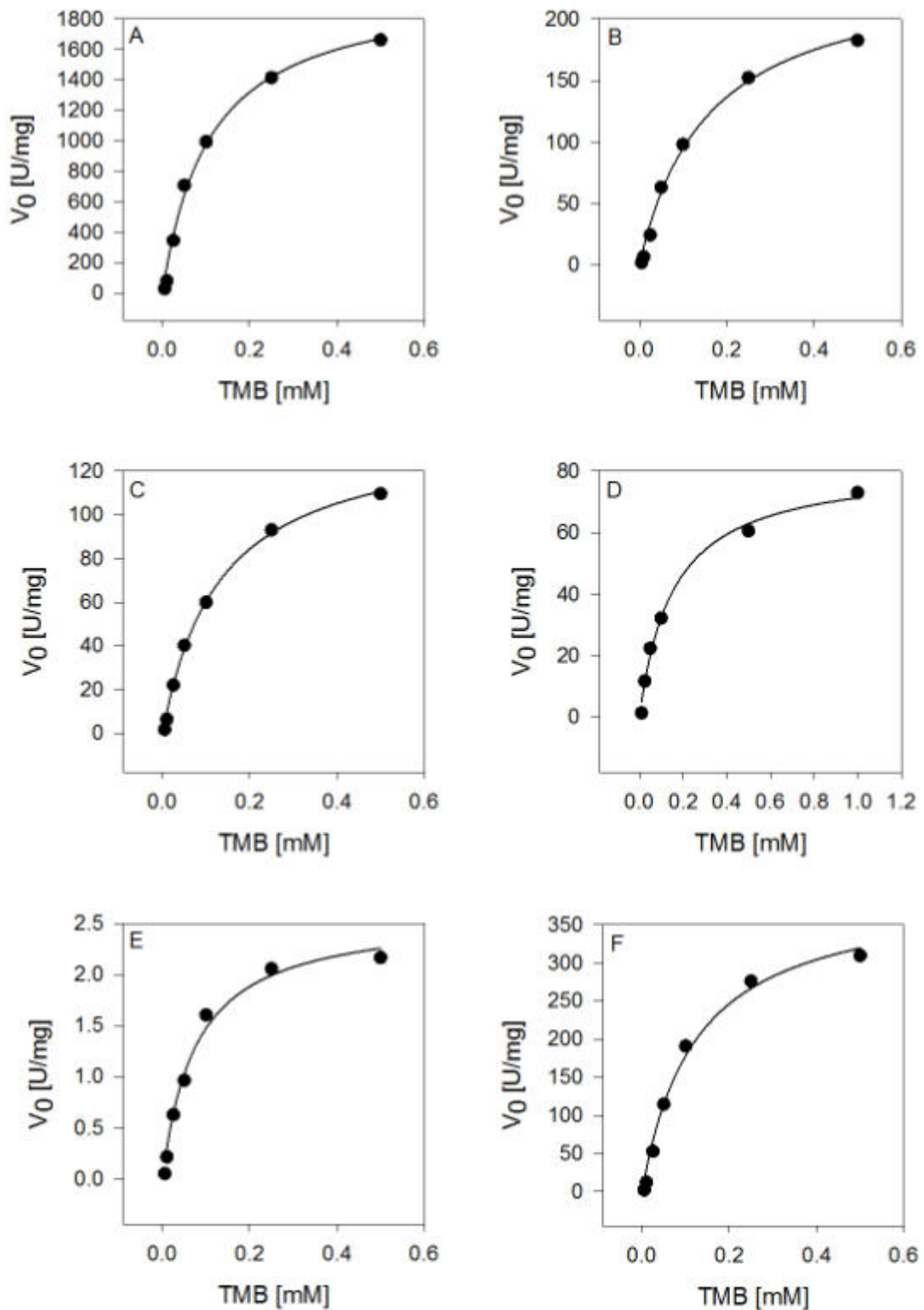
**Supplementary Figure 1. Michaelis Menten plots of different HRP isoenzymes and ABTS as electron donor. A, C1A; B, 25148.1 (C1C); C, 25148.2 (C1D); D, 04627 (C2); E, C3; F, A2A.**



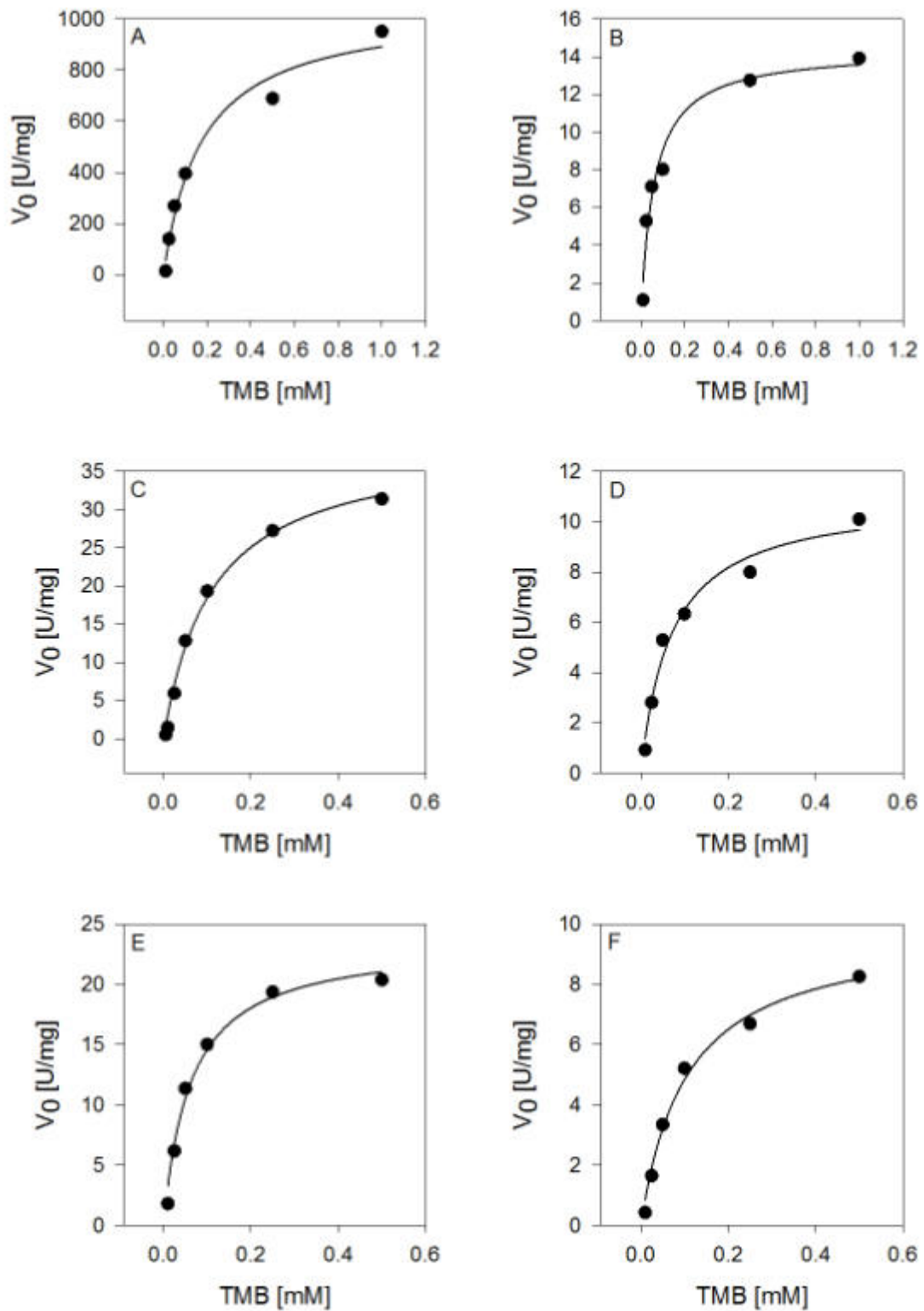
**Supplementary Figure 2. Michaelis Menten plots of different HRP isoenzymes and ABTS as electron donor. A, A2B; B, E5; C, 1805; D, 22684.2; E, 1350; F, 5508.**



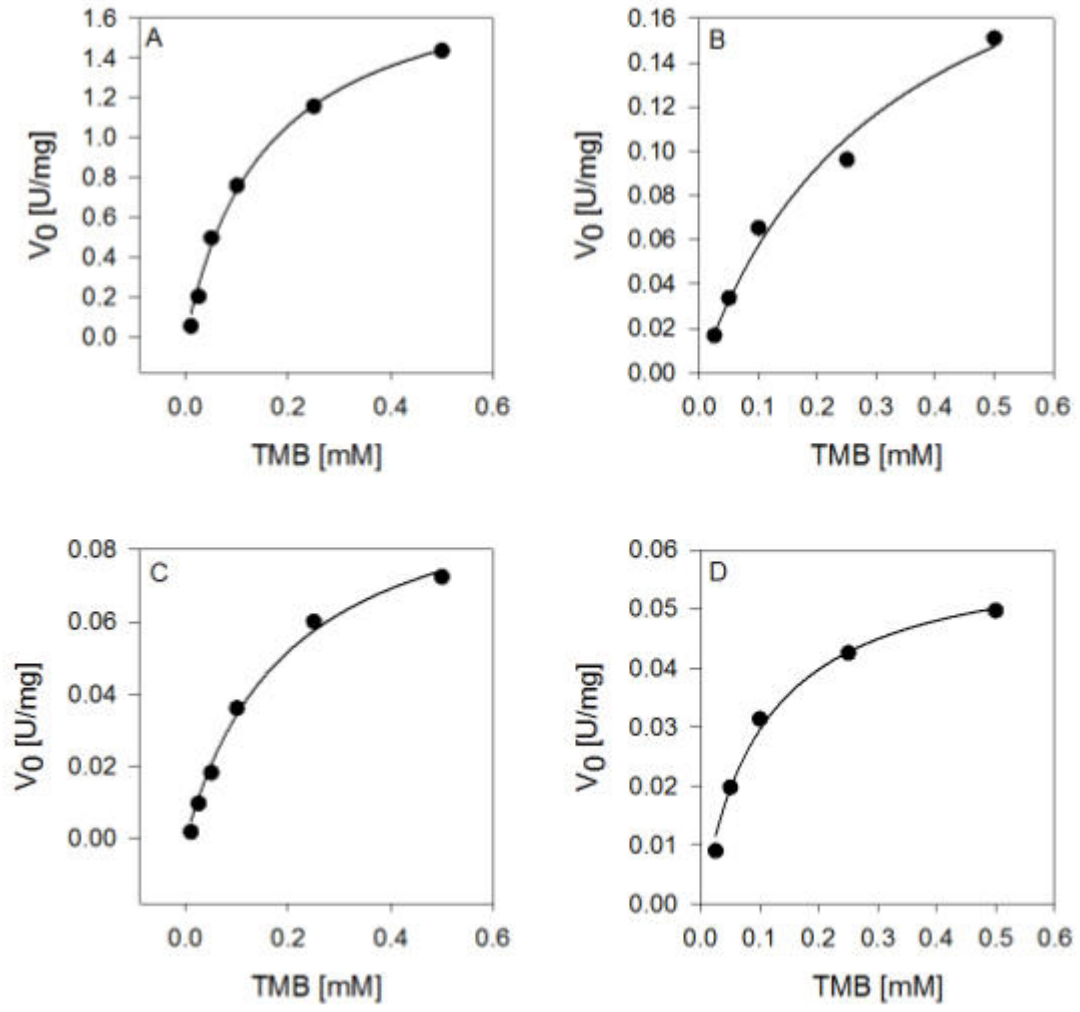
**Supplementary Figure 3. Michaelis Menten plots of different HRP isoenzymes and ABTS as electron donor. A, 22489.1; B, 22489.2; C, 17517.2; D, 08562.4.; E; 08562.1.**



**Supplementary Figure 4. Michaelis Menten plots of different HRP isoenzymes and TMB as electron donor. A, C1A; B, 25148.1 (C1C); C, 25148.2 (C1D); D, 04627 (C2); E, C3; F, A2A.**



Supplementary Figure 5. Michaelis Menten plots of different HRP isoenzymes and TMB as electron donor. A, A2B; B, E5; C, 1805; D, 22684.2; E, 1350; F, 5508.



**Supplementary Figure 6. Michaelis Menten plots of different HRP isoenzymes and TMB as electron donor. A, 22489.1; B, 17517.2; C, 08562.4.; D, 08562.1.**

## **CHAPTER II:**

**Can glycoengineering help in tailoring HRP for  
medical applications, especially in terms of reducing  
hyperglycosylation?**

# **Glyco-variant library of the versatile enzyme horseradish peroxidase**

## **Running title: Glyco-variant library of horseradish peroxidase**

Published in the journal Glycobiology Volume 24, May 2014

DOI: 10.1093/glycob/cwu047

Simona Capone<sup>1</sup>, **Robert Pletzenauer**<sup>1</sup>, Daniel Maresch<sup>2</sup>, Karl Metzger<sup>1</sup>, Friedrich Altmann<sup>2</sup>, Christoph Herwig<sup>1</sup> and Oliver Spadiut<sup>1\*</sup>

<sup>1</sup> Vienna University of Technology, Institute of Chemical Engineering, Research Area Biochemical Engineering, 1060 Vienna, Austria

<sup>2</sup> Department of Chemistry, University of Natural Resources and Life Sciences, 1190 Vienna Austria

\*Correspondence should be addressed to:

Oliver Spadiut, Vienna University of Technology, Institute of Chemical Engineering, Research Area Biochemical Engineering, Gumpendorfer Strasse 1a, A-1060 Vienna, Austria. Tel: +43 1 58801 166473, Fax: +43 1 58801 166980, email: oliver.spadiut@tuwien.ac.at

### **Keywords:**

bioprocess technology / glyco-engineering / glycosylation / horseradish peroxidase / *Pichia pastoris*

## 1 Abstract

When the glycosylated plant enzyme horseradish peroxidase (HRP) is conjugated to specific antibodies, it presents a powerful tool for medical applications. The isolation and purification of this enzyme from plant is difficult and only gives low yields. However, HRP recombinantly produced in the yeast *Pichia pastoris* experiences hyperglycosylation which impedes the use of this enzyme in medicine. Enzymatic and chemical deglycosylation are cost intensive and cumbersome and hitherto existing *P. pastoris* strain engineering approaches with the goal to avoid hyperglycosylation only resulted in physiologically impaired yeast strains not useful for protein production processes. Thus, the last resort to obtain less glycosylated recombinant HRP from *P. pastoris* is to engineer the enzyme itself.

In the present study we mutated all the 8 N-glycosylation sites of HRP C1A. After determination of the most suitable mutation at each N-glycosylation site, we physiologically characterized the respective *P. pastoris* strains in the bioreactor and purified the produced HRP C1A glyco-variants. The biochemical characterization of the enzyme variants revealed great differences in catalytic activity and stability and allowed the combination of the most promising mutations to potentially give an unglycosylated, active HRP C1A variant useful for medical applications. Interestingly, site directed mutagenesis proved to be a valuable strategy not only to reduce the overall glycan content of the recombinant enzyme, but also to improve catalytic activity and stability. In the present study, we performed an integrated bioprocess covering strain generation, bioreactor cultivations, downstream processing and product characterization and present the biochemical data of the HRP glyco-library.

## 2 Introduction

The heme-containing plant enzyme horseradish peroxidase (HRP; EC 1.11.1.7) is a Class-III peroxidase catalysing the oxidation of various substrates (e.g. amines, aromatic phenols, indoles, phenolic acids, sulfonates) using H<sub>2</sub>O<sub>2</sub> as oxidant. Horseradish peroxidase exists in at least 19 different isoenzyme forms in the horseradish root (*Armoracia rusticana*), of which isoenzyme C1A is the most

abundant and thus the most studied one (e.g. [1-6]). It is a 34 kDa monomeric oxidoreductase containing a heme-group as well as 2 Ca<sup>2+</sup>-ions as prosthetic groups. The crystal structure of HRP C1A led to the identification of 9 N-glycosylation sites of the Asn–X–Ser/Thr type, where X can be any amino acid but proline, of which 8 are occupied when the enzyme is expressed in plant [7], which is why the molecular mass of HRP C1A increases from 34 kDa to around 44 kDa [2, 5]. Due to glycosylation and the presence of both, the heme-group and disulfide bridges, the recombinant production and subsequent preparative purification of HRP has proven to be very difficult [7-10], which is why HRP is still mainly isolated from plant [10]. However, HRP preparations from plant describe a mixture of isoenzymes, which seasonally varies in composition and concentration, and yields are extremely low [11-13]. Since HRP is a versatile enzyme used in numerous, quite diverse industrial and medical applications, like waste water treatment, fine chemical synthesis, immunoassays, biosensors and coupled enzyme assays (e.g. [14]), the controllable recombinant production and subsequent efficient purification of single HRP isoenzymes is highly desired. Thus, we have not only investigated and improved the recombinant production of the isoenzyme HRP C1A with *Pichia pastoris* in the past few years [15-19], but also developed an efficient downstream process for the hypermannosylated enzyme recombinantly derived from this yeast [6, 9]. However, for medical applications where HRP is conjugated to antibodies, like antibody-directed enzyme-prodrug therapy [20, 21] and medical diagnostics [22-25], the degree of glycosylation of HRP is of utmost importance, since not only the stability of the enzyme, but also the conjugation with antibodies is expected to change with varying glycosylation. Besides, the untrimmed yeast-derived high-mannose containing glycosylation can trigger immune responses in humans (personal communication with Dr. Lisa Folkes; Gray Institute for Radiation Oncology and Biology, Department of Oncology, University of Oxford).

Obviously, the availability of an enzyme without or at least with reduced surface glycosylation would solve abovementioned problems. However, the biological role and importance of glycans for plant peroxidases is still not completely understood and is topic of numerous studies in glycobiology. So far, some studies report stabilizing effects of the glycans [26, 27], whereas other studies do not show such effects [28, 29]. In 1990, Smith *et al.* were able to produce active and correctly folded

HRP without any glycans in *Escherichia coli* [7]. In a following study, Tams and Welinder analysed the importance of the glycosylation for HRP in more detail [30]. They showed that the removal of most of the glycans, except the N-Acetylglucosamine (GlcNAc) residues, by a mild chemical deglycosylation with trifluoromethanesulfonic acid (TFMS) resulted in a fully active, but less stable enzyme [30, 31]. Both studies showed that glycans on the surface of HRP affect the physico-chemical properties of the enzyme, but are not required for catalytic activity. However, chemical deglycosylation only left 60 % of HRP active and also describes a quite cumbersome procedure [30, 31], which is why it is not a useful method to obtain unglycosylated HRP. Although recombinant proteins from *P. pastoris* can also be deglycosylated enzymatically [32, 33], also this option has to be reconsidered, since 1) enzymatic deglycosylation is only quantitative when the target protein is denatured and 2) the additional endo-glycosidases have to be removed again to obtain pure product. Another way to control and reduce the complexity of native yeast-like glycosylation on glycoproteins secreted from *P. pastoris* is through glycoengineering [34-37]. A key event in such engineering is the knock-out of the OCH1 gene, which initiates outer-chain elongation, leading to hypermannosylation. However, in a previous study, where we knocked-out this gene, we observed that HRP with reduced glycan complexity possessed hampered downstream processing and that the glycoengineered *P. pastoris* strains generated were physiologically impaired, impeding efficient production processes [38]. Consequently, the last resort to efficiently produce HRP with a reduced amount of surface glycosylation is to glyco-engineer the enzyme itself. In a recent study, two selected Asn residues of HRP were mutated to Asp to analyse effects on the stability of the enzyme and to produce more properly folded HRP in *E. coli* [39]. Asad *et al.* showed that introducing the mutations Asn13Asp and Asn268Asp did not just affect the production of HRP in *E. coli*, but also increased the catalytic constants as well as the thermal stability [39]. These results did not only underline the possibility of obtaining active and correctly folded HRP with reduced glycosylation, but also showed that mutating the glycosylation sites may even have beneficial effects on catalytic activity and stability.

In the present study we generated a glyco-variant library of HRP C1A exchanging all the eight Asn serving as glycosylation sites by the structurally similar amino acids

Asp, Gln or Ser. We did not only investigate the effects of the single mutations on enzyme activity and stability, but also on protein purification following an integrated bioprocess technology approach. After determining the most suitable mutation at the single N-glycosylation sites, we physiologically characterized the respective *P. pastoris* strains in the controlled environment of a bioreactor. A 2-step purification procedure, where both chromatography steps were performed in the flow-through mode, enabled us to recover purified HRP glyco-variants for subsequent biochemical characterization. Based thereon, we combined the most suitable mutations to potentially obtain an unglycosylated, active HRP variant suitable for medical applications. Summarizing, we conducted an integrated bioprocess study and present the bioprocess technological and biochemical results for the HRP C1A glyco-variant library.

### **3 Results and Discussion**

#### **3.1 Screening procedure**

Every transformation into *P. pastoris* CBS7435 Mut<sup>S</sup> yielded several dozens of transformants. We randomly picked 5 transformants per mutation and screened them for cell growth and production of active HRP in shake flasks. With only few exceptions all the picked transformants produced active HRP, however on average only 3 out of 5 showed comparable growth and productivity. PCR analysis confirmed the presence of the target gene in the genome of *P. pastoris*. Although we did not analyse the exact number of gene integration events by real-time polymerase chain reaction (qPCR), we assumed the integration of a comparable amount of gene copies into the yeast genome due to the fact that we always transformed the same amount of linearized vector DNA into the *P. pastoris* cells (i.e. 2 µg DNA). We had observed such a correlation in a previous study [17]. Although we did not check for the exact integration site of the target gene in the host genome, we ascribe the observed differences in protein production during the screening procedure to a fair amount of non-homologous recombination of the transformed HRP C1A gene into the genome of *P. pastoris* [40], most likely at different loci in the chromosome, which consequently influences the accessibility of the transcription machinery to the

transformed gene [17]. In Table 1 we compared the growth of the best transformant per mutation as well as the specific activity and thermal stability of the produced HRP C1A glyco-variants. Although diagnostic applications are normally not performed at 60°C, we determined the stability of HRP at this temperature since we observed nice differences for the glyco-variants at this temperature and the assay could be easily performed in the laboratory. Furthermore, we used the thermal stability as a measure for kinetic stability, as also discussed elsewhere [41, 42]. We always included a *P. pastoris* strain expressing the unmutated wildtype HRPC1A in the screening experiments as control. Although we obtained slightly different results for the wildtype depending on the screening round, we included the average values for growth, protein production, enzyme activity and thermal stability in Table 1 for comparison.

**Table 1:** Results of screening experiments to identify the most suitable mutation at the single N-glycosylation sites of HRP C1A.

Results after 96 h of induction						
Mutation	OD <sub>600</sub>	Cat. activity [U·mL <sup>-1</sup> ]	Protein content [mg mL <sup>-1</sup> ]	Spec. activity [U·mg <sup>-1</sup> ]	Residual activity after 4 hours at 60°C [%]	Chosen mutation
wt	25.2	7.5	0.13	48.4	75.0	
N13D	31.8	0.69	0.09	7.29	27.0	
N13Q	42.3	0.74	0.08	9.10	10.5	→ N13D
N13S	35.1	-	-	-	-	
N57D	31.4	0.77	0.11	7.00	53	
N57Q	23.4	2.48	0.13	19.1	43	→ N57S
N57S	30.3	7.20	0.13	55.4	74	
N158D	32.7	6.11	0.23	26.6	100	
N158Q	34.1	0.49	0.37	1.32	81.8	→ N158D
N158S	30.0	0.87	0.13	6.23	90.8	
N186D	36.8	0.10	0.09	1.06	43.1	
N186Q	47.6	0.07	0.10	0.70	0	→ N186D
N186S	46.2	0.14	0.09	1.60	36.2	
N198D	21.3	12.1	0.23	53.1	68.1	
N198Q	19.7	4.31	0.22	20.1	34.1	→ N198D
N198S	25.1	1.25	0.22	5.84	20.5	
N214D	17.9	5.03	0.11	46.6	46.1	
N214Q	18.1	4.92	0.13	39.0	41.5	→ N214S
N214S	14.2	3.17	0.12	25.6	96.0	
N255D	13.6	7.24	0.13	53.9	66.5	
N255Q	14.2	8.59	0.18	48.3	78.8	→ N255D
N255S	11.9	5.49	0.15	35.9	74.9	
N268D	13.6	0.56	0.27	2.07	70.6	
N268Q	12.9	0.40	0.26	1.54	71.0	→ N268D
N268S	12.6	0.43	0.32	1.34	54.0	

Based on the determined specific activity and thermal stability, we chose the most suitable mutation at the single N-glycosylation sites. Except for N13S all the produced HRP glyco-variants showed catalytic activity, however replacement of Asn by Gln never turned out to be the most suitable mutation at any of the 8 N-glycosylation sites. Since we did not measure any detectable extracellular protein content for N13S either, we speculate that this mutation caused problems in protein folding and/or secretion, a phenomenon described before [43-46]. Interestingly, we observed significant differences in enzyme activity and stability depending on the introduced mutation (Table 1), and identified 3 mutations which had been described before, namely at positions N13 and N268 [39] and N255 [47], respectively.

### 3.2 Physiological strain characterization in the bioreactor

The different *P. pastoris* strains carrying the respective mutated HRP gene were physiologically characterized in single dynamic batch cultivations in the controlled environment of a bioreactor. After exhaustion of glycerol which was indicated by an increase in the off-gas signal, a 0.5 % (v/v) methanol adaptation pulse was applied which was followed by several, subsequent 1.0 % (v/v) methanol pulses (an example for this procedure is illustrated for the *P. pastoris* strains expressing the wildtype enzyme and variant N57S in Figure 1, while illustrations for the other strains are shown in Supplementary Figure 1).

This dynamic strategy has repeatedly proven to be a very efficient method to physiologically characterize *P. pastoris* strains in a fast and simple manner [15-18]. In Table 2 the determined strain characteristic parameters of all the strains are summarized. Apparently, the introduction of the respective recombinant HRP C1A gene had an impact on the physiology of the *P. pastoris* strains. Although the majority of the strains showed similar maximum specific growth rates on glycerol ( $\mu_{\max \text{ gly}}$ ) between 0.24 – 0.28 h<sup>-1</sup>, the strain carrying the gene HRP C1A N13D showed a nearly 1.3-fold higher  $\mu_{\max \text{ gly}}$ . This effect was even more pronounced with respect to the specific methanol uptake rate during the adaptation pulse ( $q_{\text{s adapt}}$ ). Surprisingly, when we calculated the average specific methanol uptake rate during the consecutive 1 % (v/v) methanol pulses ( $q_{\text{s average MeOH}}$ ), we observed striking differences between all the strains.

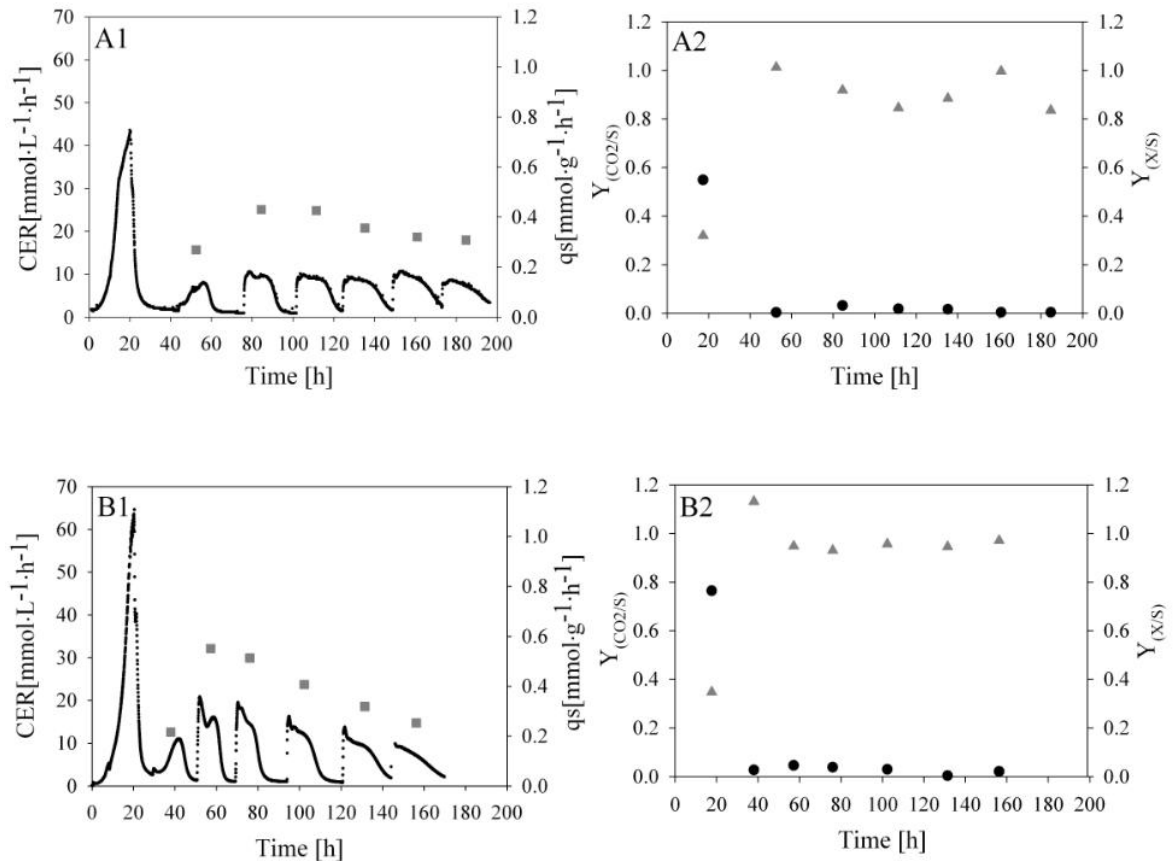


**Figure 1:** Batch cultivation of a *P. pastoris* CBS7435 Mut<sup>S</sup> strain carrying either the unmutated HRP C1A gene (designated as “wt”) or the glyco-variant HRP C1A N57S. A1, batch cultivation with methanol pulses of wt; B1, batch cultivation with methanol pulses of N57S. Solid black line, carbon dioxide evolution rate (CER); grey square, specific substrate uptake rate ( $q_s$ ). A2, calculated yields of wt; B2, calculated yields of N57S. Grey triangle, carbon dioxide yield ( $Y_{\text{CO}_2/\text{S}}$ ); black dot, biomass yield ( $Y_{\text{X/S}}$ ).

One can speculate that the reason for the altered strain physiology lies in the produced HRP glyco-variant itself, since it is known that N-glycosylation can influence protein folding and protein production and thus might affect cell physiology [43-46]. However, as shown in Table 2 the amount of total extracellular protein for each strain at the end of the dynamic batch cultivation was basically the same indicating that the single mutations did not cause significant problems in protein folding or secretion. We also analysed the cell-free cultivation broths on SDS gels and obtained the same pattern of protein bands at comparable intensity (graphs not shown). Thus, apparently not the mutated product but rather the locus of the respective introduced gene in the yeast genome had a significant influence on the methanol metabolism of the cells.

**Table 2:** Strain characteristic parameters determined for recombinant *P. pastoris* strains harbouring either the wildtype HRP C1A gene (wt) or a glyco-variant thereof and the amount of total extracellular protein at the end of cultivation.

Strain	$\mu_{\text{max gly}}$ [h <sup>-1</sup> ]	$\Delta_{\text{time adapt}}$ [h]	$q_{\text{s adapt}}$ [mmol/g h]	$q_{\text{s average MeOH}}$ [mmol/g h]
wt	0.277	11.1	0.269	0.370
N13D	0.330	8.7	0.317	0.592
N57S	0.245	12.8	0.216	0.409
N158D	0.251	13.5	0.211	0.304
N186D	0.268	13.1	0.211	0.273
N198D	0.244	8.3	0.292	0.372
N214S	0.267	14.4	0.219	0.213
N255D	0.253	8.4	0.291	0.537
N268D	0.258	14.4	0.253	0.256

Strain	$Y_{X/S}$ [C <sub>mol</sub> /C <sub>mol</sub> ]	$Y_{\text{CO}_2/S}$ [C <sub>mol</sub> /C <sub>mol</sub> ]	C- balance	Protein [mg/mL]
wt	0.013	0.92	0.93	0.08
N13D	0.063	0.88	0.95	0.08
N57S	0.027	0.95	1.02	0.09
N158D	0.065	1.00	1.07	0.09
N186D	0.019	1.00	1.02	0.10
N198D	0.022	0.90	0.96	0.08
N214S	0.012	0.95	0.95	0.08
N255D	0.006	0.96	1.00	0.11
N268D	0.038	1.00	1.04	0.08

This influence is also obvious in both yield coefficients (biomass yield,  $Y_{X/S}$ ; carbon dioxide yield,  $Y_{\text{CO}_2/S}$ ). However, we did not investigate the exact locus of gene integration for the single strains in more detail. Closing C-balances for all cultivations confirm the accuracy of the calculated strain specific parameters. It is remarkable that although we used the same *P. pastoris* strain CBS7435 Mut<sup>S</sup>, the same vector and basically the same gene except for single point mutations, we obtained physiologically diverging strains. This actually underlines the importance of a detailed physiological strain characterisation using the dynamic method applying methanol pulses, especially if subsequent fed-batch cultivations for protein production are envisioned.

### 3.3 Protein purification

After cultivation, the respective HRP glyco-variant was purified from the cell-free cultivation broth using a previously reported 2-step flow-through strategy [6, 9]. Total protein content and enzymatic activity were determined in the flow-through and the

eluates and the respective recovery yield of HRP activity in percentage (R%) and the purification factor (PF) were calculated for each single purification step (Table 3). After hydrophobic charge induction chromatography (HCIC), we recovered more than 80 % of wildtype HRP C1A (wt HRP C1A) and of most enzyme variants except for N158D and N198D. In agreement with our previous observations [6, 9], the whole activity was found in the flow-through. The remaining 5 – 20 % of the enzymes did not elute from the column under the conditions applied, which actually proves the existence of a variety of enzyme species in the cultivation broth differing in glycosylation and thus a varying degree of interaction with the resin. Interestingly, for glyco-variant N158D and N198D we only recovered 50 % of the enzyme in total, which we also found in the flow-through. Apparently, by mutating these two glycosylation sites and thus reducing the overall amount of surface N-glycosylation, the masking effect thereof was reduced leading to a different HCIC performance for these two enzyme variants. However, compared to the other glycosylation sites we could not identify a particular location of these two sites which could potentially explain this phenomenon (Supplementary Figure 2). By HCIC the wt enzyme was purified 2-fold, whereas the success of purification varied between 1.3 and 3.4-fold for the different glyco-variants highlighting the importance of an integrated bioprocess aspect – already little changes of protein properties, as the degree of surface N-glycosylation, might have a significant impact on following unit operations. The difference in the PF for wt HRP C1A compared to previous studies where we achieved a PF of 7.0 [6] might be explained by the different cultivation strategies. In our previous study, we cultivated *P. pastoris* in shake flasks, where conditions were not controlled and limitations in nutrients and oxygen occurred, which is why cells were more sensitive to cell lysis. Consequently, more contaminating proteins were found in the cell-free cultivation broth. In the present study, we cultivated the different strains in a bioreactor where parameters, like pH and temperature, were controlled and thus undesired cell lysis was reduced. Consequently, the cell-free cultivation broth contained less contaminating proteins. This is also obvious when looking at the cell-free cultivation broth before purification, which showed a specific activity of only 20 U·mg<sup>-1</sup> from shake flasks [6], but around 40 U·mg<sup>-1</sup> in the present study.

**Table 3:** Results of the 2-step purification approach for HRP C1A applying HCIC and AEC both operated in flow-through mode.

Variant	HCIC			AEC			Combined		Spec. activity [U·mg <sup>-1</sup> ]
	R% total	R% FT	PF	R% total	R% FT	PF	R%	PF	
<b>wt</b>	83.6	83.6	1.95	85.9	77.1	3.46	64.5	6.7	248
<b>N13D</b>	91.5	91.5	2.94	85.6	24.5	7.92	22.4	23.3	689
<b>N57S</b>	80.7	80.4	2.70	86.2	70.9	3.32	56.3	9.0	461
<b>N158D</b>	53.8	53.6	1.85	90.1	75.0	5.02	40.2	9.3	167
<b>N186D</b>	86.8	86.8	1.48	91.4	57.1	10.2	49.6	15.1	198
<b>N198D</b>	51.3	51.1	1.30	84.0	50.4	1.89	25.8	2.5	114
<b>N214S</b>	82.4	82.3	1.66	94.4	45.3	4.53	37.3	7.5	113
<b>N255D</b>	94.9	94.9	2.95	96.4	75.4	6.59	71.6	19.4	236
<b>N268D</b>	94.7	94.7	3.43	82.0	74.9	4.21	70.9	14.4	274

In the subsequent anion exchange chromatography (AEC) step we recovered more than 80 % of the initially applied HRP for all enzyme variants (Table 3). However, the amount of HRP we found in the flow-through vastly differed between the glyco-variants. For the wt enzyme and variants N57S, N158D, N155D and N268D we found a comparable amount of around 75 % of HRP in the flow-through, whereas for variants N13D, N186D, N198D and N214S the recovery in the flow-through was only 50 % or less. For N13D we even only found 25 % of the enzyme in the flow-through, whereas the rest was found in the eluate together with contaminating proteins. However, when we looked at the location of N13 in comparison to the other glycosylation sites we could not identify a particularity which could explain this phenomenon (Supplementary Figure 2). This again highlights the importance of the single N-glycosylation sites and the respective surface N-glycosylation for the physico-chemical properties of HRP and the applicability of the flow-through chromatography approach. With regard to AEC purification success, we obtained a PF of more than 3 for the wt enzyme and similar values for N57S, N214S and N268D. Although we only recovered 25 % of the initial amount of N13D in the flow-through, this glyco-variant was purified nearly 8-fold. Also N158D, N186D and N255D were purified with great success (5-fold, 10-fold and more than 6-fold, respectively), whereas for variant N198D a PF of only 2 was determined in the flow-through.

With respect to the overall purification efficiency for the glyco-variant library of HRP C1A using a 2-step flow-through approach, we observed vastly different results

(Table 3). The overall recovery of the initial amount of HRP after the 2 purification steps varied from only 20 % to more than 70 %. Also the obtained total PF varied immensely between 2.5 for variant N198D and more than 23 for N13D. Remarkably, these vast differences only originated from single point mutations of HRP C1A and consequent changes in surface N-glycosylation. Hence, for some of these variants, like for N198D, we recommend to adapt the downstream strategy to obtain an enzyme preparation with higher purity.

### 3.4 Biochemical enzyme characterization

After protein purification, the enzyme variants were biochemically characterized. In Table 4 the kinetic constants for the substrates 2,2'-azino-bis(3-ethyl-benzothiazoline-6-sulphonic acid) (ABTS) and hydrogen peroxide ( $H_2O_2$ ) are shown. The here presented apparent  $K_m$  of 1.60 mM of the wt HRP C1A preparation for ABTS was higher than the previously published  $K_m$  values of 0.27 mM and 0.18 mM for C1A preparations from plant and *E. coli*, respectively [48]. However, in previous studies on recombinant HRP C1A from *P. pastoris*,  $K_m$  values of 0.68 mM [49] and 1.01 [6] were reported. Apparently, yeast-derived HRP C1A preparations generally have a tendency for a lowered affinity to ABTS compared to preparations from plant and *E. coli*, indicating a crucial role of glycosylation for enzyme activity. As shown in Table 4, the  $K_m$  values of the glyco-variants for ABTS were higher than for the wt, except for variant N198D. Mutating the N-glycosylation sites on the surface of enzyme HRP C1A also affected the reaction rate (Table 4). Summarizing, in terms of catalytic efficiency with ABTS only variants N57S and N255D showed slightly higher or similar values compared to the wt. A similar effect for glyco-variant N255D had already been described elsewhere [47]. The other glyco-variants were characterized by an up to 5-fold reduced catalytic efficiency. Interestingly, in the work of Asad *et al.* HRP variants N13D and N268D also showed higher catalytic activity compared to the wt [39]. However, Asad *et al.* used a different reducing substrate as well as different assay conditions, which is why a direct comparison with the present study is not feasible.

We observed similar trends of  $K_m$  and  $V_{max}$  for the substrate  $H_2O_2$ , as the majority of HRP glyco-variants showed a reduced catalytic efficiency compared to the wt enzyme (Table 4).

**Table 4:** Kinetic constants of wt HRP C1A and the glyco-variants for the substrates ABTS and H<sub>2</sub>O<sub>2</sub> as well as thermal stability.

Variant	ABTS			H <sub>2</sub> O <sub>2</sub>			$\tau_{1/2}$ [min]
	K <sub>m</sub> [mM]	V <sub>max</sub> [U·mg <sup>-1</sup> ]	V <sub>max</sub> /K <sub>m</sub> [U·mg <sup>-1</sup> ·mM <sup>-1</sup> ]	K <sub>m</sub> [mM]	V <sub>max</sub> [U·mg <sup>-1</sup> ]	V <sub>max</sub> /K <sub>m</sub> [U·mg <sup>-1</sup> ·mM <sup>-1</sup> ]	
wt	1.60	44.2	27.7	0.003	16.3	5,433	20.6
N13D	2.90	47.2	16.3	0.005	14.7	3,066	28.9
N57S	2.98	113	38.1	0.004	23.7	5,378	38.5
N158D	3.08	16.3	5.30	0.005	51.7	10,342	3.2
N186D	4.24	77.4	18.2	0.004	7.63	2,179	18.8
N198D	1.21	14.9	12.3	0.003	19.1	5,795	18.5
N214S	3.48	41.1	11.8	0.004	9.36	2,531	6.3
N255D	1.72	51.5	29.9	0.005	21.6	4,506	11.6
N268D	1.89	32.5	17.2	0.003	10.6	3,642	61.9

In fact, N57S was the only glyco-variant showing similar or even higher catalytic efficiency with both substrates compared to the wt. The Michaelis-Menten kinetics for the wt enzyme and for variant N57S for both substrates is exemplarily shown in Figure 2, while illustrations for the other enzyme variants are shown in the Supplementary Figure 3.

To potentially explain the observed effects of the mutations on the surface of the enzyme on the catalytic activity we determined the distance of the respective N-glycosylation site to the amino acid His170, which is linked to the heme group in the active site (Figure 3). However, we were not able to identify a direct correlation between the distance of the N-glycosylation site to the active site and observed changes in catalytic activity. Only resolving the crystal structures of the single HRP C1A glyco-variants and the subsequent analysis of structure-function relationships could potentially explain the observed effects of the respective mutation on the catalytic behaviour.

Finally, we also tested the enzymes for thermal stability, since it is known that mutating N-glycosylation sites on the surface of proteins might affect stability [39]. In order to investigate if the protein concentration affects thermal stability, as described elsewhere [39], two different concentrations, *i.e.* 0.01 mg·mL<sup>-1</sup> and 0.02 mg·mL<sup>-1</sup>, of the wt HRP were tested. In fact, we observed a huge difference in the half-life time at 60°C, which we determined with 20.6 min for the less concentrated protein solution and with 121 min for the more concentrated one.

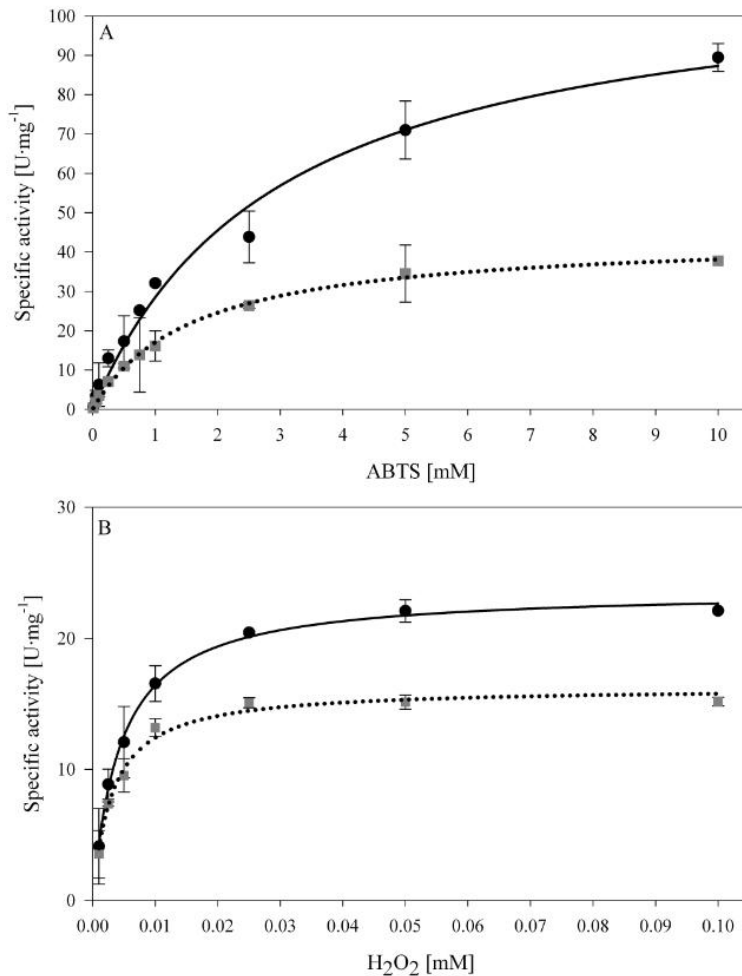
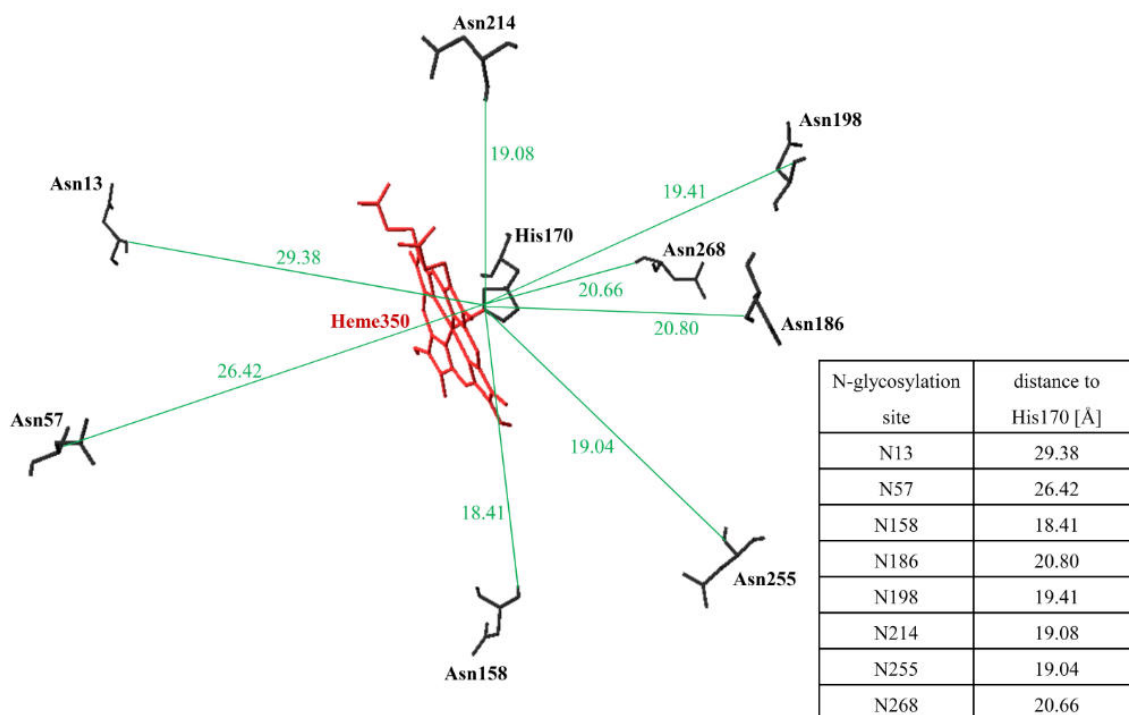


**Figure 2:** Michaelis-Menten kinetics of the unmutated wt HRP C1A and the glyco-variant N57S for ABTS and H<sub>2</sub>O<sub>2</sub>. A, kinetics for ABTS; B, kinetics for H<sub>2</sub>O<sub>2</sub>. Black dots, N57S; grey squares, wt.

Consequently, we normalized all the different HRP glyco-variant solutions to a concentration of 0.01 mg·mL<sup>-1</sup> before heat treatment. Interestingly, we found striking differences in the thermal stability of the enzyme glyco-variants (Table 4). For N158D, N214S and N255D stability was significantly reduced, whereas N186D and N198D showed half-life times comparable to the wt. Interestingly, N13D and N57S showed a higher thermal stability and N268D had an even 3-fold higher half-life time ( $\tau_{1/2}$ ) than the fully glycosylated enzyme.

Comparable observations for variants N13D and N268D were also made by Asad *et al.* [39]. The differences between the determined half-life times in this study compared to the study of Asad *et al.*, who determined the stability at 50°C, can be explained by differences in the assay conditions. Whereas Asad *et al.* used a 200 mM phosphate buffer, we only used a 50 mM phosphate buffer, which is known to positively affect HRP stability [50]. Summarizing, it is remarkable that mutating glycosylation sites of a protein and thus reducing its overall glycosylation pattern does not only reduce protein stability but might also increase it.

**Figure 3:** Distances of the N-glycosylation sites on the surface of HRP C1A to the heme binding site His170 in the active site.



### 3.4.1 Glycosylation analysis

To prove the absence of surface glycosylation on the respective mutated N-glycosylation site, we exemplarily performed glycosylation analysis for the glyco-variant N57S by digesting the protein with either chymotrypsin or trypsin and subsequently analysing the peptides by liquid-chromatography mass spectrometry. Furthermore, aliquots of the chymotryptic digest were incubated with PNGase A and released glycans were analysed by mass spectrometry (Figure 4). The success of mutating Asn57 to a non-glycosylated Ser was confirmed by mass spectrometric analysis of chymotryptic peptides. We clearly see the absence of surface N-glycosylation on N57S (Figure 4).

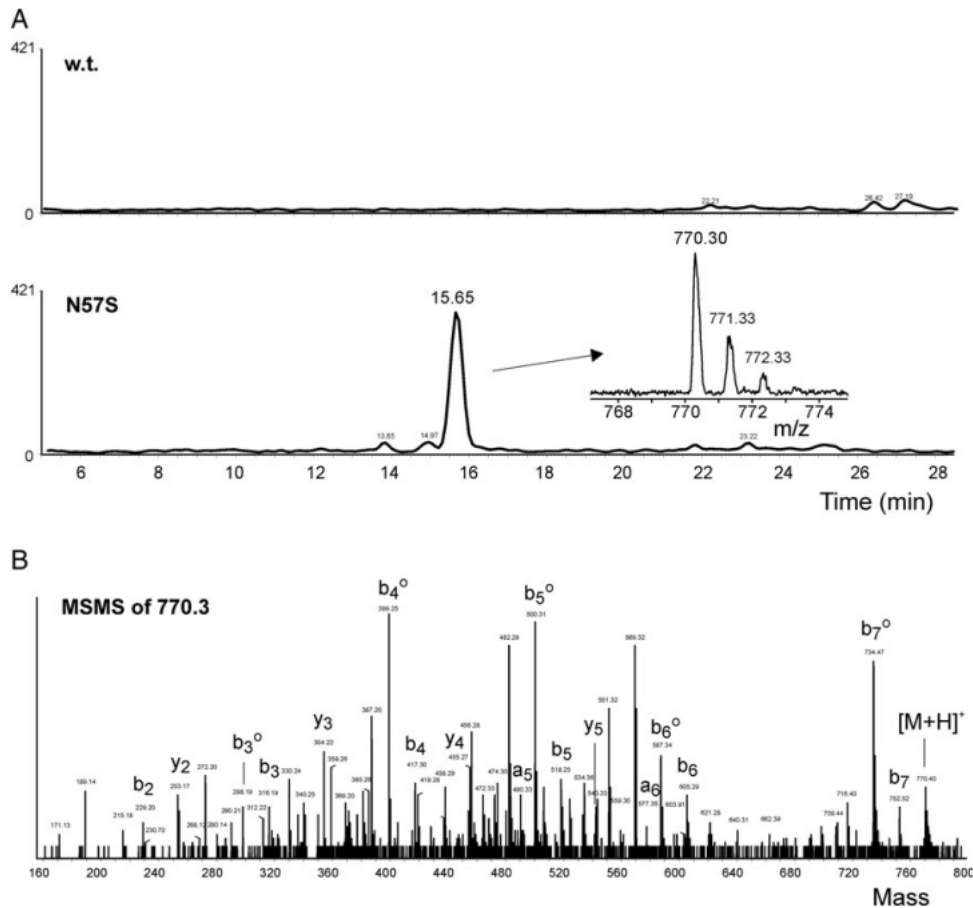


**Figure 4:** Verification of the mutated peptide LD<sup>57</sup>STTSF by MS. Panel A shows the extracted ion chromatograms for the mass of LDSTTSF (M+H<sup>+</sup> 770.36 Da) in N57S HRP. The mutant exhibited the relevant peak, whose identity was confirmed by CID fragmentation as shown in panel B. B-fragments with loss of H<sub>2</sub>O are designated as b<sup>o</sup> fragments.

### 3.5 Combination of mutations

To potentially obtain an enzyme variant without any N-glycosylation, we combined all the 8 mutations described above (hereafter called “mutant”). The resulting *P. pastoris* strain was again cultivated in a batch with consecutive methanol pulses for physiological strain characterization (Table 5). Again, we observed very different strain characteristic parameters although we used the same *P. pastoris* strain CBS7435 Mut<sup>S</sup>, the same vector and basically the same gene except for 8 point mutations. Closing C-balances for both cultivations confirm the accuracy of the calculated strain specific parameters. In contrast to the strain carrying the wt HRP C1A gene, we were not able to detect any HRP activity in the cell free cultivation broth for the strain carrying the mutated gene. Only after ultrafiltration and 20-fold concentration of the cultivation broth, we were able to measure activity for

the mutated HRP C1A glyco-variant. We concentrated the enzyme further and diafiltrated it before we determined the catalytic constants with ABTS and H<sub>2</sub>O<sub>2</sub> as well as thermal stability.

**Table 5:** Strain characteristic parameters determined for recombinant *P. pastoris* strains harboring either the wildtype HRP C1A gene (wt) or a variant where all the 8 N-glycosylation sites were mutated (mutant).

Strain	$\mu_{\max \text{ gly}}$ [h <sup>-1</sup> ]	$\Delta_{\text{time adapt}}$ [h]	$Q_s \text{ adapt}$ [mmol·g <sup>-1</sup> ·h <sup>-1</sup> ]	$Q_s \text{ average MeOH}$ [mmol·g <sup>-1</sup> ·h <sup>-1</sup> ]
wt	0.277	11.1	0.269	0.370
mutant	0.222	4.7	0.660	0.882
Strain	$Y_{X/S}$ [C <sub>mol</sub> ·C <sub>mol</sub> <sup>-1</sup> ]	$Y_{CO_2/S}$ [C <sub>mol</sub> ·C <sub>mol</sub> <sup>-1</sup> ]	C- balance	Protein [mg·mL <sup>-1</sup> ]
wt	0.013	0.92	0.93	0.08
mutant	0.153	0.81	0.97	0.10

**Table 6:** Kinetic constants of wt HRP C1A and the variant where all the 8 N-glycosylation sites were mutated (mutant) for the substrates ABTS and H<sub>2</sub>O<sub>2</sub> as well as thermal stability.

Variant	ABTS			H <sub>2</sub> O <sub>2</sub>			$\tau_{1/2}$ [min]
	Km [mM]	V <sub>max</sub> [U·mg <sup>-1</sup> · h <sup>-1</sup> ]	V <sub>max</sub> /Km [U·mg <sup>-1</sup> ·mM <sup>-1</sup> ]	Km [mM]	V <sub>max</sub> [U·mg <sup>-1</sup> · h <sup>-1</sup> ]	V <sub>max</sub> /Km [U·mg <sup>-1</sup> ·mM <sup>-1</sup> ]	
wt	1.60	44.2	27.7	0.003	16.3	5,433	20.6
mutant	1.44	0.15	0.10	0.026	0.14	5.38	3.2

As shown in Table 6, the combination of all 8 mutations to obtain a HRP C1A variant without any N-glycans resulted in an enzyme variant with extremely reduced catalytic efficiency and thermal stability. Although the affinity towards ABTS basically remained the same, the catalytic activity was reduced nearly 300-fold. The effects for H<sub>2</sub>O<sub>2</sub> were even more severe, as Km was increased more than 8-fold and V<sub>max</sub> decreased more than 100-fold resulting in a nearly 1,000-fold reduced catalytic efficiency. As judged by SDS-PAGE analysis, the size of this variant was significantly reduced compared to the glycosylated wt enzyme (Figure not shown). However, since catalytic activity and stability were that low, making this variant not useful for medical applications, we did not analyse the surface N-glycosylation of this glyco-variant in more detail.

Summarizing, enzyme engineering describes a valid approach to obtain active HRP C1A variants with a reduced amount of surface N-glycosylation. Although an

enzyme variant where all the 8 N-glycosylation sites were mutated hardly showed catalytic activity and thus does not describe a meaningful tool for medical applications, the here described glyco-library of HRP C1A describes a very useful basis for further enzyme engineering approaches. Studies, where we only combine up to 4 mutations, namely N13D, N57S, N255D and N268D, and then express these variants in a *P. pastoris* *OCH1* knockout strain [38] to obtain a HRP C1A variant useful for targeted cancer treatment are currently ongoing.

## 4 Material and Methods

### 4.1 Chemicals

Enzymes were purchased from Fermentas GmbH (Austria). 2,2'-azino-bis(3-ethylbenzthiazoline-6-sulphonic acid) diammonium salt (ABTS) was obtained from Sigma-Aldrich Handels GmbH (Austria). Difco™ yeast nitrogen base w/o amino acids (YNB), Bacto™ tryptone and Bacto™ yeast extract were obtained from Becton Dickinson and Company (Austria). Zeocin™ was obtained from Invitrogen (Austria). D-Biotin was obtained from Fluka Chemia AG (Switzerland). All other chemicals were purchased from Carl Roth GmbH & Co. KG (Germany).

### 4.2 Strain and gene

*P. pastoris* CBS7435 Mut<sup>S</sup> [15-19, 38] and vector pPpT4\_S harbouring the HRP isoenzyme C1A, which was codon-optimized for high-level expression in *P. pastoris* [17], were used in this study. The codon table described in [51] was applied for codon optimization. Secretion of HRP C1A to the cultivation broth was facilitated by an N-terminally fused prepro-signal sequence of the *S. cerevisiae* alpha-factor.

### 4.3 Site-directed mutagenesis

The 8 Asn, representing the glycosylation sites of HRP C1A, were mutated to either Asp, Gln or Ser, which are amino acids providing a certain structural similarity to Asn, by site directed mutagenesis and subsequent digestion with *DpnI* [52]. The mutagenic PCR was performed as: 98°C for 30 sec; then 10 cycles of 98°C for 10 sec, 57°C for 20 sec, 72°C for 1 min - 10 cycles of 98°C for 10 sec, 60°C for 20 sec, 72°C for 1 min - 10 cycles of 98°C for 10 sec, 63°C for 20 sec, 72°C for 1 min; with

a final incubation at 72°C for 10 min. Each reaction contained 1× HF buffer (Fermentas), 0.1 µg of plasmid DNA, 2.5 U *Phusion* DNA polymerase (Fermentas), 10 µM of each dNTP and 5 pmol of each primer in a total volume of 50 µL. All primers are listed in Table 7 and were purchased from Microsynth (Austria).

After PCR, the methylated template DNA was degraded by digestion with 10 U of *DpnI* at 37°C for at least 3 hours. The remaining PCR products were purified using the QIAquick PCR purification kit (QIAGEN; Austria) and 5 µL of each purified PCR product were transformed into electro-competent *E. coli* TOP10 F' cells. The successful introduction of the desired mutation and the absence of further mutations were confirmed by DNA sequencing (Microsynth). Transformation of approximately 2 µg *Swal*-linearized pPpT4\_S plasmid DNA harbouring the respective mutated HRP C1A gene (Supplementary Figure 4) into *P. pastoris* was done as described by Lin-Cereghino *et al.* [53]. Stable transformants were generated via homologous recombination between the linearized plasmid DNA and genomic yeast DNA. Selection of successfully transformed clones was performed on Yeast Extract Peptone Dextrose medium (YPD; 10 g·L<sup>-1</sup> yeast extract, 20 g·L<sup>-1</sup> peptone, 20 g·L<sup>-1</sup> glucose, 20 g·L<sup>-1</sup> agar) supplemented with 100 mg·L<sup>-1</sup> Zeocin.

#### 4.4 Screening procedure

Screening of 5 randomly picked *P. pastoris* transformants per mutation was done in 1000 mL shaking flasks. We also included a *P. pastoris* CBS7435 Mut<sup>S</sup> strain carrying the unmutated HRP C1A gene (henceforth designated as “wt”) as well as an untransformed *P. pastoris* CBS7435 Mut<sup>S</sup> strain as negative control, resulting in a total of 17 shaking flasks per screening experiment. First the clones were cultivated in 10 mL Buffered Glycerol Complex Medium supplemented with 100 mg·L<sup>-1</sup> Zeocin (BMGY\_Zeo; 10 g·L<sup>-1</sup> yeast extract; 20 g·L<sup>-1</sup> peptone; 3.4 g·L<sup>-1</sup> YNB w/o amino acids and ammonia sulfate, 10 g·L<sup>-1</sup> (NH<sub>4</sub>)<sub>2</sub>SO<sub>4</sub>, 400 mg·L<sup>-1</sup> biotin; 1 g·L<sup>-1</sup> glycerol; 0.1 M potassium phosphate buffer, pH 6.0) in 100 mL shaking flasks at 30°C and 230 rpm over night. The next day the OD<sub>600</sub> was measured, an appropriate aliquot of the culture was taken, and after centrifugation the cells were resuspended in selective Buffered Methanol Complex Medium supplemented with 100 mg·L<sup>-1</sup> Zeocin (BMMY\_Zeo; 10 g·L<sup>-1</sup> yeast extract; 20 g·L<sup>-1</sup> peptone; 3.4 g·L<sup>-1</sup> YNB w/o

amino acids and ammonia sulfate, 10 g·L<sup>-1</sup> (NH<sub>4</sub>)<sub>2</sub>SO<sub>4</sub>, 400 mg·L<sup>-1</sup> biotin; 0.5 % methanol; 0.1 M potassium phosphate buffer, pH 6.0) to an OD<sub>600</sub> of 1.0.

**Table 7:** Oligonucleotide primers to mutate the 8 Asn residues of the enzyme HRP C1A, which act as N-glycosylation sites, to either Asp, Gln or Ser. The mutation sites are depicted in italics.

<b>N-site</b>	<b>Name</b>	<b>Sequence (5'→3')</b>
N13	N13D_fwd	AAC TCT TGT CCT <i>GAT</i> GTG TCC AAC ATC
	N13Q_fwd	AAC TCT TGT CCT <i>CAG</i> GTG TCC AAC ATC
	N13S_fwd	AAC TCT TGT CCT <i>AGT</i> GTG TCC AAC ATC
	N13_rev	AGG ACA AGA GTT ATC GTA GAA GGT TGG AGT
N57	N57D_fwd	TCC ATC TTG CTG GAC <i>GAC</i> ACT ACC TC
	N57Q_fwd	TCC ATC TTG CTG GAC <i>CAG</i> ACT ACC TC
	N57S_fwd	TCC ATC TTG CTG GAC <i>AGC</i> ACT ACC TC
	N57_rev	GTC CAG CAA GAT GGA AGC ATC ACA ACC
N158	N158D_fwd	C AGA AAC GTT GGT CTT <i>GAC</i> AGA TCA TCC
	N158Q_fwd	C AGA AAC GTT GGT CTT <i>CAG</i> AGA TCA TCC
	N158S_fwd	C AGA AAC GTT GGT CTT <i>AGC</i> AGA TCA TCC
	N158_rev	AAG ACC AAC GTT TCT GAA AGA GTC TTT CAA TTG
N186	N186D_fwd	ATG GAT CGT CTG TAC <i>GAC</i> TTC TCT AAC AC
	N186Q_fwd	ATG GAT CGT CTG TAC <i>CAG</i> TTC TCT AAC AC
	N186S_fwd	ATG GAT CGT CTG TAC <i>AGC</i> TTC TCT AAC AC
	N186_rev	GTA CAG ACG ATC CAT GAT GAA TCT ACA TTG GTT
N198	N198D_fwd	CCA GAT CCT ACT CTG <i>GAC</i> ACC ACT TAC
	N198Q_fwd	CCA GAT CCT ACT CTG <i>CAG</i> ACC ACT TAC
	N198S_fwd	CCA GAT CCT ACT CTG <i>AGC</i> ACC ACT TAC
	N198_rev	CAG AGT AGG ATC TGG CAA ACC GG
N214	N214D_fwd	CCA CTT AAC GGA <i>GAC</i> CTG TCT GC
	N214Q_fwd	CCA CTT AAC GGA <i>CAG</i> CTG TCT GC
	N214S_fwd	CCA CTT AAC GGA <i>AGC</i> CTG TCT GC
	N214_rev	TCC GTT AAG TGG GCA CAA ACC TC
N255	N255D_fwd	TTG TTC TCC TCT CCT <i>GAC</i> GCT ACT GAT
	N255Q_fwd	TTG TTC TCC TCT CCT <i>CAG</i> GCT ACT GAT
	N255S_fwd	TTG TTC TCC TCT CCT <i>AGC</i> GCT ACT GAT
	N255_rev	AGG AGA GGA GAA CAA CTC CTG GTC
N268	N268D_fwd	G AGA TCC TTC GCA <i>GAC</i> TCC ACT CAA
	N268Q_fwd	G AGA TCC TTC GCA <i>CAG</i> TCC ACT CAA
	N268S_fwd	G AGA TCC TTC GCA <i>AGC</i> TCC ACT CAA
	N268_rev	TGC GAA GGA TCT CAC CAA TGG AAT G

The cells were again cultivated at 30°C and 230 rpm. Every day, 1 % (v/v) methanol was pulsed to the culture and a 1 mL sample was taken, analysed for optical density (OD<sub>600</sub>), catalytic activity and protein content. The catalytic activity of HRP was measured using an ABTS assay in a CuBiAn XC enzymatic robot (Innovatis, Germany). 10 µl of sample were mixed with 140 µl 1 mM ABTS solution (50 mM

KH<sub>2</sub>PO<sub>4</sub>, pH 6.5). The reaction mixture was incubated at 37°C for 5 min before the reaction was started by the addition of 20 µl 0.078 % H<sub>2</sub>O<sub>2</sub> (v/v). Changes in absorbance at 415 nm were measured for 80 seconds and rates were calculated. The standard curve was prepared using a commercially available HRP preparation (Type VI-A; Sigma-Aldrich, USA) in the range from 0.02 to 2.0 U·mL<sup>-1</sup>. Protein concentrations were determined at 595 nm by the Bradford assay using the Sigma-Aldrich (Austria) Protein Assay Kit with bovine serum albumin as standard in the range of 0.2-1.2 mg·mL<sup>-1</sup>.

After 96 h of induction, the HRP glyco-variants in the cell-free supernatants were tested for thermal stability. Therefore, aliquots of 1 mL were incubated in a waterbath at 60°C for up to 4 h, before the samples were centrifuged (10,000 x g; 10 min) and the supernatants were analysed for remaining HRP activity. These values were then compared to the initial activity before heat treatment. Based on activity and stability measurements the most suitable mutation at a respective N-glycosylation site was chosen and the corresponding *P. pastoris* strain was physiologically characterized in the bioreactor. Before bioreactor cultivation, the presence of the correctly mutated HRP gene in the respective *P. pastoris* transformant was verified by colony PCR using the primers AOX\_fwd (5'-ACTCCAACCTTCTACGATAACTC-3') and AOX\_rev (5'-ACTGTGTCATGTGCTGACC-3') and subsequent sequencing (Microsynth).

## 4.5 Strain characterization in the bioreactor

### 4.5.1 Culture Media

Precultures were done in yeast nitrogen base medium with 100 mg·L<sup>-1</sup> Zeocin (YNBM\_Zeo; 3.4 g·L<sup>-1</sup> YNB w/o amino acids and ammonia sulfate, 10 g·L<sup>-1</sup> (NH<sub>4</sub>)<sub>2</sub>SO<sub>4</sub>, 400 mg·L<sup>-1</sup> biotin, 20 g·L<sup>-1</sup> glucose, 0.1 M potassium phosphate buffer pH 6.0). Batch cultivations were performed in basal salt medium (26.7 mL·L<sup>-1</sup> 85 % phosphoric acid, 1.17 g·L<sup>-1</sup> CaSO<sub>4</sub>·2H<sub>2</sub>O, 18.2 g·L<sup>-1</sup> K<sub>2</sub>SO<sub>4</sub>, 14.9 g·L<sup>-1</sup> MgSO<sub>4</sub>·7H<sub>2</sub>O, 4.13 g·L<sup>-1</sup> KOH, 40 g·L<sup>-1</sup> glycerol, 0.2 mL·L<sup>-1</sup> Antifoam Struktol J650, 4.35 mL·L<sup>-1</sup> PTM1, NH<sub>4</sub>OH as N-source). Trace element solution (PTM1) was made of 6.0 g·L<sup>-1</sup> CuSO<sub>4</sub>·5H<sub>2</sub>O, 0.08 g·L<sup>-1</sup> NaI, 3.0 g·L<sup>-1</sup> MnSO<sub>4</sub>·H<sub>2</sub>O, 0.2 g·L<sup>-1</sup> Na<sub>2</sub>MoO<sub>4</sub>·2H<sub>2</sub>O, 0.02 g·L<sup>-1</sup> H<sub>3</sub>BO<sub>3</sub>, 0.5 g·L<sup>-1</sup> CoCl<sub>2</sub>, 20.0 g·L<sup>-1</sup> ZnCl<sub>2</sub>, 65.0 g·L<sup>-1</sup> FeSO<sub>4</sub>·7H<sub>2</sub>O, 0.2 g·L<sup>-1</sup> biotin, 5 mL·L<sup>-1</sup> H<sub>2</sub>SO<sub>4</sub>. Induction was carried out in presence of 1 mM Δ-

aminolevulinic acid. The concentration of the base  $\text{NH}_4\text{OH}$  was determined by titration with 0.25 M potassium hydrogen phthalate.

#### **4.5.2 Experimental Procedure**

**Preculture:** Frozen stocks ( $-80^\circ\text{C}$ ) were cultivated in 100 mL YNBM in 1000 mL shake flasks at  $30^\circ\text{C}$  and 230 rpm. The grown preculture was transferred aseptically to the respective culture vessel. The inoculation volume was 10 % of the final starting volume.

**Batch cultivation:** Batch cultivations were carried out in either a 3 L or a 5 L working volume glass bioreactor (Infors, Switzerland). Basal salt medium was sterilized in the bioreactor and pH was adjusted to pH 5.0 by using concentrated  $\text{NH}_4\text{OH}$  solution after autoclaving. Sterile filtered trace elements were transferred to the reactor aseptically. Dissolved oxygen ( $\text{dO}_2$ ) was measured with a sterilizable  $\text{dO}_2$  electrode (Visiferm™, Hamilton, Switzerland). The pH was measured with a sterilizable electrode (Easyferm™, Hamilton, Switzerland) and maintained constant with a PID controller using  $\text{NH}_4\text{OH}$  solution (1 to 2 M). Base consumption was determined gravimetrically. Cultivation temperature was set to  $30^\circ\text{C}$  and agitation was fixed to 1,200 rpm. The culture was aerated with 1.0 vvm dried air and off-gas of the culture was measured by using an infrared cell for  $\text{CO}_2$  and a paramagnetic cell for  $\text{O}_2$  concentration (Servomax, Switzerland). Temperature, pH,  $\text{dO}_2$ , agitation as well as  $\text{CO}_2$  and  $\text{O}_2$  in the off-gas were measured online and logged in a process information management system (PIMS; Lucillus, Biospectra, Switzerland). After the complete consumption of the substrate glycerol, indicated by an increase of  $\text{dO}_2$  and a drop in off-gas activity, the first methanol pulse of a final concentration of 0.5 % (v/v) was conducted with methanol supplemented with  $12 \text{ mL}\cdot\text{L}^{-1}$  PTM1. Following pulses were performed with 1 % methanol/PTM1 (v/v) (Figure 2). For each pulse, two samples were taken to determine the concentrations of substrate and product, as well as dry cell weight to calculate specific rates and yields.

#### **4.5.3 Analysis of growth- and expression-parameters**

Dry cell weight was determined by centrifugation of 5 mL culture broth (5,000 rpm,  $4^\circ\text{C}$ , 10 min) in a laboratory centrifuge (Sigma 4K15, rotor 11156), washing the pellet

twice with 5 mL deionized water and subsequent drying at 105°C to a constant weight.

#### **4.5.4 Substrate concentrations**

Concentrations of methanol were determined in cell free samples by HPLC (Agilent Technologies, USA) equipped with an ion-exchange column (Supelcogel C-610H Sigma-Aldrich, USA) and a refractive index detector (Agilent Technologies, USA). The mobile phase was 0.1 % H<sub>3</sub>PO<sub>4</sub> with a constant flow rate of 0.5 mL·min<sup>-1</sup> and the system was run isocratic at 30°C. Calibration was done by measuring standard points in the range from 0.1 to 10 g·L<sup>-1</sup> methanol. Measurements of biomass, product and substrate concentration were executed in duplicates.

#### **4.6 Protein purification**

After bioreactor cultivation, the cell-free cultivation broth was diafiltrated for subsequent hydrophobic charge induction chromatography (HCIC) using a Centrimate 500S TFF system (PALL; Austria) with a 10 kDa MWCO membrane. The buffer was HCIC-A (500 mM NaCl, 20 mM NaOAc, pH 6.0) and the protein solution was concentrated to a final volume of 40-50 mL. All further steps of concentration and buffer change were performed using Amicon Ultra-15 Centrifugal Filter Units with 10 kDa MWCO (Merck Millipore; Austria). The HCIC resin MEP HyperCel™ was obtained from PALL and HCIC was performed in flow-through mode: a column containing 25 mL of MEP HyperCel™ resin was equilibrated with at least 4 column volumes (CV) of buffer HCIC-A. 40-50 mL concentrated HRP solution in HCIC-A were loaded onto the column which was then washed with at least 5 CV of HCIC-A at a flow rate of 55 cm·h<sup>-1</sup>. Then a step elution to 100 % buffer HCIC-B (1.0 M NaCl, 20 mM NaOAc, pH 8.0) was performed. After elution, the column was washed with 5 CV 0.8 M NaOH before it was stored in EtOH 20 %, 1.0 M NaCl. During all the different steps fractions of 10 mL were collected and analyzed for protein content and catalytic activity.

HCIC-flow-through fractions showing HRP activity were pooled, concentrated and rebuffed in AEC-A (50 mM Tris-HCl, pH 8.0) for subsequent anion exchange chromatography (AEC) using an 8 mL CIM®-DEAE monolithic column [6] (BIAseparations; Slovenia). The column was equilibrated with 5 CV of AEC-A at a

flow rate of 16.8 cm·h<sup>-1</sup>. Diafiltrated post-HCIC pools were subsequently loaded onto the AEC column at an average linear flow rate of 16.8 cm·h<sup>-1</sup> before a post-load wash with 5 CV of AEC-A was performed. Elution was performed in a single step from 0 % to 100 % AEC-B (50 mM Tris-HCl, 1.0 M NaCl, pH 8.0). The column was washed with 5 CV of a 1 M NaOH/1 M NaCl solution at an average linear flow rate of 33.6 cm·h<sup>-1</sup> for column recovery, before the column was stored in 20 % EtOH. The efficiency of each purification step was evaluated by determining the purification factor (PF) and the recovery yield of HRP activity in percentage (R%). PF and R% were calculated by equations 1 and 2 [6]. The suffixes “pre” and “post” indicate the respective values before and after a purification step.

$$\mathbf{PF} = \frac{\mathbf{specific\ activity}_{\mathbf{post}}}{\mathbf{specific\ activity}_{\mathbf{pre}}} \quad \mathbf{Equation\ 1}$$

$$\mathbf{R\%} = \mathbf{100} * \frac{\mathbf{volumetric\ activity}_{\mathbf{post}} * \mathbf{volume}_{\mathbf{post}}}{\mathbf{volumetric\ activity}_{\mathbf{pre}} * \mathbf{volume}_{\mathbf{pre}}} \quad \mathbf{Equation\ 2}$$

Finally, the pooled active fractions after AEC were diafiltrated in 50 mM potassium phosphate buffer pH 6.5 and concentrated to a volume of approximately 1.5 mL for the subsequent biochemical characterization.

#### 4.7 Biochemical enzyme characterization

Biochemical characterization of the purified HRP glyco-variants included the determination of the basic kinetic parameters  $K_M$  and  $V_{max}$  for the two substrates H<sub>2</sub>O<sub>2</sub> and ABTS in a spectrophotometer UV-1601 from Shimadzu (Austria). The reaction mixture with a final volume of 1.0 mL contained 20 µL of HRP glyco-variant, 50 mM potassium phosphate buffer, pH 6.5 and either varying concentrations of ABTS (0.01-10 mM) and a saturating concentration of H<sub>2</sub>O<sub>2</sub> of 1.0 mM or varying concentrations of H<sub>2</sub>O<sub>2</sub> (0.001-1.0 mM) and a saturating concentration of ABTS of 10.0 mM, respectively. The increase in absorption was followed at 420 nm at 30°C for 180 s. Absorption curves were recorded with a software program (UVPC Optional Kinetics software, Shimadzu). The maximum reaction rate ( $V_{max}$ ) and the Michaelis constant ( $K_m$ ) were calculated with the Sigma Plot software (Version 11.0; Systat Software Inc., USA).

The thermal stability of individual HRP glyco-variants was tested at 60°C. The residual activity towards ABTS was measured after 1, 5, 10, 15, 30, 45, 60, 90 and 120 min of incubation at 60°C in a water bath. Protein concentrations were

normalized to 0.01 mg/ml to limit possible effects of the different protein concentrations on thermal stability [39] and to obtain comparability. Residual activities were plotted versus the incubation time and the half-life times of thermal inactivation at 60°C ( $\tau_{1/2}$ ) were calculated using equation 3:

$$\tau_{1/2} = \frac{\ln 2}{k_{in}} \quad \text{Equation 3}$$

$k_{in}$  rate of inactivation (slope of the logarithmic residual activity)

#### 4.7.1 Glycosylation analysis

Purified HRP sample was buffered in 0.1 M  $\text{NH}_4\text{HCO}_3$  and reduced with dithiothreitol (DTT) (5 mM) for 45 min at 56°C and alkylated using iodoacetamide (25 mM) at room temperature for 30 min. The protein was precipitated with four volumes of acetone for 45 min at -20°C, dried in a vacuum centrifuge and resuspended in 0.1 M  $\text{NH}_4\text{HCO}_3$  buffer to yield a protein concentration of approx.  $1 \mu\text{g} \cdot \mu\text{L}^{-1}$ . Digests were performed overnight with either chymotrypsin or trypsin (Promega; Mannheim, Germany) at 37°C at an enzyme-to-substrate ratio of 1:50 (w/w). The digested peptides were analyzed by liquid-chromatography mass spectrometry as follows: 1  $\mu\text{g}$  of sample was loaded on a BioBasic-18 column (150 x 0.32 mm; 5  $\mu\text{m}$ ; Thermo Scientific) and eluted with a gradient from 1 to 60 % acetonitrile in 0.3 % formic acid buffered to pH 3.0 at flow rate of 6  $\mu\text{L}/\text{min}$ . Eluted peptides were analysed on an Ultima Global Q-TOF mass spectrometer (Waters; Manchester, United Kingdom) operated in positive-ion mode, which was previously calibrated with a caesium iodide standard in the range of 400 – 1800  $m/z$ . Additionally, the peptide harbouring the site N57S within the mutated HRP variant was subjected to collision-induced dissociation MS/MS with Argon as collision gas. Data was manually evaluated and deconvoluted using the Software MassLynx V4.00.00 (Waters).

An aliquot of the chymotryptic digest was heat-inactivated and then incubated with 0.03 mU PNGase A (proglycan; Vienna, Austria) in 50 mM citrate buffer pH 5.5. Glycans were purified using porous graphitic carbon cartridges (Thermo Scientific) as described [54]. Glycans were analysed by mass spectrometry as described above for peptides with the sole divergence of using a 100 x 0.32 mm hypercarb column (Thermo Scientific; Vienna, Austria) and 1 h gradient from 1 to 50 % acetonitrile.

## 5 Abbreviations

ABTS	2,2'-azino-bis(3-ethylbenzothiazoline-6-sulphonic acid)
AEC	anion exchange chromatography
DTT	dithiothreitol
GlcNAc	N-Acetylglucosamine
HCIC	hydrophobic charge induction chromatography
HRP	horseradish peroxidase
H <sub>2</sub> O <sub>2</sub>	hydrogen peroxide
mutant	HRP C1A, where all 8 N-glycosylation sites were mutated
qPCR	real-time polymerase chain reaction
PF	purification factor
R%	recovery yield of HRP activity in percentage
TFMS	trifluoromethanesulfonic acid
T <sub>½</sub>	thermal half-life time
wt	wildtype HRP C1A
X	any amino acid but proline
Y <sub>X/S</sub>	biomass yield [C-mol·C-mol <sup>-1</sup> ]
Y <sub>CO<sub>2</sub>/S</sub>	carbon dioxide yield [C-mol·C-mol <sup>-1</sup> ]

## 6 Acknowledgments

The authors are very grateful to the Austrian Science Fund FWF: project P24861-B19 for financial support. We further thank the company BIA separations (Slovenia) for providing the tube monolithic columns. The authors declare that there is no conflict of interest.

## 7 References

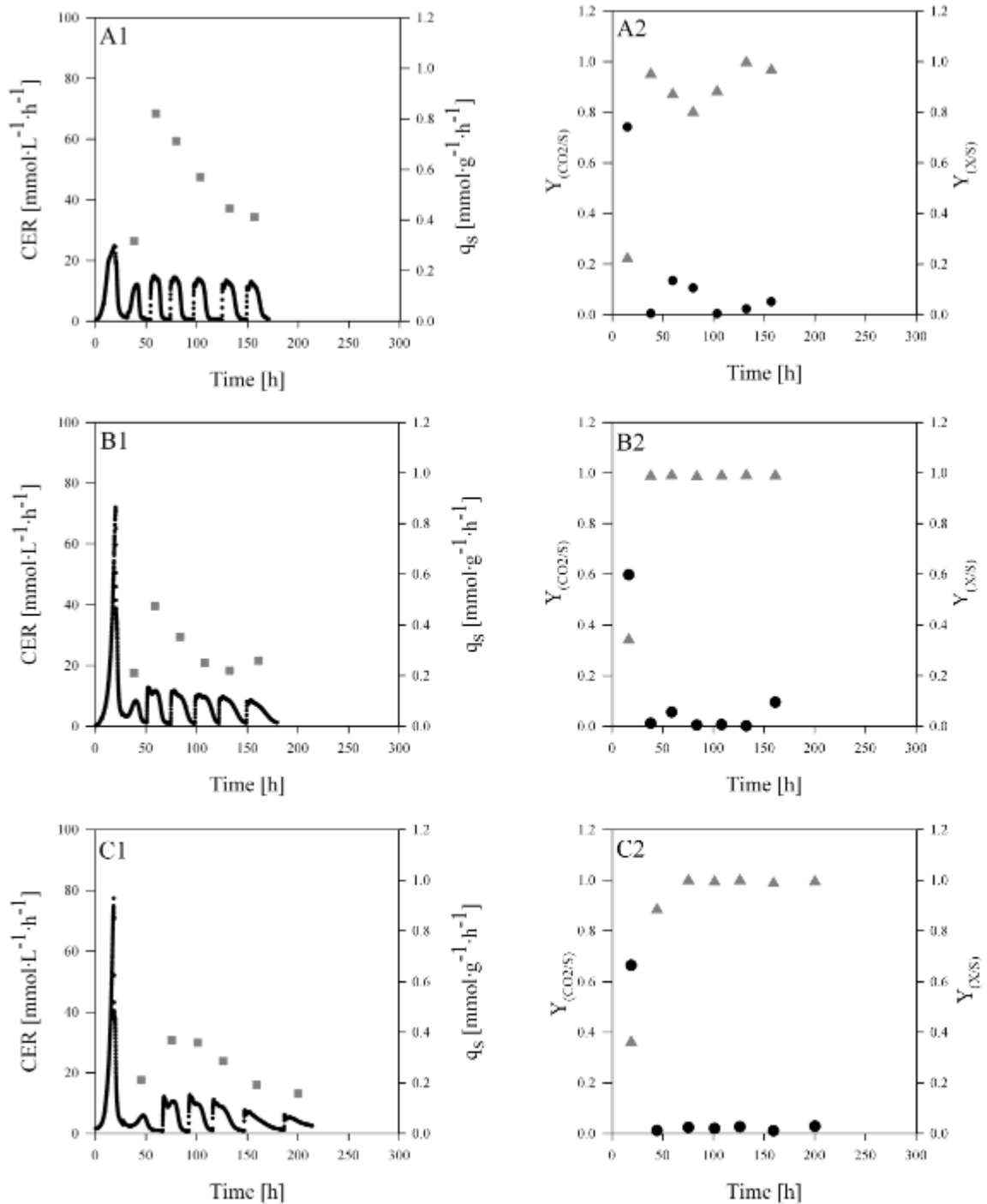
1. Dunford, H.B., *Heme peroxidases*. Wiley-VCH, New York, 1999.
2. Veitch, N.C., *Horseradish peroxidase: a modern view of a classic enzyme*. *Phytochem*, 2004. **65**(3): p. 249-259.
3. Veitch, N.C. and A.T. Smith, *Horseradish peroxidase*. *Adv Inorg Chem*, 2001. **51**: p. 107-162.

4. Carlsson, G.H., et al., *Complexes of horseradish peroxidase with formate, acetate, and carbon monoxide*. *Biochem*, 2005. **44**(2): p. 635-642.
5. Spadiut, O. and C. Herwig, *Production and purification of the multifunctional enzyme horseradish peroxidase: a review*. *Pharm Bioproc*, 2013. **1**(2): p. 283-295.
6. Krainer, F.W., et al., *Purification and basic biochemical characterization of 19 recombinant plant peroxidase isoenzymes produced in Pichia pastoris*. *Protein Expr Purif*, 2013. **95C**: p. 104-112.
7. Smith, A.T., et al., *Expression of a Synthetic Gene for Horseradish Peroxidase-C in Escherichia-Coli and Folding and Activation of the Recombinant Enzyme with Ca-2+ and Heme*. *J Biol Chem*, 1990. **265**(22): p. 13335-13343.
8. Gajhede, M., et al., *Crystal structure of horseradish peroxidase C at 2.15 angstrom resolution*. *Nat Struct Biol*, 1997. **4**(12): p. 1032-1038.
9. Spadiut, O., et al., *Purification of a recombinant plant peroxidase produced in Pichia pastoris by a simple 2-step strategy*. *Protein Expr Purif*, 2012. **86**(2): p. 89-97.
10. Lavery, C.B., et al., *Purification of Peroxidase from Horseradish (Armoracia rusticana) Roots*. *J Agric Food Chem*, 2010. **58**(15): p. 8471-8476.
11. Jermyn, M.A., *Horseradish peroxidase*. *Nature*, 1952. **169**(4299): p. 488-9.
12. Jermyn, M.A. and R. Thomas, *Multiple components in horse-radish peroxidase*. *Biochem J*, 1954. **56**(4): p. 631-9.
13. Shannon, L.M., E. Kay, and J.Y. Lew, *Peroxidase Isozymes from Horseradish Roots .I. Isolation and Physical Properties*. *J Biol Chem*, 1966. **241**(9): p. 2166-2172.
14. Krieg, R. and K.J. Halbhuber, *Recent advances in catalytic peroxidase histochemistry*. *Cell Mol Bio*, 2003. **49**(4): p. 547-563.
15. Dietzsch, C., O. Spadiut, and C. Herwig, *A fast approach to determine a fed batch feeding profile for recombinant Pichia pastoris strains*. *Microb Cell Fact*, 2011. **10**: p. 85.
16. Dietzsch, C., O. Spadiut, and C. Herwig, *A dynamic method based on the specific substrate uptake rate to set up a feeding strategy for Pichia pastoris*. *Microb Cell Fact*, 2011. **10**: p. 14.
17. Krainer, F.W., et al., *Recombinant protein expression in Pichia pastoris strains with an engineered methanol utilization pathway*. *Microb Cell Fact*, 2012. **11**: p. 22.
18. Zalai, D., et al., *A dynamic fed batch strategy for a Pichia pastoris mixed feed system to increase process understanding*. *Biotechnol Prog*, 2012. **doi:10.1002/btpr.1551**.
19. Spadiut, O., et al., *Quantitative comparison of dynamic physiological feeding profiles for recombinant protein production with Pichia pastoris*. *Bioprocess Biosyst Eng*, 2013. **doi: 10.1007/s00449-013-1087-z**.
20. Folkes, L.K. and P. Wardman, *Oxidative activation of indole-3-acetic acids to cytotoxic species - a potential new role for plant auxins in cancer therapy*. *Biochem Pharmacol*, 2001. **61**(2): p. 129-136.
21. Wardman, P., *Indole-3-acetic acids and horseradish peroxidase: A new prodrug/enzyme combination for targeted cancer therapy*. *Curr Pharm Des*, 2002. **8**(15): p. 1363-1374.

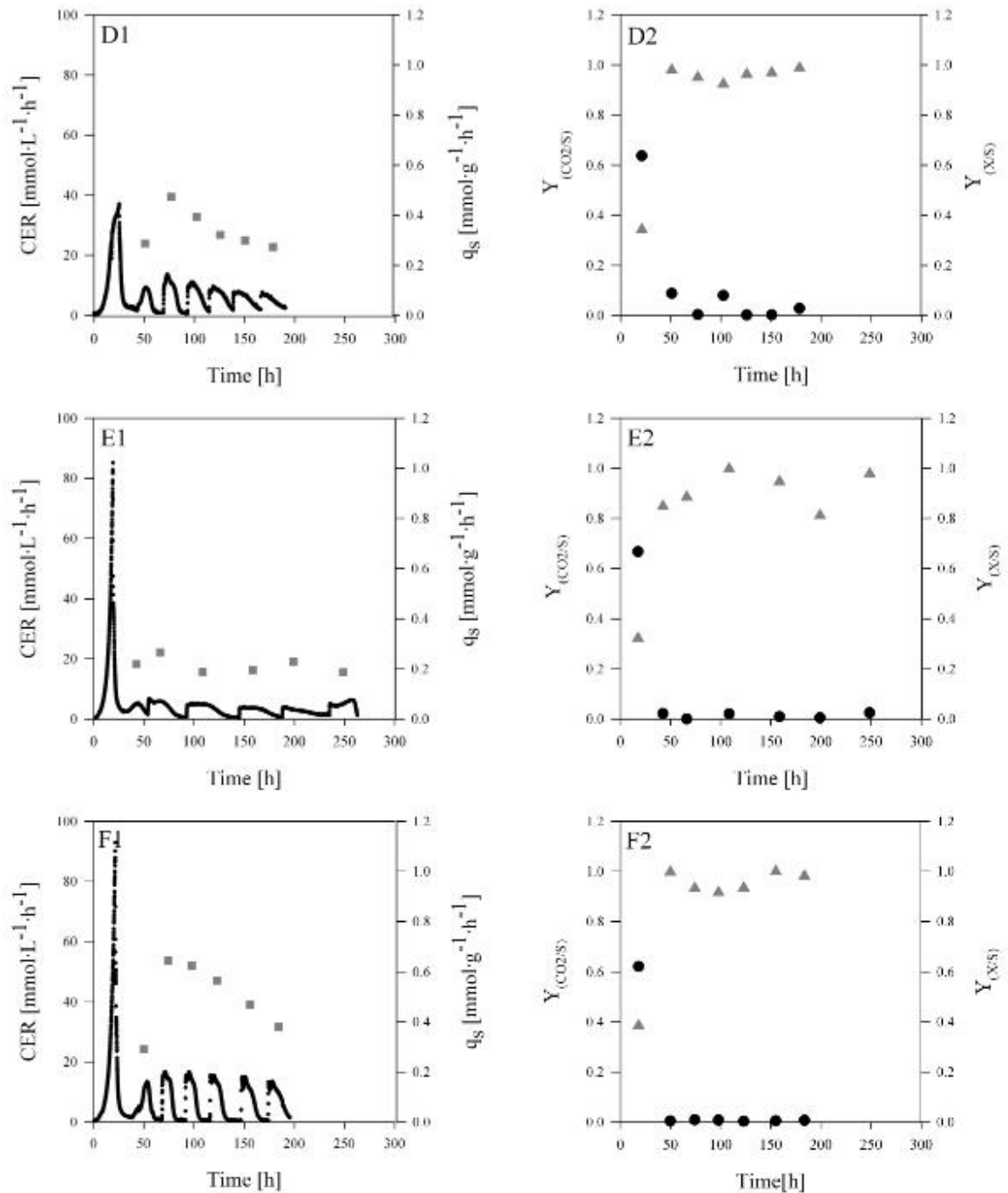
22. Huang, R.P., *Detection of multiple proteins in an antibody-based protein microarray system*. J Immunol Methods, 2001. **255**(1-2): p. 1-13.
23. Dotsikas, Y. and Y.L. Loukas, *Improved performance of antigen-HRP conjugate-based immunoassays after the addition of anti-HRP antibody and application of a liposomal chemiluminescence marker*. Anal Sci, 2012. **28**(8): p. 753-7.
24. Palmgren, B., et al., *Horseradish peroxidase dye tracing and embryonic statoacoustic ganglion cell transplantation in the rat auditory nerve trunk*. Brain Res, 2011. **1377**: p. 41-9.
25. Romero, M.I., M.A. Romero, and G.M. Smith, *Visualization of axonally transported horseradish peroxidase using enhanced immunocytochemical detection: a direct comparison with the tetramethylbenzidine method*. J Histochem Cytochem, 1999. **47**(2): p. 265-72.
26. Narhi, L.O., et al., *The Effect of Carbohydrate on the Structure and Stability of Erythropoietin*. J Biol Chem, 1991. **266**(34): p. 23022-23026.
27. Wang, C.Q., et al., *Influence of the carbohydrate moiety on the stability of glycoproteins*. Biochem, 1996. **35**(23): p. 7299-7307.
28. Ehlers, M.R.W., Y.N.P. Chen, and J.F. Riordan, *The Unique N-Terminal Sequence of Testis Angiotensin-Converting Enzyme Is Heavily O-Glycosylated and Unessential for Activity or Stability*. Biochem Biophys Res Commun, 1992. **183**(1): p. 199-205.
29. Powell, L.M. and R.H. Pain, *Effects of Glycosylation on the Folding and Stability of Human, Recombinant and Cleaved Alpha-1-Antitrypsin*. J Mol Biol, 1992. **224**(1): p. 241-252.
30. Tams, J.W. and K.G. Welinder, *Glycosylation and thermodynamic versus kinetic stability of horseradish peroxidase*. Febs Lett, 1998. **421**(3): p. 234-236.
31. Tams, J.W. and K.G. Welinder, *Mild Chemical Deglycosylation of Horseradish-Peroxidase Yields a Fully Active, Homogeneous Enzyme*. Anal Biochem, 1995. **228**(1): p. 48-55.
32. Kang, L.X., et al., *Recombinant expression of chitosanase from Bacillus subtilis HD145 in Pichia pastoris*. Carbohydr Res, 2012. **352**: p. 37-43.
33. Sainz-Pastor, N., et al., *Deglycosylation to obtain stable and homogeneous Pichia pastoris-expressed N-A1 domains of carcinoembryonic antigen*. Int J Biol Macromol, 2006. **39**(1-3): p. 141-50.
34. Hamilton, S.R., et al., *Production of complex human glycoproteins in yeast*. Science, 2003. **301**(5637): p. 1244-1246.
35. Choi, B.K., et al., *Use of combinatorial genetic libraries to humanize N-linked glycosylation in the yeast Pichia pastoris*. PNAS, 2003. **100**(9): p. 5022-5027.
36. Hamilton, S.R. and T.U. Gerngross, *Glycosylation engineering in yeast: the advent of fully humanized yeast*. Curr Opin Biotechnol, 2007. **18**(5): p. 387-92.
37. Vervecken, W., et al., *In vivo synthesis of mammalian-like, hybrid-type N-glycans in Pichia pastoris*. Appl Environ Microbiol, 2004. **70**(5): p. 2639-46.
38. Krainer, F.W., et al., *Knockout of an endogenous mannosyltransferase increases the homogeneity of glycoproteins produced in Pichia pastoris*. Sci Rep, 2013. **3**: p. 3279.

39. Asad, S., K. Khajeh, and N. Ghaemi, *Investigating the Structural and Functional Effects of Mutating Asn Glycosylation Sites of Horseradish Peroxidase to Asp*. Appl Biochem Biotechnol, 2011. **164**(4): p. 454-463.
40. Naatsaari, L., et al., *Deletion of the Pichia pastoris KU70 homologue facilitates platform strain generation for gene expression and synthetic biology*. PLoS One, 2012. **7**(6): p. e39720.
41. Spadiut, O., et al., *Improving thermostability and catalytic activity of pyranose 2-oxidase from Trametes multicolor by rational and semi-rational design*. FEBS J, 2009. **276**(3): p. 776-92.
42. Polizzi, K.M., et al., *Stability of biocatalysts*. Current Opinion in Chemical Biology, 2007. **11**(2): p. 220-225.
43. Zhu, A., Z.K. Wang, and R. Beavis, *Structural studies of alpha-N-acetylgalactosaminidase: effect of glycosylation on the level of expression, secretion efficiency, and enzyme activity*. Arch Biochem Biophys, 1998. **352**(1): p. 1-8.
44. Ito, K., et al., *Site-specific glycosylation at Asn-292 in ovalbumin is essential to efficient secretion in yeast*. J Biochem, 2007. **141**(2): p. 193-9.
45. Ito, K., et al., *Importance of N-glycosylation positioning for secretion and folding of ovalbumin*. Biochem Biophys Res Commun, 2007. **361**(3): p. 725-31.
46. Zou, S., et al., *N-Glycosylation enhances functional and structural stability of recombinant beta-glucuronidase expressed in Pichia pastoris*. J Biotechnol, 2013. **164**(1): p. 75-81.
47. Lin, Z., T. Thorsen, and F.H. Arnold, *Functional expression of horseradish peroxidase in E. coli by directed evolution*. Biotechnol Prog, 1999. **15**(3): p. 467-71.
48. Gilfoyle, D.J., J.N. Rodriguez-Lopez, and A.T. Smith, *Probing the aromatic-donor-binding site of horseradish peroxidase using site-directed mutagenesis and the suicide substrate phenylhydrazine*. Eur J Biochem, 1996. **236**(2): p. 714-22.
49. Morawski, B., et al., *Functional expression of horseradish peroxidase in Saccharomyces cerevisiae and Pichia pastoris*. Protein Eng, 2000. **13**(5): p. 377-384.
50. Asad, S., et al., *Phosphate buffer effects on thermal stability and H<sub>2</sub>O<sub>2</sub>-resistance of horseradish peroxidase*. Int J Biol Macromol, 2011. **48**(4): p. 566-70.
51. Abad, S., et al., *Stepwise engineering of a Pichia pastoris D-amino acid oxidase whole cell catalyst*. Microb Cell Fact, 2010. **9**: p. 24.
52. Li, S. and M.F. Wilkinson, *Site-directed mutagenesis: a two-step method using PCR and DpnI*. Biotechniques, 1997. **4**: p. 588-590.
53. Lin-Cereghino, J., et al., *Condensed protocol for competent cell preparation and transformation of the methylotrophic yeast Pichia pastoris*. Biotechniques, 2005. **38**(1): p. 44-48.
54. Pabst, M., et al., *Isomeric analysis of oligomannosidic N-glycans and their dolichol-linked precursors*. Glycobiology, 2012. **22**(3): p. 389-99.

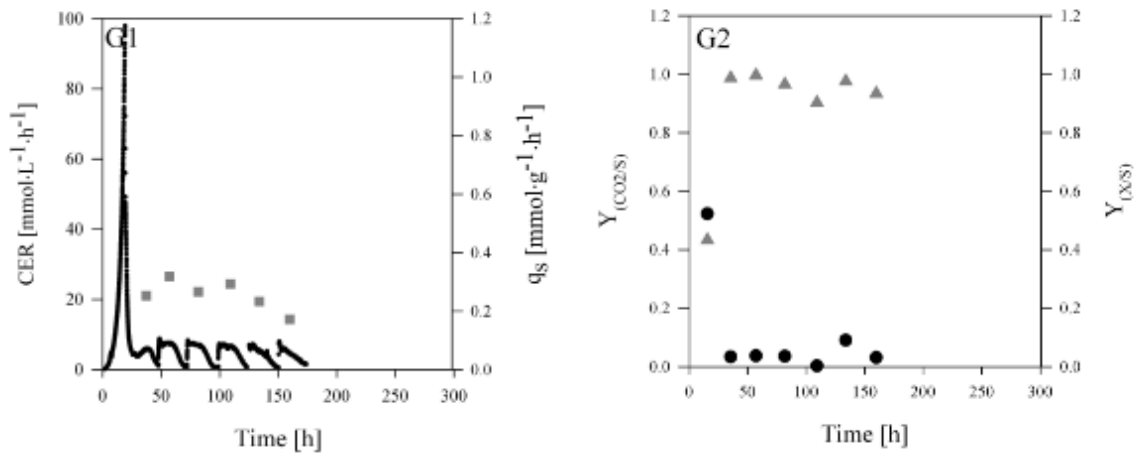
## 8 Supplementary Figures



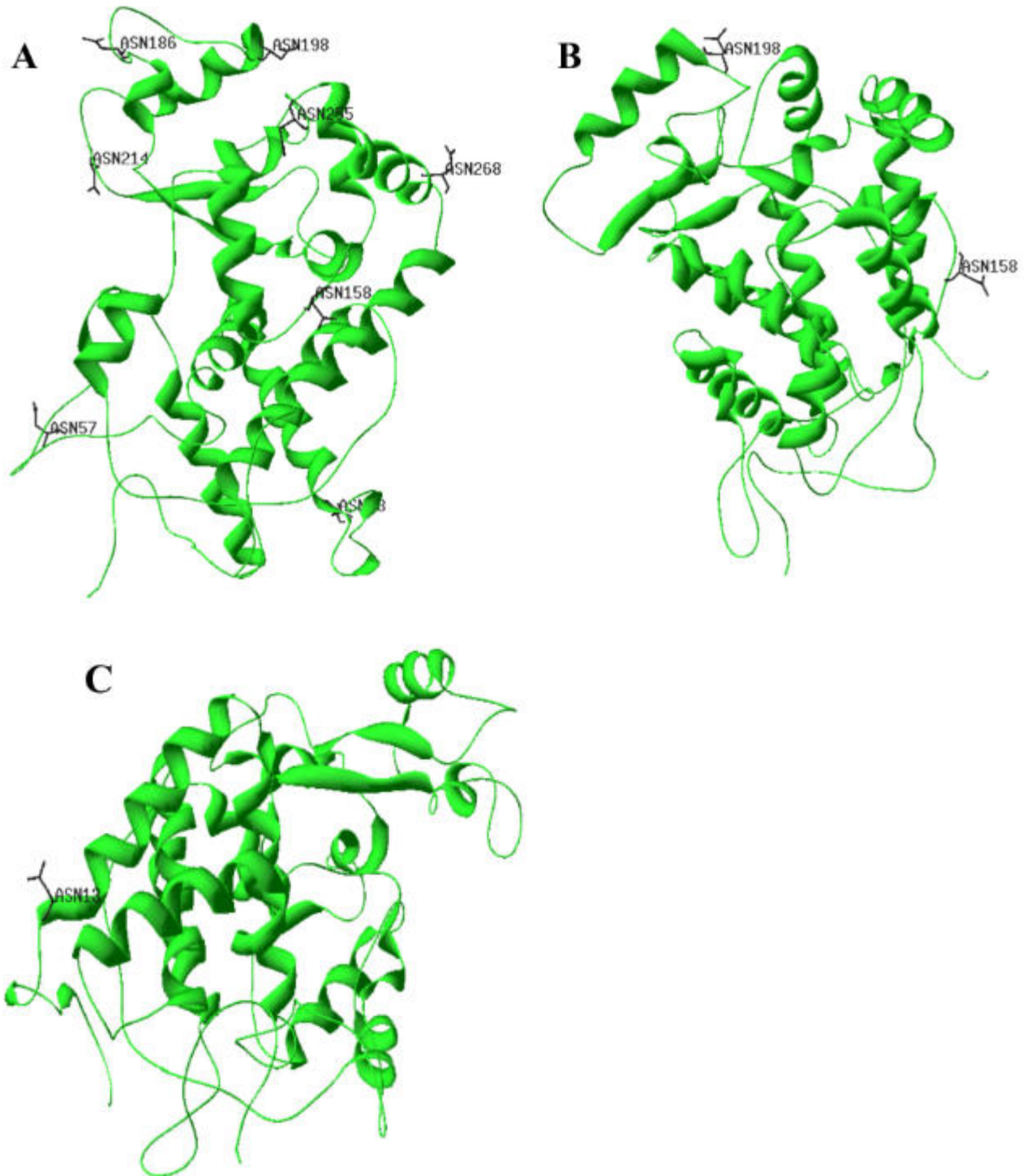
**Supplementary Figure 1:** In the left graphs (1) carbon dioxide evolution rate (CER; black line) and specific methanol uptake rate (grey square) over time are shown. In the right graphs (2), the carbon dioxide yield ( $Y_{CO_2/S}$ ; grey triangle) and the biomass yield ( $Y_{X/S}$ ; black dot) are represented. A) N13D; B) N158D; C) N186D; D) N198D; E) N214S; F) N255D; G) N268D.



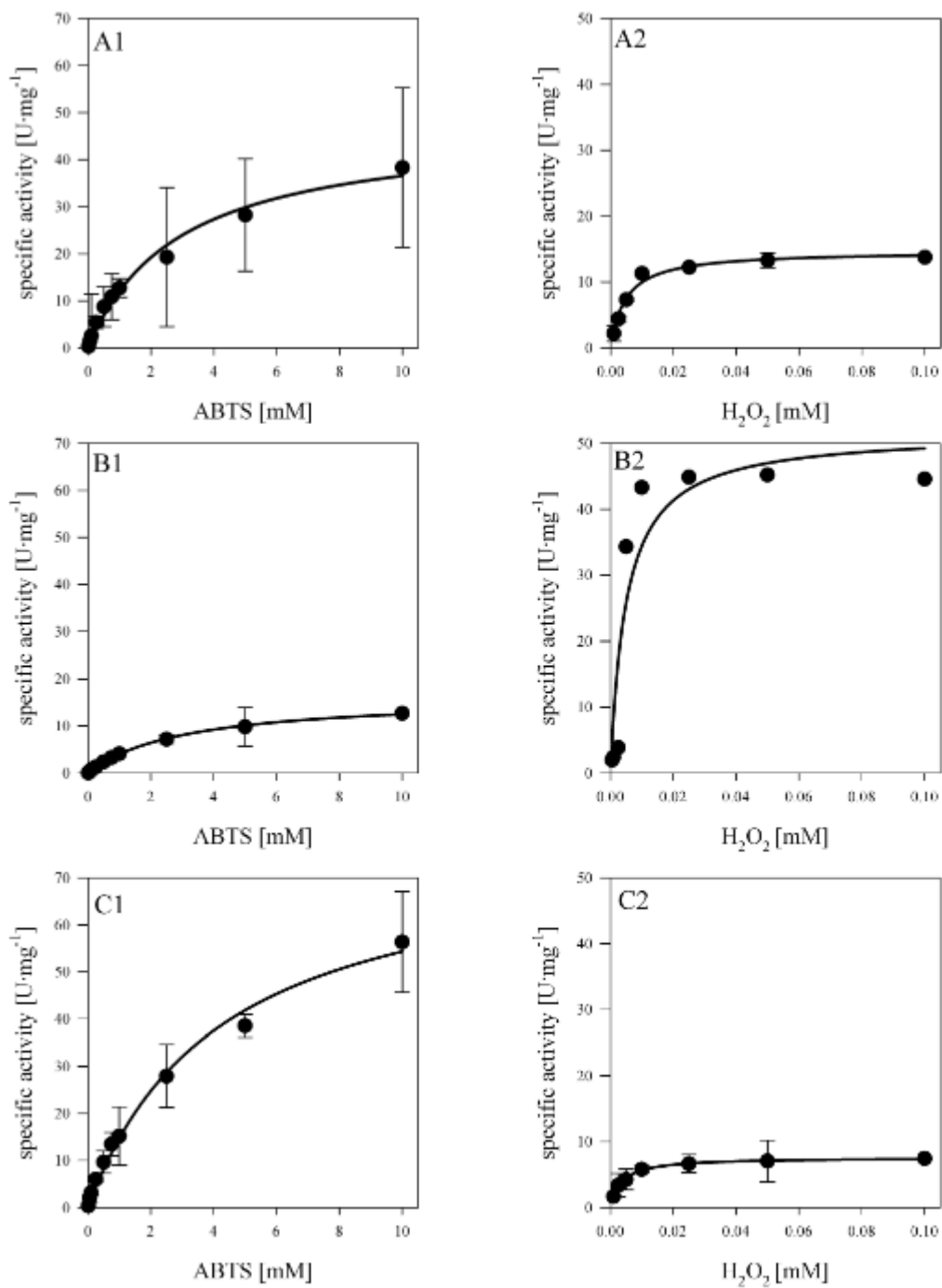
**Supplementary Figure 2:** In the left graphs (1) carbon dioxide evolution rate (CER; black line) and specific methanol uptake rate (grey square) over time are shown. In the right graphs (2), the carbon dioxide yield ( $Y_{CO_2/S}$ ; grey triangle) and the biomass yield ( $Y_{X/S}$ ; black dot) are represented. A) N13D; B) N158D; C) N186D; D) N198D; E) N214S; F) N255D; G) N268D.



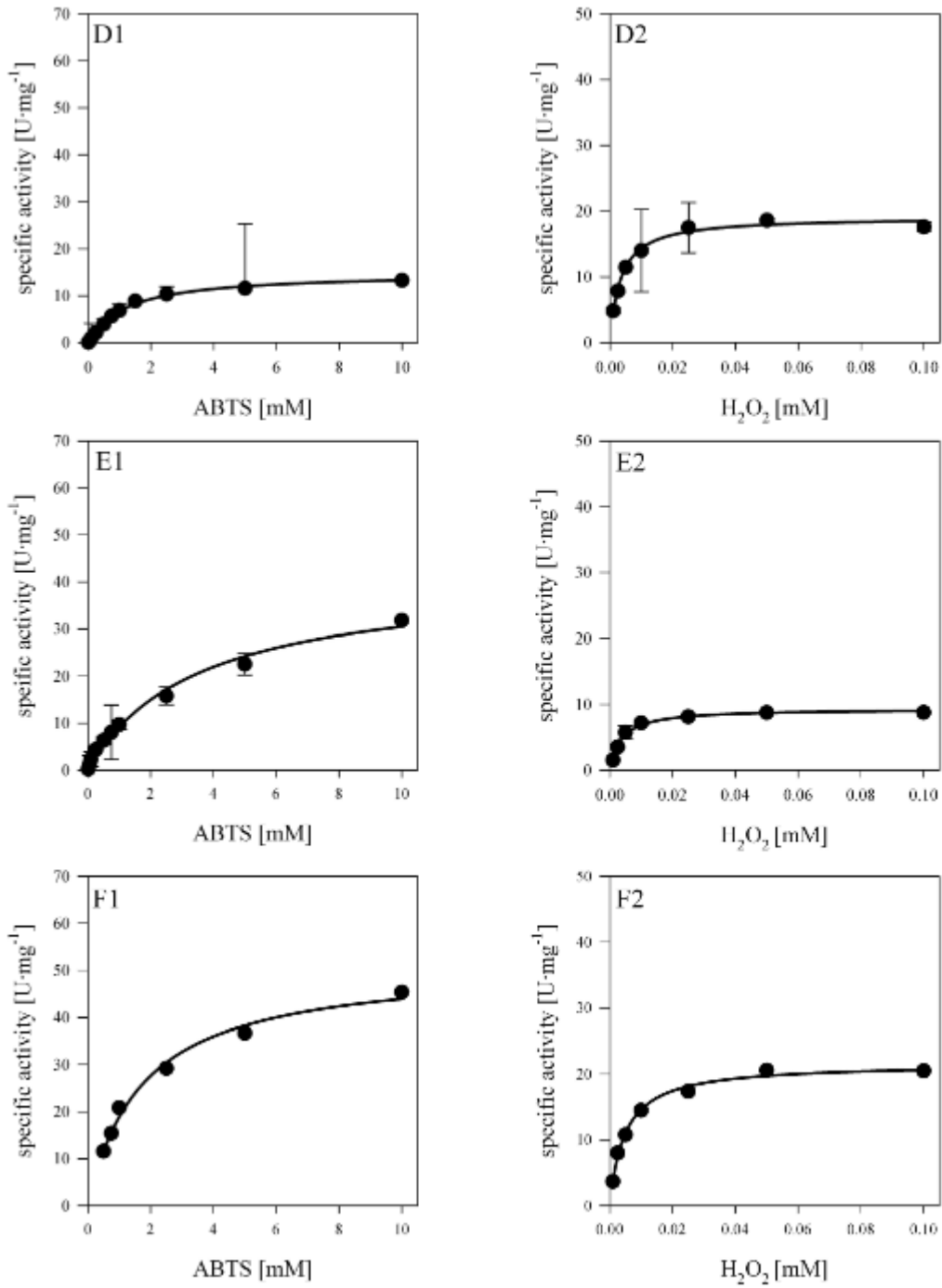
**Supplementary Figure 3:** In the left graphs (1) carbon dioxide evolution rate (CER; black line) and specific methanol uptake rate (grey square) over time are shown. In the right graphs (2), the carbon dioxide yield ( $Y_{CO_2/S}$ ; grey triangle) and the biomass yield ( $Y_{X/S}$ ; black dot) are represented. A) N13D; B) N158D; C) N186D; D) N198D; E) N214S; F) N255D; G) N268D.



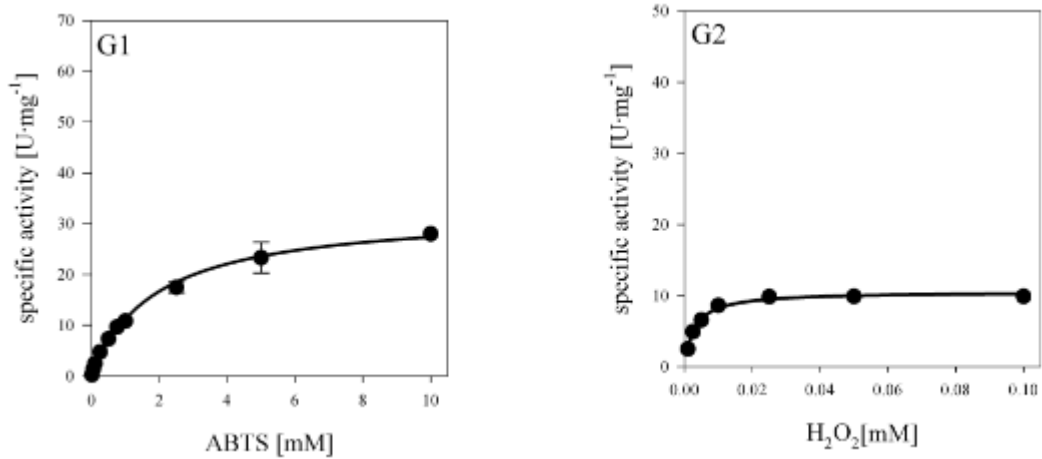
**Supplementary Figure 4:** Representation of the protein structure of HRP C1A (PDB 1ATJ). A, all the 8 N-glycosylation sites are visualized; B, the protein was rotated in a way to clearly see the location of N158 and N198; C, the protein was rotated in a way to clearly see the location of N13.



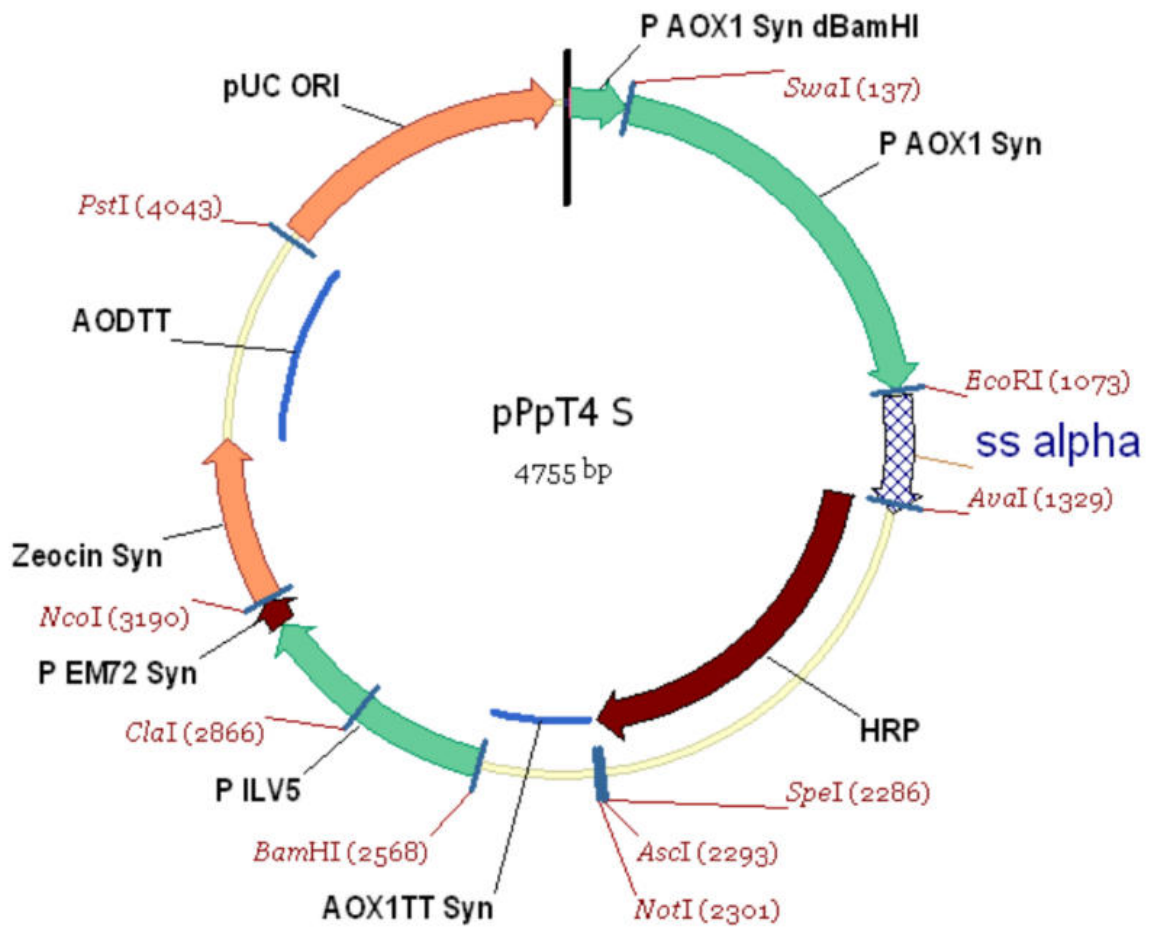
**Supplementary Figure 5:** In the left graphs (1) specific activity towards ABTS is shown. In the right graphs (2) specific activity towards H<sub>2</sub>O<sub>2</sub> is represented. A) N13D; B) N158D; C) N186D; D) N198D; E) N214S; F) N255D; G) N268D.



**Supplementary Figure 6:** In the left graphs (1) specific activity towards ABTS is shown. In the right graphs (2) specific activity towards H<sub>2</sub>O<sub>2</sub> is represented. A) N13D; B) N158D; C) N186D; D) N198D; E) N214S; F) N255D; G) N268D.



**Supplementary Figure 7:** In the left graphs (1) specific activity towards ABTS is shown. In the right graphs (2) specific activity towards H<sub>2</sub>O<sub>2</sub> is represented. A) N13D; B) N158D; C) N186D; D) N198D; E) N214S; F) N255D; G) N268D.



**Supplementary Figure 8.** Schematic illustration of the vector pPpT4\_S harboring the HRP isoenzyme C1A.

## **CHAPTER III**

### **Expression of HRP C1A in glyco-engineered *P.* *pastoris***

# Knockout of an endogenous mannosyltransferase increases the homogeneity of glycoproteins produced in *Pichia pastoris*

Published in the journal Scientific Reports, November 2013

DOI: 10.1038/srep03279

Florian W. Krainer<sup>1</sup>, Christoph Gmeiner<sup>2</sup>, Lukas Neutsch<sup>3</sup>, Markus Windwarder<sup>4</sup>, **Robert Pletzenauer**<sup>2</sup>, Friedrich Altmann<sup>4</sup>, Anton Glieder<sup>5</sup> and Oliver Spadiut<sup>2\*</sup>

<sup>1</sup> Graz University of Technology, Institute of Molecular Biotechnology, Graz, Austria

<sup>2</sup> Vienna University of Technology, Institute of Chemical Engineering, Research Area Biochemical Engineering, Vienna, Austria

<sup>3</sup> University of Vienna, Department of Pharmaceutical Technology and Biopharmaceutics, Vienna, Austria

<sup>4</sup> Department of Chemistry, University of Natural Resources and Life Sciences, Vienna Austria

<sup>5</sup> Austrian Centre of Industrial Biotechnology (ACIB GmbH), Graz, Austria

\*Corresponding Author: Oliver Spadiut, Vienna University of Technology, Institute of Chemical Engineering, Research Area Biochemical Engineering, Gumpendorfer Strasse 1a, A-1060 Vienna, Austria. Tel: +43 1 58801 166473, Fax: +43 1 58801 166980; e-mail: oliver.spadiut@tuwien.ac.at

## Keywords

*Pichia pastoris*, glycoprotein, glycosylation, glycoengineering, *OCH1*, mannosyltransferase, horseradish peroxidase, bioreactor cultivation, recombinant protein production

## 1 Abstract

The yeast *Pichia pastoris* is a common host for the recombinant production of biopharmaceuticals, capable of performing posttranslational modifications like glycosylation of secreted proteins. However, the activity of the *OCH1* encoded  $\alpha$ -1,6-mannosyltransferase triggers hypermannosylation of secreted proteins at great heterogeneity, considerably hampering downstream processing and reproducibility. Horseradish peroxidases are versatile enzymes with applications in diagnostics, bioremediation and cancer treatment. Despite the importance of these enzymes, they are still isolated from plant at low yields with different biochemical properties. Here we show the production of homogeneous glycoprotein species of recombinant horseradish peroxidase by using a *P. pastoris* platform strain in which *OCH1* was deleted. This *och1* knockout strain showed a growth impaired phenotype and considerable rearrangements of cell wall components, but nevertheless secreted more homogeneously glycosylated protein carrying mainly Man8 instead of Man10 N-glycans as a dominant core glycan structure at a volumetric productivity of 70 % of the wildtype strain.

## 2 Introduction

The methylotrophic yeast *Pichia pastoris* has long been used for the production of recombinant proteins at high titers. Up to 22 g·L<sup>-1</sup> have been reported for intracellularly produced recombinant hydroxynitrile lyase [1] and approximately 15 g·L<sup>-1</sup> [1] for secreted recombinant gelatin [2], demonstrating the high production capacity of this microbial host while being able to grow on comparatively simple and inexpensive media. Not only can *P. pastoris* be grown to cell densities as high as 160 g·L<sup>-1</sup> dry cell weight [3], it is also capable of performing posttranslational modifications, including the formation of correct disulfide bridges and the glycosylation of secretory proteins, rendering *P. pastoris* specifically suitable for the production of complex eukaryotic proteins [4].

Glycosylation has long been known to affect various protein properties such as solubility, stability and enzymatic activity (e.g. [5,6]), which need to be evaluated on a case-by-case basis.

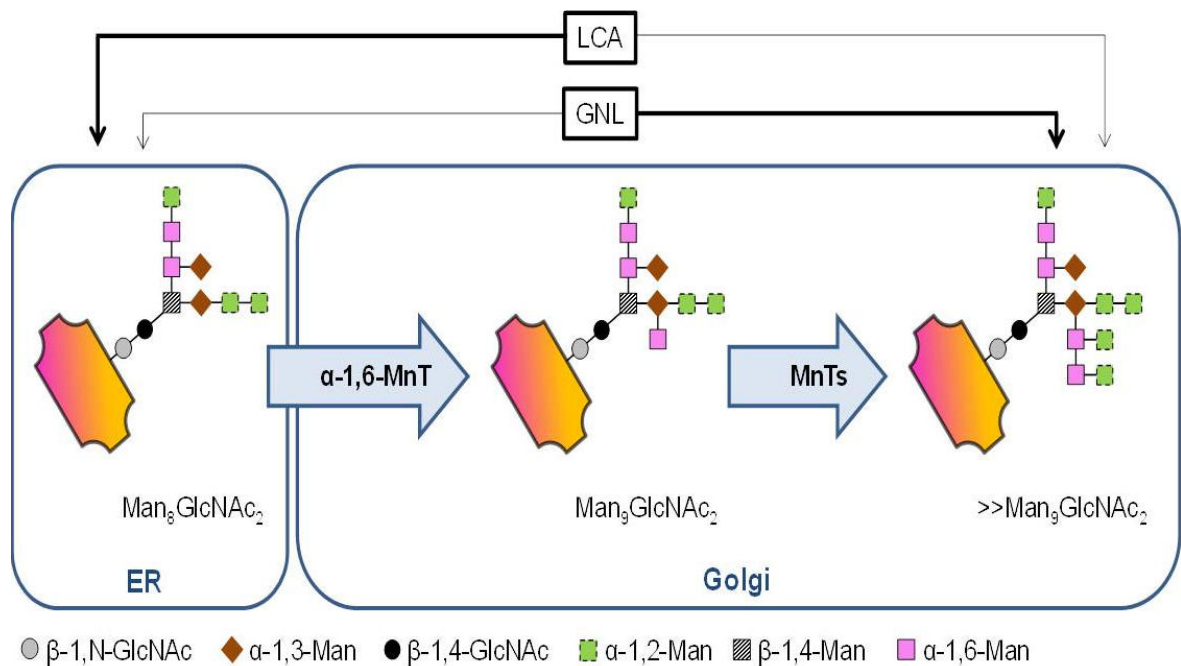


**Figure 1: Och1p in N-glycan biosynthesis.** In the Golgi, the  $\alpha$ -1,6-mannosyltransferase activity ( $\alpha$ -1,6-MnT) of Och1p extends the N-linked  $\text{Man}_8\text{GlcNAc}_2$  core glycan, which is then heterogeneously hyperglycosylated by several additional (phospho-) mannosyltransferases (MnTs). *Galanthus nivalis* lectin (GNL) and *Lens culinaris* lectin (LCA) bind to the different glycan structures either with high (thick arrow) or low (thin arrow) specificity.

Whereas only little is known about O-linked glycosylation, the biosynthesis of N-glycans is well understood. N-glycans are linked to the amido groups of asparagine residues that are recognized by glycotransferases in the sequence motif N-X-S/T, where X is any amino acid but proline. Initially, the biosynthesis steps of N-glycans in yeast and mammals are identical. Dolichol phosphate-linked N-acetylglucosamine (DoIP-GlcNAc) is synthesized by the transfer of GlcNAc from uridine diphosphate (UDP) onto DoIP on the cytoplasmic side of the ER. After extension to DoIP-linked  $\text{Man}_5\text{GlcNAc}_2$ , this structure is enzymatically flipped to the ER lumen, where further glucose (Glc) and Man residues are added to form a core glycan,  $\text{Glc}_3\text{Man}_9\text{GlcNAc}_2$ , which is transferred to an asparagine within the N-X-S/T sequence motif of a nascent protein chain. Subsequently, the three terminal Glc residues and one Man residue are trimmed by glucosidases I and II and an ER-residing  $\alpha$ -1,2-mannosidase to form  $\text{Man}_8\text{GlcNAc}_2$ . At this point, the newly formed glycoprotein is transported to the Golgi apparatus, which is where the yeast and mammalian N-glycosylation pathways diverge [7–9]. In the mammalian Golgi apparatus,  $\alpha$ -1,2-mannosidases trim the core glycan further to form  $\text{Man}_5\text{GlcNAc}_2$ . Ultimately, addition of GlcNAc by a  $\alpha$ -N-acetylglucosaminyltransferase I (GnTI),

trimming of two further Man residues by a mannosidase II and yet further addition of GlcNAc, galactose (Gal) and sialic acid (Sia) residues by the respective transferases result in the complex N-glycan structures of mammalian proteins [10]. In the yeast Golgi, on the other hand, the Man<sub>8</sub>GlcNAc<sub>2</sub> glycan is not subjected to further trimming reactions but is substantially extended. In *Saccharomyces cerevisiae*, more than 100 Man residues may account for hypermannosyl N-glycans on secretory proteins. However, the extent of hypermannosylation varies considerably and seems to depend on so far unknown influences, causing vast heterogeneity in the N-glycan pattern of secreted glycoproteins. In *S. cerevisiae* as well as in *P. pastoris* and other yeasts, the first reaction in hypermannosylation is catalyzed by an  $\alpha$ -1,6-mannosyltransferase (Och1p) that is encoded by the gene Outer CHain elongation 1 (*OCH1*), which was first discovered and characterized in *S. cerevisiae* [11,12]. Och1p uses Man from guanosin diphosphate and links it to the core glycan by an  $\alpha$ -1,6-glycosidic bond, forming a substrate that triggers additional mannosylation (Figure 1). Whereas *S. cerevisiae* holds a repertoire of Golgi-resident  $\alpha$ -1,2-,  $\alpha$ -1,3 and  $\alpha$ -1,6-mannosyl and mannosylphosphate transferases, *P. pastoris* seems to lack the Golgi-resident  $\alpha$ -1,3-mannosyltransferase, but to possess four additional  $\alpha$ -mannosyltransferases instead [7,13,14].

Although not as extensive as those of *S. cerevisiae*, the N-glycans of *P. pastoris* are also of the high mannose type and the humanization of the N-glycosylation machinery of *P. pastoris* has been the subject of several studies (Table1).

Here, we report the deletion of the *OCH1* gene from the *P. pastoris* genome in an irreversible and straight forward approach. Thereby, we generated a new *P. pastoris* platform strain that allows the production of recombinant proteins with shorter glycan structures of considerably increased homogeneity compared to proteins produced in a wildtype strain. In contrast to previous glycoengineering studies, which required several time- and labor-intensive steps of strain engineering, we achieved more homogeneously glycosylated protein with a single gene knockout step. Horseradish peroxidase (HRP) is a versatile enzyme with applications in diagnostics and histochemistry, bioremediation and cancer treatment. However, due to the lack of an appropriate recombinant production process, HRP preparations are still derived from horseradish roots as mixtures of different isoenzymes [15]. In the present

study, we produced recombinant HRP in an *och1* knockout strain in the controlled environment of a bioreactor, purified and characterized the enzyme, thus demonstrating the general applicability of this new platform strain by the example of this industrially and medically relevant enzyme.

**Table 1: Humanization of N-glycans in *P. pastoris*.** Selected studies focusing on the humanization of the N-glycans on *P. pastoris* derived glycoproteins. Bmt,  $\beta$ -mannosyltransferase; Mns, mannosidase; GnT,  $\beta$ -N-acetylglucosaminyltransferase; UDP-GlcNAc, uridine diphosphate-N-acetylglucosamine; *OCH1*, outer chain elongation gene 1.

Content	References
Introduction of $\alpha$ -1,2-Mns, GnTI and an UDP-GlcNAc transporter via a combinatorial genetic library approach in a $\Delta och1::URA3$ strain	13,50
Introduction of an UDP-GlcNAc transporter, $\alpha$ -1,2-MnsIA, MnsII, GntI, GntII in a $\Delta och1::URA3$ strain	51
Introduction of $\alpha$ -1,2-Mns and GnTI, <i>OCH1</i> inactivation via a knockin plasmid	10
GlycoSwitch plasmids for <i>OCH1</i> inactivation and introduction of glycosidase and glycosyltransferase activities to produce complex terminally galactosylated glycoproteins	52
Introduction of sialic acid biosynthesis pathway and corresponding transporter and transferase activities to produce complex terminally sialylated glycoproteins	53
Elimination of $\alpha$ -Mns resistant glycan structures by inactivation of the activities of Bmt1p, Bmt2p and Bmt3p	54

## 3 Results

### 3.1 Knockout of *OCH1* from *Ppku70-* and *PpMutS*

In yeast, the *OCH1* gene encodes an  $\alpha$ -1,6-mannosyltransferase whose activity triggers the subsequent transfer of further mannose and phosphomannose residues onto the N-glycans of secreted proteins in the Golgi apparatus, resulting in heterogeneously hyperglycosylated protein species that appear as a smear on SDS gels, e.g. [16,17]. This hyperglycosylation not only limits the use of yeast derived proteins as biopharmaceuticals but also greatly impedes traditional downstream processing. Hence, a *P. pastoris* strain that allows the production of less

heterogeneously glycosylated proteins would considerably relieve protein production processes with *P. pastoris*.

A flipper cassette targeting to the *OCH1* locus was transformed to a *Ppku70-* strain to replace the *OCH1* open reading frame. This *Ppku70-* strain has to rely on homologous recombination for gene integration events, in contrast to a wildtype strain [18]. The cassette construct and the knockout workflow are schematically shown in Figure 2.

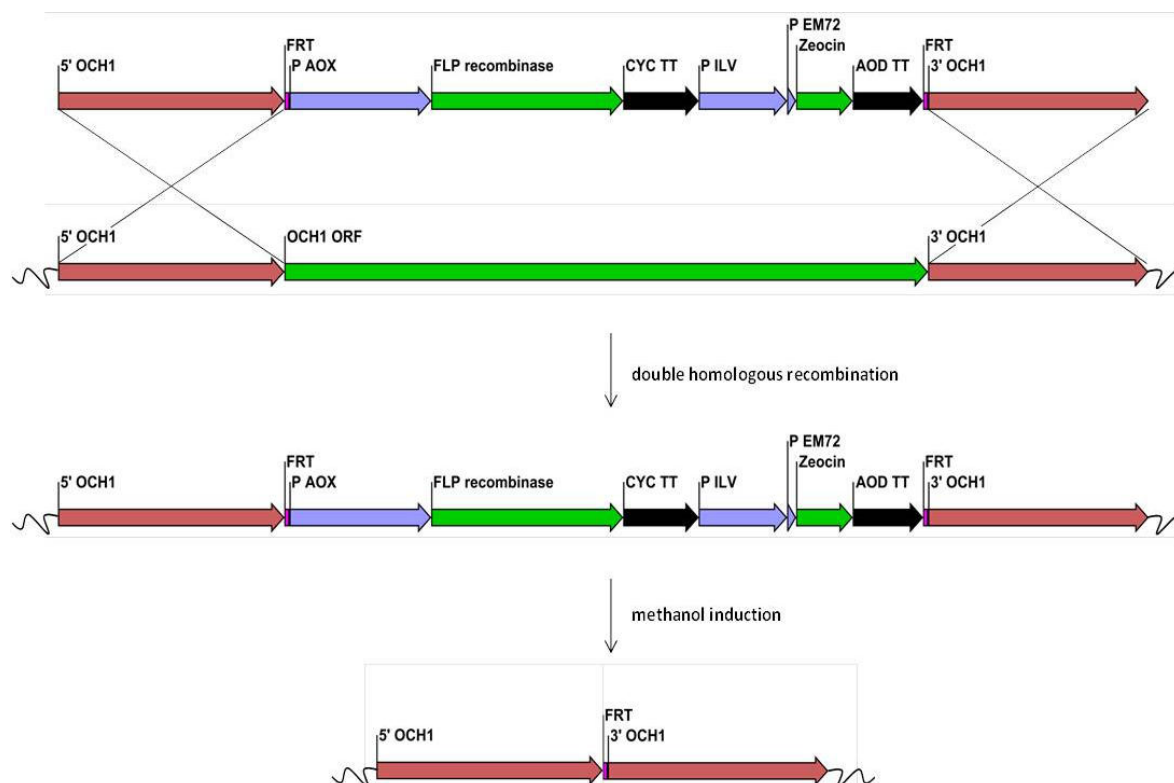


**Figure 2: Schematic workflow of the knockout of *OCH1* using a flipper cassette.** The regions 5' *OCH1* and 3' *OCH1* represent sequences upstream and downstream of the *OCH1* ORF, respectively. The 34 bp flipper recombinase target (*FRT*) sequences flank the *AOX1* promoter (*P AOX1*), the *FLP recombinase* ORF, the *CYC1* transcription terminator (*CYC TT*), a constitutive eukaryotic and a prokaryotic promoter (*P ILV* and *P EM72*, respectively), a *ble* ORF mediating *Zeocin*<sup>TM</sup> resistance and an *AOD* transcription terminator (*AOD TT*). A double homologous recombination event replaced the *OCH1* ORF in the genome with the flipper cassette. Growth of recombinant cells on methanol induced the production of the *FLP recombinase* which recognized the two *FRT* sites and excised the inner sequence, leaving only one *FRT* site in the genome. Single fragments are not drawn to scale.

Transformation of the flipper cassette to the *Ppku70-* strain resulted in only few *Zeocin*<sup>TM</sup> resistant clones. However, Sanger sequencing of a PCR amplified fragment of the *OCH1* locus from genomic DNA showed that the majority of the tested transformants had correct integration of the transformed cassette. The transformants grew slowly and formed colonies of abnormal shape. This phenotype

was preserved when the strains were grown on minimal methanol agar plates to induce the production of the FLP recombinase and subsequent excision of the inner part of the flipper cassette containing the expression cassettes for the FLP recombinase and the Zeocin™ resistance enzyme. Reconstituted sensitivity to Zeocin™, PCR and Sanger sequencing of the former *OCH1* locus confirmed the successful excision of the inner part of the flipper cassette and the efficient replacement of the former *OCH1* ORF with a single *FRT* site of 34 bp.

Transformation of the same *OCH1* flipper cassette to *PpMutS* resulted in hundreds of clones resistant to Zeocin™. Initial PCR based screenings of over 100 randomly chosen clones did not give any positive hits, analogously to what has been described by Vervecken *et al.* [10]. However, after having identified the corresponding phenotype of positive transformants in the *Ppku70*- based *och1* knockout strain, designated *PpFWK1*, also *PpMutS* based transformants with correct integration of the flipper cassette could be spotted easily on the agar plates since they showed the same unusual colony phenotype as colonies of *PpFWK1* (Figure 3).

Increasing the incubation time of the transformed cells on the agar plates to at least four days allowed growth of the *och1* knockout colonies to a size at which their abnormal shape was an obvious hint to their genotype (Figure 3). Again, Zeocin™ sensitivity was reconstituted by induction of the FLP recombinase on minimal methanol agar plates and the replacement of the *OCH1* ORF by a single *FRT* site was shown by PCR and Sanger sequencing. The observed phenotype of the generated *och1* knockout strain *PpFWK3* included slow growth, abnormal colony shape and temperature sensitivity at 37 °C (data not shown). Upon transformation of the wildtype *OCH1* promoter and *OCH1* ORF to *PpFWK3*, the detrimental phenotype was found to be complemented. PCR analyses confirmed the unaltered replacement of the former *OCH1* ORF by a *FRT* site, but the presence of the complementing *OCH1* ORF somewhere else in the genome due to ectopic integration of the transformed plasmid pPpT4\_BamHI\_*OCH1*rescue.

## 3.2 Strain morphology

**Cell morphology and cell division of an *och1* knockout strain.** Consistent with previous reports on *Och1p* deficient *S. cerevisiae* strains [19,20], we found the N-

glycosylation mutant to be characterized by an altered phenotype and growth profile (Table 2). In contrast to the wildtype based strain *PpMutS*, the *och1* knockout strain *PpFWK3* grew in the form of large cell clusters with clumpy appearance and multibudded cells (Figure 4). Daughter cells within these clusters displayed clearly

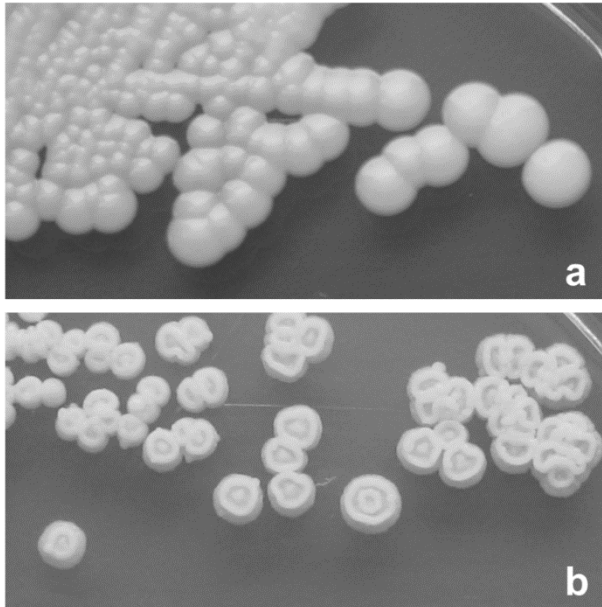


**Figure 3: Colony phenotypes.** a, *PpMutS*; b, *PpFWK3*. Both strains were grown on YPD agar.

segregated vacuoles, but remained stably attached to the wall of mother cells (Supplementary Figure 1).

Knockout induced stress response is reflected by a spatial rearrangement of WGA/STL binding sites. The direct functional implication of the altered N-glycosylation in *PpFWK3* for cell morphology and cytokinesis was further illustrated by a striking difference in the chitin deposition after *OCH1* knockout (Supplementary Figure 1). In lectin based glycoprofiling studies, we observed substantially

altered binding patterns for the GlcNAc-specific lectin WGA, with the reactive carbohydrate motifs being homogeneously distributed across the entire cell surface in the *och1* knockout strain, instead of remaining confined to the bud scars as in *PpMutS* (Figure 5 and Supplementary Figure 1).

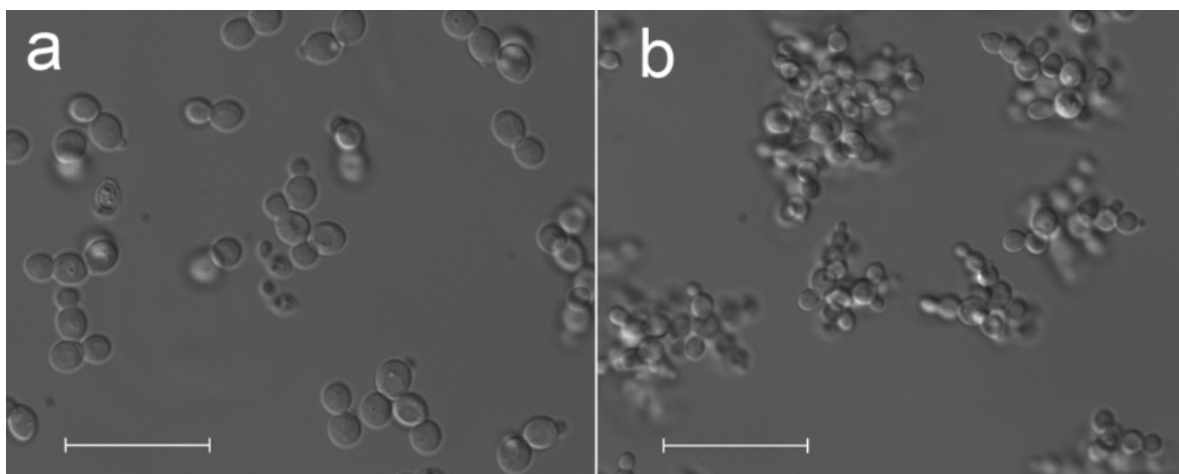


**Figure 4: Phenotypic change in *P. pastoris* upon *OCH1* knockout.** Representative DIC micrographs of *PpMuts* and *PpFWK3*. a, *PpMutS* cells in batch culture. b, covalently linked clusters of multibudded cells in *PpFWK3* during the same cultivation phase. Scale bars represent 25 µm.

In order to assess whether a mere alteration in the steric accessibility of chitin chains in the lateral wall was responsible for the difference in the WGA staining behavior or whether chitin was actually specifically localized at bud scars, *PpMutS* cells were subjected to the same fluorescence microscopic analysis after treatment with concentrated methanol, leading to denaturation of mannoproteins and a substantial increase in cell wall permeability [21]. The efficiency of the cell wall permeabilization protocol was validated by concomitant incubation with a usually non-membrane penetrating DAPI dye, which could readily access the nuclear space after methanol treatment.

**Table 2: Strain specific parameters of the different *P. pastoris* strains.** Parameters are defined in the footnote <sup>x</sup>.

	<i>PpMutS</i>	<i>PpMutS</i> <sup>HRP</sup>	<i>PpFWK3</i>	<i>PpFWK3</i> <sup>HRP</sup>
<b>max. <math>\mu_{\text{Gly}}</math> (<math>\text{h}^{-1}</math>)</b>	0.30	0.31	0.20	0.20
<b><math>q_{\text{Gly}}</math> (<math>\text{mmol}\cdot\text{g}^{-1}\cdot\text{h}^{-1}</math>)</b>	2.90	3.10	1.90	1.90
<b><math>Y_{\text{X/Gly}}</math> (<math>\text{Cmol}\cdot\text{Cmol}^{-1}</math>)</b>	0.63	0.41	0.61	0.54
<b><math>Y_{\text{CO}_2/\text{Gly}}</math> (<math>\text{Cmol}\cdot\text{Cmol}^{-1}</math>)</b>	0.33	0.64	0.37	0.44
<b><math>\Delta \text{time}_{\text{adapt}}</math> (h)</b>	15.7	19.9	6.60	8.90
<b><math>q_{\text{MeOH}}</math> (<math>\text{mmol}\cdot\text{g}^{-1}\cdot\text{h}^{-1}</math>)</b>	0.62	0.70	0.52	0.43
<b>max. <math>q_{\text{MeOH}}</math> (<math>\text{mmol}\cdot\text{g}^{-1}\cdot\text{h}^{-1}</math>)</b>	0.67	0.78	0.69	0.53
<b><math>Y_{\text{X/MeOH}}</math> (<math>\text{Cmol}\cdot\text{Cmol}^{-1}</math>)</b>	0.39	0.07	0.05	0.04
<b><math>Y_{\text{CO}_2/\text{MeOH}}</math> (<math>\text{Cmol}\cdot\text{Cmol}^{-1}</math>)</b>	0.57	1.02	constantly decreasing	constantly decreasing
<b>C-balance</b>	0.97	1.04	constantly decreasing	constantly decreasing
<b><math>q_{\text{p}}</math> (<math>\text{U}\cdot\text{g}^{-1}\cdot\text{h}^{-1}</math>)</b>	-	0.77	-	0.50
<b>vol. productivity (<math>\text{U}\cdot\text{L}^{-1}\cdot\text{h}^{-1}</math>)</b>	-	2.60	-	1.80
<b>efficiency factor (<math>\eta</math>) (<math>\text{U}\cdot\text{mmol}^{-1}</math>; [26])</b>	-	1.10	-	1.20

<sup>x</sup> max.  $\mu_{\text{Gly}}$ , maximum specific growth rate on glycerol;  $q_{\text{Gly}}$ , specific uptake rate of glycerol during the batch;  $Y_{\text{X/Gly}}$ , biomass yield on glycerol;  $Y_{\text{CO}_2/\text{Gly}}$ ,  $\text{CO}_2$  yield on glycerol;  $\Delta \text{time}_{\text{adapt}}$ , time from first addition of methanol to a maximum in offgas activity;  $q_{\text{MeOH}}$ , average specific uptake rate of methanol during consecutive methanol pulses; max.  $q_{\text{MeOH}}$ , maximum specific uptake rate of methanol during consecutive methanol pulses;  $Y_{\text{X/MeOH}}$  biomass yield on methanol;  $Y_{\text{CO}_2/\text{MeOH}}$ ,  $\text{CO}_2$  yield on methanol; C-balance, sum of biomass and  $\text{CO}_2$  yields;  $q_{\text{p}}$ , specific productivity of HRP; vol. productivity, volumetric productivity of HRP; efficiency factor; efficiency of the conversion of substrate methanol into product HRP

Still, methanol permeabilized *PpMutS* cells displayed only the conventional, bud scar selective staining pattern, contrasting to the generalized binding of GNL, which served as a control (Supplementary Figure 2).

Quantitatively, comparative overall ratios of WGA/FM<sup>®</sup> 4-64 were found for *PpMutS* and the *och1* knockout strain *PpFWK3* (Figure 6), indicating that mainly a spatial redistribution of chitin may be induced by altering the glycosylation machinery, but without general enhancement of the total cellular chitin level. In other words, the rather high chitin concentration at the bud scars in *PpMutS* seemed to be reduced in favor of an increased chitin deposition in the lateral cell walls of *PpFWK3*.

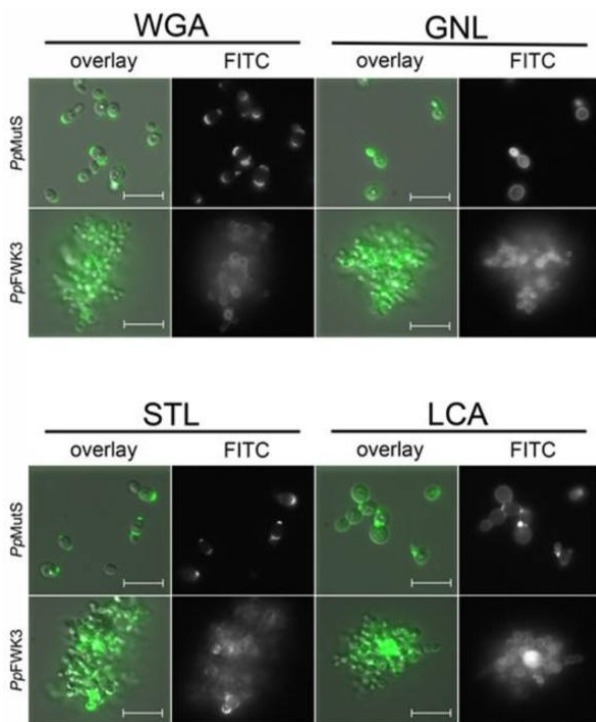


**Figure 5: Lectin based glycoprofiling of surface carbohydrate motifs in *PpMutS* and *PpFWK3*.** Live cells harvested in the exponential growth phase of batch cultivation were incubated with fluorescein labelled lectins. Micrographs show the isolated channel for FITC detection and merged images with DIC (overlay). Scale bars represent 10  $\mu$ m.

These results were also confirmed via the chitin binding lectin STL, which has a similar carbohydrate specificity profile as WGA but only limited affinity to isolated GlcNAc residues (Figure 6). Inactivation of the Och1p activity shifted the interaction capacity of mannose specific lectins. The *och1* knockout cells of the *PpFWK3* strain displayed a lower binding capacity for the lectin GNL than *PpMutS* cells (Figure 6). GNL interacts with high mannose N-glycans and preferably reacts with  $\alpha$ -1,3-Man residues, but also binds to  $\alpha$ -1,6 linked Man residues [22,23]. In the current study, the GNL/FM<sup>®</sup> 4-64 ratio was reduced by 50 % in *PpFWK3* as compared to *PpMutS*, but still remained the lectin

with highest binding capacity for this strain (Figure 6). In striking contrast, the binding levels of the glycan core-binding lectin LCA were increased upon *OCH1* knockout (Figure 6). Both, GNL and LCA showed an equal distribution across the entire cell wall (Figure 5), corresponding to the established localization of their putative targets, high-mannose N-glycans and core glycans, respectively.

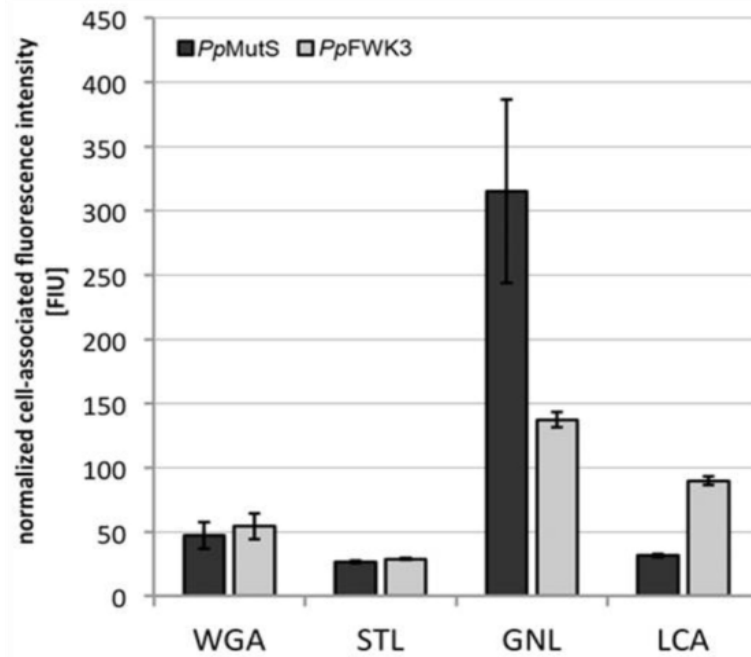


**Figure 6: Quantitative determination of lectin binding on *PpMutS* and *PpFWK3* cells.** Cell suspensions adjusted to the same concentration level were incubated with FITC labelled lectins. After thorough washing, cells were lysed and the fluorescence intensity of the lysis buffer recorded. Binding data was normalized to the average cellular content of FM<sup>®</sup> 4-64, which was shown to be similar in both strains via FACS analysis. Values represent mean  $\pm$  SD of three independent experiments.

### 3.3 Production of HRP in the strains *PpMutS*<sup>HRP</sup> and *PpFWK3*<sup>HRP</sup>

To show the applicability of the generated *och1* knockout strain for the production of recombinant proteins, a vector harboring a gene coding for an acidic HRP isoenzyme was transformed into either *PpMutS* or *PpFWK3*. Transformation of the linearized constructs into *PpFWK3* resulted in fewer Zeocin<sup>™</sup> resistant clones than for *PpMutS*, but sufficient to allow screening for HRP activity after cultivation in a 96-deep well plate in minimal media. Despite the apparent growth defect of *PpFWK3*, the volumetric yields in HRP activity in these micro-scale cultivations were comparable to those of *PpMutS* based transformants. Prior to cultivation of *PpMutS*<sup>HRP</sup> or *PpFWK3*<sup>HRP</sup> in the bioreactor, both strains were analyzed in terms of copy number of the transformed HRP gene to ensure comparability on this level. Both strains were found to have a single copy integration of the HRP encoding gene and were thus considered suitable for comparative bioreactor cultivations.

### 3.4 Strain characterization in bioreactors

We characterized four *P. pastoris* strains (Table 2) with a recently published method of conducting dynamic experiments during batch cultivations in the controlled environment of a bioreactor [16,24,25]. After depletion of glucose, a first methanol adaption pulse with a final concentration of 0.5 % (v/v) was applied. The adaptation times to the new substrate methanol ( $\Delta\text{time}_{\text{adapt}}$ ), defined as the maximum in offgas activity, were determined for all four *P. pastoris* strains and are shown in Table 2.

The calculated carbon dioxide evolution rate (CER), illustrating the metabolic activity of the different strains, the specific substrate uptake rate ( $q_s$ ) and, where appropriate, the specific productivity ( $q_p$ ), during the methanol pulses are shown in Supplementary Figure 3-6. As shown in Supplementary Figure 3 and 4, the CER profiles for the strains *PpMutS* and *PpMutS*<sup>HRP</sup> showed a similar pattern during the consecutive methanol pulses and  $q_s$  values stayed constant over time. In contrast, the CER profiles for the strains *PpFWK3* and *PpFWK3*<sup>HRP</sup> substantially changed over time (Supplementary Figures 5 and 6). After each methanol pulse, less CO<sub>2</sub> was produced per time and volume, indicating that the *P. pastoris* cells became metabolically less active. Thus, the consumption of 1 % (v/v) methanol took longer after each consecutive pulse (compare Supplementary Figures 3 and 4 with Supplementary Figures 5 and 6). The altered metabolic activity of the *och1* knockout strains was also depicted in the calculated yields ( $Y_{X/S}$  and  $Y_{CO_2/S}$ ), which are shown in Figure 7.

For the strains *PpMutS* and *PpMutS*<sup>HRP</sup> both the carbon dioxide yield ( $Y_{CO_2/S}$ ) and the biomass yield ( $Y_{X/S}$ ) stayed constant during the six conducted consecutive methanol pulses (Figure 7a and b). Evidently, the insertion of the HRP gene into strain *PpMutS* affected its physiology as  $Y_{X/S}$  decreased, whereas  $Y_{CO_2/S}$  increased (compare Figure 7a and b). Hence, *PpMutS*<sup>HRP</sup> mainly used the substrate methanol for protein production and dissimilation than for biomass growth.

Interestingly, the calculated yields for *PpFWK3* and *PpFWK3*<sup>HRP</sup> strains showed a very different behaviour. Although  $Y_{X/S}$  was again rather constant,  $Y_{CO_2/S}$  decreased dramatically in the course of the six to seven consecutive methanol pulses (Figure 7c and d), indicating that these two strains became more and more metabolically inactive. Since HPLC analysis revealed that no undesired metabolites were produced in substantial amounts during any of the four cultivations, the C-balances

for strains *PpFWK3* and *PpFWK3<sup>HRP</sup>* were determined close to 1.0 only at the beginning of the cultivation but rapidly decreased over time, whereas the C-balances for strains *PpMutS* and *PpMutS<sup>HRP</sup>* were always determined to be close to 1.0 (Supplementary Figure 7).

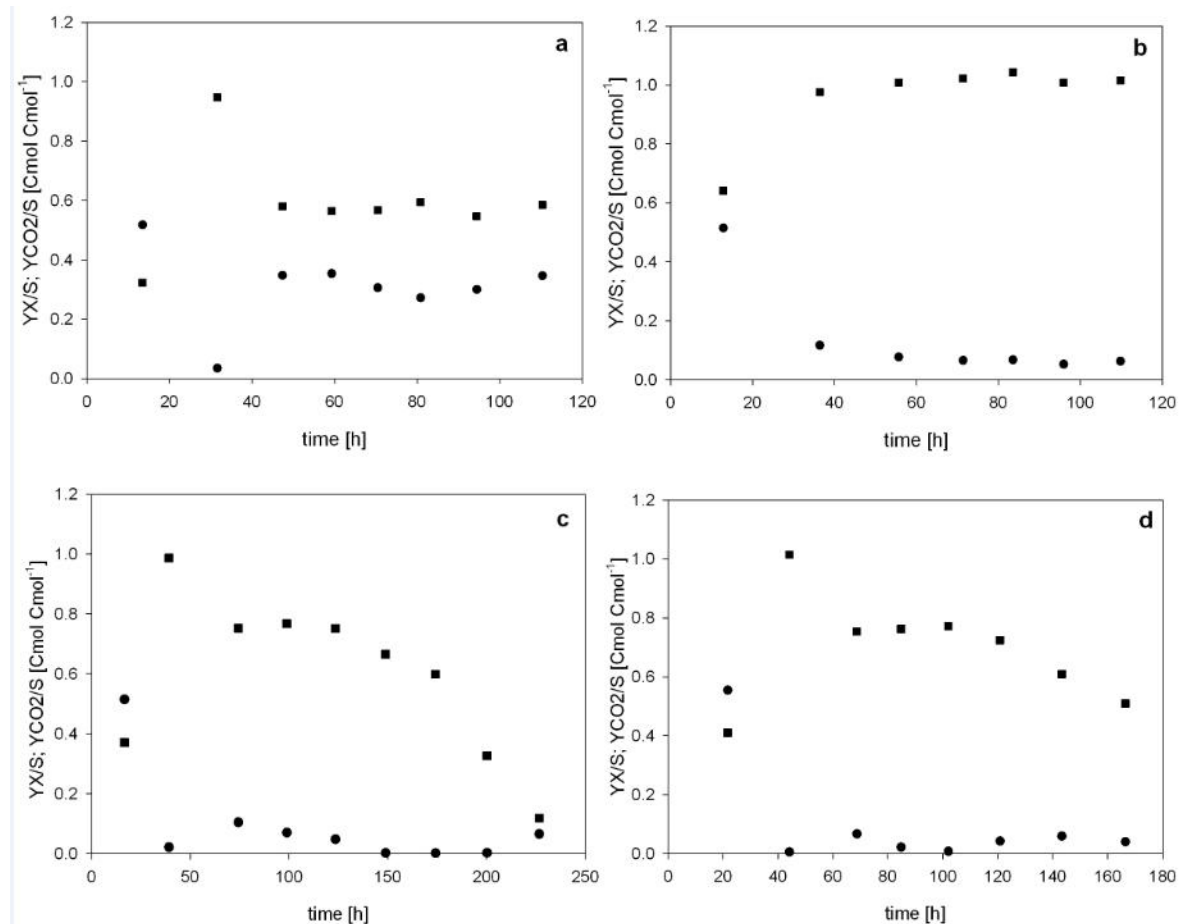


**Figure 7: Calculated yields for the different *P. pastoris* strains during batch cultivations with methanol pulses.** a, *PpMutS*; b, *PpMutS<sup>HRP</sup>*; c, *PpFWK3*; d, *PpFWK3<sup>HRP</sup>*. Black square, carbon dioxide yield ( $Y_{CO_2/S}$ ); black dot, biomass yield ( $Y_{X/S}$ ).

A summary of the determined strain specific parameters of the four different *P. pastoris* strains is given in Table 2.

As shown in Table 2, the maximum specific growth rates on glycerol (max.  $\mu_{Gly}$ ) for *PpFWK3* strains were approximately 1.5-fold lower than for *PpMutS* strains. The yields on glycerol showed a similar pattern for *PpMutS* and *PpFWK3* strains, as the yields were shifted towards production of carbon dioxide rather than biomass when the strains were hosting the gene for recombinant HRP. Both *PpFWK3* strains needed less than half of the adaptation time to methanol ( $\Delta t_{adapt}$ ) compared to the *PpMutS* strains. The altered glycosylation machinery in the *PpFWK3* strains

seems to allow a faster adaptation to methanol, which could be of great significance for industrial applications where fast and efficient bioprocesses are required. As expected, the adaptation times of the strains hosting the recombinant enzyme were longer compared to the strains not carrying this additional gene. The average specific substrate uptake rates for both substrates ( $q_s$ ) glycerol and methanol were lower for the *PpFWK3* strains than for *PpMutS* strains. In respect to the maximum specific uptake rate for methanol ( $\max. q_{\text{MeOH}}$ ) the values for the different strains were quite similar. However, these values were determined during the 3<sup>rd</sup> and the 5<sup>th</sup> methanol pulse for *PpMutS* and *PpMutS*<sup>HRP</sup>, respectively. The values during the other pulses were alike. For *PpFWK3* strains on the other hand, these maxima could only be determined during the 1<sup>st</sup> methanol pulse. After that, the values for  $q_s$  constantly decreased, indicating a progressive reduction of the metabolic activity of the *PpFWK3* strains during consecutive methanol pulses. This was also underlined by constantly decreasing  $Y_{\text{CO}_2/\text{S}}$  and C-balances. However, despite this seemingly negative impact, *PpFWK3*<sup>HRP</sup> produced the HRP isoenzyme at specific and volumetric productivities which were only reduced by 35 % and 30 %, respectively, compared to *PpMutS*<sup>HRP</sup>. In a previous study, we introduced the efficiency factor  $\eta$ , which puts the productivity of the strains in direct relation to the consumed substrate [26]. In this respect, the *och1* knockout strain *PpFWK3*<sup>HRP</sup> even showed a higher ratio than *PpMutS*<sup>HRP</sup> and thus proved to be of justifiable interest for the production of recombinant proteins.

### 3.5 Enzyme purification and characterization

In order to demonstrate the successful decrease of heterogeneity in the glycosylation of HRP when produced in an *och1* knockout strain, size exclusion chromatography (SEC) was performed with cell free cultivation broth (Figure 8). A SEC elution profile has higher specificity and sensitivity than an image of an SDS polyacrylamide gel and was therefore preferably used for this purpose. HRP produced in *PpMutS*<sup>HRP</sup> eluted with higher heterogeneity than HRP produced in *PpFWK3*<sup>HRP</sup>.

Judging by the size exclusion chromatogram (Figure 8), HRP produced in a *PpMutS*<sup>HRP</sup> strain substantially differed in its surface glycosylation pattern compared to HRP produced in a *PpFWK3*<sup>HRP</sup> strain, which showed higher homogeneity. To

analyse this phenomenon in detail, we enzymatically released the glycans from the produced recombinant HRPs and analysed them via liquid chromatography-mass spectrometry (LC-MS). Reducing glycans were observed mainly as doubly charged  $[M+H+NH_4]^{2+}$  ions (Figure 9). Analysis of enzymatically released glycans from HRP produced in either *PpMutS*<sup>HRP</sup> or *PpFWK3*<sup>HRP</sup> confirmed the expected decrease in both N-glycan size and heterogeneity. The dominant core glycan structure shifted from Man10 to Man8 in strain *PpFWK3*<sup>HRP</sup> (Table 3). As shown in Fig. 9, HRP produced in the strain *PpMutS*<sup>HRP</sup> carried a greater variety of different glycan chains consisting of up to 17 mannoses and a higher amount of phosphorylated sugars than HRP produced in *PpFWK3*<sup>HRP</sup>.

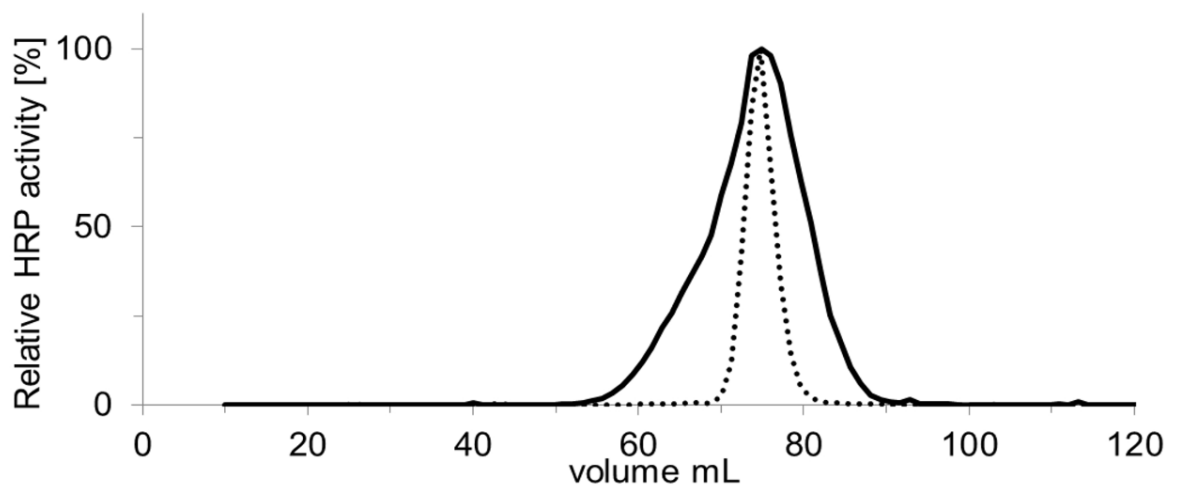


**Figure 8: Size exclusion chromatogram of HRP glycovariants.** Solid line, HRP produced in *PpMutS*<sup>HRP</sup>; dashed line, HRP produced in *PpFWK3*<sup>HRP</sup>. The run was performed at a flow of 9 cm·h<sup>-1</sup> and fractions of 1.2 mL were collected. The measured HRP activities per fraction are shown as relative activities with the respective maximum activities set to 100 % for better comparability. The unnormalized maximum activities were 2.6 and 15.1 U·mL<sup>-1</sup> for HRP from *PpMutS*<sup>HRP</sup> and from *PpFWK3*<sup>HRP</sup>, respectively. The loaded volumen was approximately 200 µL for HRP from either *PpMutS*<sup>HRP</sup> or *PpFWK3*<sup>HRP</sup>.

The evaluation of the relative peak areas underlined this observation (Table 3), as around 60 % of the identified glycan structures cleaved off from HRP produced in the *och1* knockout strain *PpFWK3*<sup>HRP</sup> were of the Man8 type, whereas no structure of that type was identified for HRP from *PpMutS*<sup>HRP</sup>. As shown in Table 3 there were also much more different glycan-chains identified on HRP from *PpMutS*<sup>HRP</sup> and interestingly no phosphorylated mannose structures were found on HRP from *PpFWK3*<sup>HRP</sup>.

To check whether the kinetic constants or the stability of the enzyme were affected by the altered glycosylation pattern, we characterized purified preparations of HRP. HRP preparations produced by either *PpMutS*<sup>HRP</sup> or *PpFWK3*<sup>HRP</sup> in bioreactor cultivations were purified by using a recently described strategy for HRP isoenzyme C1A [27]. Both HRP preparations did not bind to the mixed mode HCIC resin but were found in the flowthrough, *i.e.* 93 % of HRP produced in *PpMutS*<sup>HRP</sup> and 87 % of HRP produced in *PpFWK3*<sup>HRP</sup>. Contaminating proteins were retained on the resin, leading to a partial purification at a factor of approximately 2.5 for both enzyme solutions. A subsequent size exclusion step gave an additional purification factor of approximately 2.0. After purification, the fractions with the highest purification factor were pooled and ultrafiltrated. The enzyme HRP produced in *PpMutS*<sup>HRP</sup> was concentrated to around 3.0 mg·mL<sup>-1</sup>, whereas HRP produced in *PpFWK3*<sup>HRP</sup> could not be concentrated due to the immediate formation of precipitates during ultrafiltration and the resulting clogging of the membrane, indicating a reduced solubility of the extracellular proteins in this preparation. We determined the kinetic constants for both enzyme preparations with H<sub>2</sub>O<sub>2</sub> as electron donor at saturating concentration and ABTS as electron acceptor in varying concentrations (Table 4; Supplementary Figure 8).

As shown in Table 4, the affinity of HRP towards the substrate ABTS was increased, as the  $K_M$  was found to be decreased by approximately 15 % by the altered surface glycosylation. However,  $V_{max}$  was decreased by nearly 20 %. Also, the thermal stability of the produced HRP glycovariants at 60 °C was studied (Supplementary Figure 9) and the half life times ( $\tau_{1/2}$ ) were determined [28]. The  $\tau_{1/2}$  of HRP produced in *PpMutS*<sup>HRP</sup> was determined with 384 s, whereas HRP from *PpFWK3*<sup>HRP</sup> showed a reduction in its thermal half life time of around 50 % with 198 s.

## 4 Discussion

Despite the numerous advantages of using *P. pastoris* as a host organism for recombinant protein production, its inherent heterogeneous yeast type hyperglycosylation of secreted proteins has to be addressed by extensive and elaborated strain modifications. Here, we present a straight forward approach for the generation of a wildtype based *P. pastoris* platform strain that allows the

production of more homogeneously glycosylated recombinant proteins due to an irreversible deletion of the *OCH1* gene.

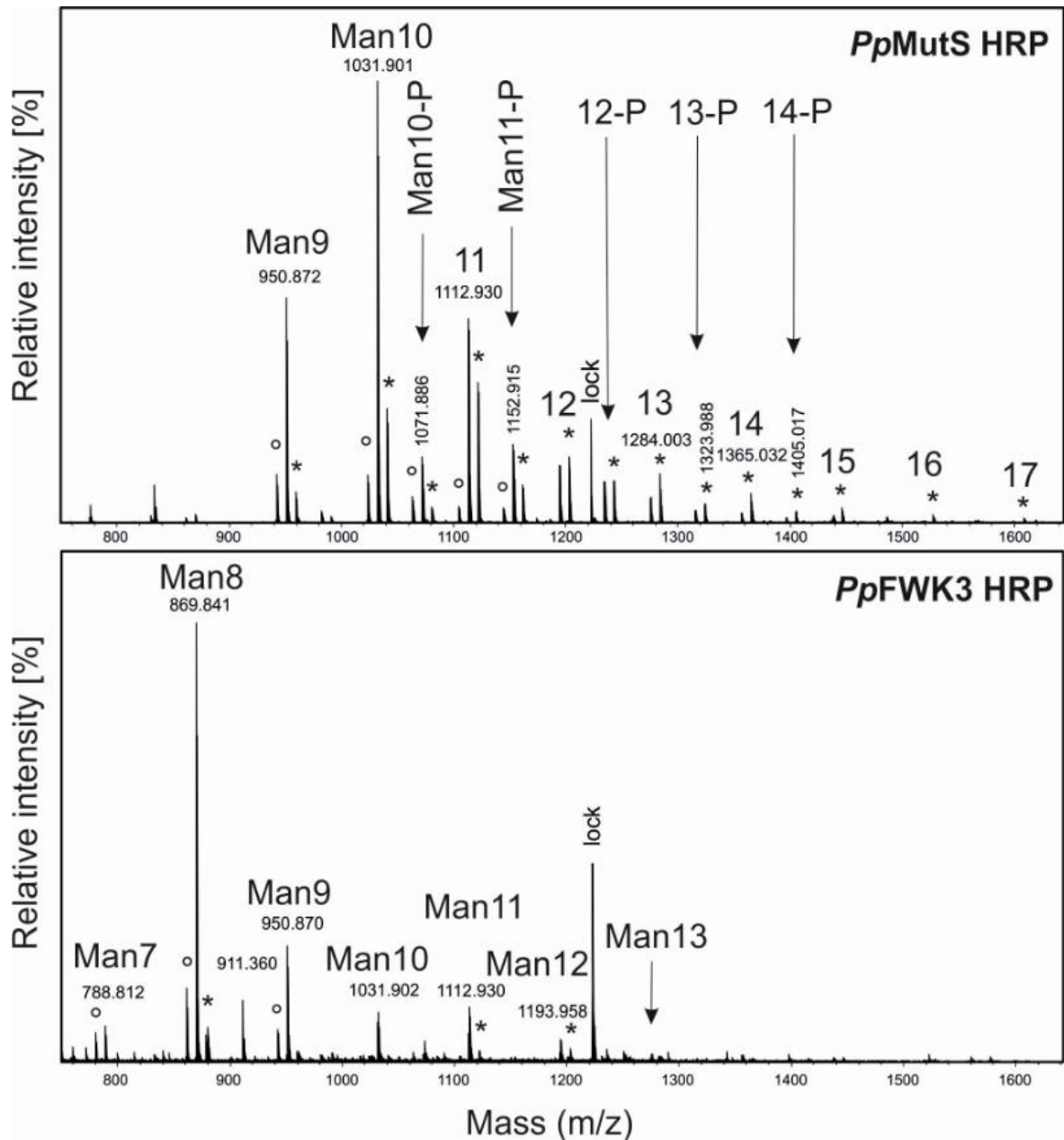


**Figure 9. Chromatogram of liquid chromatography-mass spectrometry of glycans released from HRP produced in either *PpMutS*<sup>HRP</sup> or in *PpFWK3*<sup>HRP</sup>. HRP [M+2H]<sup>2+</sup> and [M+2NH<sub>4</sub>]<sup>2+</sup> ions are marked with ° and \*, respectively. “Man10-P” or just “12-P” indicate phosphorylated glycans. lock, lock mass.**

Yeast hypermannosylation largely depends on the initial activity of an  $\alpha$ -1,6-mannosyltransferase in the Golgi apparatus. Elimination of this activity was achieved by replacement of the *OCH1* ORF with a single 34 bp *FRT* site by using a flipper cassette. However, this approach required double homologous

recombination at the correct locus in the genome. Unfortunately, homologous integration events only play a minor part in *P. pastoris*, as recently demonstrated by Näätsaari *et al.* [18] and which was found to be especially true for the *OCH1* locus by Vervecken *et al.* [10]. A new *P. pastoris* strain with inactivated non-homologous end joining pathway, designated *Ppku70-*, proved to be a particularly convenient tool to identify the phenotype of the specific knockout strain in this study. Since homologous integration was the sole possibility for recombination events in the *Ppku70-* strain, the total number of positive transformants was predominantly made up by transformants with homologous integration. The fact that particularly few colonies were obtained by targeting of the transformed flipper cassette to the *OCH1* locus when using the *Ppku70-* strain also supported the hypothesis of increased difficulty of homologous recombination in that locus.

An *och1* knockout strain of *S. cerevisiae* was described to show several defects such as impaired budding and increased temperature sensitivity [11]. Choi *et al.* mentioned temperature sensitivity and increased flocculation for their *P. pastoris och1* knockout strain [13], but neither they nor Vervecken *et al.* [10] described any further severe growth defects. However, the *och1* knockout strain in the present study was found to show not only formation of cell clusters and temperature sensitivity, but also decreased growth which might be due to an impaired cell wall structure and thus complicated bud formation. Similarly, a recently generated *och1* knockout strain based on the *his4* mutant strain *P. pastoris* GS115 was described with slower growth and rough colony surface. Explanations for these divergent findings remain speculative, but might be due to single nucleotide polymorphisms and hence different strain backgrounds. Also, a secondary integration event of the transformed flipper cassette cannot be completely excluded. However, considering that as little as 100 ng of the cassette were transformed and that all clones that exposed the described phenotype had the correct integration of the cassette in the *OCH1* locus indicates that the observed phenotype can be ascribed rather to the knockout of *OCH1* than to any additional genomic rearrangement. Also, the similarity of the observed phenotype in the present *P. pastoris och1* knockout strain to the phenotype described for a *S. cerevisiae och1* knockout strain [11] very much suggests that the deletion of the *OCH1* gene is actually responsible for the phenotype observed in this study. Most strikingly, reintroduction of the wildtype

*OCH1* gene to the *och1* knockout strain *PpFWK3* restored its phenotype, thus conclusively linking the observed phenotype of *PpFWK3* to the deletion of the *OCH1* gene. Transformation of the *och1* knockout strain with a linearized vector harboring an expression cassette for the production of an HRP isoenzyme via electroporation was found to result in lower transformation efficiency than electroporation of a *P. pastoris* wildtype strain. This increased sensitivity to electroporation might be another reflection of the altered cell wall composition that could be shown by lectin based glycoprofiling.

**Table 3: Relative peak areas of identified glycan structures cleaved off from HRP recombinantly produced in either *PpMutS*<sup>HRP</sup> or in *PpFWK3*<sup>HRP</sup>.**

glycan structure	<i>PpMutS</i> <sup>HRP</sup>	<i>PpFWK3</i> <sup>HRP</sup>
	relative peak area [%]	
Man7	0.0	7.9
Man8	0.0	57.3
Man9	15.7	16.8
Man10	31.4	6.1
Man10-P	5.6	0.0
Man11	18.7	6.8
Man11-P	6.7	0.0
Man12	6.7	3.2
Man12-P	4.4	0.0
Man13	3.7	1.8
Man13-P	1.8	0.0
Man14	2.1	0.0
Man14-P	1.1	0.0
Man15	1.2	0.0
Man16	0.5	0.0
Man17	0.4	0.0
total	100.0	100.0

The highly specific interaction of the lectin WGA with the exposed chitin ring of bud scars [30] has previously been reported for other yeasts and can be used for the precise determination of the number of cell divisions performed [31,32]. To the best of our knowledge, this is the first confirmation of this structure-related specificity for *P. pastoris*. However, in the *och1* knockout strain, we noticed an almost complete loss of bud scar selectivity. The reasons for the regionally diverse distribution of chitin in *PpFWK3* may either lie in an increased accessibility of previously cryptic chitin chains in the lateral cell wall (*i.e.* when the protective polymannan layer is missing), or in an actively increased chitin synthesis and deposition at the cell wall,

*i.e.* as a compensatory response to the cell wall stress caused by the impaired barrier function. Such stimulation of counter-regulatory pathways upon impairment of cell wall integrity has been observed in several yeast species [33,34] and involves diverse mechanisms and signaling cascades [35], which are believed to be directly or indirectly connected to the deletion of Och1p activity [20]. Especially the osmotic stress exerted on the cell as a result of the impaired cell wall integrity is known to present an important factor for the induction of counter-regulatory pathways [36]. Due to the persistence of bud scar specific binding of WGA in methanol treated *PpMutS* cells, we concluded that the strong affinity of WGA to the overall cell wall of *PpFWK3* cells traced back to a *de novo* deposition of carbohydrate epitopes (most probably chitin) in this *och1* knockout strain, and not an increased exposure of constitutive cell wall glycans that are invariably present but usually shielded by an outer chain hypermannan structure in the wildtype strain. The somewhat reduced STL/FM<sup>®</sup> 4-64 ratio compared to the WGA/FM<sup>®</sup> 4-64 ratio may be connected to the minor differences regarding the preferentially binding ligand. Based on the similarity between STL and WGA staining patterns, it is unlikely that any GlcNAc motifs other than chitin (*e.g.* in the core glycan of mannoproteins) were the primary binding epitopes detected by either of the two lectins. As a side aspect of the current work, we were able to demonstrate the use of fluorescence labeled lectins as convenient and versatile probes for visualizing stress responses derived from impaired cell wall integrity in yeast. The decreased GNL/FM<sup>®</sup> 4-64 ratio of *PpFWK3* compared to *PpMutS* could be explained by the minimized amount of high mannose N-glycans and the therefore inherently lower amount of potential GNL target ligands (*i.e.*  $\alpha$ -1,3- and  $\alpha$ -1,6-Man residues) of *PpFWK3* compared to *PpMutS*. Nevertheless, the remaining core glycan provided sufficient GNL targets for a distinct signal. The increased LCA/FM<sup>®</sup> 4-64 signal of *PpFWK3* on the other hand, may be explained by the preference of this lectin for short chain X- $\alpha$ -1,2-Man–Man motifs, with X representing either  $\alpha$ -Man or  $\beta$ -GlcNAc [37]. In mannoproteins, such short motifs may be found in the core glycans, the accessibility of which may be enhanced in absence of the usually highly branched polymannan structures of a *P. pastoris* wildtype strain [33,34].

The detailed characterization of the different *P. pastoris* strains in the controlled environment of a bioreactor revealed that the *och1* knockout strains were

physiologically impaired compared to their wildtype equivalents. During the consecutive pulses, the carbon dioxide yield  $Y_{CO_2/S}$  and the C-balances constantly decreased, indicating a loss in metabolic activity. This was also apparent in the CER signals during the single methanol pulses (Supplementary Figure 5 and 6). At the beginning of the cultivation, methanol was metabolized much faster than during later methanol pulses. We followed the morphology of the *P. pastoris* cells during cultivations via microscopy and identified formation of cell clusters by the *och1* knockout strains. Obviously, the altered surface glycosylation of *och1* knockout cells also affected the budding process. Instead of budding off, the daughter cells stayed attached to the mother cell. The microscopically observed increased tendency for cluster formation may be regarded as an effect which is intrinsically linked to the loss of the polymannan layer upon Och1p inactivation. Cell disruption experiments showed that neither treatment with Triton X-100, 0.5 % EDTA or 5 M urea, nor extensive mechanic shearing via sonication allowed breaking the clusters to single cells. Thus, we conclude that deficiencies in the constitutive cell division machinery upon Och1p inactivation led to a strong, covalent linkage between the cell walls, which remained intact even after the end of the normal budding process. The exact nature of this linkage remains speculative at the current point, but may be associated to aberrant glycosylation steps in the glycan backbone, occurring as a compensatory adaptation to the lack of Och1p activity [20,38]. Due to these very dense and compact formations we hypothesize that the cells in the center of these clusters became limited in oxygen and nutrients and showed no more metabolic activity. Since these cell clusters increased in size over time, the overall metabolic activity of the total amount of cells in the bioreactor decreased, which we observed in decreasing  $Y_{CO_2/S}$  and C-balances. However, these cell clusters were still able to produce recombinant protein. In fact, both the specific productivity and the volumetric productivity, the main focus of industrial bioprocesses, were only reduced by 35 % and 30 %, respectively, compared to the *P. pastoris* strain with an intact *OCH1* gene. However, due to the constant decrease in metabolic activity over time, use of the *och1* knockout strain in industrial processes will require considerable modifications to current standard protocols to optimize recombinant protein production in this strain.

When we analyzed the HRP produced by either a *PpMutS*<sup>HRP</sup> strain or the *och1* knockout strain *PpFWK3*<sup>HRP</sup>, we found the enzyme preparation from *PpFWK3*<sup>HRP</sup> to be considerably more homogeneously glycosylated. More detailed analyses of the surface glycan chains of HRP by mass spectrometry revealed striking differences in the glycosylation pattern between HRP produced in *PpMutS*<sup>HRP</sup> and *PpFWK3*<sup>HRP</sup>. HRP produced in *PpMutS*<sup>HRP</sup> carried a more heterogeneous glycopattern with several high-mannose structures and a great amount of phosphorylated sugars. The most dominant glycan was found to be a Man10 structure. In contrast, the most dominant glycan of HRP produced in *PpFWK3*<sup>HRP</sup> was a Man8 core glycan structure. This reduction is in agreement with our expectations since no Och1p could act on Man<sub>8</sub>GlcNac<sub>2</sub> core glycan structures in the Golgi of the *PpFWK3*<sup>HRP</sup> strain as it could in *PpMutS*<sup>HRP</sup>. Due to the missing Och1p activity, other glycosyltransferases, especially mannosylphosphate transferases, were reduced in their activity resulting in a more homogeneous glycopattern on the surface of recombinantly produced HRP from *PpFWK3*<sup>HRP</sup> (Table 3).

Enzymatic characterizations of HRP revealed an increase in the affinity to the substrate ABTS, but a decrease of  $V_{max}$  for HRP with a more homogeneous glycopattern. Also, a decreased stability at 60 °C for the homogeneously glycosylated HRP compared to the heterogeneously hyperglycosylated glycovariant was observed.

**Table 4:** Enzymatic characterization of homogeneously glycosylated HRP. Kinetic constants of HRP produced in either *PpMutS*<sup>HRP</sup> or *PpFWK3*<sup>HRP</sup> with H<sub>2</sub>O<sub>2</sub> as electron donor at saturating concentration and ABTS as electron acceptor in varying concentrations were determined at 420 nm and 30 °C.

production strain	$K_M_{ABTS}$ [mM]	$V_{max}$ [ $\mu\text{mol}\cdot\text{s}^{-1}\cdot\mu\text{g}^{-1}$ ]
<i>PpMutS</i> <sup>HRP</sup>	2.40	3.07
<i>PpFWK3</i> <sup>HRP</sup>	2.03	2.46

In conclusion, we irreversibly eliminated the *OCH1* encoded  $\alpha$ -1,6-mannosyltransferase activity of *P. pastoris*. The phenotype of the generated *och1* knockout platform strain resembled the phenotype described for the same knockout in *S. cerevisiae*. Nevertheless, the strain was successfully employed for the production of recombinant HRP as a reporter enzyme. Strain specific parameters were determined in comparative bioreactor cultivations. Recombinant HRP from

either an unaltered *P. pastoris* strain or the *och1* knockout strain was purified and characterized. The main findings of this study can be summarized as:

- The *och1* knockout strains were characterized by slow growth, increased temperature sensitivity and formation of cell clusters. The altered N-glycosylation pathway and resultant structural impacts in the *PpFWK3* strain appears to have triggered the dynamic reorganization of surface mannose residues and other glycan structures. The cellular response seemed to be more diverse than just a simple lack of an outer chain hypermannan structure, and may also involve secondary counter-regulatory mechanisms on the metabolic or structural level [20,38]. Our results in this regard are in direct agreement with previous work on *och1* deletion strains of *S. cerevisiae* [19,39]. Lectin based glycoprofiling represented a rapid and reliable method to provide functional proof for the successful deletion of Och1p activity in *P. pastoris*.
- In the course of consecutive methanol pulses, the *och1* knockout strains lost their metabolic activity due to the formation of cell clusters, thus making the adaption of current production processes necessary.
- As shown by detailed LC-MS data, the produced recombinant enzyme exhibited a more homogeneous surface glycosylation, which is beneficial for subsequent downstream processing and applications.
- $V_{\max}$  with ABTS as substrate and the thermal stability at 60 °C were reduced for the homogeneously glycosylated HRP, whereas its affinity for ABTS was increased, rendering the enzyme suitable for most applications.

Here, we report the thorough biotechnological characterization of a *P. pastoris* platform strain that allows the production of recombinant proteins with considerably increased homogeneity in their glycosylation pattern due to an irreversible knockout of the *OCH1* gene. Currently, efforts are driven forward to elucidate the potential benefits of the cell morphological changes in glycoengineered *P. pastoris* strains for the expression of recombinant proteins [40]. Also, future studies will focus on rescuing the growth impaired phenotype to generate a strain that shares the favorable growth phenotype of a wildtype strain but still allows the production of homogeneously glycosylated secreted proteins.

## 5 Methods

### 5.1 Chemicals

Enzymes and deoxynucleotide triphosphates were obtained from Thermo Scientific (formerly Fermentas, Germany). Phusion™ High-Fidelity DNA-polymerase was from Finnzymes (Finland). 2,2'-azino-bis(3-ethylbenzthiazoline-6-sulfonic acid) diammonium salt (ABTS) was purchased from Sigma-Aldrich (Austria). Difco™ yeast nitrogen base w/o amino acids (YNB), Difco™ yeast nitrogen base w/o amino acids and ammonia sulfate (YNB2), Bacto™ tryptone and Bacto™ yeast extract were purchased from Becton Dickinson (Austria). Zeocin™ was purchased from InvivoGen (France) via Eubio (Austria). Fluorescein isothiocyanate (FITC) labeled lectins for microscopic analysis were obtained from Vector Laboratories (USA), comprising wheat germ agglutinin (WGA) from *Triticum vulgare*, *Lens culinaris* agglutinin (LCA), *Galanthus nivalis* lectin (GNL) and *Solanum tuberosum* lectin (STL). FM® 4-64 membrane stain and Hoechst 33342 or 4',6-diamidino-2-phenylindole (DAPI) nucleic acid stains were purchased from Life Technologies (USA). Other chemicals were obtained from Carl Roth (Germany).

### 5.2 Microorganisms

DNA manipulations were performed in accordance to standard protocols [41] in *E. coli* Top10F' (Life Technologies, formerly Invitrogen, Austria). All *P. pastoris* strains in this study were based on the wildtype strain CBS 7435 (identical to NRRL Y-11430 or ATCC 76273). Initial *OCH1* knockout studies were performed in a *ku70* deletion strain, previously described by Näätäsaari *et al.* [18], hereafter called *Ppku70-*. Since *P. pastoris* strains with Mut<sup>S</sup> phenotype have been repeatedly shown to be superior over strains with Mut<sup>+</sup> phenotype for the production of recombinant proteins (e.g. [26]), the ultimate *och1* knockout strain was based on a Mut<sup>S</sup> strain described in [18], hereafter called *PpMutS*.

### 5.3 Deletion of the *OCH1* gene

Based on the genome sequence of the *P. pastoris* wildtype strain CBS 7435 [42], the primers OCH1-5int-fw1 and OCH1-5int-rv1 were designed to amplify a DNA fragment upstream the *OCH1* open reading frame from genomic DNA isolated

according to [43]. Primers OCH1-3int-fw1b and OCH1-3int-rv1b were designed to amplify a fragment downstream of the *OCH1* ORF. OCH1-5int-rv1 and OCH1-3int-fw1b were designed to add sequences that overlap with the *FRT* flanked inner part of a flipper cassette. All primer sequences are listed in Table 5.

**Table 5. Oligonucleotide primer list.** Primers used for the amplification of upstream and downstream sequences of the *OCH1* locus from genomic DNA, for amplification of the whole *OCH1* locus for Sanger sequencing, for amplification of fragments to assemble pPpT4\_BamHI\_OCH1rescue and to amplify the *OCH1* ORF.

Primer name	Sequence (5' - 3')
OCH1-5int-fw1	GAACTGTGTAACCTTTTAAATGACGGGATCTAAATACG TCATG
OCH1-5int-rv1	CTATTCTCTAGAAAGTATAGGAACTTCGGCTGATGATA TTTGCTACGAACACTG
OCH1-3int-fw1b	GTTCCCTATACTTTCTAGAGAATAGGAACTTCGCGAGAT TAGAGAATGAATACCTTCTTCTAAGCGATCG
OCH1-3int-rv1b	GAAGTATTAGGAGCTGAAGAAGCAGAGGCAGAG
OCH1check-fw1	CACACATATAAAGGCAATCTACG
OCH1check-rv2	CAATAACTTCTGCAATAGACTGC
OCH1rescue-fw1	TTCATAGGCTTGGGGTAATAG
OCH1rescue-rv1	CTTGAGCGGCCGCTTAGTCCTTCCAACTTCCTTC
OCH1rescue_T4fw	GCATACATTTGAAGGAAGTTGGAAGGACTAAGCGGCC GCTCAAGAGGAT
OCH1rescue_T4rv	CTATTTCTCTGTCACTATCTATTACCCCAAGCCTATGA AGGATCTGGGTACCGCAGG
OCH1-ORF-fw	ATGGCGAAGGCAGATGGC
OCH1-ORF-rv	TTAGTCCTTCCAACTTCCTTCAAATG

The two *OCH1* targeting fragments of approximately 1.5 kb each were used to assemble a flipper cassette via overlap extension PCR [18]. Transformation of 100 ng of the assembled flipper cassette into either *Ppku70-* or *PpMutS* was performed as described by Lin-Cereghino *et al.* [44]. Transformants were identified on yeast extract-peptone-dextrose (YPD) agar plates containing 100 mg·L<sup>-1</sup> Zeocin™. Double homologous recombination of the flipper cassette in the *OCH1* locus was verified by PCR using the primers OCH1check-fw1 and OCH1check-rv2 (Table 4)

and Sanger sequencing, using isolated genomic DNA as template. Expression of the FLP recombinase gene was induced by growing positive transformants on minimal methanol agar plates. The FLP recombinase mediated excision of the *FRT* flanked inner part of the flipper cassette was shown by restored sensitivity of the cells towards Zeocin™ and again by PCR and Sanger sequencing. The resulting *Ppku70- och1* knockout strain was designated *PpFWK1*, the *PpMutS och1* knockout strain was designated *PpFWK3*.

Complementation of the observed phenotype of the *PpFWK3* strain was performed by transforming a plasmid that was constructed by assembly [45] of two fragments, which were generated by PCR using the primers OCH1rescue-fw1 and OCH1rescue-rv1 using genomic DNA from *PpMutS* as template, and OCH1rescue\_T4fw and OCH1rescue\_T4rv using the plasmid pPpT4\_S [18] as template (Table 4). The resulting plasmid contained the wildtype *OCH1* ORF plus 698 bp of upstream sequence, putatively harboring the natural *OCH1* promoter, and was designated pPpT4\_BamHI\_OCH1rescue. Approximately 500 ng of *BamHI* linearized plasmid were transformed to *PpFWK3*, aliquots were plated on YPD Zeocin™ agar plates and incubated at 28 °C for two days. PCR with the primers OCH1check-fw1 and OCH1check-rv2 from isolated genomic DNA of transformant strains was performed to confirm the unaltered replacement of the former *OCH1* ORF by a single *FRT* site. A second PCR with the primers OCH1-ORF-fw and OCH1-ORF-rv from the same genomic DNA was performed to confirm the presence of a plasmid transmitted *OCH1* ORF somewhere else in the genome. A resulting strain with restored wildtype phenotype was designated *PpFWK3<sup>R</sup>*.

**Table 6.** *P. pastoris* strains used for biotechnological characterisation during bioreactor cultivations.

strain	name
<i>P. pastoris</i> Mut <sup>S</sup>	<i>PpMutS</i>
<i>P. pastoris</i> Mut <sup>S</sup> HRP	<i>PpMutS<sup>HRP</sup></i>
<i>P. pastoris</i> Mut <sup>S</sup> <i>och1</i>	<i>PpFWK3</i>
<i>P. pastoris</i> Mut <sup>S</sup> <i>och1</i> HRP	<i>PpFWK3<sup>HRP</sup></i>

## 5.4 Phenotypic strain characterization

### 5.4.1 Lectin based glycoprofiling via fluorescence microscopy

Qualitative analysis of lectin binding was performed by incubating 500  $\mu\text{L}$  of *PpMutS* or *PpFWK3* cell suspensions in 20 mM HEPES buffer, pH 7.4, at an  $\text{OD}_{600}$  of 0.3 with 500  $\mu\text{L}$  of the respective lectin solution (250  $\text{pmol}\cdot\text{mL}^{-1}$  in 20 mM HEPES, pH 7.4) for 30 min at 4 °C. If appropriate, 5  $\mu\text{g}\cdot\text{mL}^{-1}$  HOECHST 33342 nucleic acid stain or 0.5  $\mu\text{g}\cdot\text{mL}^{-1}$  FM<sup>®</sup> 4-64 membrane stain were included in the incubation mix. After thorough washing by repeated centrifugation (1700  $\text{xg}$ , 5 min) and resuspension, cells were diluted in 1.0 mL of particle free phosphate buffered saline (PBS; 50 mM, pH 7.4) and mounted in FlexiPERM<sup>®</sup> coverslip 12-well plates for microscopic analysis. Images were acquired on a Zeiss Epifluorescence Axio Observer.Z1 deconvolution microscopy system (Carl Zeiss, Germany) equipped with LD Plan-Neofluar objectives and the LED illumination system Colibri<sup>®</sup>. Exposure wavelengths and filter sets of the individual channels were chosen according to the respective fluorophore(s) (DAPI/Hoechst 33342: ex/em 365/450 nm; FITC: ex/em 485/525 nm; FM<sup>®</sup> 4-64 ex/em 485/>620 nm), and combined with differential interference contrast (DIC) images for ease of orientation. Exposure time and illumination parameters were adjusted individually for optimal visibility. For bud scar visualization, Z-stack image series of representative spots were recorded and processed via moderate iterative deconvolution. Lectin cytoadhesion was quantified by incubating the cells with the respective lectin solutions and FM<sup>®</sup> 4-64 as described above (4°C, 30 min), followed by extensive washing. Cells were then lysed by treatment with Triton X-100/SDS (1.0/1.0 %) for 24 h under vivid agitation. The FITC fluorescence intensity in the lysis buffer was assessed in a microplate reader (TECAN, Austria) at ex/em 485/525 nm and normalized to the content of FM<sup>®</sup> 4-64 for direct comparison between the individual samples. Lectin solutions without cells were subjected to the same treatment and analyzed in order to exclude potential degradation of the fluorophore. Control experiments via fluorescence-activated cell sorting (FACS) were performed to verify similar uptake of the membrane stain in both strains.

#### 5.4.2 Membrane permeabilization experiments

To gain information on the steric accessibility of cell wall-embedded chitin and other carbohydrates, cell permeability was enhanced by treatment with concentrated methanol at -20 °C for 20 min, followed by lectin staining. The cells contained in 1.0 mL of precooled suspension (OD<sub>600</sub> of 0.3) were harvested by centrifugation, resuspended in 100 µL PBS buffer and added dropwise to 1.0 mL of icecold methanol under vivid agitation. After 20 min, cells were pelleted again and excessive solvent was removed via repeated washing and centrifugation with fresh PBS buffer. After rehydration in 1.0 mL of 20 mM HEPES buffer, pH 7.4, cells were subjected to the same lectin staining protocol as described above and analyzed via fluorescence microscopy. Efficient membrane permeabilization was verified via successful counterstaining of the nuclear DNA with a normally non-membrane permeable DAPI dye.

#### 5.5 Production of the reporter enzyme horseradish peroxidase in shake flask experiments

Aliquots of approximately 2 µg of *Smil* linearized plasmid pPpT4\_S [18], harboring a HRP gene containing nine potential N-glycosylation sites were transformed into either *PpMutS* or *PpFWK3*. The transformed HRP gene encodes for a new acidic HRP isoenzyme. A detailed description on the identification of new HRP isoenzymes will be given elsewhere (Näätäsaari *et al.*, manuscript in preparation). The HRP gene was codon optimized for expression in *P. pastoris* based on a codon table described in [46]. Expression of the gene was regulated by the *AOX1* promoter. Efficient secretion of HRP to the supernatant was facilitated by fusion of the prepro signal sequence of the *S. cerevisiae* mating factor alpha to the N-terminus of the mature HRP. Transformations were performed according to [44] with the following modification: Whereas an overnight culture of *PpMutS* was diluted to an OD<sub>600</sub> of 0.2 to grow to an OD<sub>600</sub> of 0.8-1.0 in approximately 5 h prior to preparation of the cells for electroporation, an overnight culture of *PpFWK3* was diluted to a starting OD<sub>600</sub> of 0.7 to account for its decreased growth rate. Transformants were grown on YPD Zeocin™ agar plates and randomly chosen for screening in micro scale cultivations in 96-deep well plates, similarly to [47]. The cells were cultivated in 250 µL iron-supplemented BMD1% (11 g·L<sup>-1</sup> α-D(+)-glucose monohydrate, 13.4 g·L<sup>-1</sup>

YNB, 0.4 mg·L<sup>-1</sup> D(+)-biotin, 278 mg·L<sup>-1</sup> FeSO<sub>4</sub> 7H<sub>2</sub>O, 0.1 M potassium phosphate buffer, pH 6.0) for approximately 60 h, then induced once with 250 µL BMM2 (1 % (v/v) methanol, 13.4 g·L<sup>-1</sup> YNB, 0.4 mg·L<sup>-1</sup> D(+)-biotin, 0.1 M potassium phosphate buffer, pH 6.0) and three times with 50 µL BMM10 (5 % (v/v) methanol, 13.4 g·L<sup>-1</sup> YNB, 0.4 mg·L<sup>-1</sup> D(+)-biotin, 0.1 M potassium phosphate buffer, pH 6.0) per well 12 h, 24 h and 36 h after the first addition of BMM2. Induction with the methanol containing media BMM2 and BMM10 induced the production of HRP which was under control of the *AOX1* promoter. The respective HRP production strains were designated *PpMutS*<sup>HRP</sup> and *PpFWK3*<sup>HRP</sup>.

Small scale cultivations were performed in 0.5 L Ultra Yield Flasks (BioSilta, Finland) in 45 mL iron-supplemented BMD1%. After approximately 60 h, 5 mL BMM10 were added. Twelve hours and 36 h after the first induction pulse, 0.5 mL pure methanol were added. Twentyfour hours and 48 h after the first induction pulse, 0.25 mL pure methanol were added. HRP activity in the supernatant was determined by mixing 15 µL of culture supernatant with 140 µL of assay solution (1 mM ABTS, 0.8 mM H<sub>2</sub>O<sub>2</sub>, 50 mM NaOAc buffer, pH 4.5) and following the increase in absorbance at 405 nm in a Spectramax Plus 384 platereader (Molecular Devices, Germany) at room temperature for 3 min. Promising clones were streaked to single colonies and cultivated again in quadruplicates for rescreening. The copy number of the HRP gene in selected *PpMutS* and *PpFWK3* transformant strains was determined via quantitative real-time PCR according to a protocol of Abad *et al.* [48] and as described previously in [26].

## 5.6 Bioreactor cultivations

Four different *P. pastoris* strains (Table 6) were characterized in terms of physiology, biomass growth and productivity by a novel, dynamic strategy of conducting methanol pulses during batch cultivations in the controlled environment of a bioreactor, which we have described recently [16,24,26].

### 5.6.1 Culture Media

Yeast nitrogen base medium (YNBM): 20 g·L<sup>-1</sup> α-D(+)-glucose monohydrate, 3.4 g·L<sup>-1</sup> YNB2, 10 g·L<sup>-1</sup> (NH<sub>4</sub>)<sub>2</sub>SO<sub>4</sub>, 0.4 g·L<sup>-1</sup> D(+)-biotin, 0.1 M potassium phosphate buffer, pH 6.0.

Trace element solution (PTM1): 6 g·L<sup>-1</sup> CuSO<sub>4</sub>·5H<sub>2</sub>O, 0.08 g·L<sup>-1</sup> NaI, 3 g·L<sup>-1</sup> MnSO<sub>4</sub>·H<sub>2</sub>O, 0.2 g·L<sup>-1</sup> Na<sub>2</sub>MoO<sub>4</sub>·2H<sub>2</sub>O, 0.02 g·L<sup>-1</sup> H<sub>3</sub>BO<sub>3</sub>, 0.5 g·L<sup>-1</sup> CoCl<sub>2</sub>, 20 g·L<sup>-1</sup> ZnCl<sub>2</sub>, 65 g·L<sup>-1</sup> FeSO<sub>4</sub>·7H<sub>2</sub>O, 0.2 g·L<sup>-1</sup> D(+)-biotin, 5 mL·L<sup>-1</sup> 95-98 % H<sub>2</sub>SO<sub>4</sub>.

Basal salt medium (BSM): 44 g·L<sup>-1</sup> α-D(+)-glucose monohydrate, 1.17 g·L<sup>-1</sup> CaSO<sub>4</sub>·2H<sub>2</sub>O, 18.2 g·L<sup>-1</sup> K<sub>2</sub>SO<sub>4</sub>, 14.9 g·L<sup>-1</sup> MgSO<sub>4</sub>·7H<sub>2</sub>O, 4.13 g·L<sup>-1</sup> KOH, 26.7 mL·L<sup>-1</sup> 85 % (v/v) o-phosphoric acid, 0.2 mL·L<sup>-1</sup> Antifoam Struktol J650, 4.35 mL·L<sup>-1</sup> PTM1, NH<sub>4</sub>OH as N-source (see experimental procedure).

Base: NH<sub>4</sub>OH, concentration was determined by titration with 0.25 M potassium hydrogen phthalate.

### 5.6.2 Preculture

Frozen stocks (-80 °C) of either *PpMutS*<sup>HRP</sup> and *PpFWK3*<sup>HRP</sup> were precultivated in 100 mL of YNBM in 1 L shake flasks at 30 °C and 230 rpm for max. 24 h. The preculture was transferred aseptically to the respective culture vessel. The inoculation volume was 10 % of the final starting volume.

### 5.6.3 Batch cultivation

Batch cultivations were carried out in a 3 L working volume Labfors glass bioreactor (Infors, Switzerland). BSM was sterilized in the bioreactor and pH was adjusted to pH 5.0 by using concentrated ammonia solution after autoclaving. Sterile filtered PTM1 was transferred to the reactor aseptically. Dissolved oxygen (dO<sub>2</sub>) was measured with a sterilizable polarographic dissolved oxygen electrode (Mettler Toledo, Switzerland). The pH was measured with a sterilizable electrode (Mettler Toledo, Switzerland) and maintained constant with a step controller using 2.5 M ammonia solution. Base consumption was determined gravimetrically. Cultivation temperature was set to 30 °C and agitation was fixed to 1495 rpm. The culture was aerated with 2.0 vvm dried air and offgas of the culture was measured by using an infrared cell for CO<sub>2</sub> and a paramagnetic cell for O<sub>2</sub> concentration (Servomax, Switzerland). Temperature, pH, dO<sub>2</sub>, agitation as well as CO<sub>2</sub> and O<sub>2</sub> in the offgas were measured online and logged in a process information management system (PIMS Lucullus; Biospectra, Switzerland).

After the complete consumption of the substrate glucose, which was indicated by an increase of dO<sub>2</sub> and a drop in offgas activity, the first methanol pulse (adaptation

pulse) of a final concentration of 0.5 % (v/v) was conducted with methanol supplemented with PTM1 (12 mL PTM1 per 1 L of methanol). Subsequently, between five and seven pulses were performed with 1 % or 2 % (v/v) methanol for each strain. For each pulse, at least two samples were taken to determine the concentrations of the substrate methanol and product as well as dry cell weight (DCW) and OD<sub>600</sub> to calculate the strain specific parameters. The induction period for *PpMutS*<sup>HRP</sup> and *PpFWK3*<sup>HRP</sup> was carried out in the presence of 1 mM of the heme precursor  $\delta$ -aminolevulinic acid.

#### **5.6.4 Analysis of growth- and expression-parameters**

DCW was determined by centrifugation of 5 mL culture broth (4,000 x g, 10 min, 4 °C), washing the pellet with 5 mL deionized water and subsequent drying at 105 °C to a constant weight in an oven. OD<sub>600</sub> of the culture broth was measured using a spectrophotometer (Genesys 20; Thermo Scientific, Austria). The activity of HRP was determined using a CuBiAn XC enzymatic robot (Innovatis, Germany). Cell free samples (10  $\mu$ L) were added to 140  $\mu$ L of 1 mM ABTS in 50 mM potassium phosphate buffer, pH 6.5. The reaction mixture was incubated at 37 °C and was started by the addition of 20  $\mu$ L of 0.075 % H<sub>2</sub>O<sub>2</sub>. Changes of absorbance at 415 nm were measured for 80 s and rates were calculated. Calibration was done using commercially available horseradish peroxidase (Type VI-A, Sigma-Aldrich, Austria, P6782, Lot# 118K76734) as standard at six different concentrations (0.02; 0.05; 0.1; 0.25; 0.5 and 1.0 U·mL<sup>-1</sup>). Protein concentrations were determined at 595 nm using the Bradford Protein Assay Kit (Bio-Rad Laboratories GmbH, Austria) with bovine serum albumin as standard.

#### **5.6.5 Substrate concentrations**

Concentration of methanol was determined in cell free samples by HPLC (Agilent Technologies, USA) equipped with a Supelcoguard column, a Supelcogel C-610H ion-exchange column (Sigma-Aldrich, Austria) and a refractive index detector (Agilent Technologies, USA). The mobile phase was 0.1 % H<sub>3</sub>PO<sub>4</sub> with a constant flow rate of 0.5 mL·min<sup>-1</sup> and the system was run isocratically. Calibration was done by measuring standard points in the range of 0.1 to 10 g·L<sup>-1</sup> methanol.

### 5.6.6 Data analysis

Strain characteristic parameters were determined at a carbon dioxide evolution rate (CER) above  $2.5 \text{ mmol}\cdot\text{L}^{-1}\cdot\text{h}^{-1}$  during each methanol pulse. Measurements of biomass, product and substrate concentration were executed in duplicates. Along the observed standard deviation for the single measurement, the error was propagated to the specific rates  $q_s$  and  $q_p$  as well as to the yield coefficients. The error of determination of the specific rates and the yields was therefore set to 10 % and 5 %, respectively [16,24].

## 5.7 Enzyme purification

### 5.7.1 Size exclusion chromatography

The supernatants from *PpMutS*<sup>HRP</sup> and *PpFWK3*<sup>HRP</sup> produced in small scale cultures in 0.5 L Ultra Yield Flasks were concentrated to approximately 500  $\mu\text{L}$  each using Vivaspin 20 tubes (Sartorius Stedim Biotech, Germany) with 10 kDa MWCO and recovered from the tubes resulting in a volume of max. 1500  $\mu\text{L}$ , prior to size exclusion chromatography (SEC) on a HiLoad™ 16/60 Superdex 200 prep grade column (GE Healthcare Europe, Austria). SEC was performed at a flow rate of approximately  $9 \text{ cm}\cdot\text{h}^{-1}$ , fractions of 1.2 mL were collected and assayed for HRP activity using ABTS as substrate.

### 5.7.2 2-step purification protocol

To purify the secreted HRP produced in bioreactor cultivations, the fermentation broths were harvested and centrifuged (4,000  $\times g$ , 20 min) and the cell free supernatants were subjected to diafiltration with buffer (500 mM NaCl, 20 mM NaOAc, pH 6.0) for a subsequent purification step via a mixed mode resin (hydrophobic charge induction chromatography, HCIC) followed by a size exclusion step (SEC). We have recently described this 2-step flowthrough based strategy for the HRP isoenzyme C1A [27]. The catalytic activity and the protein content in all fractions were determined, active fractions were pooled and concentrated via ultrafiltration to approximately  $3 \text{ mg}\cdot\text{mL}^{-1}$  for HRP produced in *PpMuts*<sup>HRP</sup> and  $0.3 \text{ mg}\cdot\text{mL}^{-1}$  for HRP produced in *PpFWK3*<sup>HRP</sup> for subsequent enzyme characterization.

## 5.8 Enzyme characterization

The two HRP preparations produced in either *PpMuts*<sup>HRP</sup> or in *PpFWK3*<sup>HRP</sup> were characterized to determine differences between the hypermannosylated HRP from *PpMutS*<sup>HRP</sup> and its glycovariant produced in *PpFWK3*<sup>HRP</sup>.

### 5.8.1 Liquid chromatography-mass spectrometry (LC-MS) analysis

Protein N-glycosylation was analysed by releasing the N-glycans with peptide:N-glycosidase F (Roche, Mannheim). The released N-glycans were desalted and analysed using a porous graphitic carbon capillary column (ThermoScientific) coupled to a mass spectrometer (Maxis 4G, Bruker, Bremen). Deviating from previous work [49], glycans were not reduced and a steep gradient was applied leading to the elution of all glycans within approximately 2 min.

### 5.8.2 Kinetic constants with ABTS

Protein concentrations of the HRP preparations were determined at 595 nm using the Bradford Protein Assay Kit (Bio-Rad Laboratories GmbH, Austria) with bovine serum albumin as standard. The kinetic constants for ABTS were determined for both HRP glycovariants. The reaction was started by adding 10  $\mu\text{L}$  enzyme solution ( $3 \text{ mg}\cdot\text{mL}^{-1}$  HRP from *PpMutS*<sup>HRP</sup> and  $0.3 \text{ mg}\cdot\text{mL}^{-1}$  HRP from *PpFWK3*<sup>HRP</sup>) to 990  $\mu\text{L}$  reaction buffer containing ABTS in varying concentrations (0.01–10 mM), 1 mM  $\text{H}_2\text{O}_2$  and 50 mM potassium phosphate, pH 6.5. The change in absorbance at 420 nm was recorded in a spectrophotometer UV-1601 (Shimadzu, Japan) at 30 °C controlled with a temperature controller (CPS controller 240 A; Shimadzu, Japan). Absorption curves were recorded with a software program (UVPC Optional Kinetics; Shimadzu, Japan). Measurements were performed in triplicates.

### 5.8.3 Thermal stability

Both enzyme solutions were incubated at 60 °C for 1 h. At different time points, aliquots were withdrawn, the solutions were immediately cooled and centrifuged ( $20,000 \times g$ , 15 min) to pellet precipitated proteins and the remaining catalytic activity in the supernatants was measured [28].

## 6 References

1. Hasslacher, M. *et al.* High-level intracellular expression of hydroxynitrile lyase from the tropical rubber tree *Hevea brasiliensis* in microbial hosts. *Protein Expr. Purif.* **11**, 61–71 (1997).
2. Werten, M. W., van den Bosch, T. J., Wind, R. D., Mooibroek, H. & de Wolf, F. A. High-yield secretion of recombinant gelatins by *Pichia pastoris*. *Yeast* **15**, 1087–1096 (1999).
3. Jahic, M., Rotticci-Mulder, J. C., Martinelle, M., Hult, K. & Enfors, S.-O. Modeling of growth and energy metabolism of *Pichia pastoris* producing a fusion protein. *Bioprocess Biosyst. Eng.* **24**, 385–393 (2002).
4. Lin-Cereghino, G. P., Lin-Cereghino, J., Ilgen, C. & Cregg, J. M. Production of recombinant proteins in fermenter cultures of the yeast *Pichia pastoris*. *Curr. Opin. Biotechnol.* **13**, 329–332 (2002).
5. Parekh, R. B. Effects of glycosylation on protein function. *Curr. Opin. Struct. Biol.* **1**, 750–754 (1991).
6. Ryckaert, S., Martens, V., De Vusser, K. & Contreras, R. Development of a *S. cerevisiae* whole cell biocatalyst for in vitro sialylation of oligosaccharides. *J. Biotechnol.* **119**, 379–388 (2005).
7. Wildt, S. & Gerngross, T. U. The humanization of N-glycosylation pathways in yeast. *Nat. Rev. Microbiol.* **3**, 119–128 (2005).
8. Hamilton, S. R. & Gerngross, T. U. Glycosylation engineering in yeast: the advent of fully humanized yeast. *Curr. Opin. Biotechnol.* **18**, 387–392 (2007).
9. De Pourcq, K., De Schutter, K. & Callewaert, N. Engineering of glycosylation in yeast and other fungi: current state and perspectives. *Appl. Microbiol. Biotechnol.* **87**, 1617–1631 (2010).
10. Vervecken, W. *et al.* In vivo synthesis of mammalian-like, hybrid-type N-glycans in *Pichia pastoris*. *Appl. Environ. Microbiol.* **70**, 2639–2646 (2004).
11. Nagasu, T. *et al.* Isolation of new temperature-sensitive mutants of *Saccharomyces cerevisiae* deficient in mannose outer chain elongation. *Yeast* **8**, 535–547 (1992).
12. Nakayama, K., Nagasu, T., Shimma, Y., Kuromitsu, J. & Jigami, Y. OCH1 encodes a novel membrane bound mannosyltransferase: outer chain elongation of asparagine-linked oligosaccharides. *EMBO J.* **11**, 2511–2519 (1992).
13. Choi, B.-K. *et al.* Use of combinatorial genetic libraries to humanize N-linked glycosylation in the yeast *Pichia pastoris*. *Proc. Natl. Acad. Sci. U.S.A.* **100**, 5022–5027 (2003).
14. Mille, C. *et al.* Identification of a new family of genes involved in beta-1,2-mannosylation of glycans in *Pichia pastoris* and *Candida albicans*. *J. Biol. Chem.* **283**, 9724–9736 (2008).
15. Veitch, N. C. Horseradish peroxidase: a modern view of a classic enzyme. *Phytochemistry* **65**, 249–259 (2004).
16. Dietzsch, C., Spadiut, O. & Herwig, C. A dynamic method based on the specific substrate uptake rate to set up a feeding strategy for *Pichia pastoris*. *Microb. Cell Fact.* **10**, 14–22 (2011).

17. Morawski, B. *et al.* Functional expression of horseradish peroxidase in *Saccharomyces cerevisiae* and *Pichia pastoris*. *Protein Eng.* **13**, 377–384 (2000).
18. Näätäsaari, L. *et al.* Deletion of the *Pichia pastoris* KU70 homologue facilitates platform strain generation for gene expression and synthetic biology. *PLoS ONE* **7**, e39720 (2012).
19. Zhou, J., Zhang, H., Liu, X., Wang, P. G. & Qi, Q. Influence of N-glycosylation on *Saccharomyces cerevisiae* morphology: a golgi glycosylation mutant shows cell division defects. *Curr. Microbiol.* **55**, 198–204 (2007).
20. Lee, B. N. & Elion, E. A. The MAPKKK Ste11 regulates vegetative growth through a kinase cascade of shared signaling components. *Proc. Natl. Acad. Sci. U.S.A.* **96**, 12679–12684 (1999).
21. *Non-Conventional Yeasts In Genetics, Biochemistry And Biotechnology.* (Springer Berlin Heidelberg, 2003). doi:10.1007/978-3-642-55758-3
22. Shibuya, N., Goldstein, I. J., Van Damme, E. J. & Peumans, W. J. Binding properties of a mannose-specific lectin from the snowdrop (*Galanthus nivalis*) bulb. *J. Biol. Chem.* **263**, 728–734 (1988).
23. Fouquaert, E. *et al.* Related lectins from snowdrop and maize differ in their carbohydrate-binding specificity. *Biochem. Biophys. Res. Commun.* **380**, 260–265 (2009).
24. Dietzsch, C., Spadiut, O. & Herwig, C. A fast approach to determine a fed batch feeding profile for recombinant *Pichia pastoris* strains. *Microb. Cell Fact.* **10**, 85–94 (2011).
25. Zalai, D., Dietzsch, C., Herwig, C. & Spadiut, O. A dynamic fed batch strategy for a *Pichia pastoris* mixed feed system to increase process understanding. *Biotechnol. Prog.* **28**, 878–886 (2012).
26. Krainer, F. W. *et al.* Recombinant protein expression in *Pichia pastoris* strains with an engineered methanol utilization pathway. *Microb. Cell Fact.* **11**, 22–35 (2012).
27. Spadiut, O., Rossetti, L., Dietzsch, C. & Herwig, C. Purification of a recombinant plant peroxidase produced in *Pichia pastoris* by a simple 2-step strategy. *Protein Expr. Purif.* **86**, 89–97 (2012).
28. Spadiut, O. *et al.* Improving thermostability and catalytic activity of pyranose 2-oxidase from *Trametes multicolor* by rational and semi-rational design. *FEBS J.* **276**, 776–792 (2009).
29. Chen, Z. *et al.* Enhancement of the gene targeting efficiency of non-conventional yeasts by increasing genetic redundancy. *PLoS ONE* **8**, e57952 (2013).
30. Cabib, E. & Bowers, B. Chitin and yeast budding. Localization of chitin in yeast bud scars. *J. Biol. Chem.* **246**, 152–159 (1971).
31. Chen, C. *et al.* A high-throughput screening system for genes extending life-span. *Exp. Gerontol.* **38**, 1051–1063 (2003).
32. Chaudhari, R. D., Stenson, J. D., Overton, T. W. & Thomas, C. R. Effect of bud scars on the mechanical properties of *Saccharomyces cerevisiae* cell walls. *Chem. Eng. Sci.* **84**, 188–196 (2012).
33. Lesage, G. & Bussey, H. Cell wall assembly in *Saccharomyces cerevisiae*. *Microbiol. Mol. Biol. Rev.* **70**, 317–343 (2006).

34. De Groot, P. W. J., Ram, A. F. & Klis, F. M. Features and functions of covalently linked proteins in fungal cell walls. *Fungal Genet. Biol.* **42**, 657–675 (2005).
35. Klis, F. M., Boorsma, A. & De Groot, P. W. J. Cell wall construction in *Saccharomyces cerevisiae*. *Yeast* **23**, 185–202 (2006).
36. Kapteyn, J. C. *et al.* Altered extent of cross-linking of beta1,6-glucosylated mannoproteins to chitin in *Saccharomyces cerevisiae* mutants with reduced cell wall beta1,3-glucan content. *J. Bacteriol.* **179**, 6279–6284 (1997).
37. Maupin, K. A., Liden, D. & Haab, B. B. The fine specificity of mannose-binding and galactose-binding lectins revealed using outlier motif analysis of glycan array data. *Glycobiology* **22**, 160–169 (2012).
38. Hirayama, H. & Suzuki, T. Metabolism of free oligosaccharides is facilitated in the och1D mutant of *Saccharomyces cerevisiae*. *Glycobiology* **21**, 1341–1348 (2011).
39. Nakanishi-Shindo, Y., Nakayama, K., Tanaka, A., Toda, Y. & Jigami, Y. Structure of the N-linked oligosaccharides that show the complete loss of alpha-1,6-polymannose outer chain from och1, och1 mnn1, and och1 mnn1 alg3 mutants of *Saccharomyces cerevisiae*. *J. Biol. Chem.* **268**, 26338–26345 (1993).
40. Jacobs, P. P. *et al.* Pichia surface display: display of proteins on the surface of glycoengineered *Pichia pastoris* strains. *Biotechnol. Lett.* **30**, 2173–2181 (2008).
41. *Current Protocols In Molecular Biology*. (John Wiley & Sons, Inc., 2001). doi:10.1002/0471142727
42. Küberl, A. *et al.* High-quality genome sequence of *Pichia pastoris* CBS7435. *J. Biotechnol.* **154**, 312–320 (2011).
43. Harju, S., Fedosyuk, H. & Peterson, K. R. Rapid isolation of yeast genomic DNA: Bust n' Grab. *BMC Biotechnol.* **4**, 8–13 (2004).
44. Lin-Cereghino, J. *et al.* Condensed protocol for competent cell preparation and transformation of the methylotrophic yeast *Pichia pastoris*. *BioTechniques* **38**, 44–48 (2005).
45. Gibson, D. G. *et al.* Enzymatic assembly of DNA molecules up to several hundred kilobases. *Nat. Methods* **6**, 343–345 (2009).
46. Abad, S. *et al.* Stepwise engineering of a *Pichia pastoris* D-amino acid oxidase whole cell catalyst. *Microb. Cell Fact.* **9**, 24–35 (2010).
47. Weis, R. *et al.* Reliable high-throughput screening with *Pichia pastoris* by limiting yeast cell death phenomena. *FEMS Yeast Res.* **5**, 179–89 (2004).
48. Abad, S. *et al.* Real-time PCR-based determination of gene copy numbers in *Pichia pastoris*. *Biotechnol. J.* **5**, 413–420 (2010).
49. Pabst, M. *et al.* Isomeric analysis of oligomannosidic N-glycans and their dolichol-linked precursors. *Glycobiology* **22**, 389–399 (2012).
50. Nett, J. H. *et al.* A combinatorial genetic library approach to target heterologous glycosylation enzymes to the endoplasmic reticulum or the Golgi apparatus of *Pichia pastoris*. *Yeast* **28**, 237–252 (2011).
51. Hamilton, S. R. *et al.* Production of complex human glycoproteins in yeast. *Science* **301**, 1244–1246 (2003).
52. Jacobs, P. P., Geysens, S., Vervecken, W., Contreras, R. & Callewaert, N. Engineering complex-type N-glycosylation in *Pichia pastoris* using GlycoSwitch technology. *Nat. Protoc.* **4**, 58–70 (2009).

53. Hamilton, S. R. *et al.* Humanization of yeast to produce complex terminally sialylated glycoproteins. *Science* **313**, 1441–1443 (2006).
54. Hopkins, D. *et al.* Elimination of b-mannose glycan structures in *Pichia pastoris*. *Glycobiology* **21**, 1616-1626 (2011).

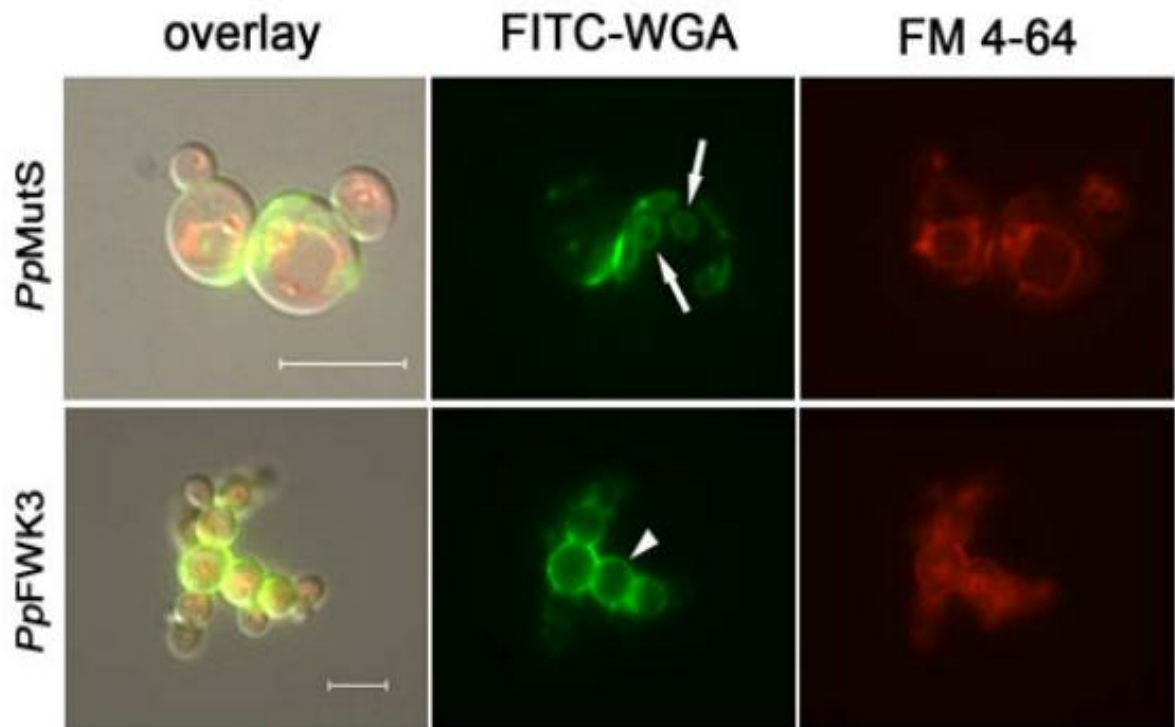
## **7 Acknowledgments**

The authors are very grateful to the Austrian Science Fund (FWF): project P24861-B19 and FWF W901 DK Molecular Enzymology for financial support. We would also like to thank Michaela Gerstmann, Astrid Weninger and Karl Metzger for excellent technical assistance in the lab and Daniel Maresch for excellent assistance with LC-MS.

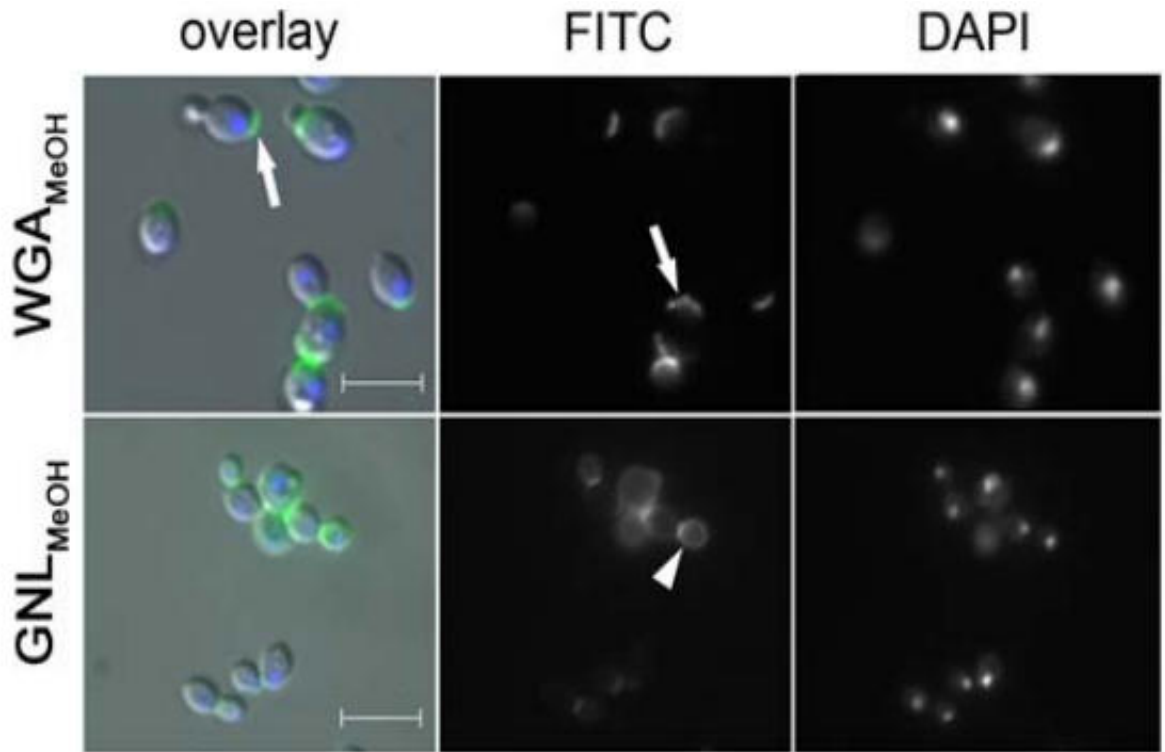
## **8 Author Contributions Statement**

FWK and OS conceived of and planned the study. FWK, CG, LN, MW, RP and OS conducted the different experiments. AG and FA supervised parts of the research. FWK and OS wrote the paper.

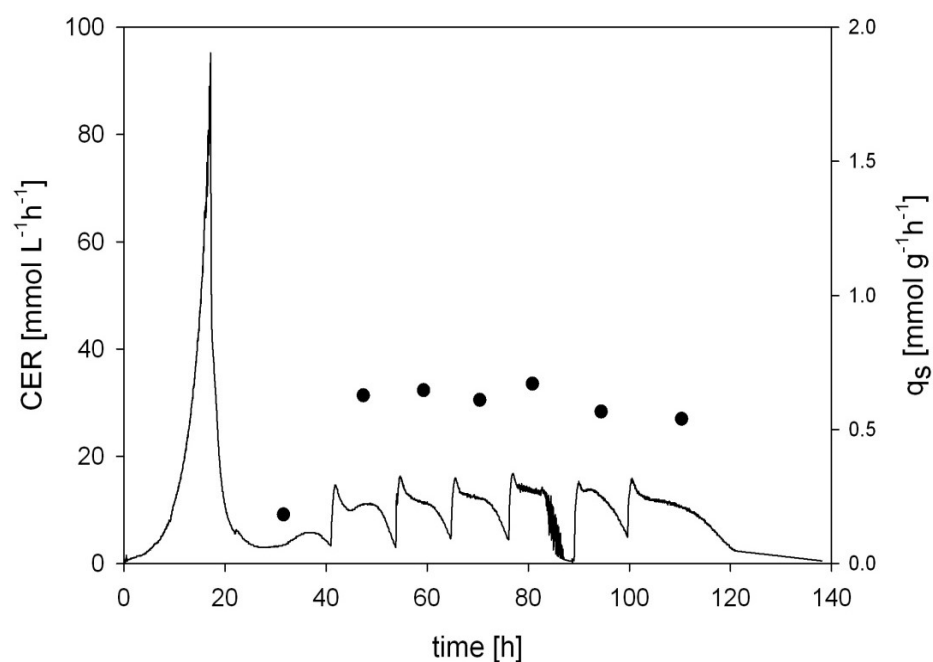
## 9 Supplementary Figures



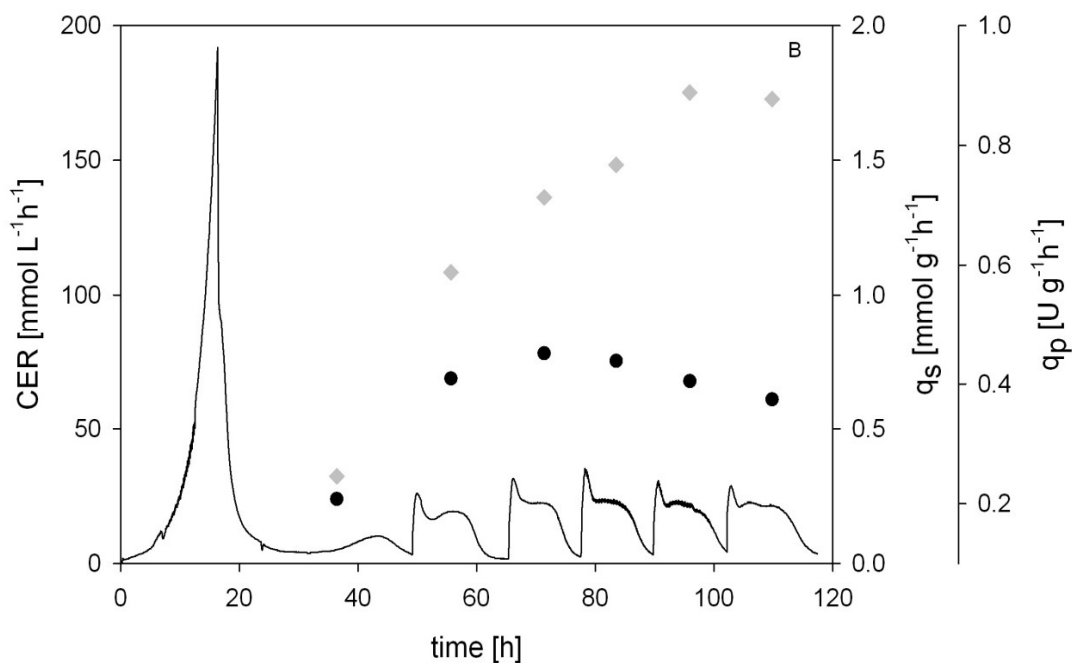
**Supplementary Figure 1:** Differential chitin deposition in response to OCH1 knockout. Surface accessible chitin was visualized via FITC-WGA staining (250 pmol·mL<sup>-1</sup>) of live yeast cells, corresponding to either the PpMutS strain (upper panel) or the PpFWK3 strain (lower panel). Vacuoles were counterstained with the lipophilic membrane dye FM® 4-64. Fluorescence micrographs show the individual channels (middle, right) and an overlay DIC image (left) for ease of orientation. Note the bud scar selective localization of chitin in the wildtype strain (arrows), in contrast to the non-specific deposition pattern in the entire cell wall after knockout of Och1p (arrowhead). Scale bars represent 5  $\mu$ m.



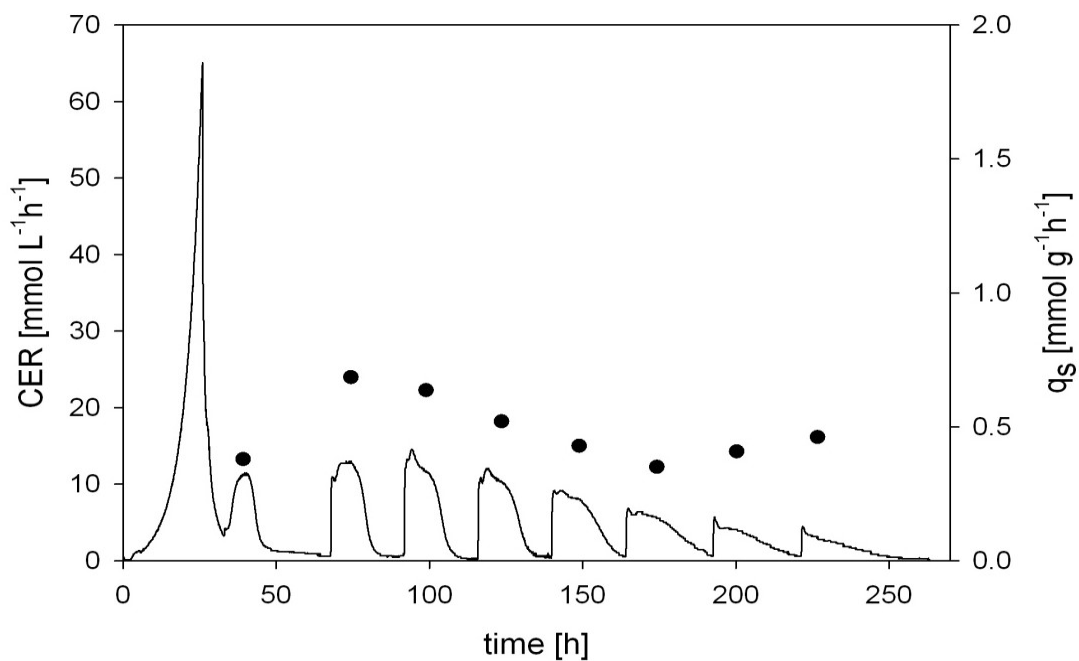
**Supplementary Figure 2:** Staining pattern of FITC-labeled chitin- (WGA) and mannosylspecific (GNL) lectins in *PpMutS* after cell permeabilization with icecold methanol. A nonmembrane penetrating DNA stain was included as a control for successful cell wall permeabilization (DAPI). Images show the individual fluorescence channels (FITC, DAPI) and an overlay with DIC micrographs. Exposure times were individually adjusted for optimal visualization of the regional distribution. WGA binding was still confined to the bud scar regions (arrows), while GNL was distributed throughout the entire cell wall (arrowhead). This corresponded to the staining pattern obtained without prior permeabilization of the cell wall. Scale bars represent 10  $\mu\text{m}$ .



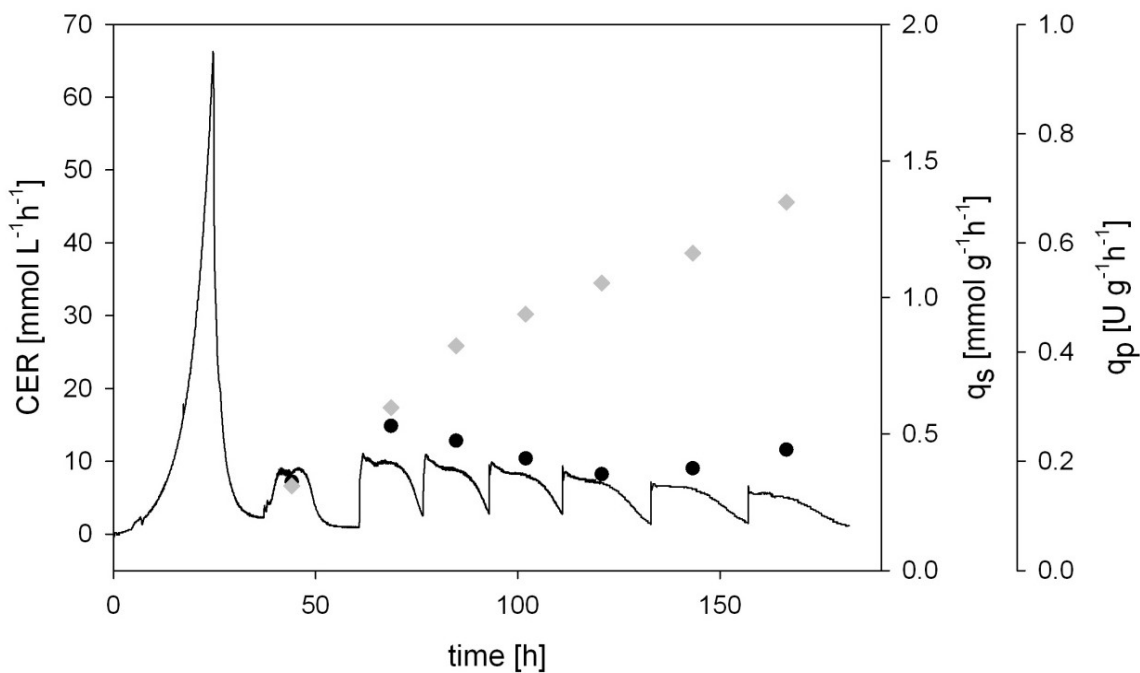
**Supplementary Figure 3:** Batch cultivation of strain *PpMutS* with a methanol adaptation pulse of 0.5 %, subsequent 1 % pulses and a last 2 % pulse (v/v). Solid line, carbon dioxide evolution rate (CER); black dot, specific substrate uptake rate ( $q_s$ ).



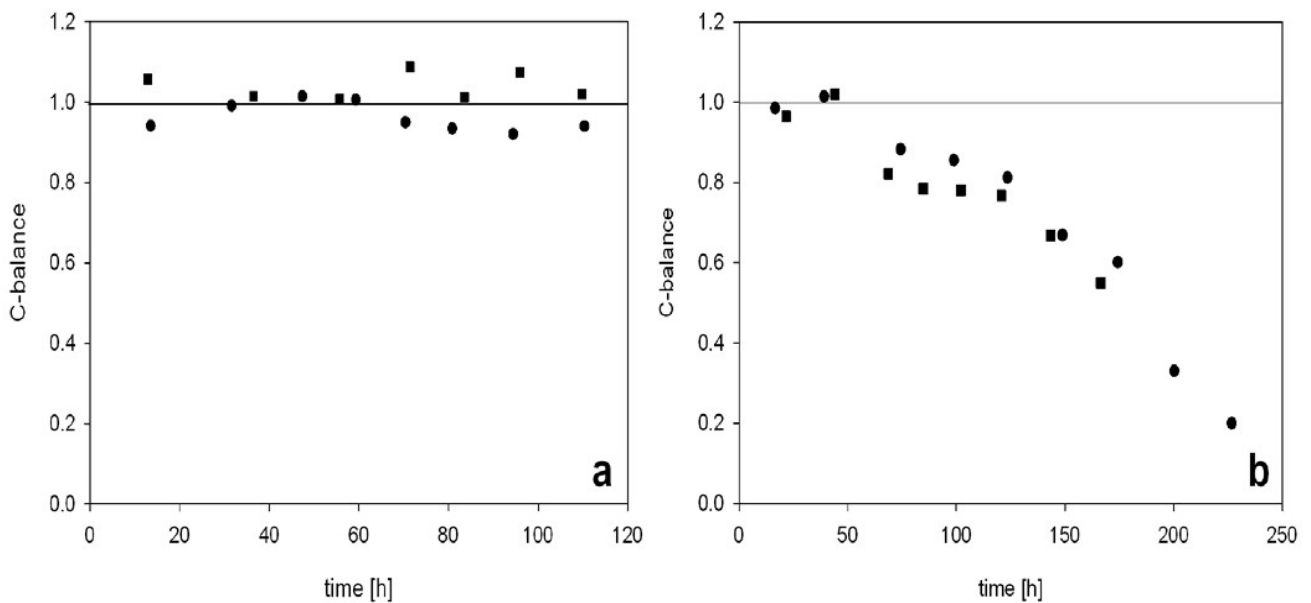
**Supplementary Figure 4:** Batch cultivation of strain *PpMutS*<sup>HRP</sup> with a methanol adaptation pulse of 0.5 % and subsequent 1 % pulses (v/v). Solid line, carbon dioxide evolution rate (CER); black dot, specific substrate uptake rate ( $q_s$ ), grey diamond, specific productivity ( $q_p$ ).



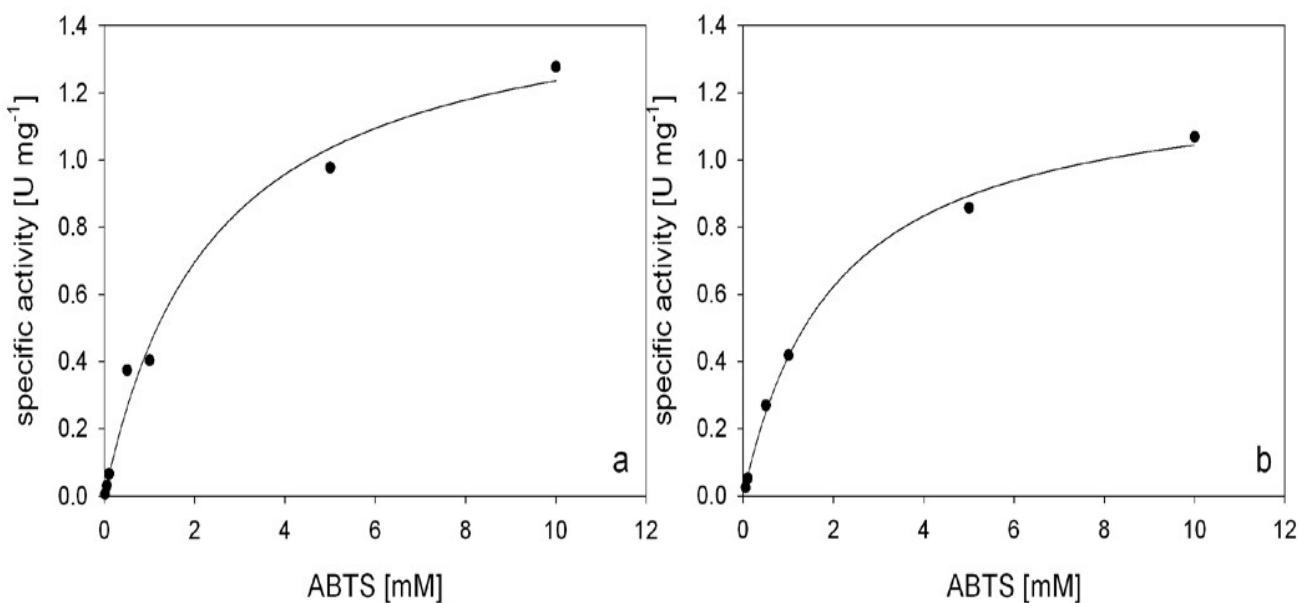
**Supplementary Figure 5:** Batch cultivation of strain *PpFWK3* with a methanol adaptation pulse of 0.5 % and subsequent 1 % pulses (v/v). Solid line, carbon dioxide evolution rate (CER); black dot, specific substrate uptake rate ( $q_s$ ).



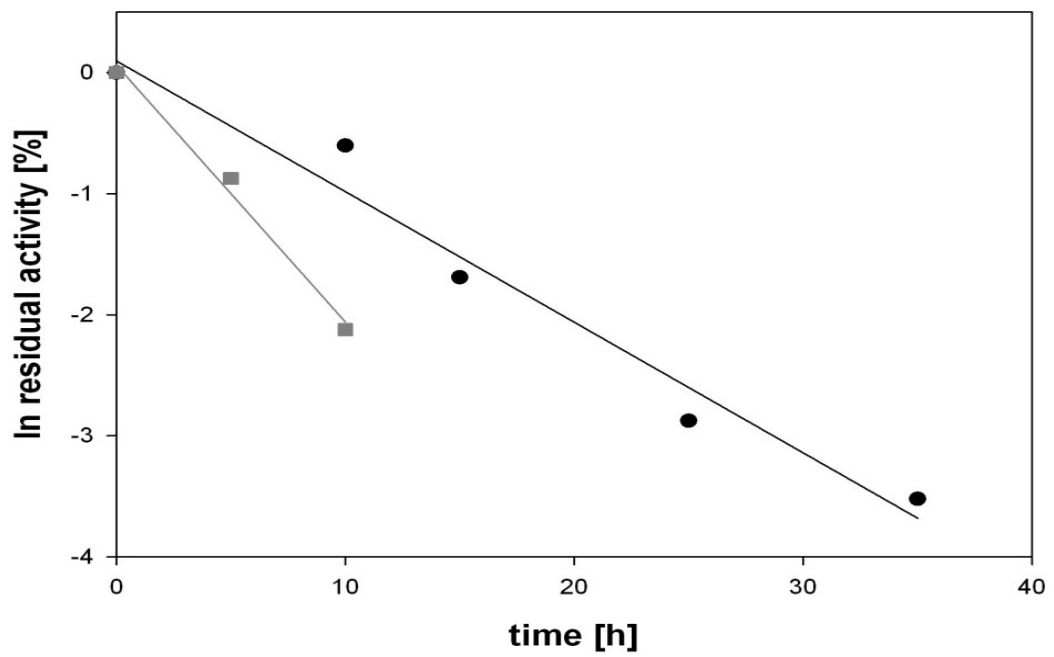
**Supplementary Figure 6:** Batch cultivation of strain *PpFWK3*<sup>HRP</sup> with a methanol adaptation pulse of 0.5 % and subsequent 1 % pulses (v/v). Solid line, carbon dioxide evolution rate (CER); black dot, specific substrate uptake rate ( $q_s$ ), grey diamond, specific productivity ( $q_p$ ).



**Supplementary Figure 7:** C-balances of the different *P. pastoris* strains during the consecutive methanol pulses. A, *PpMutS* strains; black dot, *PpMutS*; black square, *PpMutS<sup>HRP</sup>*; B, *PpFWK3* strains; black dot, *PpFWK3*; black square, *PpFWK3<sup>HRP</sup>*.



**Supplementary Figure 8:** Michaelis-Menten curves of HRP with H<sub>2</sub>O<sub>2</sub> as electron donor in a saturating concentration of 1 mM and ABTS as electron acceptor in varying concentrations between 0.1 and 10.0 mM. The reaction was started by adding 10  $\mu$ L enzyme solution to 990  $\mu$ L reaction buffer containing ABTS, H<sub>2</sub>O<sub>2</sub> and 50 mM potassium phosphate, pH 6.5. The change in absorbance at 420 nm was recorded in a spectrophotometer UV-1601 at 30 °C. Absorption curves were recorded with a software program (UVPC Optional Kinetics; Shimadzu, Japan). Measurements were performed in triplicates.



**Supplementary Figure 9:** Thermal stability of HRP glycovariants at 60 °C. Black dots and line, HRP produced in strain *PpMutS*<sup>HRP</sup>; dark grey dots and line, HRP produced in *PpFWK3*<sup>HRP</sup>.

## **OVERALL CONCLUSIONS**

Summarizing I was able to answer the 4 scientific questions which were raised at the beginning of my Thesis, and to give a future perspective:

**Are there any other HRP isoenzymes useful for medical applications?**

I recombinantly expressed, purified and biochemically characterized 19 different HRP isoenzymes. Isoenzymes HRP A2A and HRP A2B might be potentially good candidates for diagnostic applications with ABTS. However, for targeted cancer treatment HRP C1A prevailed.

**Is it possible to develop a more efficient downstream process for hyperglycosylated enzyme preparations recombinantly produced in *P. pastoris*?**

I developed an efficient 2-step Downstream Process for recombinant HRP C1A from *P. pastoris* where both steps can be operated in the flowthrough mode. The purity of the final enzyme preparation is competitive to the purity of commercially available enzyme preparation from plant.

**Can glyco-engineering help in tailoring HRP for medical applications, especially in terms of reducing hyperglycosylation?**

Rational protein design proved to be a useful tool to reduce glycosylation of HRP C1A. However, a glyco-variant, where all glycosylation sites were removed, showed drastically reduced catalytic activity and stability and thus cannot be used for targeted cancer treatment.

**Can we produce HRP in a humanized, glyco-engineered *P. pastoris* strain?**

Yes, HRP C1A can be produced in a glyco-engineered OCH1 ko *P. pastoris* strain, although this engineered strain is hard to cultivate and physiologically impaired. However, production of HRP C1A in humanized yeast presents the most promising strategy to make this enzyme applicable for targeted cancer treatment.

## **Outlook and to do's**

As shown in my Master Thesis, only the expression of HRP C1A in glyco-engineered yeast is a potential solution to make this enzyme more useful for targeted cancer therapy. Thus, my Outlook focuses in this direction. In my opinion several point still have to be addressed:

- Development of a robust fed-batch production strategy for the physiologically impaired *P. pastoris* OCH1 ko strain
- Expression of HRP C1A in a humanized yeast, which also allows the attachment of sialic acid as terminal residue of surface glycans
- Boost of volumetric recombinant HRP C1A productivity
- Conjugation of HRP C1A derived from the *P. pastoris* OCH1 ko strain to antibodies and application on cancer cell lines

## **APPENDIX**

**I: Purification and basic biochemical characterization of 19 recombinant plant peroxidase isoenzymes produced in *Pichia pastoris*,  
9 pages**

**II: Glyco-variant library of the versatile enzyme horseradish peroxidase,  
12 pages**

**III: Knockout of an endogenous mannosyltransferase increases the homogeneity of glycoproteins produced in *Pichia pastoris*,  
13 pages**



Contents lists available at ScienceDirect

## Protein Expression and Purification

journal homepage: [www.elsevier.com/locate/yprep](http://www.elsevier.com/locate/yprep)Purification and basic biochemical characterization of 19 recombinant plant peroxidase isoenzymes produced in *Pichia pastoris*<sup>☆</sup>Florian W. Krainer<sup>a,1</sup>, Robert Pletzenauer<sup>b,1</sup>, Laura Rossetti<sup>b</sup>, Christoph Herwig<sup>b</sup>, Anton Glieder<sup>c</sup>, Oliver Spadiut<sup>b,\*</sup><sup>a</sup> Graz University of Technology, Institute of Molecular Biotechnology, Graz, Austria<sup>b</sup> Vienna University of Technology, Institute of Chemical Engineering, Research Area Biochemical Engineering, Vienna, Austria<sup>c</sup> Austrian Centre of Industrial Biotechnology (ACIB, GmbH), Graz, Austria

## ARTICLE INFO

## Article history:

Received 30 October 2013  
and in revised form 27 November 2013  
Available online 14 December 2013

## Keywords:

Horseradish peroxidase  
*Pichia pastoris*  
Glycosylation  
Protein purification  
Negative chromatography  
Monolith

## ABSTRACT

The plant enzyme horseradish peroxidase (HRP) is used in several important industrial and medical applications, of which especially biosensors and diagnostic kits describe an emerging field. Although there is an increasing demand for high amounts of pure enzyme preparations, HRP is still isolated from the plant as a mixture of different isoenzymes with different biochemical properties. Based on a recent next generation sequencing approach of the horseradish transcriptome, we produced 19 individual HRP isoenzymes recombinantly in the yeast *Pichia pastoris*. After optimizing a previously reported 2-step purification strategy for the recombinant isoenzyme HRP C1A by substituting an unfavorable size exclusion chromatography step with an anion exchange step using a monolithic column, we purified the 19 HRP isoenzymes with varying success. Subsequent basic biochemical characterization revealed differences in catalytic activity, substrate specificity and thermal stability of the purified HRP preparations. The preparations of the isoenzymes HRP A2A and HRP A2B were found to be highly interesting candidates for future applications in diagnostic kits with increased sensitivity.

© 2013 The Authors. Published by Elsevier Inc. All rights reserved.

## Introduction

Horseradish peroxidase (HRP<sup>2</sup>; EC 1.11.1.7) is a class III peroxidase or classical secretory plant peroxidase which oxidizes different substrates (e.g. aromatic phenols, indoles, phenolic acids, amines, sulfonates) using peroxides, commonly H<sub>2</sub>O<sub>2</sub>, as initial electron acceptors [1–3]. This enzyme has been studied for more than 200 years. Already in 1810, horseradish roots were observed to cause a color reaction when mixed with the resin of *Guaiacum* plants [4],

probably the oxidation of  $\alpha$ -guaiaconic acid to guaiacum blue by HRP [5]. In plants, HRP is involved in numerous reactions, such as the crosslinking of phenolic molecules and the regulation of H<sub>2</sub>O<sub>2</sub> levels, the cell wall network and auxin catabolism [6–8]. Correlating with the large number of different *in vivo* functions, horseradish was found to contain a multitude of different HRP isoenzymes. Up to 42 isoenzymes were detected by isoelectric focusing of commercial HRP preparations [9]. Jermyn et al. observed multiple proteins in the horseradish plant with peroxidase activity and found seasonal variation in their relative amounts as well as differences in substrate affinity [10,11]. This biochemical versatility of HRP isoenzymes was further demonstrated in several subsequent studies (e.g. [12–16]).

Until now, however, most studies have focused on the isoenzyme C1A [17], which is the only isoenzyme with a solved structure [18]. HRP C1A contains nine potential N-glycosylation sites, defined by the N-X-S/T motif, with X being any amino acid but proline, of which eight are glycosylated when isolated from plant [19]. Plant-derived HRP C1A has a total carbohydrate content of 21.8% [20]. Interestingly, plant-derived HRP isoenzymes with a basic isoelectric point (pI) of >12 were found to be less glycosylated, e.g. only 0.8–4.2% carbohydrate content for isoenzymes E3–E6 [15]. Tams et al. studied the effect of the N-glycans on the biochemical properties of HRP C1A and found that pI, absorption spectrum,

<sup>☆</sup> This is an open-access article distributed under the terms of the Creative Commons Attribution-NonCommercial-No Derivative Works License, which permits non-commercial use, distribution, and reproduction in any medium, provided the original author and source are credited.

\* Corresponding author. Address: Vienna University of Technology, Institute of Chemical Engineering, Research Area Biochemical Engineering, Gumpendorfer Strasse 1a, A-1060 Vienna, Austria. Tel.: +43 1 58801 166473.

E-mail address: [oliver.spadiut@tuwien.ac.at](mailto:oliver.spadiut@tuwien.ac.at) (O. Spadiut).

<sup>1</sup> These authors contributed equally to this work.

<sup>2</sup> Abbreviations used: HRP, horseradish peroxidase; pI, isoelectric point; HClC, hydrophobic charge induction chromatography; HIC, hydrophobic interaction chromatography; SEC, size exclusion chromatography; AEC, anion exchange chromatography; ONC, overnight culture; YPD, yeast extract-peptone-dextrose; CV, column volumes; PF, purification factor; R%, recovery yield of HRP activity in percentage; ELISA, enzyme-linked immunosorbent assays; ABTS, 2,2'-azino-bis(3-ethylbenzothiazoline-6-sulfonic acid) diammonium salt; TMB, 3,3',5,5'-tetramethylbenzidine HCl.

peroxidase activity towards *o*-dianisidine and thermal stability remained the same, whereas the kinetic stability and the solubility in ammonium sulfate were decreased upon deglycosylation [21,22]. Thus, the presence of glycan structures on the enzyme surface has a considerable impact on HRP.

Today, the roots of the horseradish plant are the main source for commercially available HRP preparations. These preparations commonly describe mixtures of isoenzymes whose expression patterns change seasonally and in response to uncontrollable environmental factors [8]. The yields of HRP are rather low with less than 10 mg of total HRP protein, which presents a mixture of different isoenzymes, from 100 g of horseradish roots [23]. Thus, the yield of specific isoenzymes purified from such a mixture is extremely low, e.g. Aibara et al. reported as little as 40 mg of isoenzyme E1 from 200 kg of horseradish roots [15]. Unfortunately, due to intrinsic enzyme properties such as intramolecular disulfide bridges [18], the recombinant production of HRP is challenging. Recombinant production as inclusion bodies in *Escherichia coli* is possible (e.g. [24,25]), but refolding yields are as low as 10 mg L<sup>-1</sup> [25]. Beside the recombinant production of HRP in insect cell cultures (e.g. [26,27]), the currently most promising production systems are yeasts such as *Saccharomyces cerevisiae* [28–30] and *Pichia pastoris* [29,31]. However, HRP produced in *P. pastoris* is heterogeneously hyperglycosylated, causing the enzyme to appear as a smear on a SDS polyacrylamide gel at a size of approximately 65 kDa instead of its unglycosylated size of 35 kDa [29,32,33]. These excessive yeast-type glycans considerably impede classical downstream processing approaches. Whereas plant-derived HRP can be purified either by several consecutive steps of column chromatography (e.g. [12,15,16]) or by affinity chromatography using the lectin concanavalin A (e.g. [34–37]) as an isoenzyme mixture in a quite simple way, yeast-derived HRP cannot be purified by these strategies [33].

One obvious advantage of the recombinant production of single HRP isoenzymes in *P. pastoris* is the fact that this isoenzyme does not need to be isolated from an isoenzyme mixture, an otherwise time-intensive and tedious purification effort. Consequently, all HRP activity can be ascribed to the produced individual isoenzyme, allowing its specific enzymatic characterization. However, for that purpose, the HRP isoenzyme still has to be purified from yeast proteins. Hyperglycosylated HRP isoenzyme C1A from *P. pastoris* was previously purified by subsequent steps of hydrophobic interaction chromatography (HIC), size exclusion chromatography (SEC) and anion exchange chromatography (AEC) [29,30]. Recently, we addressed the issue of this cumbersome purification strategy by even making use of the high carbohydrate content of recombinant HRP C1A. We applied hydrophobic charge induction chromatography (HCIC) operated in flowthrough mode to remove contaminating proteins that bound to the resin, whereas the hyperglycosylated HRP eluted in the flowthrough. The glycan coat surrounding HRP C1A seemed to mask the physicochemical properties of the enzyme, allowing this rather unconventional, negative chromatography approach. An additional polishing step by SEC gave a preparation of HRP C1A with a specific activity comparable to the purest commercially available HRP preparation from plant [33].

Recently, we performed a next generation sequencing approach of the horseradish transcriptome which greatly increased the amount of available HRP isoenzyme sequences [38], and thus allowed more detailed studies of single isoenzymes. Considering the numerous applications of HRP as a reporter enzyme in diagnostic assays and histochemical staining as well as in strain engineering studies (e.g. [31,39,40]), biocatalysis (e.g. [41]), wastewater cleanup systems (e.g. [42]) and antibody-directed enzyme-prodrug cancer therapy (e.g. [43]), it is highly interesting to biochemically characterize the different HRP isoenzymes to find the most suitable one for a certain application.

Here, we report the production, purification and basic biochemical characterization of 19 individual HRP isoenzyme preparations. We significantly improved our recently reported 2-step purification procedure [33], replacing the rather inefficient and slow SEC polishing step by using a tube monolithic AEC column. Finally, we performed a basic enzymatic characterization of the final HRP preparations to determine potential differences in their catalytic activities, substrate specificities and thermal stabilities.

## Materials and methods

### Chemicals

Enzymes were obtained from Thermo Scientific (formerly Fermentas, Germany). 2,2'-Azino-bis(3-ethylbenzthiazoline-6-sulfonic acid) diammonium salt (ABTS), 3,3',5,5'-tetramethylbenzidine HCl (TMB) and D(+)-biotin were purchased from Sigma–Aldrich (Austria). Difco™ yeast nitrogen base w/o amino acids (YNB), Bacto™ tryptone and Bacto™ yeast extract were obtained from Becton Dickinson (Austria). Zeocin™ was obtained from *in vivo* Gen (France). Other chemicals were obtained from Carl Roth (Germany).

### *P. pastoris* strains for HRP production

All *P. pastoris* strains in this study were based on the *P. pastoris* wildtype strain CBS 7435 (identical to NRRL Y-11430 and ATCC 76273). The Mut<sup>S</sup> (methanol utilization slow) phenotype of *P. pastoris* was shown to be superior over the Mut<sup>+</sup> phenotype in terms of volumetric productivity and production efficiency of HRP [31]. Thus, all HRP production strains in this study were strains with Mut<sup>S</sup> phenotype [44]. A detailed description of the identification of new HRP isoenzyme sequences and the generation of the *P. pastoris* strains producing the various HRP isoenzymes was given elsewhere [38]. Calculated basic protein parameters and the corresponding database accession codes are shown in Table 1. Synthetic codon-optimized genes encoding mature HRP isoenzymes were N-terminally fused to the prepro signal peptide of the *S. cerevisiae* mating factor alpha to facilitate efficient secretion of the recombinant HRP to the cultivation supernatant. The expression of the HRP

**Table 1**

Calculated basic characteristics of HRP isoenzymes. The isoelectric point (pI) and the molecular weight (MW) were calculated using the Compute pI/Mw tool of the ExpASY server [55,56] and the number of potential N-glycosylation sites (N-X-S/T) was deduced from the NetNGlyc 1.0 Server [57]. All calculations were based on a cleavage of the prepro signal peptide of the *S. cerevisiae* mating factor alpha between A87 and E88, upstream of the mature HRP peptide.

HRP isoenzyme	pI	MW [kDa]	N-X-S/T	GenBank	UniProt
C1A	5.41	35.82	9	HE963800.1	K7ZWW6
25148.1 (C1C)	6.13	35.86	7	HE963802.1	K7ZWQ1
25148.2 (C1D)	6.50	35.89	7	HE963803.1	K7ZW56
04627 (C2)	8.38	35.67	4	HE963804.1	K7ZW02
C3	7.05	35.48	3	HE963805.1	K7ZWW7
A2A	4.84	32.09	9	HE963806.1	K7ZW28
A2B	4.84	32.12	9	HE963807.1	K7ZWQ2
E5	8.99	33.92	3	HE963808.1	K7ZW57
1805	5.75	35.96	5	HE963809.1	K7ZW05
22684.1	6.39	35.06	4	HE963810.1	K7ZWW8
22684.2	6.00	35.15	4	HE963811.1	K7ZW29
1350	8.47	31.42	3	HE963812.1	K7ZWQ3
5508	8.22	31.35	3	HE963815.1	K7ZWW9
6351	5.99	32.89	2	HE963816.1	K7ZW31
22489.1	8.24	31.37	2	HE963818.1	K7ZW59
22489.2	8.24	31.39	2	HE963819.1	K7ZW11
17517.2	9.30	32.69	4	HE963823.1	K7ZW60
08562.4	8.91	33.26	3	HE963825.1	K7ZWX1
08562.1	8.89	33.81	3	HE963824.1	K7ZW15

encoding genes was regulated by the methanol-inducible promoter of the *P. pastoris* AOX1 gene.

#### Production of recombinant HRP isoenzymes

Recombinant production of 19 different HRP isoenzymes in *P. pastoris* was performed in 2.5 L Ultra Yield Flasks from BioSilta (Finland), applying a protocol based on [45] with the following modifications: An overnight culture (ONC) of 30 mL YPD (yeast extract-peptone-dextrose) in 250 mL baffled shake flasks was inoculated with a single colony of a *P. pastoris* strain producing a specific HRP isoenzyme and incubated at 28 °C, 90 rpm and approximately 50% humidity for at least 12 h. 1.5 mL of this ONC were transferred to 270 mL of iron-supplemented BMD1% (11 g L<sup>-1</sup> α-D(+)-glucose monohydrate, 13.4 g L<sup>-1</sup> YNB, 0.4 mg L<sup>-1</sup> D(+)-biotin, 278 mg L<sup>-1</sup> FeSO<sub>4</sub>·7H<sub>2</sub>O, 0.1 M potassium phosphate buffer, pH 6.0) per Ultra Yield Flask and cultivated under the same conditions for approximately 60 h. A first induction pulse was performed by addition of 30 mL BMM10 (5% (v/v) methanol, 13.4 g L<sup>-1</sup> YNB, 0.4 mg L<sup>-1</sup> D(+)-biotin, 0.1 M potassium phosphate buffer, pH 6.0). 3.0 mL of pure methanol were added approximately 12 h and 36 h after the first induction pulse, 1.5 mL of pure methanol were added approximately 24 h and 48 h after the first induction pulse. 72 h after the first induction pulse, the culture broth was centrifuged (15,000×g, 30 min, 4 °C) and the supernatant was filtered through a 0.2 μm cellulose acetate filter (Sartorius Stedim Biotech, Germany).

#### Purification of recombinant HRP isoenzymes

In accordance to our previous study, the supernatant was concentrated using the Vivaflow 50 system (Sartorius Stedim Biotech, Germany) with a 10 kDa MWCO membrane prior to hydrophobic charge induction chromatography (HCIC; [33]). The buffer was changed to HCIC-A (500 mM NaCl, 20 mM NaOAc, pH 6.0) and concentrated to a final volume of 10–15 mL. All further steps of concentration and buffer change were performed using Vivaspin 20 tubes (Sartorius Stedim Biotech, Germany) with 10 kDa MWCO. The HCIC resin MEP HyperCel™ was obtained from Pall (Austria), and HCIC was performed in flowthrough mode based on [33]: A column containing approximately 25 mL of MEP HyperCel™ resin was equilibrated with at least 4 column volumes (CV) of buffer HCIC-A. 10–15 mL concentrated HRP solution in HCIC-A were loaded onto the column and washed with at least 220 mL of HCIC-A at a flow rate of approximately 55 cm h<sup>-1</sup>. Fractions of 10 mL were collected. Fractions containing HRP activity were pooled and concentrated to 500–1000 μL. The column was washed with 5 CV of 800 mM NaOH, then re-equilibrated with HCIC-A for subsequent runs.

Univariate screenings for a potential application of CIM® tube monolithic columns (BIA separations, Slovenia) as a second chromatographic purification step were performed with the partially purified isoenzyme C1A after HCIC. Flowthrough fractions from HCIC purifications were pooled, concentrated and rebuffed in either of the loading buffers: 50 mM Tris-HCl, pH 7.4, 50 mM Tris-HCl, pH 8.0 or 50 mM potassium phosphate, pH 6.0. The respective elution buffers contained 1 M NaCl. The tube monolithic columns tested were 1 mL CIM®-DEAE, 1 mL CIM®-QA and 1 mL CIM®-OH (BIA separations, Slovenia), which were equilibrated in the respective loading buffer at a flow rate of 156 cm h<sup>-1</sup>. A post-load wash of 4 CV binding buffer was performed before elution was conducted by either increasing the elution buffer in a single step to 100% or in a linear gradient to 100% over 30 CV.

Ultimately, anion exchange chromatography (AEC) with an 8 mL CIM®-DEAE tube monolithic column was performed as a second purification step for all the HRP isoenzymes. The column was equilibrated in loading buffer AEC-A (50 mM Tris-HCl, pH 8.0) at a flow rate of 16.8 cm h<sup>-1</sup>. Post-HCIC pools of each HRP isoenzyme

were subjected to diafiltration in AEC-A and were subsequently loaded onto the AEC column at an average linear flow rate of 16.8 cm h<sup>-1</sup>. Elution was performed in a single step from 0% to 100% AEC-B (50 mM Tris-HCl, 1 M NaCl, pH 8.0). For column recovery the column was washed with 5 CV of a 1 M NaOH/1 M NaCl solution at an average linear flow rate of 33.6 cm h<sup>-1</sup>.

#### Electrophoresis

To check the electrophoretic purity of HRP isoenzyme preparations SDS-PAGE was performed using a 5% stacking gel and a 10% separating gel in 1× Tris-glycine buffer. Unless otherwise stated, samples were diluted to a protein concentration between 0.1 and 0.5 mg mL<sup>-1</sup> before loading. Gels were run in a vertical electrophoresis Mini-PROTEAN Tetra Cell apparatus (Biorad, Austria) and stained with Coomassie blue. The protein mass standard used was the PageRuler Prestained Ladder (Fermentas, Austria).

#### Data analysis and basic enzymatic characterization of purified recombinant HRP isoenzymes

Protein concentrations were determined at 595 nm by the Bradford assay using the Sigma-Aldrich (Austria) Protein Assay Kit with bovine serum albumin as standard in the range of 0.2–1.2 mg mL<sup>-1</sup>.

The enzymatic activity of HRP was measured using an ABTS assay in a CuBiAn XC enzymatic robot (Innovatis, Germany). 10 μL of sample were mixed with 140 μL 1 mM ABTS solution (50 mM potassium phosphate buffer, pH 6.5). The reaction mixture was incubated at 37 °C for 5 min before the reaction was started by the addition of 20 μL 0.078% (w/w) H<sub>2</sub>O<sub>2</sub>. Changes in absorption at 415 nm were measured for 80 s and rates were calculated. The standard curve was prepared using a commercially available HRP preparation (Type VI-A, Sigma-Aldrich, Austria) in the range from 0.02 to 2.0 U mL<sup>-1</sup>.

The efficiency of the applied purification approach was evaluated by determining the purification factor (PF) and the recovery yield of HRP activity in percentage (R%). PF and R% were calculated by Eqs. (1) and (2):

$$PF = \frac{\text{specific activity}_{\text{post}}}{\text{specific activity}_{\text{pre}}}, \quad (1)$$

$$R(\%) = 100 \times \frac{\text{volumetric activity}_{\text{post}} \times \text{volume}_{\text{post}}}{\text{volumetric activity}_{\text{pre}} \times \text{volume}_{\text{pre}}}. \quad (2)$$

The suffixes “pre” and “post” indicate the respective values before and after a purification step. To obtain an overall PF and R% for the 2-step purification approach, we combined the values we determined for the single purification steps (Table 2). In case one purification step did not work or could not be evaluated, e.g. due to too low HRP activity, we only presented the successful purification step. The pooled active fractions after AEC were concentrated using Amicon Ultra-15 Centrifugal Filter Units with 10 kDa MWCO (Merck-Millipore, Austria) to the final enzyme preparation of a volume of approximately 1.5 mL.

Characterization of the purified HRP isoenzyme preparations included the determination of the basic kinetic parameters,  $V_{\text{max}}$  and  $K_M$ , for the electron acceptors ABTS and TMB in a spectrophotometer UV-1601 from Shimadzu (Austria). These peroxidase substrates are commonly used in enzyme-linked immunosorbent assays (ELISA). The reaction mixture with a final volume of 1.0 mL contained a concentration of 1 mM H<sub>2</sub>O<sub>2</sub>, 10 μL of HRP isoenzyme preparation and varying concentrations of ABTS (0.05–10 mM) or TMB (0.005–0.5 mM) in 50 mM potassium phosphate buffer, pH 6.5. The increase in absorption was followed at 420 nm for ABTS and at 653 nm for

**Table 2**

Summary of the 2-step purification approach of 19 recombinant HRP isoenzymes. The purification factor (PF) and the recovery of HRP activity in percentage (R%) of the applied HCIC and AEC flowthrough steps, as well as the combined purification results are shown. Some isoenzymes did not show any detectable peroxidase activity. In these cases, no values for PF or R% are available (n/a). The combined PF value is a product of the PFs of the HCIC and AEC step; in case no values were available for one purification step (n/a), the combined value only describes the working step.

HRP isoenzyme	HCIC		AEC		Combined	
	PF	R%	PF	R%	PF	R%
C1A	7.02	95.4	10.92	58.5	76.66	55.8
25148.1 (C1C)	6.80	95.5	2.28	66.4	15.50	63.4
25148.2 (C1D)	8.96	32.9	2.42	66.5	21.68	21.9
04627 (C2)	10.08	100.0	6.17	45.7	62.19	45.7
C3	2.17	17.6	2.50	100.0	5.43	17.6
A2A	15.85	100.0	43.18	15.6	684.40	15.6
A2B	5.82	92.0	6.64	80.0	38.64	73.6
E5	3.89	33.1	0.54	81.0	2.10	26.8
1805	n/a	n/a	15.68	38.4	15.68	38.4
22684.1	0.11	1.4	n/a	n/a	n/a	n/a
22684.2	n/a	n/a	n/a	n/a	n/a	n/a
1350	n/a	n/a	n/a	n/a	n/a	n/a
5508	2.18	33.2	66.25	31.5	144.43	10.5
6351	3.01	32.6	n/a	n/a	n/a	n/a
22489.1	0.42	3.8	n/a	n/a	n/a	n/a
22489.2	0.02	0.3	2.09	74.6	0.04	0.2
17517.2	3.48	38.9	0.98	75.0	3.41	29.2
08562.4	n/a	n/a	0.89	32.6	0.89	32.6
08562.1	1.18	16.5	0.27	45.5	0.32	7.5

TMB at 30 °C for 180 s, respectively. Absorption curves were recorded with an adapted software program (UVPC Optional Kinetics software, Shimadzu). The maximum reaction rate ( $V_{max}$ ) and the Michaelis constant ( $K_m$ ) were calculated with the Sigma Plot software (Version 11.0, Systat Software Inc., USA).

The thermal stability of individual HRP isoenzyme preparations was tested at 60 °C. The residual activity towards ABTS was measured after 5, 10, 15, 20, 30 and 60 min of incubation at 60 °C. The residual activities were plotted versus the incubation time and the half life times of thermal inactivation at 60 °C ( $\tau_{1/2}$ ) were calculated using Eq. (3) [46]:

$$\tau^{1/2} = \frac{\ln 2}{k_{in}}, \quad (3)$$

$k_{in}$  rate of inactivation (slope of the logarithmic residual activity).

## Results and discussion

HRP is a well-studied enzyme which is used in numerous industrial and medical applications (e.g. [31,39–43]). Due to certain intrinsic enzyme features, the recombinant production and purification of this important enzyme is quite cumbersome, and HRP is still isolated from horseradish roots as a mixture of isoenzymes at low yields. A recombinant production process in combination with an efficient purification strategy would allow the reliable production of individual HRP isoenzymes for the various applications in large amounts.

### HRP production

In this study, 19 HRP isoenzymes were recombinantly produced in the methylotrophic yeast *P. pastoris* in shake flask cultivations. By fusing the genes to the prepro signal sequence of the *S. cerevisiae* mating factor alpha, the HRP isoenzymes were secreted to the cultivation broth. Due to the fact that *P. pastoris* actively secretes only few endogenous proteins [47,48], the subsequent downstream process was thereby considerably facilitated already. After centrifugation and diafiltration, the HRP isoenzymes could

already be subjected to chromatography. Typical total protein concentrations in the cultivation broth at the time of harvesting were in the range of 200–500 mg L<sup>-1</sup>. The amount of obtainable purified HRP isoenzyme preparation differed vastly; for the isoenzymes which could be purified best using the here presented 2-step strategy the following protein contents per liter cultivation broth were obtained: 1.0 mg C1A, 0.6 mg C2, 0.1 mg A2A and 0.15 mg 5508. Also volumetric HRP activities with ABTS as reducing substrate varied considerably from isoenzyme to isoenzyme. For instance, the HRP isoenzymes 8562.1, 22489.1, A2A, C1A and E5 gave approximately 3, 70, 220, 440 and 670 U L<sup>-1</sup>, respectively.

### Hydrophobic charge induction chromatography (HCIC)

In a recent multivariate Design of Experiments screening study, we found HCIC operated in the flowthrough mode to be very effective for the purification of the hyperglycosylated recombinant HRP C1A, allowing a 5-fold purification at almost 100% recovery [33]. However, in the present study the application of this flowthrough purification step to the 19 different HRP isoenzymes produced in *P. pastoris* led to quite diverse results in terms of purification factor (PF) and recovery yield (R%; Table 2), indicating significant differences in the physicochemical properties, to some extent probably caused by the different degrees of glycosylation of the individual HRP isoenzymes. However, the HCIC elution profile of the HRP isoenzyme C1A that was shown previously [33], could be reproduced under the conditions applied in the present study as the whole HRP activity was found in the flowthrough (Fig. 1). The higher PF for HRP C1A in this study compared to our previous results [33] (i.e. 7-fold versus 5-fold, respectively) might be explained by the different cultivation approaches. In the present study, we produced HRP C1A in shake flask cultivations, whereas previous cultivations were done in the controlled environment of a bioreactor [33]. The latter allowed cultivation under optimized conditions, thus limiting cell lysis and contamination of the cultivation broth by intracellular proteins. Presumably, the amount of contaminating proteins in the starting solution was therefore lower, causing an overall lower PF for the C1A preparation from the bioreactor.

Elution profiles similar to the one shown in Fig. 1 were found for ten other HRP isoenzymes (graphs not shown), indicating the applicability of the HCIC flowthrough purification for these isoenzymes (Table 2). Remarkably, a 16-fold purification at 100% recovery was achieved for isoenzyme HRP A2A (Table 2). However, for some isoenzymes the flowthrough based HCIC step could not be applied successfully as no purification was achieved (e.g. HRP 22489.1; Table 2). To find an explanation for that phenomenon, we looked at the single isoenzymes in more detail. Predictions of potential N-glycosylation sites, based on the identification of the conserved N-X-S/T motif, were performed using the NetNGlyc 1.0 Server (Table 1). Interestingly, the number of predicted potential N-glycosylation sites correlated well with both the PF and the recovery yield (R%; Fig. 2). This observation strongly underlines our previous hypothesis that extensive glycosylation prevents the interaction of recombinant HRP from *P. pastoris* with the HCIC material, hence allowing the negative chromatography purification step [33]. For example, HRP C1A and HRP A2A each contain nine N-X-S/T motifs and could be purified 7.0- and 15.9-fold at 95.4 and 100.0% recovery, respectively. HRP 6351 and HRP C3, on the other hand, contain only 2 and 3 N-X-S/T motifs and could only be purified 3.0- and 2.2-fold at 32.6 and 17.6% recovery, respectively (Tables 1 and 2). Outliers from that correlation, e.g. HRP 22684.1, which could not be purified via HCIC (PF of 0.1; Table 2) despite containing four N-X-S/T motifs, might be explained by varying degrees in glycosylation due to steric hindrance at certain N-glycosylation sites. However, the generally high correlation between the number of glycosylation sites and both the PF and

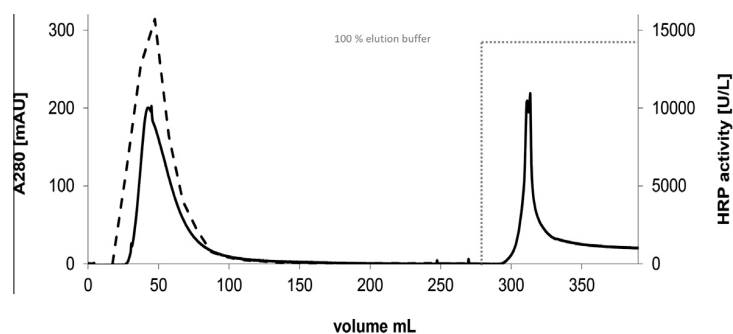


**Fig. 1.** HIC chromatogram of the recombinant HRP isoenzyme C1A. The HRP activity (dashed line) was determined by using ABTS as reducing substrate. Protein content was followed throughout the run by recording the absorption at 280 nm (solid line).

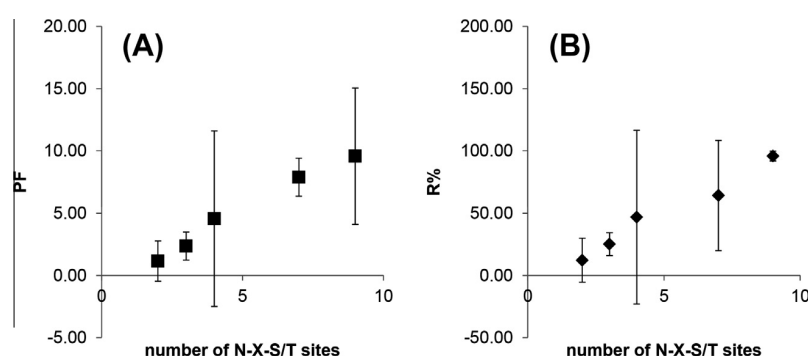


**Fig. 2.** Correlation of the number of N-glycosylation sites and HIC purification parameters. A, purification factor (PF); B, recovery yield of HRP activity in percentage (R%). The average PF and R% for HRPs with  $n$  N-X-S/T sites are shown with the corresponding calculated standard deviations;  $n_2 = 3$ ,  $n_3 = 4$ ,  $n_4 = 3$ ,  $n_7 = 2$ ,  $n_9 = 3$ .

the R%, as evident in Fig. 2, allows the design of an appropriate purification strategy for extensively glycosylated enzymes produced in *P. pastoris*.

#### Anion exchange chromatography (AEC)

Recently, monolithic columns were discovered as a powerful tool for both analytical purposes and preparative protein purification [49–51]. The solid support, a uniform monolithic porous material (e.g. glycidyl methacrylate-based materials), is simple to handle and to scale up, allows elevated operating flow rates and pressures (e.g. flow rates of up to  $336 \text{ cm h}^{-1}$  and a back pressure of up to 20 bar for an 8 mL tube monolithic column from BIA separations), and provides high binding capacity ( $>20 \text{ mg mL}^{-1}$ ). These beneficial features are mainly enabled by the convective mass transfer of the target molecule through the highly interconnected channel structure of the porous polymer block. In convective processes, both resolution and binding capacity are not affected by the flow rate, an effect that is emphasized when large biomolecules such as proteins are separated due to their high diffusion coefficients [49]. On the other hand, porous particles which are applied in conventional chromatographic media require diffusive transport of the molecules which have to enter the pores to get in contact with the active surface. This diffusive transport results in increased separation times and void volumes.

In our previous study, we polished partially purified recombinant HRP C1A after HCIC by SEC [33]. Although this strategy gave a good PF of  $>2.0$  and a recovery yield of 100%, SEC has several uneconomical disadvantages such as low flow rates, sample dilution, temperature effects due to long process times, limited sample volumes and limited scalability. Thus, we tested monolithic columns as an alternative to SEC. A wide range of monolithic formats

and ligands is available today [52]. In this study, we tested two AEC resins and a HIC resin, since these two purification principles had shown promising results using particle-based resins for recombinant HRP C1A before [33]. We used different buffer systems and elution profiles for the potential application of CIM<sup>®</sup> tube monolithic columns as polishing step for recombinant HRP C1A, partially purified after HCIC. Active flowthrough fractions from HCIC purifications were pooled, concentrated via diafiltration and loaded on the different CIM<sup>®</sup> tube columns. The HIC resin CIM<sup>®</sup>-OH was not able to purify recombinant HRP C1A after HCIC any further, regardless of the buffers applied. We believe that this was due to the fact that the vast majority of hydrophobic proteins had already been retained on the HCIC resin. Using the strong AEC resin CIM<sup>®</sup>-QA, the enzyme preparation could not be purified more than 1.3-fold regardless of the buffer, a phenomenon which we also observed with particle-based strong AEC materials before [33]. However, the weak AEC tube monolithic column CIM<sup>®</sup>-DEAE gave satisfactory results. Using Tris-HCl (50 mM, pH 8.0) as loading buffer, a PF of nearly 11.0 was obtained for recombinant HRP C1A when the negative chromatography approach was applied.

Interestingly, similar to the HCIC flowthrough step, operation of AEC in the flowthrough mode also gave diverse results in terms of PF and R% for the different recombinant HRP isoenzymes (Table 2). Some isoenzymes could not be purified by this strategy, whereas other isoenzymes were purified up to 66-fold. Remarkably, for isoenzymes 1805, 5508 and 22489.2 only the second purification step via the CIM<sup>®</sup>-DEAE monolithic column worked, whereas HCIC could not improve the preparations in terms of enzyme purity; in fact, PFs of more than 30 showed that for some HRP isoenzymes the AEC step alone already described an efficient purification strategy (Table 2). The HRP isoenzymes 22684.1, 6351 and 22489.1 did not show any detectable peroxidase activity after diafiltration

indicating instability under the conditions applied. Furthermore, no HRP activity was detected prior to AEC for 22684.2 and 1350 due to the high dilution of the enzyme at that stage (Table 2). Therefore, we cannot comment on the applicability of the AEC strategy for these five isoenzymes.

Summarizing, the CIM<sup>®</sup>-DEAE tube monolith describes a highly interesting alternative to SEC as a polishing step for partially purified recombinant HRP isoenzymes. Compared to the PF of around 2.0 which we achieved for the recombinant HRP isoenzyme C1A using SEC before [33], the flowthrough step applying an anion exchange monolith presented here is not only advantageous in terms of flow rates, sample volumes and thus process time, but also gave a 5-fold higher PF of nearly 11.0. In Fig. 3 we exemplarily show a SDS gel of the different steps during AEC purification of the HRP isoenzyme C1A. Although there are no striking bands indicating contaminant proteins in the flowthrough fraction of AEC, the specific activity of the purified HRP C1A preparation in this study was remarkably lower than in our previous study [33]: The preparation of HRP C1A in this study yielded a specific activity of only approximately 100 U mg<sup>-1</sup>, whereas the C1A preparation in our previous study yielded a specific activity of approximately 1000 U mg<sup>-1</sup> [33]. We ascribe this phenomenon to the different cultivation procedures. Whereas HRP C1A was produced in the controlled environment of a bioreactor constantly providing optimal conditions for *P. pastoris* in our previous work [33], in the present study the HRP isoenzymes, including HRP C1A, were produced in shake flasks where conditions were not controlled. Limitations in oxygen and nutrients as well as gradients, which can occur in shake flasks, apparently influence the physiology of the cells and hence their ability to produce catalytically active enzyme. In fact, this is a very good example how the upstream process might influence the downstream process and the final product quality.

#### Basic biochemical characterization of HRP isoenzyme preparations

After the chromatographic 2-step purification procedure, the flowthrough fractions of the single HRP isoenzymes were pooled and concentrated by ultrafiltration before basic biochemical characterization was done. Especially, for HRP isoenzymes 22684.2 and 1350, where the concentration of HRP in the collected fractions was very low, this step was essential to be able to obtain reliable kinetic data.

As anticipated from our preliminary data [38], the preparations of the recombinant HRP isoenzymes featured significantly different biochemical properties. Not only physicochemical parameters, such as the predicted pI (Table 1), covered a broad range, but also the enzymatic activity towards the two tested electron donors ABTS and TMB were found to be highly versatile (Table 3; examples for Michaelis–Menten plots shown in Fig. 4).

For the oxidation of ABTS, the highest  $V_{max}$  values were obtained for the preparations of the isoenzymes A2A and A2B. These two isoenzyme preparations were able to oxidize ABTS 4- to 5-fold better than the preparation of the well-studied isoenzyme C1A (Table 3), rendering our preparations of HRP A2A and A2B particularly interesting for diagnostic bioassays with increased sensitivity. In a previous study on commercial preparations of acidic HRP isoenzymes from the plant, a comparatively high  $K_M$  value of 4.0 mM was reported for ABTS as the reducing substrate [53]. In contrast, the here reported  $K_M$  values of recombinant preparations of the acidic isoenzymes A2A and A2B were significantly lower with 1.95 and 1.73 mM, respectively. An explanation for this difference in substrate affinity remains speculative, but might be ascribed to the slightly different amino acid sequences of isoenzymes A2A and A2B used in this study compared to the commercial isoenzymes.

The here presented apparent  $K_M$  of 1.01 mM for ABTS for the HRP C1A preparation was higher than the previously published  $K_M$  values of 0.27 mM and 0.18 mM for C1A preparations from plant and *E. coli*, respectively [54]. In a previous study on recombinant HRP C1A from *P. pastoris* a  $K_M$  of 0.68 mM was reported [30]. Apparently, yeast-derived HRP C1A preparations generally have a tendency for a lowered affinity for ABTS, probably related to the yeast-type hyperglycosylation compared to preparations from plant and *E. coli*.

Interestingly, some HRP isoenzyme preparations did not show any (e.g. 22684.1) or only very low (e.g. 08562.4) catalytic activity with H<sub>2</sub>O<sub>2</sub> and ABTS. Nevertheless, bearing the biochemical diversity of HRP isoenzymes in mind, these isoenzymes might be more active towards other substrates that were not tested in this study.

The oxidation of TMB was catalyzed best by the HRP C1A preparation, followed by HRP A2A and A2B (Table 3). Interestingly, HRP A2A oxidized TMB slower than ABTS, whereas most other isoenzymes – including C1A and A2B – oxidized TMB faster than ABTS (Table 3). Once more, these kinetic differences demonstrate the diverse substrate affinities and biochemical properties of the individual HRP isoenzymes. Keeping this variance in mind, it is of

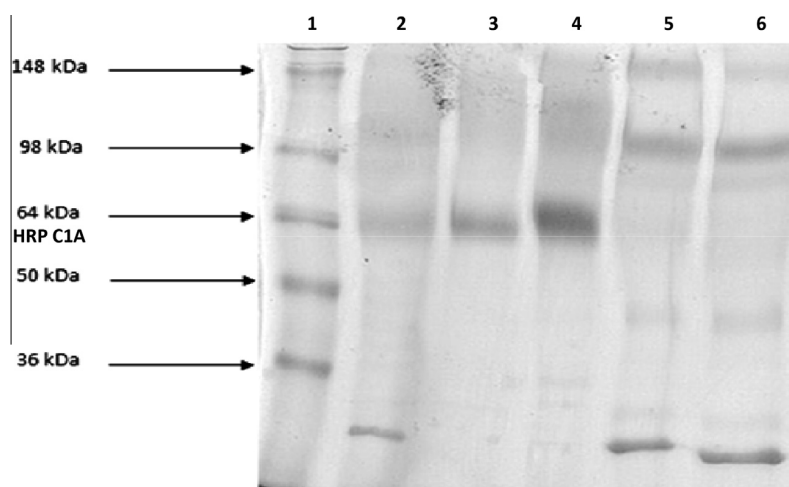


**Fig. 3.** SDS-PAGE of fractions from AEC with HRP C1A. Lane 1, molecular mass standard; lane 2, cell-free cultivation supernatant (5 µg); lane 3, flowthrough (5 µg); lane 4, flowthrough (10 µg); lanes 5 and 6, fractions eluted with buffer AEC-B (5 µg).

**Table 3**

Kinetic parameters of recombinant HRP isoenzyme preparations after 2-step flow-through purification. Kinetic data of the purified HRP isoenzyme preparations were recorded for the electron donors ABTS and TMB at a concentration of 1.0 mM H<sub>2</sub>O<sub>2</sub>. In some preparations, no peroxidase activity could be detected. In these cases, no values for V<sub>max</sub> or K<sub>M</sub> are available (n/a).

HRP isoenzyme	ABTS		TMB	
	V <sub>max</sub> [U mg <sup>-1</sup> ]	K <sub>M</sub> [mM]	V <sub>max</sub> [U mg <sup>-1</sup> ]	K <sub>M</sub> [mM]
C1A	105.54	1.01	2031.50	0.11
25148.1 (C1C)	8.13	4.02	243.14	0.16
25148.2 (C1D)	9.94	3.55	139.77	0.13
04627 (C2)	5.52	4.49	82.34	0.15
C3	0.31	12.5	2.60	0.08
A2A	483.02	1.95	397.99	0.12
A2B	538.40	1.73	1049.11	0.18
E5	33.15	3.51	14.38	0.06
1805	2.95	2.36	39.02	0.11
22684.1	n/a	n/a	n/a	n/a
22684.2	1.08	3.36	11.02	0.07
1350	2.64	2.62	23.62	0.06
5508	42.40	0.46	9.89	0.10
6351	n/a	n/a	n/a	n/a
22489.1	0.17	3.03	n/a	n/a
22489.2	2.42	2.70	1.89	0.16
17517.2	0.11	0.39	0.24	0.32
08562.4	0.05	0.31	0.10	0.20
08562.1	0.10	0.18	0.06	0.11

considerable importance to choose the most suitable isoenzyme for a certain application in the future, e.g. to use a HRP A2B preparation for a diagnostic kit with ABTS as substrate, but a HRP C1A preparation for diagnostics with TMB as substrate, to achieve optimal assay sensitivity. On that note, the here described efficient purification strategy is a prerequisite for the application of specific HRP isoenzyme preparations. Also, the possibility for the recombi-

nant production of a certain HRP isoenzyme with favorable characteristics for a given application in *P. pastoris* is superior to the currently applied, but unpredictable and irreproducible isolation of a mixture of HRP isoenzymes from horseradish roots.

**Table 4**

Calculated half life times at 60 °C (τ<sub>1/2</sub>) of recombinant HRP isoenzyme preparations. Some isoenzymes did not show any detectable loss in HRP activity after 60 min. The thermal stability of recombinant HRP preparations with an initial V<sub>max</sub> lower than 0.5 U mg<sup>-1</sup> for ABTS were not determined (n.d.). Due to a limited amount of purified enzyme, HRP 04627 (C2) and HRP E5 were not included in this study (n.i.).

HRP isoenzyme	τ <sub>1/2</sub> [min]
C1A	Stable for 60
25148.1 (C1C)	159
25148.2 (C1D)	21
04627 (C2)	n.i.
C3	n.d.
A2A	64
A2B	55
E5	n.i.
1805	Stable for 60
22684.1	n.d.
22684.2	46
1350	62
5508	17
6351	n.d.
22489.1	n.d.
22489.2	11
17517.2	n.d.
08562.4	n.d.
08562.1	n.d.

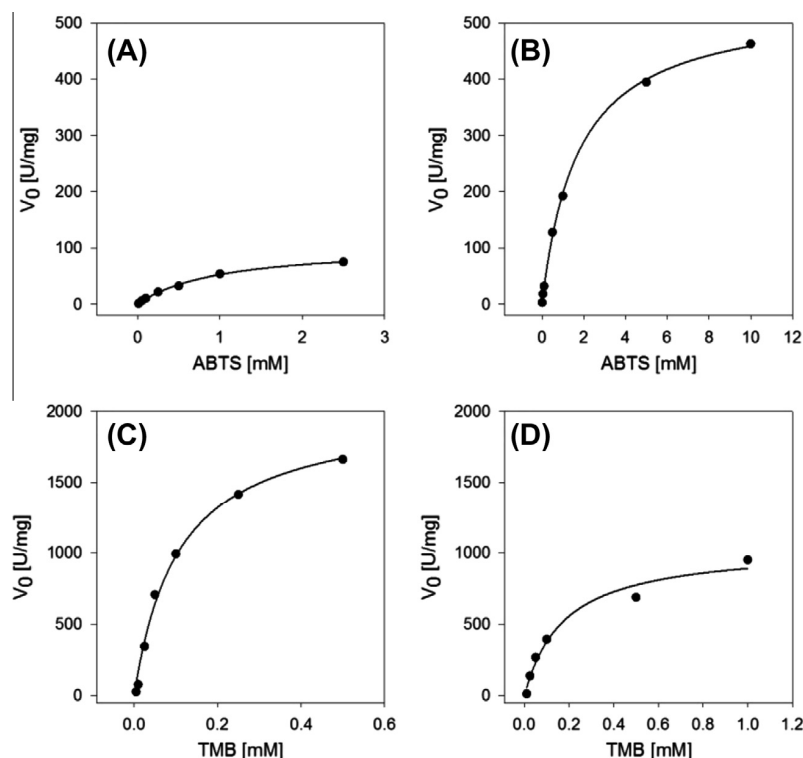


**Fig. 4.** Michaelis-Menten plots for preparations of recombinant HRP C1A and A2B. (A) HRP C1A with ABTS; (B) HRP A2B with ABTS; (C) HRP C1A with TMB; (D) HRP A2B with TMB. The Michaelis-Menten plots for all HRP isoenzyme preparations of this study are shown in [Supplementary Figs. 1–6](#).

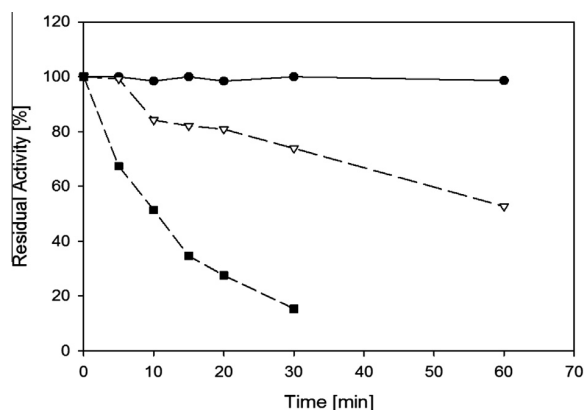


**Fig. 5.** Thermal stability profiles of selected recombinant HRP preparations. Filled circles, HRP C1A; open triangles, HRP A2A; filled squares, HRP 22489.2. Residual HRP activity was determined over 60 min of incubation at 60 °C.

#### Thermostability of HRP isoenzyme preparations

The HRP isoenzyme preparations did not only differ in terms of enzymatic activity and substrate specificity, but also in thermal stability (Table 4). The preparations of HRP C1A and HRP 1805 did not show a detectable decrease in catalytic activity after 60 min of incubation at 60 °C, whereas the activity of HRP 22489.2 was already below 20% of the initial activity after 30 min. A summary of all the calculated thermal half-life times ( $\tau_{1/2}$ ) is given in Table 4. The thermal stability profiles of the stable HRP C1A preparation, the moderately stable HRP A2A and the quite unstable HRP 22489.2 at 60 °C over time are exemplarily shown in Fig. 5. As shown in Table 4, the most thermostable HRP preparations of this study were HRP C1A and HRP 1805, which both did not show any detectable loss in catalytic activity at 60 °C after 60 min. HRP A2A and A2B, which are highly interesting in terms of catalytic activity with ABTS and TMB (Table 3), showed a significantly lower thermal stability (Table 4, Fig. 5). However, for possible future applications of these isoenzymes in sensitive bioassays, their stability is supposedly sufficient. In addition, no significant loss of peroxidase activity of these two isoenzymes could be detected over weeks when stored at 4 °C.

#### Conclusions

In the present study, we recombinantly produced 19 single HRP isoenzymes in *P. pastoris* in shake flask cultivations. We optimized our recently reported 2-step purification approach for recombinant hyperglycosylated HRP replacing the tedious SEC step with an AEC step using a tube monolithic column. After purification, we biochemically characterized the individual HRP isoenzyme preparations with different substrates and evaluated their thermal stability. The main outcomes of this study can be summarized as:

- The novel 2-step flowthrough purification strategy gave a recovery yield of 55% and a PF of approximately 77 for the recombinant HRP isoenzyme C1A. Although the recovery yield was lower, the PF was more than 7-fold higher compared to our previous study, where we achieved a recovery yield of 93% but only a PF of 10. Despite the lower recovery, the here presented strategy is superior, since the second purification step can be run in flowthrough mode, thus allowing both high sample volumes and flow rates.

- Regarding the other isoenzymes especially HRP 04627 (C2), A2A and 5508 could be purified very efficiently with PFs of 62, 684 and 144, respectively. HRP 25148.1 (C1C), 25148.2 (C1D), 04627 (C2), A2B and 1805 were purified 15- to 38-fold.
- The correlation between the amount of potential N-glycosylation sites and the success in flowthrough purification can be used to design an efficient purification strategy for glycosylated proteins expressed in *P. pastoris* in general.
- Basic biochemical characterization using ABTS and TMB revealed significant differences of the individual isoenzyme preparations. The preparations of HRP A2A and HRP A2B turned out to be highly active with H<sub>2</sub>O<sub>2</sub> and ABTS and hence are especially interesting for applications in diagnostic assays with high sensitivity.

The data provided in this study pave the way for cost-effective recombinant production of HRP isoenzymes in *P. pastoris*. Current efforts are made in our lab to provide detailed information on the identification of new HRP isoenzymes from a next generation sequencing of the horseradish transcriptome and to show classifying data on the new HRP isoenzyme sequences (Näättsaari et al., in preparation). Future in-depth studies will provide information on the molecular mechanisms underlying the differences in activity and stability of the various interesting HRP isoenzymes.

#### Acknowledgments

The authors are very grateful to the Austrian Science Fund FWF: project P24861-B19 and FWF: W901 DK Molecular Enzymology for financial support. We further thank the company BIA separations (Slovenia) for providing the monolithic columns and Ms. Astrid Wening for excellent technical assistance in the lab.

#### Appendix A. Supplementary data

Supplementary data associated with this article can be found, in the online version, at <http://dx.doi.org/10.1016/j.pep.2013.12.003>.

#### References

- [1] B. Chance, The kinetics and stoichiometry of the transition from the primary to the secondary peroxidase peroxide complexes, *Arch. Biochem. Biophys.* 41 (1952) 416–424.
- [2] P. George, Chemical nature of the secondary hydrogen peroxide compound formed by cytochrome-c peroxidase and horseradish peroxidase, *Nature* 169 (1952) 612–613.
- [3] P. George, The chemical nature of the second hydrogen peroxide compound formed by cytochrome c peroxidase and horseradish peroxidase. I. Titration with reducing agents, *Biochem. J.* 54 (1953) 267–276.
- [4] L.A. Planche, Note sur la sophistication de la résine de jalap et sur les moyens de la reconnaître, *Bull. Pharm.* 2 (1810) 578–580.
- [5] J.F. Kratochvil, R.H. Burris, M.K. Seikel, J.M. Harkin, Isolation and characterization of  $\alpha$ -guaiacolic acid and the nature of guaiacum blue, *Phytochemistry* 10 (1971) 2529–2531.
- [6] A.J. Gross, I.W. Sizer, The oxidation of tyramine, tyrosine, and related compounds by peroxidase, *J. Biol. Chem.* 234 (1959) 1611–1614.
- [7] F. Passardi, C. Penel, C. Dunand, Performing the paradoxical: how plant peroxidases modify the cell wall, *Trends Plant Sci.* 9 (2004) 534–540.
- [8] F. Passardi, C. Cosio, C. Penel, C. Dunand, Peroxidases have more functions than a Swiss army knife, *Plant Cell Rep.* 24 (2005) 255–265.
- [9] M.C. Hoyle, High resolution of peroxidase-indoleacetic acid oxidase isoenzymes from horseradish by isoelectric focusing, *Plant Physiol.* 60 (1977) 787–793.
- [10] M.A. Jermyn, Horseradish peroxidase, *Nature* 169 (1952) 488–489.
- [11] M.A. Jermyn, R. Thomas, Multiple components in horseradish peroxidase, *Biochem. J.* 56 (1954) 631–639.
- [12] L.M. Shannon, E. Kay, J.Y. Lew, Peroxidase isozymes from horseradish roots. I. Isolation and physical properties, *J. Biol. Chem.* 241 (1966) 2166–2172.
- [13] E. Kay, L.M. Shannon, J.Y. Lew, Peroxidase isozymes from horseradish roots. II. Catalytic properties, *J. Biol. Chem.* 242 (1967) 2470–2473.

- [14] S. Marklund, P.I. Ohlsson, A. Opara, K.G. Paul, The substrate profiles of the acidic and slightly basic horseradish peroxidases, *Biochim. Biophys. Acta* 350 (1974) 304–313.
- [15] S. Aibara, T. Kobayashi, Y. Morita, Isolation and properties of basic isoenzymes of horseradish peroxidase, *J. Biochem.* 90 (1981) 489–496.
- [16] S. Aibara, H. Yamashita, E. Mori, M. Kato, Y. Morita, Isolation and characterization of five neutral isoenzymes of horseradish peroxidase, *J. Biochem.* 92 (1982) 531–539.
- [17] K. Fujiyama, H. Takemura, S. Shibayama, K. Kobayashi, J.K. Choi, A. Shinmyo, et al., Structure of the horseradish peroxidase isozyme C genes, *Eur. J. Biochem.* 173 (1988) 681–687.
- [18] M. Gajhede, D.J. Schuller, A. Henriksen, A.T. Smith, T.L. Poulos, Crystal structure of horseradish peroxidase C at 2.15 Å resolution, *Nat. Struct. Biol.* 4 (1997) 1032–1038.
- [19] K.G. Welinder, Amino acid sequence studies of horseradish peroxidase. Amino and carboxyl termini, cyanogen bromide and tryptic fragments, the complete sequence, and some structural characteristics of horseradish peroxidase C, *Eur. J. Biochem.* 96 (1979) 483–502.
- [20] B.Y. Yang, J.S. Gray, R. Montgomery, The glycans of horseradish peroxidase, *Carbohydr. Res.* 287 (1996) 203–212.
- [21] J.W. Tams, K.G. Welinder, Mild chemical deglycosylation of horseradish peroxidase yields a fully active, homogeneous enzyme, *Anal. Biochem.* 228 (1995) 48–55.
- [22] J.W. Tams, K.G. Welinder, Glycosylation and thermodynamic versus kinetic stability of horseradish peroxidase, *FEBS Lett.* 421 (1998) 234–236.
- [23] C.B. Lavery, M.C. Macinnis, M.J. Macdonald, J.B. Williams, C.A. Spencer, A.A. Burke, et al., Purification of peroxidase from Horseradish (*Armoracia rusticana*) roots, *J. Agric. Food Chem.* 58 (2010) 8471–8476.
- [24] A.T. Smith, N. Santama, S. Dacey, M. Edwards, R.C. Bray, R.N. Thorneley, et al., Expression of a synthetic gene for horseradish peroxidase C in *Escherichia coli* and folding and activation of the recombinant enzyme with Ca<sup>2+</sup> and heme, *J. Biol. Chem.* 265 (1990) 13335–13343.
- [25] V. Grigorenko, T. Chubar, Y. Kapeliuch, T. Borchers, F. Spener, A. Egorov, New approaches for functional expression of recombinant horseradish peroxidase C in *Escherichia coli*, *Biocatalysis Biotransformation* 17 (1999) 359–379.
- [26] C. Hartmann, P.R. Ortiz de Montellano, Baculovirus expression and characterization of catalytically active horseradish peroxidase, *Arch. Biochem. Biophys.* 297 (1992) 61–72.
- [27] M. de las, M. Segura, G. Levin, M.V. Miranda, F.M. Mendive, H.M. Targovnik, O. Cascone, High-level expression and purification of recombinant horseradish peroxidase isozyme C in SF-9 insect cell culture, *Process Biochem.* 40 (2005) 795–800.
- [28] A. Vlamis-Gardikas, A.T. Smith, J.M. Clements, J.F. Burke, Expression of active horseradish peroxidase in *Saccharomyces cerevisiae*, *Biochem. Soc. Trans.* 20 (1992) 1115.
- [29] B. Morawski, Z. Lin, P. Cirino, H. Joo, G. Bandara, F.H. Arnold, Functional expression of horseradish peroxidase in *Saccharomyces cerevisiae* and *Pichia pastoris*, *Protein Eng.* 13 (2000) 377–384.
- [30] B. Morawski, S. Quan, F.H. Arnold, Functional expression and stabilization of horseradish peroxidase by directed evolution in *Saccharomyces cerevisiae*, *Biotechnol. Bioeng.* 76 (2001) 99–107.
- [31] F.W. Krainer, C. Dietzsch, T. Hajek, C. Herwig, O. Spadiut, A. Glieder, Recombinant protein expression in *Pichia pastoris* strains with an engineered methanol utilization pathway, *Microb. Cell Factor* 11 (2012) 22–35.
- [32] C. Dietzsch, O. Spadiut, C. Herwig, A dynamic method based on the specific substrate uptake rate to set up a feeding strategy for *Pichia pastoris*, *Microb. Cell Factor* 10 (2011) 14–22.
- [33] O. Spadiut, L. Rossetti, C. Dietzsch, C. Herwig, Purification of a recombinant plant peroxidase produced in *Pichia pastoris* by a simple 2-step strategy, *Protein Expr. Purif.* 86 (2012) 89–97.
- [34] M.G. Brattain, M.E. Marks, T.G. Pretlow, The purification of horseradish peroxidase by affinity chromatography on Sepharose-bound concanavalin A1,2, *Anal. Biochem.* 72 (1976) 346–352.
- [35] M.V. Miranda, H.M. Fernández-Lahore, J. Dobrecky, O. Cascone, The extractive purification of peroxidase from plant raw materials in aqueous two-phase systems, *Acta Biotechnol.* 18 (1998) 179–188.
- [36] W. Guo, E. Ruckenstein, Separation and purification of horseradish peroxidase by membrane affinity chromatography, *J. Membr. Sci.* 211 (2003) 101–111.
- [37] L.F. Fraguas, F. Batista-Viera, J. Carlsson, Preparation of high-density concanavalin A adsorbent and its use for rapid, high-yield purification of peroxidase from horseradish roots, *J. Chromatogr. B Analyt. Technol. Biomed. Life Sci.* 803 (2004) 237–241.
- [38] A. Glieder, F.W. Krainer, M. Kulterer, L. Näätäsaari, V. Reichel, Horseradish peroxidase isoenzymes, EP2584035 A1, 2013.
- [39] S.K. Sharma, N. Sehgal, A. Kumar, A quick and simple biostrip technique for detection of lactose, *Biotechnol. Lett.* 24 (2002) 1737–1739.
- [40] C.C. Chiou, P.Y. Chang, E.C. Chan, T.L. Wu, K.C. Tsao, J.T. Wu, Urinary 8-hydroxydeoxyguanosine and its analogs as DNA marker of oxidative stress: development of an ELISA and measurement in both bladder and prostate cancers, *Clin. Chim. Acta* 334 (2003) 87–94.
- [41] A. Singh, D. Ma, D.L. Kaplan, Enzyme-mediated free radical polymerization of styrene, *Biomacromolecules* 1 (2000) 592–596.
- [42] N. Vasileva, T. Godjevargova, D. Ivanova, K. Gabrovska, Application of immobilized horseradish peroxidase onto modified acrylonitrile copolymer membrane in removing of phenol from water, *Int. J. Biol. Macromol.* 44 (2009) 190–194.
- [43] O. Greco, S. Rossiter, C. Kanthou, L.K. Folkes, P. Wardman, G.M. Tozer, et al., Horseradish peroxidase-mediated gene therapy: choice of prodrugs in oxic and anoxic tumor conditions, *Mol. Cancer Ther.* 1 (2001) 151–160.
- [44] L. Näätäsaari, B. Mistlberger, C. Ruth, T. Hajek, F.S. Hartner, A. Glieder, Deletion of the *Pichia pastoris* KU70 homologue facilitates platform strain generation for gene expression and synthetic biology, *PLoS One* 7 (2012) e39720.
- [45] R. Weis, R. Luiten, W. Skranc, H. Schwab, M. Wubbolts, A. Glieder, Reliable high-throughput screening with *Pichia pastoris* by limiting yeast cell death phenomena, *FEMS Yeast Res.* 5 (2004) 179–189.
- [46] O. Spadiut, C. Leitner, C. Salaheddin, B. Varga, B.G. Vertessy, T.-C. Tan, et al., Improving thermostability and catalytic activity of pyranose 2-oxidase from *Trametes multicolor* by rational and semi-rational design, *FEBS J.* 276 (2009) 776–792.
- [47] D. Mattanovich, A. Graf, J. Stadlmann, M. Dragosits, A. Redl, M. Maurer, et al., Genome, secretome and glucose transport highlight unique features of the protein production host *Pichia pastoris*, *Microb. Cell Factor* 8 (2009) 29.
- [48] C.-J. Huang, L.M. Damasceno, K.A. Anderson, S. Zhang, L.J. Old, C.A. Batt, A proteomic analysis of the *Pichia pastoris* secretome in methanol-induced cultures, *Appl. Microbiol. Biotechnol.* 90 (2011) 235–247.
- [49] H. Podgornik, A. Podgornik, A. Perdih, A method of fast separation of lignin peroxidases using convective interaction media disks, *Anal. Biochem.* 272 (1999) 43–47.
- [50] H. Podgornik, A. Podgornik, P. Milavec, A. Perdih, The effect of agitation and nitrogen concentration on lignin peroxidase (LiP) isoform composition during fermentation of *Phanerochaete chrysosporium*, *J. Biotechnol.* 88 (2001) 173–176.
- [51] H. Podgornik, A. Podgornik, Separation of manganese peroxidase isoenzymes on strong anion-exchange monolithic column using pH-salt gradient, *J. Chromatogr. B Analyt. Technol. Biomed. Life Sci.* 799 (2004) 343–347.
- [52] M. Barut, A. Podgornik, P. Brne, A. Strancar, Convective interaction media short monolithic columns: enabling chromatographic supports for the separation and purification of large biomolecules, *J. Sep. Sci.* 28 (2005) 1876–1892.
- [53] A.N. Hiner, J. Hernández-Ruiz, M.B. Arnao, F. García-Cánovas, M. Acosta, A comparative study of the purity, enzyme activity, and inactivation by hydrogen peroxide of commercially available horseradish peroxidase isoenzymes A and C, *Biotechnol. Bioeng.* 50 (1996) 655–662.
- [54] D.J. Gilfoyle, J.N. Rodríguez-Lopez, A.T. Smith, Probing the aromatic-donor-binding site of horseradish peroxidase using site-directed mutagenesis and the suicide substrate phenylhydrazine, *Eur. J. Biochem.* 236 (1996) 714–722.
- [55] B. Bjellqvist, G.J. Hughes, C. Pasquali, N. Paquet, F. Ravier, J.C. Sanchez, et al., The focusing positions of polypeptides in immobilized pH gradients can be predicted from their amino acid sequences, *Electrophoresis* 14 (1993) 1023–1031.
- [56] B. Bjellqvist, B. Basse, E. Olsen, J.E. Celis, Reference points for comparisons of two-dimensional maps of proteins from different human cell types defined in a pH scale where isoelectric points correlate with polypeptide compositions, *Electrophoresis* 15 (1994) 529–539.
- [57] R. Gupta, E. Jung, S. Brunak, Prediction of N-glycosylation sites in human proteins, 2004 (in preparation).

# Glyco-variant library of the versatile enzyme horseradish peroxidase

Simona Capone<sup>2</sup>, Robert Pletzenauer<sup>2</sup>, Daniel Maresch<sup>3</sup>, Karl Metzger<sup>2</sup>, Friedrich Altmann<sup>3</sup>, Christoph Herwig<sup>2</sup>, and Oliver Spadiut<sup>1,2</sup>

<sup>2</sup>Institute of Chemical Engineering, Research Area Biochemical Engineering, Vienna University of Technology, Vienna 1060, Austria and <sup>3</sup>Department of Chemistry, University of Natural Resources and Life Sciences, Vienna 1190, Austria

Received on April 11, 2014; revised on May 20, 2014; accepted on May 20, 2014

When the glycosylated plant enzyme horseradish peroxidase (HRP) is conjugated to specific antibodies, it presents a powerful tool for medical applications. The isolation and purification of this enzyme from plant is difficult and only gives low yields. However, HRP recombinantly produced in the yeast *Pichia pastoris* experiences hyperglycosylation, which impedes the use of this enzyme in medicine. Enzymatic and chemical deglycosylation are cost intensive and cumbersome and hitherto existing *P. pastoris* strain engineering approaches with the goal to avoid hyperglycosylation only resulted in physiologically impaired yeast strains not useful for protein production processes. Thus, the last resort to obtain less glycosylated recombinant HRP from *P. pastoris* is to engineer the enzyme itself. In the present study, we mutated all the eight N-glycosylation sites of HRP C1A. After determination of the most suitable mutation at each N-glycosylation site, we physiologically characterized the respective *P. pastoris* strains in the bioreactor and purified the produced HRP C1A glyco-variants. The biochemical characterization of the enzyme variants revealed great differences in catalytic activity and stability and allowed the combination of the most promising mutations to potentially give an unglycosylated, active HRP C1A variant useful for medical applications. Interestingly, site-directed mutagenesis proved to be a valuable strategy not only to reduce the overall glycan content of the recombinant enzyme but also to improve catalytic activity and stability. In the present study, we performed an integrated bioprocess covering strain generation, bioreactor cultivations, downstream processing and product characterization and present the biochemical data of the HRP glyco-library.

**Keywords:** bioprocess technology / glyco-engineering / glycosylation / horseradish peroxidase / *Pichia pastoris*

## Introduction

The heme-containing plant enzyme horseradish peroxidase (HRP; EC 1.11.1.7) is a Class III peroxidase catalyzing the oxidation of various substrates (e.g., amines, aromatic phenols, indoles, phenolic acids and sulfonates) using hydrogen peroxide (H<sub>2</sub>O<sub>2</sub>) as oxidant. Horseradish peroxidase exists in at least 19 different isoenzyme forms in the horseradish root (*A Armoracia rusticana*), of which isoenzyme C1A is the most abundant and thus the most studied one (e.g., Dunford 1999; Veitch and Smith 2001; Veitch 2004; Carlsson et al. 2005; Krainer et al. 2013; Spadiut and Herwig 2013). It is a 34 kDa monomeric oxidoreductase containing a heme-group as well as two Ca<sup>2+</sup>-ions as prosthetic groups. The crystal structure of HRP C1A led to the identification of nine N-glycosylation sites of the Asn-X-Ser/Thr type, where X can be any amino acid but proline, of which eight are occupied when the enzyme is expressed in plant (Smith et al. 1990), which is why the molecular mass of HRP C1A increases from 34 to ~44 kDa (Veitch 2004; Spadiut and Herwig 2013). Due to glycosylation and the presence of both, the heme-group and disulfide bridges, the recombinant production and subsequent preparative purification of HRP has proven to be very difficult (Smith et al. 1990; Gajhede et al. 1997; Lavery et al. 2010; Spadiut et al. 2012), which is why HRP is still mainly isolated from plant (Lavery et al. 2010). However, HRP preparations from plant describe a mixture of isoenzymes, which seasonally varies in composition and concentration, and yields are extremely low (Jermyn 1952; Jermyn and Thomas 1954; Shannon et al. 1966). Since HRP is a versatile enzyme used in numerous, quite diverse industrial and medical applications, such as waste water treatment, fine chemical synthesis, immunoassays, biosensors and coupled enzyme assays (e.g., Krieg and Halhuber 2003), the controllable recombinant production and subsequent efficient purification of single HRP isoenzymes is highly desired. Thus, we have not only investigated and improved the recombinant production of the isoenzyme HRP C1A with *Pichia pastoris* in the past few years (Dietzsch et al. 2011a,b; Krainer et al. 2012; Zalai et al. 2012; Spadiut et al. 2013), but also developed an efficient downstream process for the hypermannosylated enzyme recombinantly derived from this yeast (Spadiut et al. 2012; Krainer, Pletzenauer, et al. 2013). However, for medical applications where HRP is conjugated to antibodies, like antibody-directed enzyme-prodrug therapy (Folkes and Wardman 2001; Wardman 2002) and medical

<sup>1</sup>To whom correspondence should be addressed: Tel: +43-1-58801-166473, Fax: +43-1-58801-166980, e-mail: oliver.spadiut@tuwien.ac.at

diagnostics (Romero et al. 1999; Huang 2001; Palmgren et al. 2011; Dotsikas and Loukas 2012), the degree of glycosylation of HRP is of utmost importance, since not only the stability of the enzyme but also the conjugation with antibodies is expected to change with varying glycosylation. Besides, the untrimmed yeast-derived high-mannose containing glycosylation can trigger immune responses in humans (personal communication with Dr. Lisa Folkes; Gray Institute for Radiation Oncology and Biology, Department of Oncology, University of Oxford).

Obviously, the availability of an enzyme without or at least with reduced surface glycosylation would solve abovementioned problems. However, the biological role and importance of glycans for plant peroxidases is still not completely understood and is topic of numerous studies in glycobiology. So far, some studies report stabilizing effects of the glycans (Narhi et al. 1991; Wang et al. 1996), whereas other studies do not show such effects (Ehlers et al. 1992; Powell and Pain 1992). In 1990, Smith et al. (1990) were able to produce active and correctly folded HRP without any glycans in *Escherichia coli*. In a following study, Tams and Welinder analyzed the importance of the glycosylation for HRP in more detail (Tams and Welinder 1998). They showed that the removal of most of the glycans, except the *N*-acetylglucosamine residues, by a mild chemical deglycosylation with trifluoromethanesulfonic acid resulted in a fully active, but less stable enzyme (Tams and Welinder 1995, 1998). Both studies showed that glycans on the surface of HRP affect the physicochemical properties of the enzyme but are not required for catalytic activity. However, chemical deglycosylation only left 60% of HRP active and also describes a quite cumbersome procedure (Tams and Welinder 1995, 1998), which is why it is not a useful method to obtain unglycosylated HRP. Although recombinant proteins from *P. pastoris* can also be deglycosylated enzymatically (Sainz-Pastor et al. 2006; Kang et al. 2012), also this option has to be reconsidered, since (1) enzymatic deglycosylation is only quantitative when the target protein is denatured and (2) the additional endoglycosidases have to be removed again to obtain pure product. Another way to control and reduce the complexity of native yeast-like glycosylation on glycoproteins secreted from *P. pastoris* is through glyco-engineering (Choi et al. 2003; Hamilton et al. 2003; Verweken et al. 2004; Hamilton and Gerngross 2007). A key event in such engineering is the knockout of the OCH1 gene, which initiates outer-chain elongation, leading to hypermannosylation. However, in a previous study, where we knocked out this gene, we observed that HRP with reduced glycan complexity possessed hampered downstream processing and that the glyco-engineered *P. pastoris* strains generated were physiologically impaired, impeding efficient production processes (Kraimer et al. 2013).

Consequently, the last resort to efficiently produce HRP with a reduced amount of surface glycosylation is to glyco-engineer the enzyme itself. In a recent study, two selected Asn residues of HRP were mutated to Asp to analyze effects on the stability of the enzyme and to produce more properly folded HRP in *E. coli* (Asad, Khajeh, et al. 2011). Asad, Khajeh, et al. (2011) showed that introducing the mutations Asn13Asp and Asn268Asp did not just affect the production of HRP in *E. coli*, but also increased the catalytic constants as well as the thermal stability. These results did not only underline the possibility of obtaining

active and correctly folded HRP with reduced glycosylation but also showed that mutating the glycosylation sites may even have beneficial effects on catalytic activity and stability.

In the present study, we generated a glyco-variant library of HRP C1A exchanging all the eight Asn serving as glycosylation sites by the structurally similar amino acids Asp, Gln or Ser. We did not only investigate the effects of the single mutations on enzyme activity and stability but also on protein purification following an integrated bioprocess technology approach. After determining the most suitable mutation at the single N-glycosylation sites, we physiologically characterized the respective *P. pastoris* strains in the controlled environment of a bioreactor. A two-step purification procedure, where both chromatography steps were performed in the flow-through mode, enabled us to recover purified HRP glyco-variants for subsequent biochemical characterization. Based thereon, we combined the most suitable mutations to potentially obtain an unglycosylated, active HRP variant suitable for medical applications. Summarizing, we conducted an integrated bioprocess study and present the bioprocess technological and biochemical results for the HRP C1A glyco-variant library.

## Results and discussion

### Screening procedure

Every transformation into *P. pastoris* CBS7435 Mut<sup>S</sup> yielded several dozens of transformants. We randomly picked five transformants per mutation and screened them for cell growth and production of active HRP in shake flasks. With only few exceptions, all the picked transformants produced active HRP; however, on average only three of five showed comparable growth and productivity. PCR analysis confirmed the presence of the target gene in the genome of *P. pastoris*. Although we did not analyze the exact number of gene integration events by real-time polymerase chain reaction, we assumed the integration of a comparable amount of gene copies into the yeast genome due to the fact that we always transformed the same amount of linearized vector DNA into the *P. pastoris* cells (i.e., 2 µg DNA). We had observed such a correlation in a previous study (Kraimer et al. 2012). Although we did not check for the exact integration site of the target gene in the host genome, we ascribe the observed differences in protein production during the screening procedure to a fair amount of non-homologous recombination of the transformed HRP C1A gene into the genome of *P. pastoris* (Naatsaari et al. 2012), most likely at different loci in the chromosome, which consequently influences the accessibility of the transcription machinery to the transformed gene (Kraimer et al. 2012). In Table 1, we compared the growth of the best transformant per mutation as well as the specific activity and thermal stability of the produced HRP C1A glyco-variants. Although diagnostic applications are normally not performed at 60°C, we determined the stability of HRP at this temperature since we observed nice differences for the glyco-variants at this temperature and the assay could be easily performed in the laboratory. Furthermore, we used the thermal stability as a measure for kinetic stability, as also discussed elsewhere (Polizzi et al. 2007; Spadiut et al. 2009). We always included a *P. pastoris* strain expressing the unmutated wild-type (wt) HRP C1A in the screening experiments as control. Although we obtained slightly different results for the wt depending on the screening round, we included the average values for

**Table I.** Results of screening experiments to identify the most suitable mutation at the single N-glycosylation sites of HRP C1A

Mutation	Results after 96 h of induction					Chosen mutation
	OD <sub>600</sub>	Cat. activity (U mL <sup>-1</sup> )	Protein content (mg mL <sup>-1</sup> )	Spec. activity (U mg <sup>-1</sup> )	Residual activity after 4 h at 60°C (%)	
wt	25.2	7.5	0.13	48.4	75.0	
N13D	31.8	0.69	0.09	7.29	27.0	→N13D
N13Q	42.3	0.74	0.08	9.10	10.5	
N13S	35.1	–	–	–	–	
N57D	31.4	0.77	0.11	7.00	53	→N57S
N57Q	23.4	2.48	0.13	19.1	43	
N57S	30.3	7.20	0.13	55.4	74	
N158D	32.7	6.11	0.23	26.6	100	→N158D
N158Q	34.1	0.49	0.37	1.32	81.8	
N158S	30.0	0.87	0.13	6.23	90.8	
N186D	36.8	0.10	0.09	1.06	43.1	→N186D
N186Q	47.6	0.07	0.10	0.70	0	
N186S	46.2	0.14	0.09	1.60	36.2	
N198D	21.3	12.1	0.23	53.1	68.1	→N198D
N198Q	19.7	4.31	0.22	20.1	34.1	
N198S	25.1	1.25	0.22	5.84	20.5	
N214D	17.9	5.03	0.11	46.6	46.1	→N214S
N214Q	18.1	4.92	0.13	39.0	41.5	
N214S	14.2	3.17	0.12	25.6	96.0	
N255D	13.6	7.24	0.13	53.9	66.5	→N255D
N255Q	14.2	8.59	0.18	48.3	78.8	
N255S	11.9	5.49	0.15	35.9	74.9	
N268D	13.6	0.56	0.27	2.07	70.6	→N268D
N268Q	12.9	0.40	0.26	1.54	71.0	
N268S	12.6	0.43	0.32	1.34	54.0	

growth, protein production, enzyme activity and thermal stability in Table I for comparison. Based on the determined specific activity and thermal stability, we chose the most suitable mutation at the single N-glycosylation sites. Except for N13S all the produced HRP glyco-variants showed catalytic activity; however, replacement of Asn by Gln never turned out to be the most suitable mutation at any of the eight N-glycosylation sites. Since we did not measure any detectable extracellular protein content for N13S either, we speculate that this mutation caused problems in protein folding and/or secretion, a phenomenon described before (Zhu et al. 1998; Ito, Ishimaru, et al. 2007; Ito, Seri, et al. 2007; Zou et al. 2013). Interestingly, we observed significant differences in enzyme activity and stability depending on the introduced mutation (Table I), and identified three mutations which had been described before, namely at positions N13 and N268 (Asad, Khajeh, et al. 2011) and N255 (Lin et al. 1999), respectively.

#### Physiological strain characterization in the bioreactor

The different *P. pastoris* strains carrying the respective mutated HRP gene were physiologically characterized in single dynamic batch cultivations in the controlled environment of a bioreactor. After exhaustion of glycerol which was indicated by an increase in the off-gas signal, a 0.5% (v/v) methanol adaptation pulse was applied which was followed by several, subsequent 1.0% (v/v) methanol pulses (an example for this procedure is illustrated for the *P. pastoris* strains expressing the wt enzyme and variant N57S in Figure 1, while illustrations for the other strains are shown in Supplementary data, Figure S1). This dynamic strategy has repeatedly proven to be a very efficient method to physiologically

characterize *P. pastoris* strains in a fast and simple manner (Dietzsch et al. 2011a,b; Krainer et al. 2012; Zalai et al. 2012).

In Table II, the determined strain characteristic parameters of all the strains are summarized. Apparently, the introduction of the respective recombinant HRP C1A gene had an impact on the physiology of the *P. pastoris* strains. Although the majority of the strains showed similar maximum specific growth rates on glycerol ( $\mu_{\max \text{ gly}}$ ) between 0.24 and 0.28 h<sup>-1</sup>, the strain carrying the gene HRP C1A N13D showed a nearly 1.3-fold higher  $\mu_{\max \text{ gly}}$ . This effect was even more pronounced with respect to the specific methanol uptake rate during the adaptation pulse ( $q_{\text{s adapt}}$ ). Surprisingly, when we calculated the average-specific methanol uptake rate during the consecutive 1% (v/v) methanol pulses ( $q_{\text{s average MeOH}}$ ), we observed striking differences between all the strains. One can speculate that the reason for the altered strain physiology lies in the produced HRP glyco-variant itself, since it is known that N-glycosylation can influence protein folding and protein production and thus might affect cell physiology (Zhu et al. 1998; Ito, Ishimaru, et al. 2007; Ito, Seri, et al. 2007; Zou et al. 2013). However, as shown in Table II, the amount of total extracellular protein for each strain at the end of the dynamic batch cultivation was basically the same, indicating that the single mutations did not cause significant problems in protein folding or secretion. We also analyzed the cell-free cultivation broths on SDS gels and obtained the same pattern of protein bands at comparable intensity (graphs not shown). Thus, apparently not the mutated product but rather the locus of the respective introduced gene in the yeast genome had a significant influence on the methanol metabolism of the cells. This influence is also obvious in both yield coefficients (biomass yield,

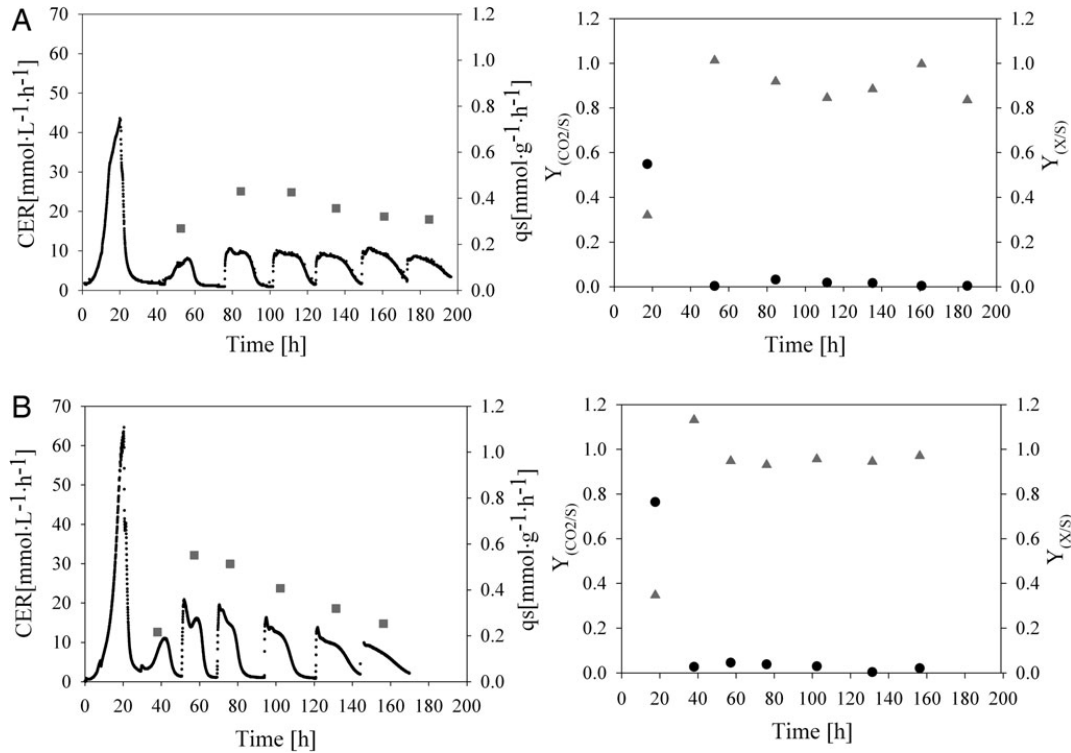


**Fig. 1.** Batch cultivation of a *P. pastoris* CBS7435 Mut<sup>S</sup> strain carrying either the unmutated HRP C1A gene (designated as “wt”) or the glyco-variant HRP C1A N57S. A1, batch cultivation with methanol pulses of wt; B1, batch cultivation with methanol pulses of N57S. Solid black line, carbon dioxide evolution rate (CER); gray square, specific substrate uptake rate ( $q_s$ ). A2, calculated yields of wt; B2, calculated yields of N57S. Gray triangle, carbon dioxide yield ( $Y_{CO_2/S}$ ); black dot, biomass yield ( $Y_{X/S}$ ).

**Table II.** Strain characteristic parameters determined for recombinant *P. pastoris* strains harboring either the wt HRP C1A gene or a glyco-variant thereof and the amount of total extracellular protein at the end of cultivation

Strain	$\mu_{max\ gly}$ (h <sup>-1</sup> )	$\Delta_{time\ adapt}$ (h)	$q_s\ adapt$ (mmol g <sup>-1</sup> h <sup>-1</sup> )	$q_s\ average_{MeOH}$ (mmol g <sup>-1</sup> h <sup>-1</sup> )	$Y_{X/S}$ (C <sub>mol</sub> C <sub>mol</sub> <sup>-1</sup> )	$Y_{CO_2/S}$ (C <sub>mol</sub> C <sub>mol</sub> <sup>-1</sup> )	C-balance	Protein (mg mL <sup>-1</sup> )
wt	0.277	11.1	0.269	0.370	0.013	0.92	0.93	0.08
N13D	0.330	8.7	0.317	0.592	0.063	0.88	0.95	0.08
N57S	0.245	12.8	0.216	0.409	0.027	0.95	1.02	0.09
N158D	0.251	13.5	0.211	0.304	0.065	1.00	1.07	0.09
N186D	0.268	13.1	0.211	0.273	0.019	1.00	1.02	0.10
N198D	0.244	8.3	0.292	0.372	0.022	0.90	0.96	0.08
N214S	0.267	14.4	0.219	0.213	0.012	0.95	0.95	0.08
N255D	0.253	8.4	0.291	0.537	0.006	0.96	1.00	0.11
N268D	0.258	14.4	0.253	0.256	0.038	1.00	1.04	0.08

$Y_{X/S}$ ; carbon dioxide yield,  $Y_{CO_2/S}$ ). However, we did not investigate the exact locus of gene integration for the single strains in more detail. Closing C-balances for all cultivations confirm the accuracy of the calculated strain specific parameters. It is remarkable that although we used the same *P. pastoris* strain CBS7435 Mut<sup>S</sup>, the same vector and basically the same gene except for single point mutations, we obtained physiologically diverging strains. This actually underlines the importance of a detailed physiological strain characterization using the dynamic method applying methanol pulses, especially if subsequent fed-batch cultivations for protein production are envisioned.

#### Protein purification

After cultivation, the respective HRP glyco-variant was purified from the cell-free cultivation broth using a previously reported two-step flow-through strategy (Spadiut et al. 2012; Krainer, Pletzenauer, et al. 2013). Total protein content and enzymatic activity were determined in the flow-through and the eluates and the respective recovery yield of HRP activity in percentage ( $R\%$ ) and the purification factor (PF) were calculated for each single purification step (Table III).

After hydrophobic charge induction chromatography (HCIC), we recovered >80% of wt HRP C1A and of most

**Table III.** Results of the two-step purification approach for HRP C1A applying HCIC and AEC both operated in flow-through mode

Variant	HCIC			AEC			Combined		Spec. activity (U mg <sup>-1</sup> )
	R% total	R% FT	PF	R% total	R% FT	PF	R%	PF	
wt	83.6	83.6	1.95	85.9	77.1	3.46	64.5	6.7	248
N13D	91.5	91.5	2.94	85.6	24.5	7.92	22.4	23.3	689
N57S	80.7	80.4	2.70	86.2	70.9	3.32	56.3	9.0	461
N158D	53.8	53.6	1.85	90.1	75.0	5.02	40.2	9.3	167
N186D	86.8	86.8	1.48	91.4	57.1	10.2	49.6	15.1	198
N198D	51.3	51.1	1.30	84.0	50.4	1.89	25.8	2.5	114
N214S	82.4	82.3	1.66	94.4	45.3	4.53	37.3	7.5	113
N255D	94.9	94.9	2.95	96.4	75.4	6.59	71.6	19.4	236
N268D	94.7	94.7	3.43	82.0	74.9	4.21	70.9	14.4	274

enzyme variants except for N158D and N198D. In agreement with our previous observations (Spadiut et al. 2012; Krainer et al. 2013), the whole activity was found in the flow-through. The remaining 5–20% of the enzymes did not elute from the column under the conditions applied, which actually proves the existence of a variety of enzyme species in the cultivation broth differing in glycosylation and thus a varying degree of interaction with the resin. Interestingly, for glyco-variant N158D and N198D, we only recovered 50% of the enzyme in total, which we also found in the flow-through. Apparently, by mutating these two glycosylation sites and thus reducing the overall amount of surface N-glycosylation, the masking effect thereof was reduced leading to a different HCIC performance for these two enzyme variants. However, compared with the other glycosylation sites we could not identify a particular location of these two sites which could potentially explain this phenomenon (Supplementary data, Figure S2). By HCIC, the wt enzyme was purified 2-fold, whereas the success of purification varied between 1.3- and 3.4-fold for the different glyco-variants highlighting the importance of an integrated bioprocess aspect—already little changes of protein properties, as the degree of surface N-glycosylation, might have a significant impact on following unit operations. The difference in the PF for wt HRP C1A compared with previous studies where we achieved a PF of 7.0 (Krainer, Pletzenauer, et al. 2013) might be explained by the different cultivation strategies. In our previous study, we cultivated *P. pastoris* in shake flasks, where conditions were not controlled and limitations in nutrients and oxygen occurred, which is why cells were more sensitive to cell lysis. Consequently, more contaminating proteins were found in the cell-free cultivation broth. In the present study, we cultivated the different strains in a bioreactor where parameters, such as pH and temperature, were controlled and thus undesired cell lysis was reduced. Consequently, the cell-free cultivation broth contained less contaminating proteins. This is also obvious when looking at the cell-free cultivation broth before purification, which showed a specific activity of only 20 U mg<sup>-1</sup> from shake flasks (Krainer, Pletzenauer, et al. 2013) but ~40 U mg<sup>-1</sup> in the present study.

In the subsequent anion exchange chromatography (AEC) step, we recovered >80% of the initially applied HRP for all enzyme variants (Table III). However, the amount of HRP we found in the flow-through vastly differed between the glyco-variants. For the wt enzyme and variants N57S, N158D, N155D and N268D, we found a comparable amount of ~75%

of HRP in the flow-through, whereas for variants N13D, N186D, N198D and N214S, the recovery in the flow-through was only 50% or less. For N13D, we even only found 25% of the enzyme in the flow-through, whereas the rest was found in the eluate together with contaminating proteins. However, when we looked at the location of N13 in comparison to the other glycosylation sites we could not identify a particularity which could explain this phenomenon (Supplementary data, Figure S2). This again highlights the importance of the single N-glycosylation sites and the respective surface N-glycosylation for the physicochemical properties of HRP and the applicability of the flow-through chromatography approach. With regard to AEC purification success, we obtained a PF of >3 for the wt enzyme and similar values for N57S, N214S and N268D. Although we only recovered 25% of the initial amount of N13D in the flow-through, this glyco-variant was purified nearly 8-fold. Also N158D, N186D and N255D were purified with great success (5-, 10- and more than 6-fold, respectively), whereas for variant N198D, a PF of only two was determined in the flow-through.

With respect to the overall purification efficiency for the glyco-variant library of HRP C1A using a two-step flow-through approach, we observed vastly different results (Table III). The overall recovery of the initial amount of HRP after the two purification steps varied from only 20% to >70%. Also the obtained total PF varied immensely between 2.5 for variant N198D and >23 for N13D. Remarkably, these vast differences only originated from single point mutations of HRP C1A and consequent changes in surface N-glycosylation. Hence, for some of these variants, such as for N198D, we recommend to adapt the downstream strategy to obtain an enzyme preparation with higher purity.

#### Biochemical enzyme characterization

After protein purification, the enzyme variants were biochemically characterized. In Table IV, the kinetic constants for the substrates 2,2'-azino-bis(3-ethylbenzothiazoline-6-sulphonic acid) (ABTS) and H<sub>2</sub>O<sub>2</sub> are shown. The here presented apparent  $K_m$  of 1.60 mM of the wt HRP C1A preparation for ABTS was higher than the previously published  $K_m$  values of 0.27 and 0.18 mM for C1A preparations from plant and *E. coli*, respectively (Gilfoyle et al. 1996). However, in previous studies on recombinant HRP C1A from *P. pastoris*,  $K_m$  values of 0.68 mM (Morawski et al. 2000) and 1.01 (Krainer, Pletzenauer, et al. 2013) were reported. Apparently, yeast-derived HRP C1A preparations generally have a

**Table IV.** Kinetic constants of wt HRP C1A and the glyco-variants for the substrates ABTS and H<sub>2</sub>O<sub>2</sub> as well as thermal stability

Variant	ABTS			H <sub>2</sub> O <sub>2</sub>			$\tau_{1/2}$ (min)
	$K_m$ (mM)	$V_{max}$ (U mg <sup>-1</sup> )	$V_{max}/K_m$ (U mg <sup>-1</sup> mM <sup>-1</sup> )	$K_m$ (mM)	$V_{max}$ (U mg <sup>-1</sup> )	$V_{max}/K_m$ (U mg <sup>-1</sup> mM <sup>-1</sup> )	
wt	1.60	44.2	27.7	0.003	16.3	5433	20.6
N13D	2.90	47.2	16.3	0.005	14.7	3066	28.9
N57S	2.98	113	38.1	0.004	23.7	5378	38.5
N158D	3.08	16.3	5.30	0.005	51.7	10,342	3.2
N186D	4.24	77.4	18.2	0.004	7.63	2179	18.8
N198D	1.21	14.9	12.3	0.003	19.1	5795	18.5
N214S	3.48	41.1	11.8	0.004	9.36	2531	6.3
N255D	1.72	51.5	29.9	0.005	21.6	4506	11.6
N268D	1.89	32.5	17.2	0.003	10.6	3642	61.9

tendency for a lowered affinity to ABTS compared with preparations from plant and *E. coli*, indicating a crucial role of glycosylation for enzyme activity.

As shown in Table IV, the  $K_m$  values of the glyco-variants for ABTS were higher than for the wt, except for variant N198D. Mutating the N-glycosylation sites on the surface of enzyme HRP C1A also affected the reaction rate (Table IV). Summarizing, in terms of catalytic efficiency with ABTS only variants N57S and N255D showed slightly higher or similar values compared with the wt. A similar effect for glyco-variant N255D had already been described elsewhere (Lin et al. 1999). The other glyco-variants were characterized by an up to 5-fold reduced catalytic efficiency. Interestingly, in the work of Asad, Khajeh, et al. (2011) HRP variants N13D and N268D also showed higher catalytic activity compared with the wt. However, Asad et al. used a different reducing substrate as well as different assay conditions, which is why a direct comparison with the present study is not feasible.

We observed similar trends of  $K_m$  and  $V_{max}$  for the substrate H<sub>2</sub>O<sub>2</sub>, as the majority of HRP glyco-variants showed a reduced catalytic efficiency compared with the wt enzyme (Table IV). In fact, N57S was the only glyco-variant showing similar or even higher catalytic efficiency with both substrates compared with the wt. The Michaelis–Menten kinetics for the wt enzyme and for variant N57S for both substrates is exemplarily shown in Figure 2, whereas illustrations for the other enzyme variants are shown in the Supplementary data, Figure S3.

To potentially explain the observed effects of the mutations on the surface of the enzyme on the catalytic activity, we determined the distance of the respective N-glycosylation site to the amino acid His170, which is linked to the heme group in the active site (Figure 3). However, we were not able to identify a direct correlation between the distance of the N-glycosylation site to the active site and observed changes in catalytic activity. Only resolving the crystal structures of the single HRP C1A glyco-variants and the subsequent analysis of structure–function relationships could potentially explain the observed effects of the respective mutation on the catalytic behavior.

Finally, we also tested the enzymes for thermal stability, since it is known that mutating N-glycosylation sites on the surface of proteins might affect stability (Asad, Khajeh, et al. 2011). In order to investigate if the protein concentration affects thermal stability, as described elsewhere (Asad, Khajeh, et al. 2011), two different concentrations, i.e., 0.01 and 0.02 mg mL<sup>-1</sup>, of the wt HRP were tested. In fact, we observed a huge

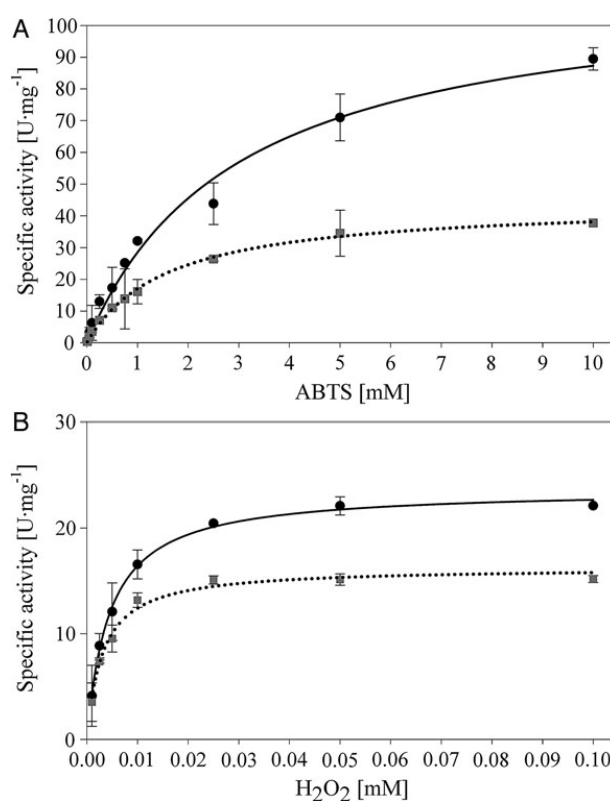


**Fig. 2.** Michaelis–Menten kinetics of the unmutated wt HRP C1A and the glyco-variant N57S for ABTS and H<sub>2</sub>O<sub>2</sub>. (A) Kinetics for ABTS, (B) kinetics for H<sub>2</sub>O<sub>2</sub>. Black dots, N57S; gray squares, wt.

difference in the half-life time at 60°C, which we determined with 20.6 min for the less concentrated protein solution and with 121 min for the more concentrated one. Consequently, we normalized all the different HRP glyco-variant solutions to a concentration of 0.01 mg mL<sup>-1</sup> before heat treatment. Interestingly, we found striking differences in the thermal stability of the enzyme glyco-variants (Table IV). For N158D, N214S and N255D stability was significantly reduced, whereas N186D and N198D showed half-life times comparable to the wt. Interestingly, N13D and N57S showed a higher thermal stability and N268D had an even 3-fold higher half-life time ( $\tau_{1/2}$ )

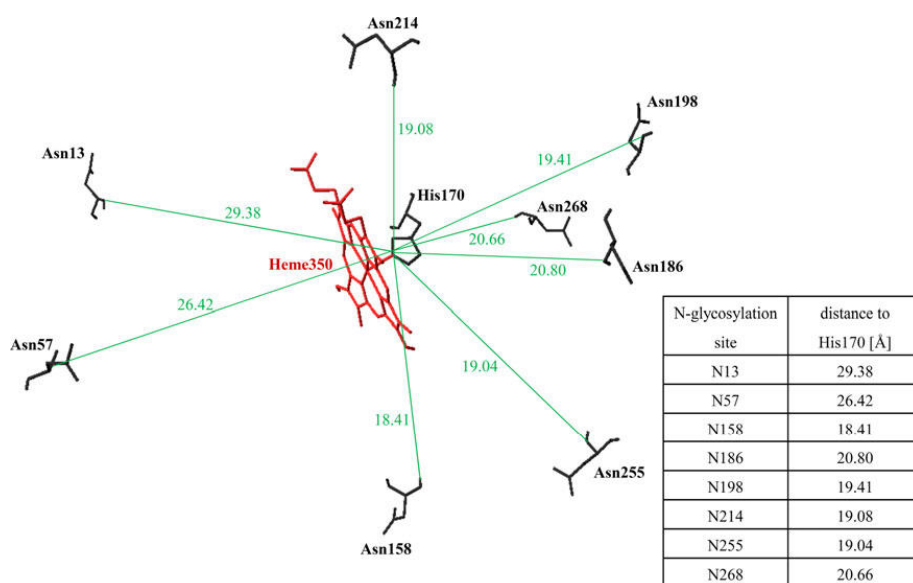


Fig. 3. Distances of the N-glycosylation sites on the surface of HRP C1A to the heme-binding site His170 in the active site.

than the fully glycosylated enzyme. Comparable observations for variants N13D and N268D were also made by Asad, Khajeh, et al. (2011). The differences between the determined half-life times in this study compared with the study of Asad et al., who determined the stability at 50°C, can be explained by differences in the assay conditions. Whereas Asad, Torabi, et al. (2011) used a 200 mM phosphate buffer, we only used a 50 mM phosphate buffer, which is known to positively affect HRP stability. Summarizing, it is remarkable that mutating glycosylation sites of a protein and thus reducing its overall glycosylation pattern does not only reduce protein stability but might also increase it.

**Glycosylation analysis.** To prove the absence of surface glycosylation on the respective mutated N-glycosylation site, we exemplarily performed glycosylation analysis for the glyco-variant N57S by digesting the protein with either chymotrypsin or trypsin and subsequently analyzing the peptides by liquid-chromatography mass spectrometry. Furthermore, aliquots of the chymotryptic digest were incubated with PNGase A and released glycans were analyzed by mass spectrometry (Figure 4). The success of mutating Asn57 to a non-glycosylated Ser was confirmed by mass spectrometric analysis of chymotryptic peptides. We clearly see the absence of surface N-glycosylation on N57S (Figure 4).

#### Combination of mutations

To potentially obtain an enzyme variant without any N-glycosylation, we combined all the eight mutations described in chapter Screening procedure (hereafter called “mutant”). The resulting *P. pastoris* strain was again cultivated in a batch with consecutive methanol pulses for physiological strain characterization (Table V). Again, we observed very different strain characteristic parameters, although we used the same *P. pastoris* strain CBS7435 Mut<sup>S</sup>, the same vector and basically the same gene except for eight point mutations. Closing C-balances for

both cultivations confirm the accuracy of the calculated strain specific parameters. In contrast to the strain carrying the wt HRP C1A gene, we were not able to detect any HRP activity in the cell-free cultivation broth for the strain carrying the mutated gene. Only after ultrafiltration and 20-fold concentration of the cultivation broth, we were able to measure activity for the mutated HRP C1A glyco-variant. We concentrated the enzyme further and diafiltrated it before we determined the catalytic constants with ABTS and H<sub>2</sub>O<sub>2</sub> as well as thermal stability (Table VI). As shown in Table VI, the combination of all eight mutations to obtain a HRP C1A variant without any N-glycans resulted in an enzyme variant with extremely reduced catalytic efficiency and thermal stability. Although the affinity towards ABTS basically remained the same, the catalytic activity was reduced nearly 300-fold. The effects for H<sub>2</sub>O<sub>2</sub> were even more severe, as  $K_m$  was increased >8-fold and  $V_{max}$  decreased >100-fold resulting in a nearly 1000-fold reduced catalytic efficiency. As judged by SDS-PAGE analysis, the size of this variant was significantly reduced compared with the glycosylated wt enzyme (figure not shown). However, since catalytic activity and stability were that low, making this variant not useful for medical applications, we did not analyze the surface N-glycosylation of this glyco-variant in more detail.

Summarizing, enzyme engineering describes a valid approach to obtain active HRP C1A variants with a reduced amount of surface N-glycosylation. Although an enzyme variant where all the eight N-glycosylation sites were mutated hardly showed catalytic activity and thus does not describe a meaningful tool for medical applications, the here described glyco-library of HRP C1A describes a very useful basis for further enzyme engineering approaches. Studies, where we only combine up to four mutations, namely N13D, N57S, N255D and N268D, and then express these variants in a *P. pastoris* OCH1 knockout strain (Krainer, Gmeiner, et al. 2013) to obtain a HRP C1A variant useful for targeted cancer treatment are currently ongoing.

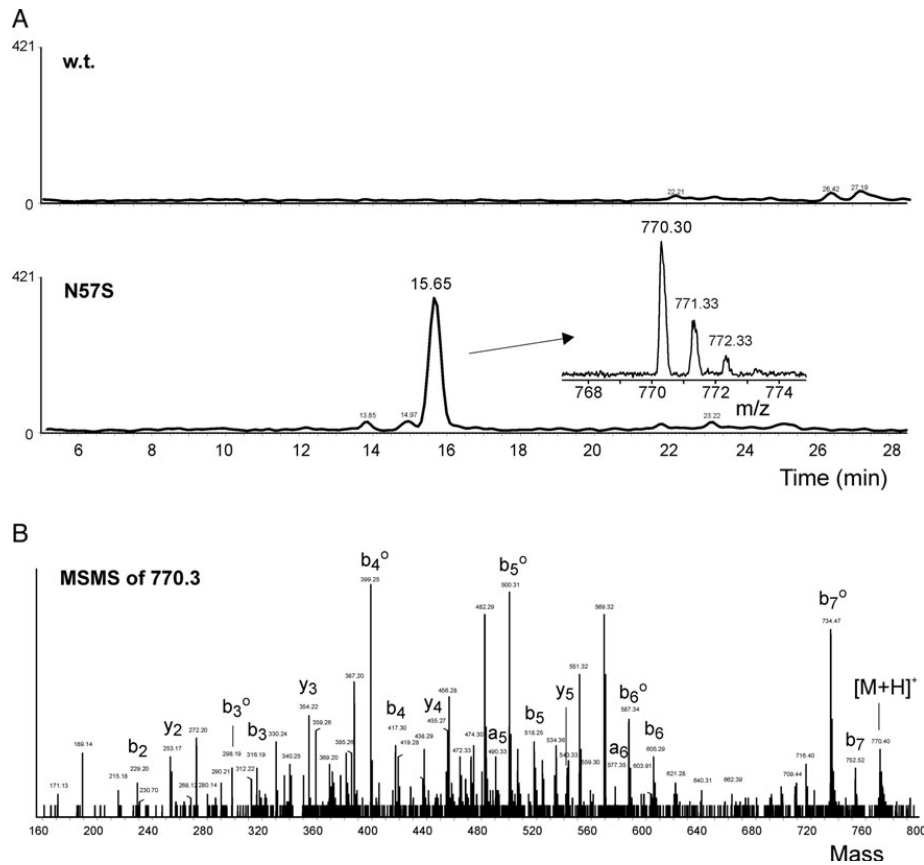


**Fig. 4.** Verification of the mutated peptide LD<sup>57</sup>STTSF by MS. (A) The extracted ion chromatograms for the mass of LDSTTSF ([M+H]<sup>+</sup> 770.36 Da) in N57S HRP. The mutant exhibited the relevant peak, whose identity was confirmed by CID fragmentation as shown in (B). B-fragments with loss of H<sub>2</sub>O are designated as b<sup>0</sup> fragments.

**Table V.** Strain characteristic parameters determined for recombinant *P. pastoris* strains harboring either the wt HRP C1A gene or a variant where all the eight N-glycosylation sites were mutated (mutant)

Strain	$\mu_{\max}$ gly (h <sup>-1</sup> )	$\Delta t_{\text{time adapt}}$ [h]	$q_s$ adapt (mmol g <sup>-1</sup> h <sup>-1</sup> )	$q_s$ average MeOH (mmol g <sup>-1</sup> h <sup>-1</sup> )	$Y_{X/S}$ (C <sub>mol</sub> C <sub>mol</sub> <sup>-1</sup> )	$Y_{CO_2/S}$ (C <sub>mol</sub> C <sub>mol</sub> <sup>-1</sup> )	C-balance	Protein (mg mL <sup>-1</sup> )
Wt	0.277	11.1	0.269	0.370	0.013	0.92	0.93	0.08
Mutant	0.222	4.7	0.660	0.882	0.153	0.81	0.97	0.10

**Table VI.** Kinetic constants of wt HRP C1A and the variant where all the eight N-glycosylation sites were mutated (mutant) for the substrates ABTS and H<sub>2</sub>O<sub>2</sub> as well as thermal stability

Variant	ABTS			H <sub>2</sub> O <sub>2</sub>			$\tau_{1/2}$ (min)
	$K_m$ (mM)	$V_{\max}$ (U mg <sup>-1</sup> )	$V_{\max}/K_m$ (U mg <sup>-1</sup> mM <sup>-1</sup> )	$K_m$ (mM)	$V_{\max}$ (U mg <sup>-1</sup> )	$V_{\max}/K_m$ (U mg <sup>-1</sup> mM <sup>-1</sup> )	
Wt	1.60	44.2	27.7	0.003	16.3	5433	20.6
Mutant	1.44	0.15	0.10	0.026	0.14	5.38	3.2

## Material and methods

### Chemicals

Enzymes were purchased from Fermentas GmbH (Vienna, Austria). ABTS diammonium salt was obtained from Sigma-Aldrich Handels GmbH (Vienna, Austria). Difco™ yeast nitrogen

base w/o amino acids (YNB), Bacto™ tryptone and Bacto™ yeast extract were obtained from Becton Dickinson and Company (Schwechat, Austria). Zeocin™ was obtained from Invitrogen (Vienna, Austria). D-Biotin was obtained from Fluka Chemia AG (St. Gallen, Switzerland). All other chemicals were purchased from Carl Roth GmbH & Co. KG (Karlsruhe, Germany).

*Strain and gene*

*P. pastoris* CBS7435 Mut<sup>S</sup> (Dietzsch et al. 2011a,b; Krainer et al. 2012; Zalai et al. 2012; Krainer, Gmeiner, et al. 2013; Spadiut et al. 2013) and vector pPpT4\_S harboring the HRP isoenzyme C1A, which was codon-optimized for high-level expression in *P. pastoris* (Krainer et al. 2012), were used in this study. The codon table described in Abad et al. (2010) was applied for codon optimization. Secretion of HRP C1A to the cultivation broth was facilitated by an N-terminally fused prepro-signal sequence of the *S. cerevisiae* alpha-factor.

*Site-directed mutagenesis*

The eight Asn, representing the glycosylation sites of HRP C1A, were mutated to either Asp, Gln or Ser, which are amino acids providing a certain structural similarity to Asn, by site-directed mutagenesis and subsequent digestion with DpnI (Li and Wilkinson 1997). The mutagenic PCR was performed as: 98°C for 30 s; then 10 cycles of 98°C for 10 s, 57°C for 20 s, 72°C for 1 min—10 cycles of 98°C for 10 s, 60°C for 20 s, 72°C for 1 min—10 cycles of 98°C for 10 s, 63°C for 20 s, 72°C for 1 min; with a final incubation at 72°C for 10 min. Each reaction contained 1 × HF buffer (Fermentas), 0.1 µg of plasmid DNA, 2.5 U *Phusion* DNA polymerase (Fermentas), 10 µM of each dNTP and 5 pmol of each primer in a total volume of 50 µL. All primers are listed in Table VII and were purchased from Microsynth (Vienna, Austria).

After PCR, the methylated template DNA was degraded by digestion with 10 U of DpnI at 37°C for at least 3 h. The remaining PCR products were purified using the QIAquick PCR purification kit (QIAGEN, Vienna, Austria) and 5 µL of each purified PCR product were transformed into electro-competent *E. coli* TOP10 F' cells. The successful introduction of the desired mutation and the absence of further mutations were confirmed by DNA sequencing (Microsynth). Transformation of ~2 µg SwaI-linearized pPpT4\_S plasmid DNA harboring the respective mutated HRP C1A gene (Supplementary data, Figure S4) into *P. pastoris* was done as described by Lin-Cereghino et al. (2005). Stable transformants were generated via homologous recombination between the linearized plasmid DNA and genomic yeast DNA. Selection of successfully transformed clones was performed on yeast extract peptone dextrose medium (YPD; 10 g L<sup>-1</sup> yeast extract, 20 g L<sup>-1</sup> peptone, 20 g L<sup>-1</sup> glucose, 20 g L<sup>-1</sup> agar) supplemented with 100 mg L<sup>-1</sup> Zeocin.

*Screening procedure*

Screening of five randomly picked *P. pastoris* transformants per mutation was done in 1000 mL shaking flasks. We also included a *P. pastoris* CBS7435 Mut<sup>S</sup> strain carrying the unmutated HRP C1A gene (henceforth designated as “wt”) as well as an untransformed *P. pastoris* CBS7435 Mut<sup>S</sup> strain as negative control, resulting in a total of 17 shaking flasks per screening experiment. First the clones were cultivated in 10 mL buffered glycerol complex medium supplemented with 100 mg L<sup>-1</sup> Zeocin (BMGY\_Zeo; 10 g L<sup>-1</sup> yeast extract; 20 g L<sup>-1</sup> peptone; 3.4 g L<sup>-1</sup> YNB w/o amino acids and ammonia sulfate, 10 g L<sup>-1</sup> (NH<sub>4</sub>)<sub>2</sub>SO<sub>4</sub>, 400 mg L<sup>-1</sup> biotin; 1 g L<sup>-1</sup> glycerol; 0.1 M potassium phosphate buffer, pH 6.0) in 100 mL shaking flasks at 30°C and 230 rpm overnight. The next day the OD<sub>600</sub> was measured, an appropriate aliquot of the culture was taken, and after

**Table VII.** Oligonucleotide primers to mutate the eight Asn residues of the enzyme HRP C1A, which act as N-glycosylation sites, to either Asp, Gln or Ser

N-site	Name	Sequence (5'→3')
N13	N13D_fwd	AAC TCT TGT CCT <i>GAT</i> GTG TCC AAC ATC
	N13Q_fwd	AAC TCT TGT CCT <i>CAG</i> GTG TCC AAC ATC
	N13S_fwd	AAC TCT TGT CCT <i>AGT</i> GTG TCC AAC ATC
N57	N13_rev	AGG ACA AGA GTT ATC GTA GAA GGT TGG AGT
	N57D_fwd	TCC ATC TTG CTG GAC <i>GAC</i> ACT ACC TC
	N57Q_fwd	TCC ATC TTG CTG GAC <i>CAG</i> ACT ACC TC
	N57S_fwd	TCC ATC TTG CTG GAC <i>AGC</i> ACT ACC TC
N158	N57_rev	GTC CAG CAA GAT GGA AGC ATC ACA ACC
	N158D_fwd	C AGA AAC GTT GGT CTT <i>GAC</i> AGA TCATCC
	N158Q_fwd	C AGA AAC GTT GGT CTT <i>CAG</i> AGA TCATCC
	N158S_fwd	C AGA AAC GTT GGT CTT <i>AGC</i> AGA TCATCC
N186	N158_rev	AAG ACC AAC GTT TCT GAA AGA GTC TTT CAA TTG
	N186D_fwd	ATG GAT CGT CTG TAC <i>GAC</i> TTC TCT AAC AC
	N186Q_fwd	ATG GAT CGT CTG TAC <i>CAG</i> TTC TCT AAC AC
	N186S_fwd	ATG GAT CGT CTG TAC <i>AGC</i> TTC TCT AAC AC
N198	N186_rev	GTA CAG ACG ATC CAT GAT GAATCTACATTG GTT
	N198D_fwd	CCA GAT CCT ACT CTG <i>GAC</i> ACC ACT TAC
	N198Q_fwd	CCA GAT CCT ACT CTG <i>CAG</i> ACC ACT TAC
	N198S_fwd	CCA GAT CCT ACT CTG <i>AGC</i> ACC ACT TAC
N214	N198_rev	CAG AGT AGG ATC TGG CAA ACC GG
	N214D_fwd	CCA CTT AAC GGA <i>GAC</i> CTG TCT GC
	N214Q_fwd	CCA CTT AAC GGA <i>CAG</i> CTG TCT GC
	N214S_fwd	CCA CTT AAC GGA <i>AGC</i> CTG TCT GC
N255	N214_rev	TCC GTT AAG TGG GCA CAA ACC TC
	N255D_fwd	TTG TTC TCC TCT CCT <i>GAC</i> GCT ACT GAT
	N255Q_fwd	TTG TTC TCC TCT CCT <i>CAG</i> GCT ACT GAT
	N255S_fwd	TTG TTC TCC TCT CCT <i>AGC</i> GCT ACT GAT
N268	N255_rev	AGG AGA GGA GAA CAA CTC CTG GTC
	N268D_fwd	G AGA TCC TTC GCA <i>GAC</i> TCC ACT CAA
	N268Q_fwd	G AGA TCC TTC GCA <i>CAG</i> TCC ACT CAA
	N268S_fwd	G AGA TCC TTC GCA <i>AGC</i> TCC ACT CAA
N268_rev	TGC GAA GGATCT CAC CAA TGG AAT G	

The mutation sites are depicted in italics.

centrifugation the cells were resuspended in selective buffered methanol complex medium supplemented with 100 mg L<sup>-1</sup> Zeocin (BMMY\_Zeo; 10 g L<sup>-1</sup> yeast extract; 20 g L<sup>-1</sup> peptone; 3.4 g L<sup>-1</sup> YNB w/o amino acids and ammonia sulfate, 10 g L<sup>-1</sup> (NH<sub>4</sub>)<sub>2</sub>SO<sub>4</sub>, 400 mg L<sup>-1</sup> biotin; 0.5% methanol; 0.1 M potassium phosphate buffer, pH 6.0) to an OD<sub>600</sub> of 1.0. The cells were again cultivated at 30°C and 230 rpm. Every day, 1% (v/v) methanol was pulsed to the culture and a 1 mL sample was taken, analyzed for optical density (OD<sub>600</sub>), catalytic activity and protein content. The catalytic activity of HRP was measured using an ABTS assay in a CuBiAn XC enzymatic robot (Bielefeld, Germany). Ten microliters of sample were mixed with 140 µL 1 mM ABTS solution (50 mM KH<sub>2</sub>PO<sub>4</sub>, pH 6.5). The reaction mixture was incubated at 37°C for 5 min before the reaction was started by the addition of 20 µL 0.078% H<sub>2</sub>O<sub>2</sub> (v/v). Changes in absorbance at 415 nm were measured for 80 s and rates were calculated. The standard curve was prepared using a commercially available HRP preparation (Type VI-A; Sigma–Aldrich) in the range from 0.02 to 2.0 U mL<sup>-1</sup>. Protein concentrations were determined at 595 nm by the Bradford assay using the Sigma–Aldrich Protein Assay Kit with bovine serum albumin as standard in the range of 0.2–1.2 mg mL<sup>-1</sup>.

After 96 h of induction, the HRP glyco-variants in the cell-free supernatants were tested for thermal stability. Therefore, aliquots of 1 mL were incubated in a waterbath at 60°C for up to 4 h, before the samples were centrifuged (14,000 rpm; 10 min)

and the supernatants were analyzed for remaining HRP activity. These values were then compared with the initial activity before heat treatment. Based on activity and stability measurements, the most suitable mutation at a respective N-glycosylation site was chosen and the corresponding *P. pastoris* strain was physiologically characterized in the bioreactor. Before bioreactor cultivation, the presence of the correctly mutated HRP gene in the respective *P. pastoris* transformant was verified by colony PCR using the primers AOX\_fwd (5'-ACTCCAACCTTCTACGATAACTC-3') and AOX\_rev (5'-ACTGTGTCATGTGCTGACC-3') and subsequent sequencing (Microsynth).

#### Strain characterization in the bioreactor

**Culture media.** Precultures were done in yeast nitrogen base medium with 100 mg L<sup>-1</sup> Zeocin (YNBM\_Zeo; 3.4 g L<sup>-1</sup> YNB w/o amino acids and ammonia sulfate, 10 g L<sup>-1</sup> (NH<sub>4</sub>)<sub>2</sub>SO<sub>4</sub>, 400 mg L<sup>-1</sup> biotin, 20 g L<sup>-1</sup> glucose, 0.1 M potassium phosphate buffer, pH 6.0). Batch cultivations were performed in basal salt medium (26.7 mL L<sup>-1</sup> 85% phosphoric acid, 1.17 g L<sup>-1</sup> CaSO<sub>4</sub>·2H<sub>2</sub>O, 18.2 g L<sup>-1</sup> K<sub>2</sub>SO<sub>4</sub>, 14.9 g L<sup>-1</sup> MgSO<sub>4</sub>·7H<sub>2</sub>O, 4.13 g L<sup>-1</sup> KOH, 40 g L<sup>-1</sup> glycerol, 0.2 mL L<sup>-1</sup> Antifoam Struktol J650, 4.35 mL L<sup>-1</sup> PTM1, NH<sub>4</sub>OH as N-source). Trace element solution (PTM1) was made of 6.0 g L<sup>-1</sup> CuSO<sub>4</sub>·5H<sub>2</sub>O, 0.08 g L<sup>-1</sup> NaI, 3.0 g L<sup>-1</sup> MnSO<sub>4</sub>·H<sub>2</sub>O, 0.2 g L<sup>-1</sup> Na<sub>2</sub>MoO<sub>4</sub>·2H<sub>2</sub>O, 0.02 g L<sup>-1</sup> H<sub>3</sub>BO<sub>3</sub>, 0.5 g L<sup>-1</sup> CoCl<sub>2</sub>, 20.0 g L<sup>-1</sup> ZnCl<sub>2</sub>, 65.0 g L<sup>-1</sup> FeSO<sub>4</sub>·7H<sub>2</sub>O, 0.2 g L<sup>-1</sup> biotin, 5 mL L<sup>-1</sup> H<sub>2</sub>SO<sub>4</sub>. Induction was carried out in presence of 1 mM Δ-aminolevulinic acid. The concentration of the base NH<sub>4</sub>OH was determined by titration with 0.25 M potassium hydrogen phthalate.

#### Experimental procedure

**Preculture.** Frozen stocks (-80°C) were cultivated in 100 mL YNB in 1000 mL shake flasks at 30°C and 230 rpm. The grown preculture was transferred aseptically to the respective culture vessel. The inoculation volume was 10% of the final starting volume.

**Batch cultivation.** Batch cultivations were carried out in either a 3 L or a 5 L working volume glass bioreactor (Infors, Bottmingen, Switzerland). Basal salt medium was sterilized in the bioreactor and pH was adjusted to pH 5.0 by using concentrated NH<sub>4</sub>OH solution after autoclaving. Sterile filtered trace elements were transferred to the reactor aseptically. Dissolved oxygen (dO<sub>2</sub>) was measured with a sterilizable dO<sub>2</sub> electrode (Visiferm™, Hamilton, Bonaduz, Switzerland). The pH was measured with a sterilizable electrode (Easyferm™, Hamilton, Bonaduz, Switzerland) and maintained constant with a PID controller using NH<sub>4</sub>OH solution (1–2 M). Base consumption was determined gravimetrically. Cultivation temperature was set to 30°C and agitation was fixed to 1200 rpm. The culture was aerated with 1.0 vvm dried air and off-gas of the culture was measured by using an infrared cell for CO<sub>2</sub> and a paramagnetic cell for O<sub>2</sub> concentration (Servomax, Hyderabad, India). Temperature, pH, dO<sub>2</sub>, agitation as well as CO<sub>2</sub> and O<sub>2</sub> in the off-gas were measured online and logged in a process information management system (Lucillus, Biospectra, Schlieren, Switzerland). After the complete consumption of the substrate glycerol, indicated by an increase of dO<sub>2</sub> and a drop in off-gas activity, the first methanol pulse of a final concentration of 0.5%

(v/v) was conducted with methanol supplemented with 12 mL L<sup>-1</sup> PTM1. Following pulses were performed with 1% methanol/PTM1 (v/v) (Figure 2). For each pulse, two samples were taken to determine the concentrations of substrate and product, as well as dry cell weight to calculate specific rates and yields.

#### Analysis of growth and expression parameters

Dry cell weight was determined by centrifugation of 5 mL culture broth (5000 rpm, 4°C, 10 min) in a laboratory centrifuge (Sigma 4K15, rotor 11156), washing the pellet twice with 5 mL deionized water and subsequent drying at 105°C to a constant weight.

#### Substrate concentrations

Concentrations of methanol were determined in cell-free samples by HPLC (Vienna, Austria) equipped with an ion-exchange column (Supelcogel C-610H Sigma–Aldrich) and a refractive index detector (Agilent Technologies). The mobile phase was 0.1% H<sub>3</sub>PO<sub>4</sub> with a constant flow rate of 0.5 mL min<sup>-1</sup> and the system was run isocratic at 30°C. Calibration was done by measuring standard points in the range from 0.1 to 10 g L<sup>-1</sup> methanol. Measurements of biomass, product and substrate concentration were executed in duplicates.

#### Protein purification

After bioreactor cultivation, the cell-free cultivation broth was diafiltered for subsequent HCIC using a Centramate 500S TFF system (PALL, Vienna, Austria) with a 10 kDa MWCO membrane. The buffer was HCIC-A (500 mM NaCl, 20 mM NaOAc, pH 6.0) and the protein solution was concentrated to a final volume of 40–50 mL. All further steps of concentration and buffer change were performed using Amicon Ultra-15 Centrifugal Filter Units with 10 kDa MWCO (Merck Millipore; Vienna, Austria). The HCIC resin MEP HyperCel™ was obtained from PALL and HCIC was performed in flow-through mode: a column containing 25 mL of MEP HyperCel™ resin was equilibrated with at least 4 column volumes (CV) of buffer HCIC-A. Forty to 50 mL concentrated HRP solution in HCIC-A were loaded onto the column which was then washed with at least 5 CV of HCIC-A at a flow rate of 55 cm h<sup>-1</sup>. Then a step elution to 100% buffer HCIC-B (1.0 M NaCl, 20 mM NaOAc, pH 8.0) was performed. After elution, the column was washed with 5 CV 0.8 M NaOH before it was stored in EtOH 20%, 1.0 M NaCl. During all the different steps, fractions of 10 mL were collected and analyzed for protein content and catalytic activity.

HCIC flow-through fractions showing HRP activity were pooled, concentrated and rebuffed in AEC-A (50 mM Tris–HCl, pH 8.0) for subsequent AEC using an 8 mL CIM®-DEAE monolithic column (Krainer, Pletzenauer, et al. 2013) (BIAseparations, Ajdovščina, Slovenia). The column was equilibrated with 5 CV of AEC-A at a flow rate of 16.8 cm h<sup>-1</sup>. Diafiltered post-HCIC pools were subsequently loaded onto the AEC column at an average linear flow rate of 16.8 cm h<sup>-1</sup> before a post-load wash with 5 CV of AEC-A was performed. Elution was performed in a single step from 0 to 100% AEC-B (50 mM Tris–HCl, 1.0 M NaCl, pH 8.0). The column was washed with 5 CV of a 1 M NaOH/1 M NaCl solution at an average linear flow rate of 33.6 cm h<sup>-1</sup> for column recovery, before the column was stored in 20% EtOH.

The efficiency of each purification step was evaluated by determining the PF and the recovery yield of HRP activity in percentage ( $R\%$ ). PF and  $R\%$  were calculated by Eqs (1) and (2) (Krainer, Pletzenauer, et al. 2013). The suffixes “pre” and “post” indicate the respective values before and after a purification step.

$$\text{PF} = \frac{\text{specific activity}_{\text{post}}}{\text{specific activity}_{\text{pre}}}, \quad (1)$$

$$R\% = 100 \times \frac{\text{volumetric activity}_{\text{post}} \times \text{volume}_{\text{post}}}{\text{volumetric activity}_{\text{pre}} \times \text{volume}_{\text{pre}}}. \quad (2)$$

Finally, the pooled active fractions after AEC were diafiltrated in 50 mM potassium phosphate buffer, pH 6.5, and concentrated to a volume of  $\sim 1.5$  mL for the subsequent biochemical characterization.

#### Biochemical enzyme characterization

Biochemical characterization of the purified HRP glyco-variants included the determination of the basic kinetic parameters  $K_m$  and  $V_{\text{max}}$  for the two substrates  $\text{H}_2\text{O}_2$  and ABTS in a spectrophotometer UV-1601 from Shimadzu (Korneuburg, Austria). The reaction mixture with a final volume of 1.0 mL contained 20  $\mu\text{L}$  of HRP glyco-variant, 50 mM potassium phosphate buffer, pH 6.5, and either varying concentrations of ABTS (0.01–10 mM) and a saturating concentration of  $\text{H}_2\text{O}_2$  of 1.0 mM or varying concentrations of  $\text{H}_2\text{O}_2$  (0.001–1.0 mM) and a saturating concentration of ABTS of 10.0 mM, respectively. The increase in absorption was followed at 420 nm at 30°C for 180 s. Absorption curves were recorded with a software program (UVPC Optional Kinetics software, Shimadzu). The maximum reaction rate ( $V_{\text{max}}$ ) and the Michaelis constant ( $K_m$ ) were calculated with the Sigma Plot software (Version 11.0; Systat Software Inc.).

The thermal stability of individual HRP glyco-variants was tested at 60°C. The residual activity towards ABTS was measured after 1, 5, 10, 15, 30, 45, 60, 90 and 120 min of incubation at 60°C in a water bath. Protein concentrations were normalized to 0.01 mg mL<sup>-1</sup> to limit possible effects of the different protein concentrations on thermal stability (Asad, Khajeh, et al. 2011) and to obtain comparability. Residual activities were plotted versus the incubation time and the half-life times of thermal inactivation at 60°C ( $\tau_{1/2}$ ) were calculated using Eq. (3):

$$\tau_{1/2} = \frac{\ln 2}{k_{\text{in}}}, \quad (3)$$

$k_{\text{in}}$  rate of inactivation (slope of the logarithmic residual activity).

**Glycosylation analysis.** Purified HRP sample was buffered in 0.1 M  $\text{NH}_4\text{HCO}_3$  and reduced with dithiothreitol (5 mM) for 45 min at 56°C and alkylated using iodoacetamide (25 mM) at room temperature for 30 min. The protein was precipitated with 4 volumes of acetone for 45 min at  $-20^\circ\text{C}$ , dried in a vacuum centrifuge and resuspended in 0.1 M  $\text{NH}_4\text{HCO}_3$  buffer to yield a protein concentration of  $\sim 1 \mu\text{g} \mu\text{L}^{-1}$ . Digests were performed overnight with either chymotrypsin or trypsin (Promega, Mannheim, Germany) at 37°C at an enzyme-to-substrate

ratio of 1:50 (w/w). The digested peptides were analyzed by liquid-chromatography mass spectrometry as follows: 1  $\mu\text{g}$  of sample was loaded on a BioBasic-18 column (150  $\times$  0.32 mm; 5  $\mu\text{m}$ ; Thermo Scientific, Vienna, Austria) and eluted with a gradient from 1 to 60% acetonitrile in 0.3% formic acid buffered to pH 3.0 at flow rate of 6  $\mu\text{L} \text{min}^{-1}$ . Eluted peptides were analyzed on an Ultima Global Q-TOF mass spectrometer (Waters, Manchester, UK) operated in positive-ion mode, which was previously calibrated with a cesium iodide standard in the range of 400–1800  $m/z$ . Additionally, the peptide harboring the site N57S within the mutated HRP variant was subjected to collision-induced dissociation MS-MS with Argon as collision gas. Data were manually evaluated and deconvoluted using the Software MassLynx V4.00.00 (Waters).

An aliquot of the chymotryptic digest was heat inactivated and then incubated with 0.03 mU PNGase A (Proglycan, Vienna, Austria) in 50 mM citrate buffer, pH 5.5. Glycans were purified using porous graphitic carbon cartridges (Thermo Scientific) as described (Pabst et al. 2012). Glycans were analyzed by mass spectrometry as described in chapter Glycosylation analysis for peptides with the sole divergence of using a 100  $\times$  0.32 mm hypercarb column (Thermo Scientific) and 1 h gradient from 1 to 50% acetonitrile.

#### Supplementary Data

Supplementary data for this article are available online at <http://glycob.oxfordjournals.org/>.

#### Funding

The authors are very grateful to the Austrian Science Fund FWF: project P24861-B19 for financial support. Funding to pay the Open Access publication charges for this article was provided by the Austrian Science Fund FWF (project P24861-B19).

#### Acknowledgements

We further thank the company BIA separations (Slovenia) for providing the tube monolithic columns.

#### Conflict of interest statement

None declared.

#### Abbreviations

ABTS, 2,2'-azino-bis(3-ethylbenzothiazoline-6-sulphonic acid); AEC, anion exchange chromatography; CV, column volumes; HCIC, hydrophobic charge induction chromatography; HRP, horseradish peroxidase;  $\text{H}_2\text{O}_2$ , hydrogen peroxide; mutant, HRP C1A, where all eight N-glycosylation sites were mutated; PF, purification factor;  $R\%$ , recovery yield of HRP activity in percentage;  $\tau_{1/2}$ , thermal half-life time; wt, wild type; X, any amino acid but proline;  $Y_{X/S}$ , biomass yield ( $\text{C-mol-C-mol}^{-1}$ );  $Y_{\text{CO}_2/S}$ , carbon dioxide yield ( $\text{C-mol-C-mol}^{-1}$ ).

#### References

- Abad S, Nahalka J, Bergler G, Arnold SA, Speight R, Fotheringham I, Nidetzky B, Glieder A. 2010. Stepwise engineering of a *Pichia pastoris* D-amino acid oxidase whole cell catalyst. *Microb Cell Fact*. 9:24.

- Asad S, Khajeh K, Ghaemi N. 2011. Investigating the structural and functional effects of mutating Asn glycosylation sites of horseradish peroxidase to Asp. *Appl Biochem Biotechnol.* 164:454–463.
- Asad S, Torabi SF, Fathi-Roudsari M, Ghaemi N, Khajeh K. 2011. Phosphate buffer effects on thermal stability and H<sub>2</sub>O<sub>2</sub>-resistance of horseradish peroxidase. *Int J Biol Macromol.* 48:566–570.
- Carlsson GH, Nicholls P, Svistunenko D, Berglund GI, Hajdu J. 2005. Complexes of horseradish peroxidase with formate, acetate, and carbon monoxide. *Biochemistry* 44:635–642.
- Choi BK, Bobrowicz P, Davidson RC, Hamilton SR, Kung DH, Li HJ, Miele RG, Nett JH, Wildt S, Gemgross TU. 2003. Use of combinatorial genetic libraries to humanize N-linked glycosylation in the yeast *Pichia pastoris*. *Proc Natl Acad Sci USA.* 100:5022–5027.
- Dietzsch C, Spadiut O, Herwig C. 2011a. A dynamic method based on the specific substrate uptake rate to set up a feeding strategy for *Pichia pastoris*. *Microb Cell Fact.* 10:14.
- Dietzsch C, Spadiut O, Herwig C. 2011b. A fast approach to determine a fed batch feeding profile for recombinant *Pichia pastoris* strains. *Microb Cell Fact.* 10:85.
- Dotsikas Y, Loukas YL. 2012. Improved performance of antigen-HRP conjugate-based immunoassays after the addition of anti-HRP antibody and application of a liposomal chemiluminescence marker. *Anal Sci.* 28:753–757.
- Dunford HB. 1999. *Heme Peroxidases*. New York: Wiley-VCH.
- Ehlers MRW, Chen YNP, Riordan JF. 1992. The unique N-terminal sequence of testis angiotensin-converting enzyme is heavily O-glycosylated and unessential for activity or stability. *Biochem Biophys Res Commun.* 183:199–205.
- Folkes LK, Wardman P. 2001. Oxidative activation of indole-3-acetic acids to cytotoxic species – a potential new role for plant auxins in cancer therapy. *Biochem Pharmacol.* 61:129–136.
- Gajhede M, Schuller DJ, Henriksen A, Smith AT, Poulos TL. 1997. Crystal structure of horseradish peroxidase C at 2.15 angstrom resolution. *Nat Struct Biol.* 4:1032–1038.
- Gilfoyle DJ, Rodriguez-Lopez JN, Smith AT. 1996. Probing the aromatic-donor-binding site of horseradish peroxidase using site-directed mutagenesis and the suicide substrate phenylhydrazine. *Eur J Biochem.* 236:714–722.
- Hamilton SR, Bobrowicz P, Bobrowicz B, Davidson RC, Li HJ, Mitchell T, Nett JH, Rausch S, Stadheim TA, Wischniewski H, et al. 2003. Production of complex human glycoproteins in yeast. *Science.* 301:1244–1246.
- Hamilton SR, Gemgross TU. 2007. Glycosylation engineering in yeast: The advent of fully humanized yeast. *Curr Opin Biotechnol.* 18:387–392.
- Huang RP. 2001. Detection of multiple proteins in an antibody-based protein microarray system. *J Immunol Methods.* 255:1–13.
- Ito K, Ishimaru T, Kimura F, Matsudomi N. 2007. Importance of N-glycosylation positioning for secretion and folding of ovalbumin. *Biochem Biophys Res Commun.* 361:725–731.
- Ito K, Seri A, Kimura F, Matsudomi N. 2007. Site-specific glycosylation at Asn-292 in ovalbumin is essential to efficient secretion in yeast. *J Biochem.* 141:193–199.
- Jermyn MA. 1952. Horseradish peroxidase. *Nature.* 169:488–489.
- Jermyn MA, Thomas R. 1954. Multiple components in horse-radish peroxidase. *Biochem J.* 56:631–639.
- Kang LX, Chen XM, Fu L, Ma LX. 2012. Recombinant expression of chitosanase from *Bacillus subtilis* HD145 in *Pichia pastoris*. *Carbohydr Res.* 352:37–43.
- Krainer FW, Dietzsch C, Hajek T, Herwig C, Spadiut O, Glieder A. 2012. Recombinant protein expression in *Pichia pastoris* strains with an engineered methanol utilization pathway. *Microb Cell Fact.* 11:22.
- Krainer FW, Gmeiner C, Neutsch L, Windwarder M, Pletzenauer R, Herwig C, Altmann F, Glieder A, Spadiut O. 2013. Knockout of an endogenous mannosyltransferase increases the homogeneity of glycoproteins produced in *Pichia pastoris*. *Sci Rep.* 3:3279.
- Krainer FW, Pletzenauer R, Rossetti L, Herwig C, Glieder A, Spadiut O. 2013. Purification and basic biochemical characterization of 19 recombinant plant peroxidase isoenzymes produced in *Pichia pastoris*. *Protein Expr Purif.* 95C:104–112.
- Krieg R, Halbhuber KJ. 2003. Recent advances in catalytic peroxidase histochemistry. *Cell Mol Biol.* 49:547–563.
- Lavery CB, MacInnis MC, MacDonald MJ, Williams JB, Spencer CA, Burke AA, Irwin DJG, D’Cunha GB. 2010. Purification of peroxidase from horseradish (*Armoracia rusticana*) roots. *J Agric Food Chem.* 58:8471–8476.
- Li S, Wilkinson MF. 1997. Site-directed mutagenesis: A two-step method using PCR and DpnI. *Biotechniques.* 4:588–590.
- Lin-Cereghino J, Wong WW, Xiong S, Giang W, Luong LT, Vu J, Johnson SD, Lin-Cereghino GP. 2005. Condensed protocol for competent cell preparation and transformation of the methylotrophic yeast *Pichia pastoris*. *Biotechniques.* 38:44–48.
- Lin Z, Thorsen T, Arnold FH. 1999. Functional expression of horseradish peroxidase in *E. coli* by directed evolution. *Biotechnol Prog.* 15:467–471.
- Morawski B, Lin ZL, Cirino PC, Joo H, Bandara G, Arnold FH. 2000. Functional expression of horseradish peroxidase in *Saccharomyces cerevisiae* and *Pichia pastoris*. *Protein Eng.* 13:377–384.
- Naatsaari L, Mistlberger B, Ruth C, Hajek T, Hartner FS, Glieder A. 2012. Deletion of the *Pichia pastoris* KU70 homologue facilitates platform strain generation for gene expression and synthetic biology. *PLoS ONE.* 7:e39720.
- Narhi LO, Arakawa T, Aoki KH, Elmore R, Rohde MF, Boone T, Strickland TW. 1991. The effect of carbohydrate on the structure and stability of erythropoietin. *J Biol Chem.* 266:23022–23026.
- Pabst M, Grass J, Toegel S, Liebming E, Strasser R, Altmann F. 2012. Isomeric analysis of oligomannosidic N-glycans and their dolichol-linked precursors. *Glycobiology.* 22:389–399.
- Palmgren B, Jin Z, Jiao Y, Kostyszyn B, Olivius P. 2011. Horseradish peroxidase dye tracing and embryonic statoacoustic ganglion cell transplantation in the rat auditory nerve trunk. *Brain Res.* 1377:41–49.
- Polizzi KM, Bommarius AS, Broering JM, Chaparro-Riggers JF. 2007. Stability of biocatalysts. *Curr Opin Chem Biol.* 11:220–225.
- Powell LM, Pain RH. 1992. Effects of glycosylation on the folding and stability of human, recombinant and cleaved alpha-1-antitrypsin. *J Mol Biol.* 224:241–252.
- Romero MI, Romero MA, Smith GM. 1999. Visualization of axonally transported horseradish peroxidase using enhanced immunocytochemical detection: A direct comparison with the tetramethylbenzidine method. *J Histochem Cytochem.* 47:265–272.
- Sainz-Pastor N, Tolner B, Huhlov A, Kogelberg H, Lee YC, Zhu D, Begent RH, Chester KA. 2006. Deglycosylation to obtain stable and homogeneous *Pichia pastoris*-expressed N-A1 domains of carcinoembryonic antigen. *Int J Biol Macromol.* 39:141–150.
- Shannon LM, Kay E, Lew JY. 1966. Peroxidase isozymes from horseradish roots. I. Isolation and physical properties. *J Biol Chem.* 241:2166–2172.
- Smith AT, Santama N, Dacey S, Edwards M, Bray RC, Thorneley RNF, Burke JF. 1990. Expression of a synthetic gene for horseradish peroxidase-C in *Escherichia coli* and folding and activation of the recombinant enzyme with Ca<sup>2+</sup> and heme. *J Biol Chem.* 265:13335–13343.
- Spadiut O, Herwig C. 2013. Production and purification of the multifunctional enzyme horseradish peroxidase: A review. *Pharm Bioproc.* 1:283–295.
- Spadiut O, Leitner C, Salaheddin C, Varga B, Vertessy BG, Tan TC, Divne C, Haltrich D. 2009. Improving thermostability and catalytic activity of pyranose 2-oxidase from *Trametes multicolor* by rational and semi-rational design. *FEBS J.* 276:776–792.
- Spadiut O, Rossetti L, Dietzsch C, Herwig C. 2012. Purification of a recombinant plant peroxidase produced in *Pichia pastoris* by a simple 2-step strategy. *Protein Expr Purif.* 86:89–97.
- Spadiut O, Zalai D, Dietzsch C, Herwig C. 2013. Quantitative comparison of dynamic physiological feeding profiles for recombinant protein production with *Pichia pastoris*. *Bioprocess Biosyst Eng.* doi: 10.1007/s00449-013-1087-z.
- Tams JW, Welinder KG. 1995. Mild chemical deglycosylation of horseradish peroxidase yields a fully active, homogeneous enzyme. *Anal Biochem.* 228:48–55.
- Tams JW, Welinder KG. 1998. Glycosylation and thermodynamic versus kinetic stability of horseradish peroxidase. *FEBS Lett.* 421:234–236.
- Veitch NC. 2004. Horseradish peroxidase: A modern view of a classic enzyme. *Phytochemistry.* 65:249–259.
- Veitch NC, Smith AT. 2001. Horseradish peroxidase. *Adv Inorg Chem.* 51:107–162.
- Vervecken W, Kaigorodov V, Callewaert N, Geysens S, De Vusser K, Contreras R. 2004. In vivo synthesis of mammalian-like, hybrid-type N-glycans in *Pichia pastoris*. *Appl Environ Microbiol.* 70:2639–2646.
- Wang CQ, Eufemi M, Turano C, Giartosio A. 1996. Influence of the carbohydrate moiety on the stability of glycoproteins. *Biochemistry.* 35:7299–7307.
- Wardman P. 2002. Indole-3-acetic acids and horseradish peroxidase: A new prodrug/enzyme combination for targeted cancer therapy. *Curr Pharm Des.* 8:1363–1374.
- Zalai D, Dietzsch C, Herwig C, Spadiut O. 2012. A dynamic fed batch strategy for a *Pichia pastoris* mixed feed system to increase process understanding. *Biotechnol Prog.* doi:10.1002/btpr.1551
- Zhu A, Wang ZK, Beavis R. 1998. Structural studies of alpha-N-acetyl galactosaminidase: Effect of glycosylation on the level of expression, secretion efficiency, and enzyme activity. *Arch Biochem Biophys.* 352:1–8.
- Zou S, Huang S, Kaleem I, Li C. 2013. N-Glycosylation enhances functional and structural stability of recombinant beta-glucuronidase expressed in *Pichia pastoris*. *J Biotechnol.* 164:75–81.



## OPEN

# Knockout of an endogenous mannosyltransferase increases the homogeneity of glycoproteins produced in *Pichia pastoris*

SUBJECT AREAS:  
ENZYMES  
GLYCOPROTEINS  
EXPRESSION SYSTEMS  
PROTEIN DESIGN

Received  
20 May 2013

Accepted  
4 November 2013

Published  
20 November 2013

Correspondence and  
requests for materials  
should be addressed to  
O.S. (oliver.spadiut@  
tuwien.ac.at)

Florian W. Krainer<sup>1</sup>, Christoph Gmeiner<sup>2</sup>, Lukas Neutsch<sup>3</sup>, Markus Windwarder<sup>4</sup>, Robert Pletzenauer<sup>2</sup>, Christoph Herwig<sup>2</sup>, Friedrich Altmann<sup>4</sup>, Anton Glieder<sup>5</sup> & Oliver Spadiut<sup>2</sup>

<sup>1</sup>Graz University of Technology, Institute of Molecular Biotechnology, Graz, Austria, <sup>2</sup>Vienna University of Technology, Institute of Chemical Engineering, Research Area Biochemical Engineering, Vienna, Austria, <sup>3</sup>University of Vienna, Department of Pharmaceutical Technology and Biopharmaceutics, Vienna, Austria, <sup>4</sup>Department of Chemistry, University of Natural Resources and Life Sciences, Vienna Austria, <sup>5</sup>Austrian Centre of Industrial Biotechnology (ACIB GmbH), Graz, Austria.

The yeast *Pichia pastoris* is a common host for the recombinant production of biopharmaceuticals, capable of performing posttranslational modifications like glycosylation of secreted proteins. However, the activity of the *OCH1* encoded  $\alpha$ -1,6-mannosyltransferase triggers hypermannosylation of secreted proteins at great heterogeneity, considerably hampering downstream processing and reproducibility. Horseradish peroxidases are versatile enzymes with applications in diagnostics, bioremediation and cancer treatment. Despite the importance of these enzymes, they are still isolated from plant at low yields with different biochemical properties. Here we show the production of homogeneous glycoprotein species of recombinant horseradish peroxidase by using a *P. pastoris* platform strain in which *OCH1* was deleted. This *och1* knockout strain showed a growth impaired phenotype and considerable rearrangements of cell wall components, but nevertheless secreted more homogeneously glycosylated protein carrying mainly Man<sub>8</sub> instead of Man<sub>10</sub> N-glycans as a dominant core glycan structure at a volumetric productivity of 70% of the wildtype strain.

The methylotrophic yeast *Pichia pastoris* has long been used for the production of recombinant proteins at high titers. Up to 22 g·L<sup>-1</sup> have been reported for intracellularly produced recombinant hydroxynitrile lyase<sup>1</sup> and approximately 15 g·L<sup>-1</sup> for secreted recombinant gelatin<sup>2</sup>, demonstrating the high production capacity of this microbial host while being able to grow on comparatively simple and inexpensive media. Not only can *P. pastoris* be grown to cell densities as high as 160 g·L<sup>-1</sup> dry cell weight<sup>3</sup>, it is also capable of performing posttranslational modifications, including the formation of correct disulfide bridges and the glycosylation of secretory proteins, rendering *P. pastoris* specifically suitable for the production of complex eukaryotic proteins<sup>4</sup>.

Glycosylation has long been known to affect various protein properties such as solubility, stability and enzymatic activity (e.g.<sup>5,6</sup>), which need to be evaluated on a case-by-case basis. Whereas only little is known about O-linked glycosylation, the biosynthesis of N-glycans is well understood. N-glycans are linked to the amido groups of asparagine residues that are recognized by glycotransferases in the sequence motif N-X-S/T, where X is any amino acid but proline. Initially, the biosynthesis steps of N-glycans in yeast and mammals are identical. Dolichol phosphate-linked N-acetylglucosamine (DolP-GlcNAc) is synthesized by the transfer of GlcNAc from uridine diphosphate (UDP) onto DolP on the cytoplasmic side of the ER. After extension to DolP-linked Man<sub>5</sub>GlcNAc<sub>2</sub>, this structure is enzymatically flipped to the ER lumen, where further glucose (Glc) and Man residues are added to form a core glycan, Glc<sub>3</sub>Man<sub>9</sub>GlcNAc<sub>2</sub>, which is transferred to an asparagine within the N-X-S/T sequence motif of a nascent protein chain. Subsequently, the three terminal Glc residues and one Man residue are trimmed by the glucosidases I and II and an ER-residing  $\alpha$ -1,2-mannosidase to form Man<sub>8</sub>GlcNAc<sub>2</sub>. At this point, the newly formed glycoprotein is transported to the Golgi apparatus, which is where the yeast and mammalian N-glycosylation pathways diverge<sup>7-9</sup>. In the mammalian Golgi apparatus,  $\alpha$ -1,2-mannosidases trim the core glycan further to form Man<sub>5</sub>GlcNAc<sub>2</sub>. Ultimately, addition of GlcNAc by a  $\beta$ -N-acetylglucosaminyltransferase I

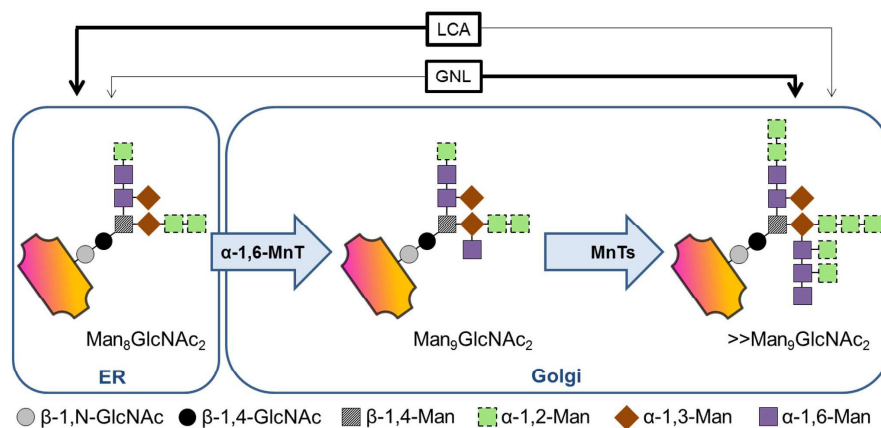


**Figure 1 | Och1p in N-glycan biosynthesis.** In the Golgi, the  $\alpha$ -1,6-mannosyltransferase activity ( $\alpha$ -1,6-MnT) of Och1p extends the N-linked  $\text{Man}_8\text{GlcNAc}_2$  core glycan, which is then heterogeneously hyperglycosylated by several additional (phospho-) mannosyltransferases (MnTs). *Galanthus nivalis* lectin (GNL) and *Lens culinaris* lectin (LCA) bind to the different glycan structures either with high (thick arrow) or low (thin arrow) specificity.

(GnTI), trimming of two further Man residues by a mannosidase II and yet further addition of GlcNAc, galactose (Gal) and sialic acid (Sia) residues by the respective transferases result in the complex N-glycan structures of mammalian proteins<sup>10</sup>. In the yeast Golgi, on the other hand, the  $\text{Man}_8\text{GlcNAc}_2$  glycan is not subjected to further trimming reactions but is substantially extended. In *Saccharomyces cerevisiae*, more than 100 Man residues may account for hypermannosyl N-glycans on secretory proteins. However, the extent of hypermannosylation varies considerably and seems to depend on so far unknown influences, causing vast heterogeneity in the N-glycan pattern of secreted glycoproteins. In *S. cerevisiae* as well as in *P. pastoris* and other yeasts, the first reaction in hypermannosylation is catalyzed by an  $\alpha$ -1,6-mannosyltransferase (Och1p) that is encoded by the gene Outer CHain elongation 1 (*OCH1*), which was first discovered and characterized in *S. cerevisiae*<sup>11,12</sup>. Och1p uses Man from guanosin diphosphate and links it to the core glycan by an  $\alpha$ -1,6-glycosidic bond, forming a substrate that triggers additional mannosylation (Figure 1). Whereas *S. cerevisiae* holds a repertoire of Golgi-resident  $\alpha$ -1,2-,  $\alpha$ -1,3 and  $\alpha$ -1,6-mannosyl and mannosylphosphate transferases, *P. pastoris* seems to lack the Golgi-resident  $\alpha$ -1,3-mannosyltransferase, but to possess four additional  $\beta$ -mannosyltransferases instead<sup>7,13,14</sup>.

Although not as extensive as those of *S. cerevisiae*, the N-glycans of *P. pastoris* are also of the high mannose type and the humanization of the N-glycosylation machinery of *P. pastoris* has been the subject of several studies (Table 1).

Here, we report the deletion of the *OCH1* gene from the *P. pastoris* genome in an irreversible and straight forward approach. Thereby, we generated a new *P. pastoris* platform strain that allows the production of recombinant proteins with shorter glycan structures of considerably increased homogeneity compared to proteins produced in a wildtype strain. In contrast to previous glycoengineering studies, which required several time- and labor-intensive steps of strain engineering, we achieved more homogeneously glycosylated protein with a single gene knockout step. Horseradish peroxidase (HRP) is a versatile enzyme with applications in diagnostics and histochemistry, bioremediation and cancer treatment. However, due to the lack of an appropriate recombinant production process, HRP preparations are still derived from horseradish roots as mixtures of different isoenzymes<sup>15</sup>. In the present study, we produced recombinant HRP in an *och1* knockout strain in the controlled environment of a bioreactor, purified and characterized the enzyme, thus demonstrating the general applicability of this new platform strain by the example of this industrially and medically relevant enzyme.

## Results

**Knockout of *OCH1* from *Ppku70-* and *PpMutS*.** In yeast, the *OCH1* gene encodes an  $\alpha$ -1,6-mannosyltransferase whose activity triggers the subsequent transfer of further mannose and phosphomannose residues onto the N-glycans of secreted proteins in the Golgi apparatus, resulting in heterogeneously hyperglycosylated protein species that appear as a smear on SDS gels, e.g.<sup>16,17</sup>. This hyperglycosylation not only limits the use of yeast derived proteins as biopharmaceuticals but also greatly impedes traditional downstream processing. Hence, a *P. pastoris* strain that allows the production of less heterogeneously glycosylated proteins would considerably relieve protein production processes with *P. pastoris*.

A flipper cassette targeting to the *OCH1* locus was transformed to a *Ppku70-* strain to replace the *OCH1* open reading frame. This *Ppku70-* strain has to rely on homologous recombination for gene integration events, in contrast to a wildtype strain<sup>18</sup>. The cassette construct and the knockout workflow are schematically shown in Fig. 2.

Transformation of the flipper cassette to the *Ppku70-* strain resulted in only few Zeocin<sup>TM</sup> resistant clones. However, Sanger sequencing of

**Table 1 | Humanization of N-glycans in *P. pastoris*.** Selected studies focusing on the humanization of the N-glycans on *P. pastoris* derived glycoproteins. Bmt,  $\beta$ -mannosyltransferase; Mns, mannosidase; GnT,  $\beta$ -N-acetylglucosaminyltransferase; UDP-GlcNAc, uridine diphosphate-N-acetylglucosamine; *OCH1*, outer chain elongation gene 1

content	references
introduction of $\alpha$ -1,2-Mns, GnTI and an UDP-GlcNAc transporter via a combinatorial genetic library approach in a $\Delta och1::URA3$ strain	13,50
introduction of an UDP-GlcNAc transporter, $\alpha$ -1,2-MnsIA, MnsII, GnTI, GnIII in a $\Delta och1::URA3$ strain	51
introduction of $\alpha$ -1,2-Mns and GnTI, <i>OCH1</i> inactivation via a knockin plasmid	10
GlycoSwitch plasmids for <i>OCH1</i> inactivation and introduction of glycosidase and glycosyltransferase activities to produce complex terminally galactosylated glycoproteins	52
introduction of sialic acid biosynthesis pathway and corresponding transporter and transferase activities to produce complex terminally sialylated glycoproteins	53
elimination of $\alpha$ -Mns resistant glycan structures by inactivation of the activities of Bmt1p, Bmt2p and Bmt3p	54



a PCR amplified fragment of the *OCH1* locus from genomic DNA showed that the majority of the tested transformants had correct integration of the transformed cassette. The transformants grew slowly and formed colonies of abnormal shape. This phenotype was preserved when the strains were grown on minimal methanol agar plates to induce the production of the FLP recombinase and subsequent excision of the inner part of the flipper cassette containing the expression cassettes for the FLP recombinase and the Zeocin<sup>TM</sup> resistance enzyme. Reconstituted sensitivity to Zeocin<sup>TM</sup>, PCR and Sanger sequencing of the former *OCH1* locus confirmed the successful excision of the inner part of the flipper cassette and the efficient replacement of the former *OCH1* ORF with a single *FRT* site of 34 bp.

Transformation of the same *OCH1* flipper cassette to *PpMutS* resulted in hundreds of clones resistant to Zeocin<sup>TM</sup>. Initial PCR based screenings of over 100 randomly chosen clones did not give any positive hits, analogously to what has been described by Vervecken *et al.*<sup>10</sup>. However, after having identified the corresponding phenotype of positive transformants in the *Ppku70*- based *och1* knockout strain, designated *PpFWK1*, also *PpMutS* based transformants with correct integration of the flipper cassette could be spotted easily on the agar plates since they showed the same unusual colony phenotype as colonies of *PpFWK1* (Figure 3).

Increasing the incubation time of the transformed cells on the agar plates to at least four days allowed growth of the *och1* knockout colonies to a size at which their abnormal shape was an obvious hint to their genotype (Figure 3). Again, Zeocin<sup>TM</sup> sensitivity was reconstituted by induction of the FLP recombinase on minimal methanol agar plates and the replacement of the *OCH1* ORF by a single *FRT* site was shown by PCR and Sanger sequencing. The observed phenotype of the generated *och1* knockout strain *PpFWK3* included slow

growth, abnormal colony shape and temperature sensitivity at 37°C (data not shown). Upon transformation of the wildtype *OCH1* promoter and *OCH1* ORF to *PpFWK3*, the detrimental phenotype was found to be complemented. PCR analyses confirmed the unaltered replacement of the former *OCH1* ORF by a *FRT* site, but the presence of the complementing *OCH1* ORF somewhere else in the genome due to ectopic integration of the transformed plasmid pPpT4\_BamHI\_*OCH1*rescue.

**Strain morphology.** *Cell morphology and cell division of an och1 knockout strain.* Consistent with previous reports on *Och1p* deficient *S. cerevisiae* strains<sup>19,20</sup>, we found the N-glycosylation mutant to be characterized by an altered phenotype and growth profile (Table 2). In contrast to the wildtype based strain *PpMutS*, the *och1* knockout strain *PpFWK3* grew in the form of large cell clusters with clumpy appearance and multibudded cells (Figure 4). Daughter cells within these clusters displayed clearly segregated vacuoles, but remained stably attached to the wall of mother cells (Supplementary Figure 1).

*Knockout induced stress response is reflected by a spatial rearrangement of WGA/STL binding sites.* The direct functional implication of the altered N-glycosylation in *PpFWK3* for cell morphology and cytokinesis was further illustrated by a striking difference in the chitin deposition after *OCH1* knockout (Supplementary Figure 1). In lectin based glycoprofiling studies, we observed substantially altered binding patterns for the GlcNAc-specific lectin WGA, with the reactive carbohydrate motifs being homogeneously distributed across the entire cell surface in the *och1* knockout strain, instead of remaining confined to the bud scars as in *PpMutS* (Figure 5 and Supplementary Figure 1).

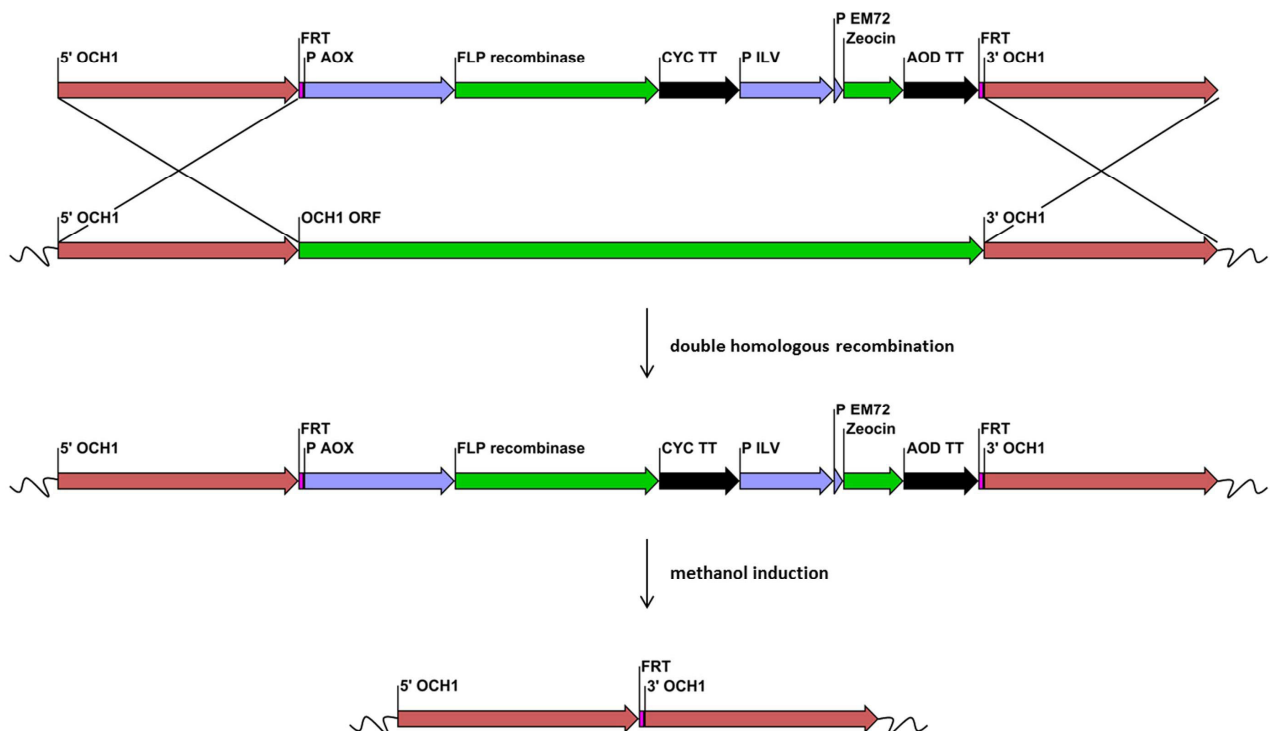


**Figure 2 | Schematic workflow of the knockout of *OCH1* using a flipper cassette.** The regions 5' *OCH1* and 3' *OCH1* represent sequences upstream and downstream of the *OCH1* ORF, respectively. The 34 bp flipper recombinase target (*FRT*) sequences flank the *AOX1* promoter (P *AOX1*), the FLP recombinase ORF, the *CYC1* transcription terminator (CYC TT), a constitutive eukaryotic and a prokaryotic promoter (P ILV and P EM72, respectively), a *ble* ORF mediating Zeocin<sup>TM</sup> resistance and an *AOD* transcription terminator (AOD TT). A double homologous recombination event replaced the *OCH1* ORF in the genome with the flipper cassette. Growth of recombinant cells on methanol induced the production of the FLP recombinase which recognized the two *FRT* sites and excised the inner sequence, leaving only one *FRT* site in the genome. Single fragments are not drawn to scale.

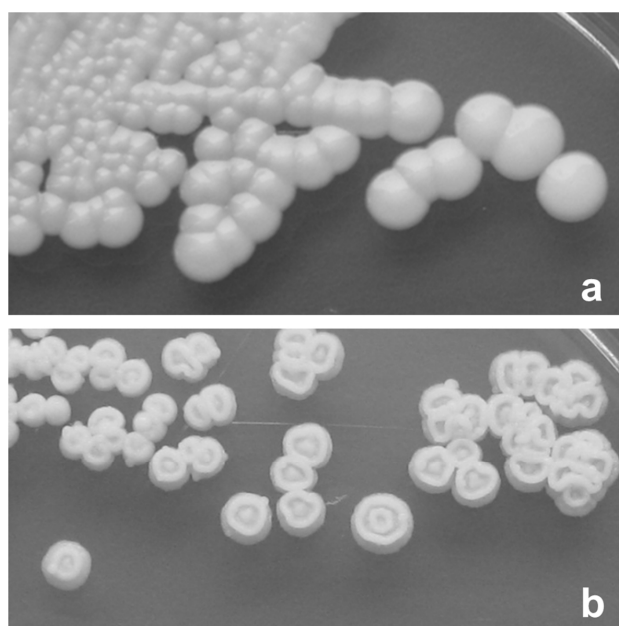


**Figure 3 | Colony phenotypes.** (a), *PpMutS*; (b), *PpFWK3*. Both strains were grown on YPD agar.

In order to assess whether a mere alteration in the steric accessibility of chitin chains in the lateral wall was responsible for the difference in the WGA staining behavior or whether chitin was actually specifically localized at bud scars, *PpMutS* cells were subjected to the same fluorescence microscopic analysis after treatment with concentrated methanol, leading to denaturation of mannoproteins and a substantial increase in cell wall permeability<sup>21</sup>. The efficiency of the cell wall permeabilization protocol was validated by concomitant incubation with a usually non-membrane penetrating DAPI dye, which could readily access the nuclear space after methanol treatment. Still, methanol permeabilized *PpMutS* cells displayed only the conventional, bud scar selective staining pattern, contrasting to the generalized binding of GNL, which served as a control (Supplementary Figure 2).

Quantitatively, comparative overall ratios of WGA/FM<sup>®</sup> 4–64 were found for *PpMutS* and the *och1* knockout strain *PpFWK3* (Figure 6), indicating that mainly a spatial redistribution of chitin

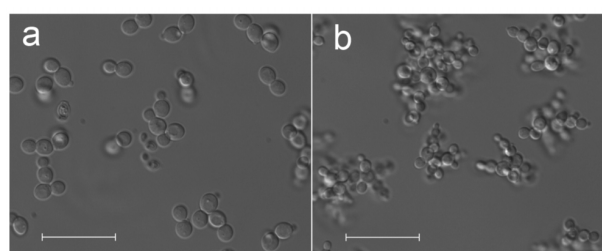


**Figure 4 | Phenotypic change in *P. pastoris* upon *OCH1* knockout.** Representative DIC micrographs of *PpMutS* and *PpFWK3*. (a), *PpMutS* cells in batch culture. (b), covalently linked clusters of multibudded cells in *PpFWK3* during the same cultivation phase. Scale bars represent 25  $\mu\text{m}$ .

may be induced by altering the glycosylation machinery, but without general enhancement of the total cellular chitin level. In other words, the rather high chitin concentration at the bud scars in *PpMutS* seemed to be reduced in favor of an increased chitin deposition in the lateral cell walls of *PpFWK3*. These results were also confirmed via the chitin binding lectin STL, which has a similar carbohydrate specificity profile as WGA but only limited affinity to isolated GlcNAc residues (Figure 6).

Inactivation of the *Och1p* activity shifted the interaction capacity of mannose specific lectins. The *och1* knockout cells of the *PpFWK3* strain displayed a lower binding capacity for the lectin GNL than *PpMutS* cells (Figure 6). GNL interacts with high mannose N-glycans and preferably reacts with  $\alpha$ -1,3-Man residues, but also binds to  $\alpha$ -1,6 linked Man residues<sup>22,23</sup>. In the current study, the GNL/FM<sup>®</sup> 4–64 ratio was reduced by 50% in *PpFWK3* as compared to *PpMutS*, but still remained the lectin with highest binding capacity for this strain (Figure 6). In striking contrast, the binding levels of the glycan core-binding lectin LCA were increased upon *OCH1* knockout (Figure 6). Both, GNL and LCA showed an equal distribution across the entire cell wall (Figure 5), corresponding to the established localization of their putative targets, high-mannose N-glycans and core glycans, respectively.

**Production of HRP in the strains *PpMutS*<sup>HRP</sup> and *PpFWK3*<sup>HRP</sup>.** To show the applicability of the generated *och1* knockout strain for the production of recombinant proteins, a vector harboring a gene coding for an acidic HRP isoenzyme was transformed into either *PpMutS* or *PpFWK3*. Transformation of the linearized constructs

**Table 2 | Strain specific parameters of the different *P. pastoris* strains.** Parameters are defined in the footnote\*

	<i>PpMutS</i>	<i>PpMutS</i> <sup>HRP</sup>	<i>PpFWK3</i>	<i>PpFWK3</i> <sup>HRP</sup>
<b>max. <math>\mu_{\text{Gly}}</math> (<math>\text{h}^{-1}</math>)</b>	0.30	0.31	0.20	0.20
<b><math>q_{\text{Gly}}</math> (<math>\text{mmol} \cdot \text{g}^{-1} \cdot \text{h}^{-1}</math>)</b>	2.90	3.10	1.90	1.90
<b><math>Y_{\text{X/Gly}}</math> (<math>\text{Cmol} \cdot \text{Cmol}^{-1}</math>)</b>	0.63	0.41	0.61	0.54
<b><math>Y_{\text{CO}_2/\text{Gly}}</math> (<math>\text{Cmol} \cdot \text{Cmol}^{-1}</math>)</b>	0.33	0.64	0.37	0.44
<b><math>\Delta\text{time}_{\text{adapt}}</math> (h)</b>	15.7	19.9	6.60	8.90
<b><math>q_{\text{MeOH}}</math> (<math>\text{mmol} \cdot \text{g}^{-1} \cdot \text{h}^{-1}</math>)</b>	0.62	0.70	0.52	0.43
<b>max. <math>q_{\text{MeOH}}</math> (<math>\text{mmol} \cdot \text{g}^{-1} \cdot \text{h}^{-1}</math>)</b>	0.67	0.78	0.69	0.53
<b><math>Y_{\text{X/MeOH}}</math> (<math>\text{Cmol} \cdot \text{Cmol}^{-1}</math>)</b>	0.39	0.07	0.05	0.04
<b><math>Y_{\text{CO}_2/\text{MeOH}}</math> (<math>\text{Cmol} \cdot \text{Cmol}^{-1}</math>)</b>	0.57	1.02	constantly decreasing	constantly decreasing
<b>C-balance</b>	0.97	1.04	constantly decreasing	constantly decreasing
<b><math>q_{\text{p}}</math> (<math>\text{U} \cdot \text{g}^{-1} \cdot \text{h}^{-1}</math>)</b>	-	0.77	-	0.50
<b>vol. productivity (<math>\text{U} \cdot \text{L}^{-1} \cdot \text{h}^{-1}</math>)</b>	-	2.60	-	1.80
<b>efficiency factor (<math>\eta</math>) (<math>\text{U} \cdot \text{mmol}^{-1} \cdot 26</math>)</b>	-	1.10	-	1.20

\*max.  $\mu_{\text{Gly}}$ , maximum specific growth rate on glycerol;  $q_{\text{Gly}}$ , specific uptake rate of glycerol during the batch;  $Y_{\text{X/Gly}}$ , biomass yield on glycerol;  $Y_{\text{CO}_2/\text{Gly}}$ ,  $\text{CO}_2$  yield on glycerol;  $\Delta\text{time}_{\text{adapt}}$ , time from first addition of methanol to a maximum in offgas activity;  $q_{\text{MeOH}}$ , average specific uptake rate of methanol during consecutive methanol pulses; max.  $q_{\text{MeOH}}$ , maximum specific uptake rate of methanol during consecutive methanol pulses;  $Y_{\text{X/MeOH}}$ , biomass yield on methanol;  $Y_{\text{CO}_2/\text{MeOH}}$ ,  $\text{CO}_2$  yield on methanol; C-balance, sum of biomass and  $\text{CO}_2$  yields;  $q_{\text{p}}$ , specific productivity of HRP; vol. productivity, volumetric productivity of HRP; efficiency factor; efficiency of the conversion of substrate methanol into product HRP.

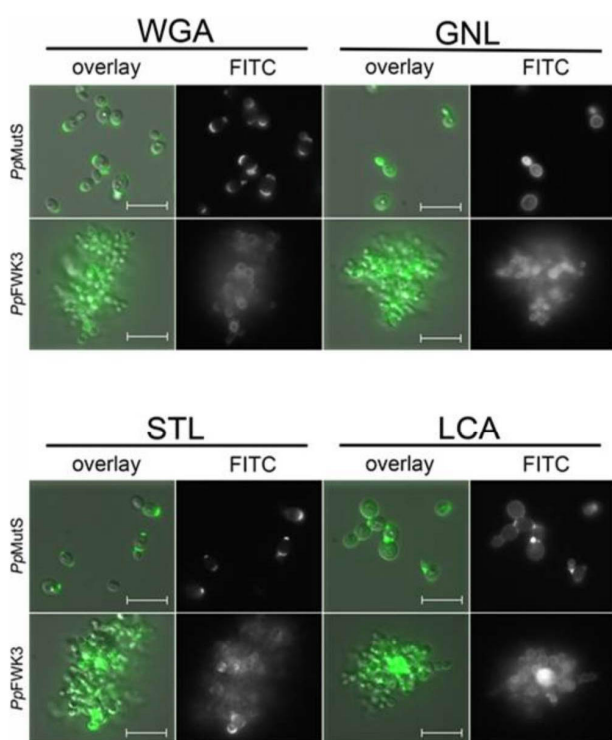


**Figure 5 | Lectin based glycoprofiling of surface carbohydrate motifs in *PpMutS* and *PpFWK3*.** Live cells harvested in the exponential growth phase of batch cultivation were incubated with fluorescein labeled lectins. Micrographs show the isolated channel for FITC detection and merged images with DIC (overlay). Scale bars represent 10  $\mu\text{m}$ .

into *PpFWK3* resulted in fewer Zeocin<sup>TM</sup> resistant clones than for *PpMutS*, but sufficient to allow screening for HRP activity after cultivation in a 96-deep well plate in minimal media. Despite the apparent growth defect of *PpFWK3*, the volumetric yields in HRP activity in these micro-scale cultivations were comparable to those of *PpMutS* based transformants. Prior to cultivation of *PpMutS*<sup>HRP</sup> or *PpFWK3*<sup>HRP</sup> in the bioreactor, both strains were analyzed in terms of copy number of the transformed HRP gene to ensure comparability on this level. Both strains were found to have a single copy integration of the HRP encoding gene and were thus considered suitable for comparative bioreactor cultivations.

**Strain characterization in bioreactors.** We characterized four *P. pastoris* strains (Table 2) with a recently published method of conducting dynamic experiments during batch cultivations in the controlled environment of a bioreactor<sup>16,24,25</sup>. After depletion of glucose, a first methanol adaption pulse with a final concentration of 0.5% (v/v) was applied. The adaptation times to the new substrate methanol ( $\Delta\text{time}_{\text{adapt}}$ ), defined as the maximum in offgas activity, were determined for all four *P. pastoris* strains and are shown in Table 2.

The calculated carbon dioxide evolution rate (CER), illustrating the metabolic activity of the different strains, the specific substrate uptake rate ( $q_s$ ) and, where appropriate, the specific productivity ( $q_p$ ), during the methanol pulses are shown in Supplementary Fig. 3–6. As shown in Supplementary Fig. 3 and 4, the CER profiles for the strains *PpMutS* and *PpMutS*<sup>HRP</sup> showed a similar pattern during the consecutive methanol pulses and  $q_s$  values stayed constant over time. In contrast, the CER profiles for the strains *PpFWK3* and *PpFWK3*<sup>HRP</sup> substantially changed over time (Supplementary Figures 5 and 6). After each methanol pulse, less CO<sub>2</sub> was produced per time and volume, indicating that the *P. pastoris* cells became

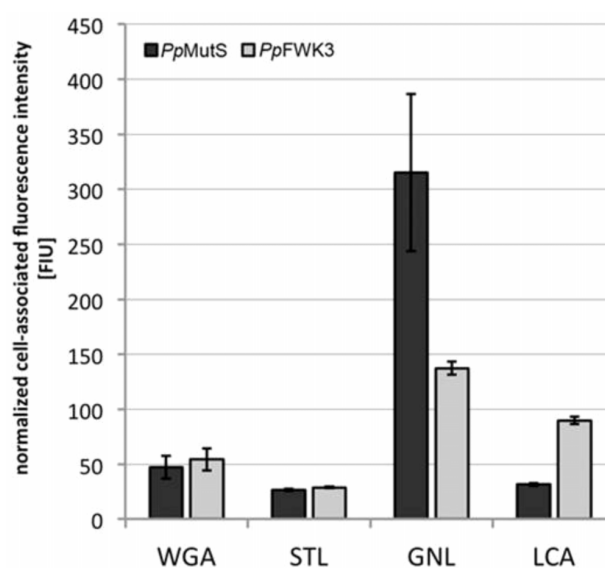


**Figure 6 | Quantitative determination of lectin binding on *PpMutS* and *PpFWK3* cells.** Cell suspensions adjusted to the same concentration level were incubated with FITC labeled lectins. After thorough washing, cells were lysed and the fluorescence intensity of the lysis buffer recorded. Binding data was normalized to the average cellular content of FM® 4–64, which was shown to be similar in both strains via FACS analysis. Values represent mean  $\pm$  SD of three independent experiments.

metabolically less active. Thus, the consumption of 1% (v/v) methanol took longer after each consecutive pulse (compare Supplementary Figures 3 and 4 with Supplementary Figures 5 and 6). The altered metabolic activity of the *och1* knockout strains was also depicted in the calculated yields ( $Y_{X/S}$  and  $Y_{CO_2/S}$ ), which are shown in Fig. 7.

For the strains *PpMutS* and *PpMutS*<sup>HRP</sup> both the carbon dioxide yield ( $Y_{CO_2/S}$ ) and the biomass yield ( $Y_{X/S}$ ) stayed constant during the six conducted consecutive methanol pulses (Figure 7a and b). Evidently, the insertion of the HRP gene into strain *PpMutS* affected its physiology as  $Y_{X/S}$  decreased, whereas  $Y_{CO_2/S}$  increased (compare Figure 7a and b). Hence, *PpMutS*<sup>HRP</sup> mainly used the substrate methanol for protein production and dissimilation than for biomass growth.

Interestingly, the calculated yields for *PpFWK3* and *PpFWK3*<sup>HRP</sup> strains showed a very different behaviour. Although  $Y_{X/S}$  was again rather constant,  $Y_{CO_2/S}$  decreased dramatically in the course of the six to seven consecutive methanol pulses (Figure 7c and d), indicating that these two strains became more and more metabolically inactive. Since HPLC analysis revealed that no undesired metabolites were produced in substantial amounts during any of the four cultivations, the C-balances for strains *PpFWK3* and *PpFWK3*<sup>HRP</sup> were determined close to 1.0 only at the beginning of the cultivation but rapidly decreased over time, whereas the C-balances for strains *PpMutS* and *PpMutS*<sup>HRP</sup> were always determined to be close to 1.0 (Supplementary Figure 7). A summary of the determined strain specific parameters of the four different *P. pastoris* strains is given in Table 2.

As shown in Table 2, the maximum specific growth rates on glycerol (max.  $\mu_{\text{Gly}}$ ) for *PpFWK3* strains were approximately 1.5-fold lower than for *PpMutS* strains. The yields on glycerol showed a similar pattern for *PpMutS* and *PpFWK3* strains, as the yields were shifted towards production of carbon dioxide rather than biomass when the strains were hosting the gene for recombinant HRP. Both *PpFWK3* strains needed less than half of the adaptation time to methanol ( $\Delta\text{time}_{\text{adapt}}$ ) compared to the *PpMutS* strains. The altered glycosylation machinery in the *PpFWK3* strains seems to allow a

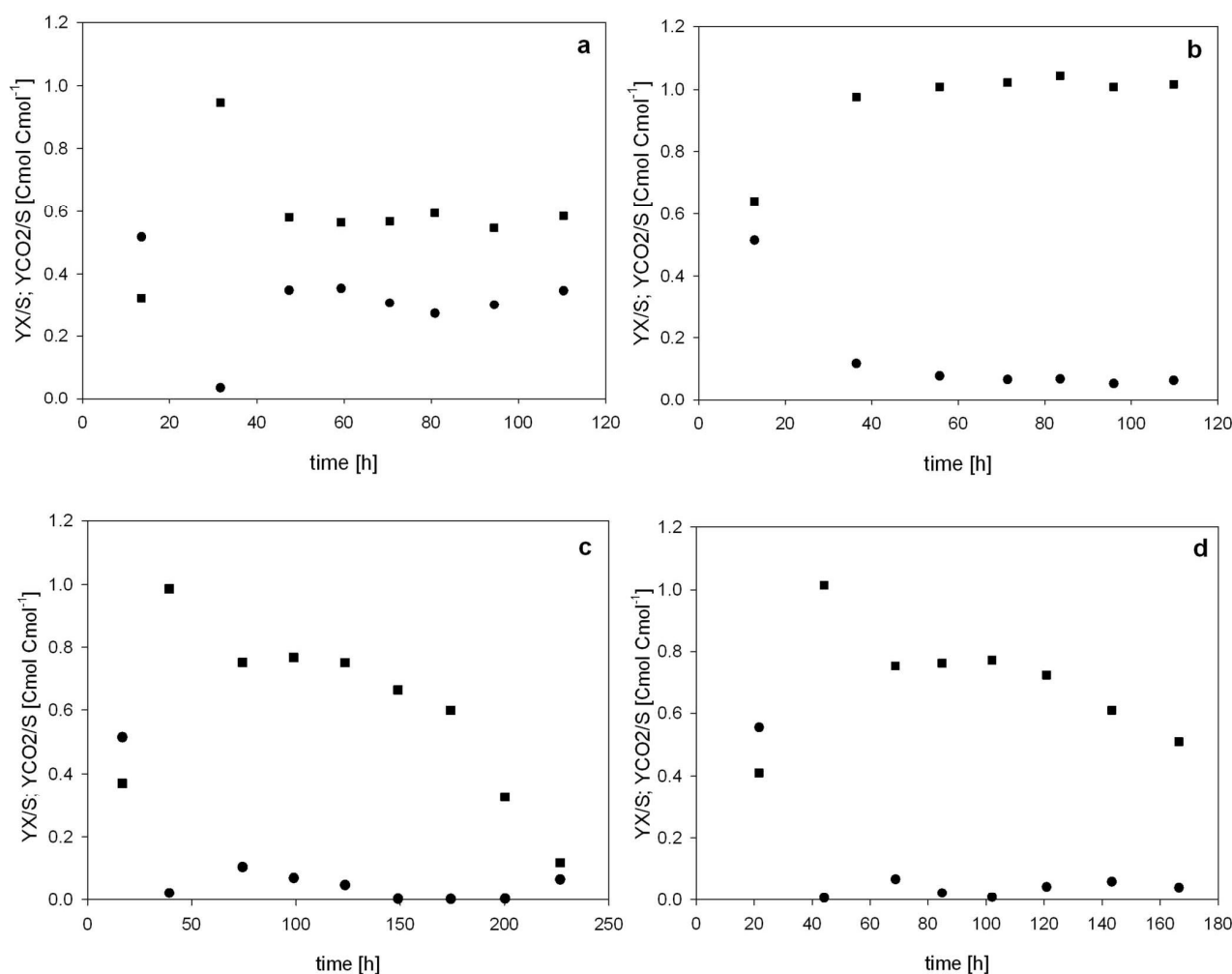


**Figure 7 |** Calculated yields for the different *P. pastoris* strains during batch cultivations with methanol pulses. (a), *PpMutS*; (b), *PpMutS<sup>HRP</sup>*; (c), *PpFWK3*; (d), *PpFWK3<sup>HRP</sup>*. Black square, carbon dioxide yield ( $Y_{CO_2/S}$ ); black dot, biomass yield ( $Y_{X/S}$ ).

faster adaption to methanol, which could be of great significance for industrial applications where fast and efficient bioprocesses are required. As expected, the adaptation times of the strains hosting the recombinant enzyme were longer compared to the strains not carrying this additional gene. The average specific substrate uptake rates for both substrates ( $q_s$ ) glycerol and methanol were lower for the *PpFWK3* strains than for *PpMutS* strains. In respect to the maximum specific uptake rate for methanol (max.  $q_{MeOH}$ ) the values for the different strains were quite similar. However, these values were determined during the 3<sup>rd</sup> and the 5<sup>th</sup> methanol pulse for *PpMutS* and *PpMutS<sup>HRP</sup>*, respectively. The values during the other pulses were alike. For *PpFWK3* strains on the other hand, these maxima could only be determined during the 1<sup>st</sup> methanol pulse. After that, the values for  $q_s$  constantly decreased, indicating a progressional reduction of the metabolic activity of the *PpFWK3* strains during consecutive methanol pulses. This was also underlined by constantly decreasing  $Y_{CO_2/S}$  and C-balances. However, despite this seemingly negative impact, *PpFWK3<sup>HRP</sup>* produced the HRP isoenzyme at specific and volumetric productivities which were only reduced by 35% and 30%, respectively, compared to *PpMutS<sup>HRP</sup>*. In a previous study, we introduced the efficiency factor  $\eta$ , which puts the productivity of the strains in direct relation to the consumed substrate<sup>26</sup>. In this respect, the *och1* knockout strain *PpFWK3<sup>HRP</sup>* even showed a higher ratio than *PpMutS<sup>HRP</sup>* and thus proved to be of justifiable interest for the production of recombinant proteins.

**Enzyme purification and characterization.** In order to demonstrate the successful decrease of heterogeneity in the glycosylation of HRP when produced in an *och1* knockout strain, size exclusion chromatography (SEC) was performed with cell free cultivation broth (Figure 8). A SEC elution profile has higher specificity and sensitivity than an image of an SDS polyacrylamide gel and was therefore preferably used for this purpose. HRP produced in *PpMutS<sup>HRP</sup>* eluted with higher heterogeneity than HRP produced in *PpFWK3<sup>HRP</sup>*.

Judging by the size exclusion chromatogram (Figure 8), HRP produced in a *PpMutS<sup>HRP</sup>* strain substantially differed in its surface glycosylation pattern compared to HRP produced in a *PpFWK3<sup>HRP</sup>* strain, which showed higher homogeneity. To analyze this phenomenon in detail, we enzymatically released the glycans from the produced recombinant HRPs and analyzed them via liquid chromatography-mass spectrometry (LC-MS). Reducing glycans were observed mainly as doubly charged  $[M + H + NH_4]^{2+}$  ions (Figure 9). Analysis of enzymatically released glycans from HRP produced in either *PpMutS<sup>HRP</sup>* or *PpFWK3<sup>HRP</sup>* confirmed the expected decrease in both N-glycan size and heterogeneity. The dominant core glycan structure shifted from Man10 to Man8 in strain *PpFWK3<sup>HRP</sup>* (Table 3). As shown in Fig. 9, HRP produced in the strain *PpMutS<sup>HRP</sup>* carried a greater variety of different glycan chains consisting of up to 17 mannoses and a higher amount of phosphorylated sugars than HRP produced in *PpFWK3<sup>HRP</sup>*.



The evaluation of the relative peak areas underlined this observation (Table 3), as around 60% of the identified glycan structures cleaved off from HRP produced in the *och1* knockout strain *PpFWK3<sup>HRP</sup>* were of the Man8 type, whereas no structure of that type was identified for HRP from *PpMutS<sup>HRP</sup>*. As shown in Table 3 there were also much more different glycan chains identified on HRP from *PpMutS<sup>HRP</sup>* and interestingly no phosphorylated mannose structures were found on HRP from *PpFWK3<sup>HRP</sup>*.

To check whether the kinetic constants or the stability of the enzyme were affected by the altered glycosylation pattern, we characterized purified preparations of HRP. HRP preparations produced by either *PpMutS<sup>HRP</sup>* or *PpFWK3<sup>HRP</sup>* in bioreactor cultivations were purified by using a recently described strategy for HRP isoenzyme C1A<sup>27</sup>. Both HRP preparations did not bind to the mixed mode HCIC resin but were found in the flowthrough, i.e. 93% of HRP produced in *PpMutS<sup>HRP</sup>* and 87% of HRP produced in *PpFWK3<sup>HRP</sup>*. Contaminating proteins were retained on the resin, leading to a partial purification at a factor of approximately 2.5 for both enzyme solutions. A subsequent size exclusion step gave an additional purification factor of approximately 2.0. After purification, the fractions with the highest purification factor were pooled and ultrafiltered. The enzyme HRP produced in *PpMutS<sup>HRP</sup>* was concentrated to around 3.0 mg·mL<sup>-1</sup>, whereas HRP produced in *PpFWK3<sup>HRP</sup>* could not be concentrated due to the immediate formation of precipitates during ultrafiltration and the resulting clogging of the membrane, indicating a reduced solubility of the extracellular proteins in this preparation. We determined the kinetic constants for both enzyme preparations with H<sub>2</sub>O<sub>2</sub> as electron donor at saturating concentration and ABTS as electron acceptor in varying concentrations (Table 4; Supplementary Figure 8).

As shown in Table 4, the affinity of HRP towards the substrate ABTS was increased, as the  $K_M$  was found to be decreased by approximately 15% by the altered surface glycosylation. However,  $V_{max}$  was decreased by nearly 20%. Also, the thermal stability of the produced HRP glycovariants at 60°C was studied (Supplementary Figure 9) and the half life times ( $\tau_{1/2}$ ) were determined<sup>28</sup>. The  $\tau_{1/2}$  of HRP produced in *PpMutS<sup>HRP</sup>* was determined with 384 s, whereas HRP from *PpFWK3<sup>HRP</sup>* showed a reduction in its thermal half life time of around 50% with 198 s.

## Discussion

Despite the numerous advantages of using *P. pastoris* as a host organism for recombinant protein production, its inherent heterogeneous yeast type hyperglycosylation of secreted proteins has to be addressed by extensive and elaborated strain modifications. Here, we present a straight forward approach for the generation of a wildtype based *P.*

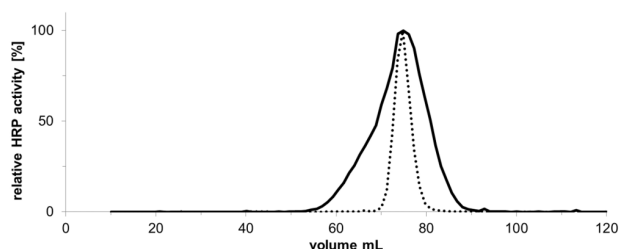


**Figure 8 |** Size exclusion chromatogram of HRP glycovariants. Solid line, HRP produced in *PpMutS<sup>HRP</sup>*; dashed line, HRP produced in *PpFWK3<sup>HRP</sup>*. The run was performed at a flow of 9 cm<sup>3</sup>·h<sup>-1</sup> and fractions of 1.2 mL were collected. The measured HRP activities per fraction are shown as relative activities with the respective maximum activities set to 100% for better comparability. The unnormalized maximum activities were 2.6 and 15.1 U·mL<sup>-1</sup> for HRP from *PpMutS<sup>HRP</sup>* and from *PpFWK3<sup>HRP</sup>*, respectively. The loaded volume was approximately 200  $\mu$ L for HRP from either *PpMutS<sup>HRP</sup>* or *PpFWK3<sup>HRP</sup>*.

*pastoris* platform strain that allows the production of more homogeneously glycosylated recombinant proteins due to an irreversible deletion of the *OCH1* gene.

Yeast hypermannosylation largely depends on the initial activity of an  $\alpha$ -1,6-mannosyltransferase in the Golgi apparatus. Elimination of this activity was achieved by replacement of the *OCH1* ORF with a single 34 bp *FRT* site by using a flipper cassette. However, this approach required double homologous recombination at the correct locus in the genome. Unfortunately, homologous integration events only play a minor part in *P. pastoris*, as recently demonstrated by Näätsaari *et al.*<sup>18</sup> and which was found to be especially true for the *OCH1* locus by Vervecken *et al.*<sup>10</sup>. A new *P. pastoris* strain with inactivated non-homologous end joining pathway, designated *Ppku70-*, proved to be a particularly convenient tool to identify the phenotype of the specific knockout strain in this study. Since homologous integration was the sole possibility for recombination events in the *Ppku70-* strain, the total number of positive transformants was predominantly made up by transformants with homologous integration. The fact that particularly few colonies were obtained by targeting of the transformed flipper cassette to the *OCH1* locus when using the *Ppku70-* strain also supported the hypothesis of increased difficulty of homologous recombination in that locus.

An *och1* knockout strain of *S. cerevisiae* was described to show several defects such as impaired budding and increased temperature sensitivity<sup>11</sup>. Choi *et al.* mentioned temperature sensitivity and increased flocculation for their *P. pastoris och1* knockout strain<sup>13</sup>, but neither they nor Vervecken *et al.*<sup>10</sup> described any further severe growth defects. However, the *och1* knockout strain in the present study was found to show not only formation of cell clusters and temperature sensitivity, but also decreased growth which might be due to an impaired cell wall structure and thus complicated bud formation. Similarly, a recently generated *och1* knockout strain based on the *his4* mutant strain *P. pastoris* GS115 was described with slower growth and rough colony surface<sup>29</sup>. Explanations for these divergent findings remain speculative, but might be due to single nucleotide polymorphisms and hence different strain backgrounds. Also, a secondary integration event of the transformed flipper cassette cannot be completely excluded. However, considering that as little as 100 ng of the cassette were transformed and that all clones that exposed the described phenotype had the correct integration of the cassette in the *OCH1* locus indicates that the observed phenotype can be ascribed rather to the knockout of *OCH1* than to any additional genomic rearrangement. Also, the similarity of the observed phenotype in the present *P. pastoris och1* knockout strain to the phenotype described for a *S. cerevisiae och1* knockout strain<sup>11</sup> very much suggests that the deletion of the *OCH1* gene is actually responsible for the phenotype observed in this study. Most strikingly, reintroduction of the wildtype *OCH1* gene to the *och1* knockout strain *PpFWK3* restored its phenotype, thus conclusively linking the observed phenotype of *PpFWK3* to the deletion of the *OCH1* gene. Transformation of the *och1* knockout strain with a linearized vector harboring an expression cassette for the production of an HRP isoenzyme via electroporation was found to result in lower transformation efficiency than electroporation of a *P. pastoris* wildtype strain. This increased sensitivity to electroporation might be another reflection of the altered cell wall composition that could be shown by lectin based glycoprofiling.

The highly specific interaction of the lectin WGA with the exposed chitin ring of bud scars<sup>30</sup> has previously been reported for other yeasts and can be used for the precise determination of the number of cell divisions performed<sup>31,32</sup>. To the best of our knowledge, this is the first confirmation of this structure-related specificity for *P. pastoris*. However, in the *och1* knockout strain, we noticed an almost complete loss of bud scar selectivity. The reasons for the regionally diverse distribution of chitin in *PpFWK3* may either lie in an increased accessibility of previously cryptic chitin chains in the

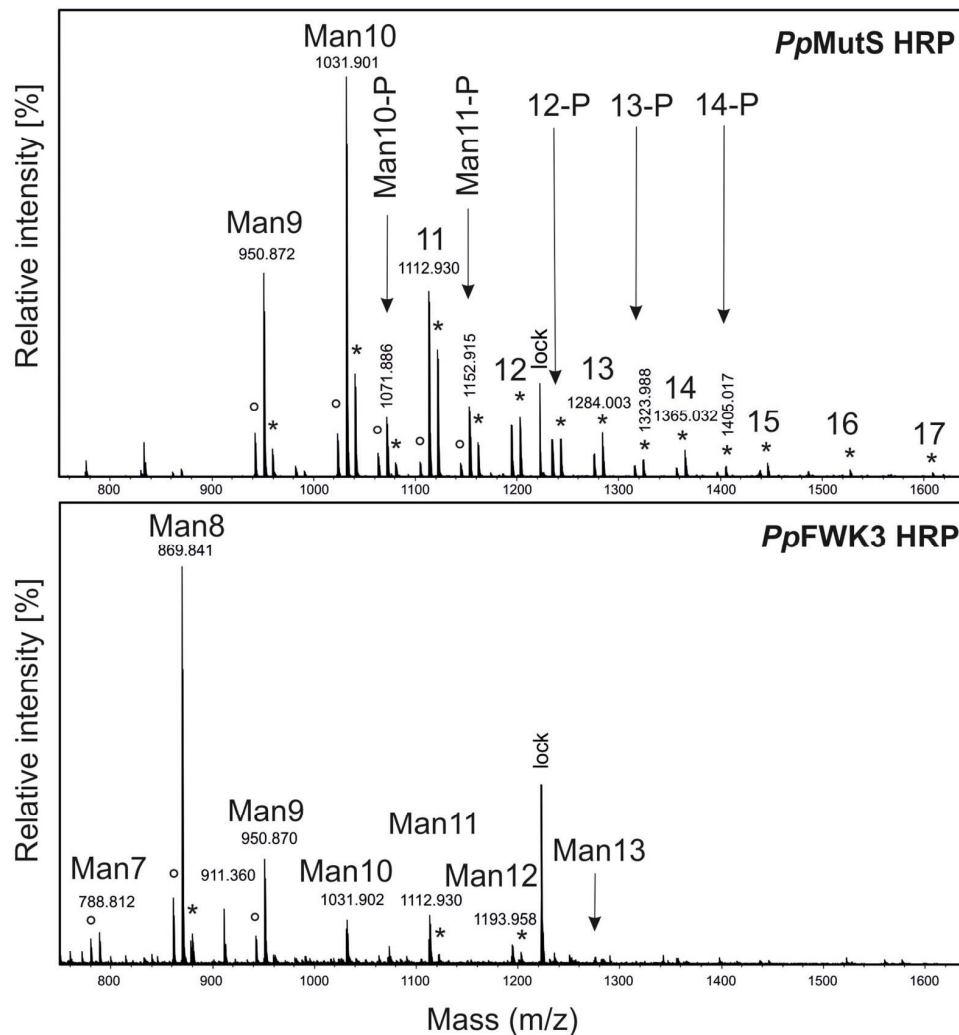


**Figure 9** | Chromatogram of liquid chromatography-mass spectrometry of glycans released from HRP produced in either *PpMutS*<sup>HRP</sup> or in *PpFWK3*<sup>HRP</sup>. HRP  $[M + 2H]^{2+}$  and  $[M + 2NH_4]^{2+}$  ions are marked with  $^{\circ}$  and  $*$ , respectively. “Man10-P” or just “12-P” indicate phosphorylated glycans. lock, lock mass.

lateral cell wall (*i.e.* when the protective polymannan layer is missing), or in an actively increased chitin synthesis and deposition at the cell wall, *i.e.* as a compensatory response to the cell wall stress caused by the impaired barrier function. Such stimulation of counter-regulatory pathways upon impairment of cell wall integrity has been observed in several yeast species<sup>33,34</sup> and involves diverse mechanisms and signaling cascades<sup>35</sup>, which are believed to be directly or indirectly connected to the deletion of Och1p activity<sup>20</sup>. Especially the osmotic stress exerted on the cell as a result of the impaired cell wall integrity is known to present an important factor for the induction of counter-regulatory pathways<sup>36</sup>. Due to the persistence of bud scar specific binding of WGA in methanol treated *PpMutS* cells, we concluded that the strong affinity of WGA to the overall cell wall of *PpFWK3* cells traced back to a *de novo* deposition of carbohydrate epitopes (most probably chitin) in this *och1* knockout strain, and not an increased exposure of constitutive cell wall glycans that are invariably present but usually shielded by an outer chain hypermannan structure in the wildtype strain. The somewhat reduced STL/FM<sup>®</sup> 4–64 ratio compared to the WGA/FM<sup>®</sup> 4–64 ratio may be connected to the minor differences regarding the preferentially binding ligand. Based on the similarity between STL and WGA staining patterns, it is unlikely that any GlcNAc motifs other than chitin (*e.g.* in the core glycan of mannoproteins) were the primary binding epitopes

detected by either of the two lectins. As a side aspect of the current work, we were able to demonstrate the use of fluorescence labeled lectins as convenient and versatile probes for visualizing stress responses derived from impaired cell wall integrity in yeast. The decreased GNL/FM<sup>®</sup> 4–64 ratio of *PpFWK3* compared to *PpMutS* could be explained by the minimized amount of high mannose N-glycans and the therefore inherently lower amount of potential GNL target ligands (*i.e.*  $\alpha$ -1,3- and  $\alpha$ -1,6-Man residues) of *PpFWK3* compared to *PpMutS*. Nevertheless, the remaining core glycan provided sufficient GNL targets for a distinct signal. The increased LCA/FM<sup>®</sup> 4–64 signal of *PpFWK3* on the other hand, may be explained by the preference of this lectin for short chain X- $\alpha$ -1,2-Man–Man motifs, with X representing either  $\alpha$ -Man or  $\beta$ -GlcNAc<sup>37</sup>. In mannoproteins, such short motifs may be found in the core glycans, the accessibility of which may be enhanced in absence of the usually highly branched polymannan structures of a *P. pastoris* wildtype strain<sup>33,34</sup>.

The detailed characterization of the different *P. pastoris* strains in the controlled environment of a bioreactor revealed that the *och1* knockout strains were physiologically impaired compared to their wildtype equivalents. During the consecutive pulses, the carbon dioxide yield  $Y_{CO_2/S}$  and the C-balances constantly decreased, indicating a loss in metabolic activity. This was also apparent in the CER signals during the single methanol pulses (Supplementary Figure 5



**Table 3 |** Relative peak areas of identified glycan structures cleaved off from HRP recombinantly produced in either *PpMutS<sup>HRP</sup>* or in *PpFWK3<sup>HRP</sup>*

glycan structure	<i>PpMutS<sup>HRP</sup></i>	<i>PpFWK3<sup>HRP</sup></i>
	relative peak area [%]	
Man7	0.0	7.9
Man8	0.0	57.3
Man9	15.7	16.8
Man10	31.4	6.1
Man10-P	5.6	0.0
Man11	18.7	6.8
Man11-P	6.7	0.0
Man12	6.7	3.2
Man12-P	4.4	0.0
Man13	3.7	1.8
Man13-P	1.8	0.0
Man14	2.1	0.0
Man14-P	1.1	0.0
Man15	1.2	0.0
Man16	0.5	0.0
Man17	0.4	0.0
total	100.0	100.0

and 6). At the beginning of the cultivation, methanol was metabolized much faster than during later methanol pulses. We followed the morphology of the *P. pastoris* cells during cultivations via microscopy and identified formation of cell clusters by the *och1* knockout strains. Obviously, the altered surface glycosylation of *och1* knockout cells also affected the budding process. Instead of budding off, the daughter cells stayed attached to the mother cell. The microscopically observed increased tendency for cluster formation may be regarded as an effect which is intrinsically linked to the loss of the polymannan layer upon Och1p inactivation. Cell disruption experiments showed that neither treatment with Triton X-100, 0.5% EDTA or 5 M urea, nor extensive mechanic shearing via sonication allowed breaking the clusters to single cells. Thus, we conclude that deficiencies in the constitutive cell division machinery upon Och1p inactivation led to a strong, covalent linkage between the cell walls, which remained intact even after the end of the normal budding process. The exact nature of this linkage remains speculative at the current point, but may be associated to aberrant glycosylation steps in the glycan backbone, occurring as a compensatory adaptation to the lack of Och1p activity<sup>20,38</sup>. Due to these very dense and compact formations we hypothesize that the cells in the center of these clusters became limited in oxygen and nutrients and showed no more metabolic activity. Since these cell clusters increased in size over time, the overall metabolic activity of the total amount of cells in the bioreactor decreased, which we observed in decreasing  $Y_{CO_2/S}$  and C-balances. However, these cell clusters were still able to produce recombinant protein. In fact, both the specific productivity and the volumetric productivity, the main focus of industrial bioprocesses, were only reduced by 35% and 30%, respectively, compared to the *P. pastoris* strain with an intact *OCH1* gene. However, due to the constant

**Table 4 |** Enzymatic characterization of homogeneously glycosylated HRP. Kinetic constants of HRP produced in either *PpMutS<sup>HRP</sup>* or *PpFWK3<sup>HRP</sup>* with  $H_2O_2$  as electron donor at saturating concentration and ABTS as electron acceptor in varying concentrations were determined at 420 nm and 30°C

production strain	$K_{M,ABTS}$ [mM]	$V_{max}$ [ $\mu\text{mol}\cdot\text{s}^{-1}\cdot\mu\text{g}^{-1}$ ]
<i>PpMutS<sup>HRP</sup></i>	2.40	3.07
<i>PpFWK3<sup>HRP</sup></i>	2.03	2.46

decrease in metabolic activity over time, use of the *och1* knockout strain in industrial processes will require considerable modifications to current standard protocols to optimize recombinant protein production in this strain.

When we analyzed the HRP produced by either a *PpMutS<sup>HRP</sup>* strain or the *och1* knockout strain *PpFWK3<sup>HRP</sup>*, we found the enzyme preparation from *PpFWK3<sup>HRP</sup>* to be considerably more homogeneously glycosylated. More detailed analyses of the surface glycan chains of HRP by mass spectrometry revealed striking differences in the glycosylation pattern between HRP produced in *PpMutS<sup>HRP</sup>* and *PpFWK3<sup>HRP</sup>*. HRP produced in *PpMutS<sup>HRP</sup>* carried a more heterogeneous glycopattern with several high-mannose structures and a great amount of phosphorylated sugars. The most dominant glycan was found to be a Man10 structure. In contrast, the most dominant glycan of HRP produced in *PpFWK3<sup>HRP</sup>* was a Man8 core glycan structure. This reduction is in agreement with our expectations since no Och1p could act on Man<sub>8</sub>GlcNAc<sub>2</sub> core glycan structures in the Golgi of the *PpFWK3<sup>HRP</sup>* strain as it could in *PpMutS<sup>HRP</sup>*. Due to the missing Och1p activity, other glycosyltransferases, especially mannosylphosphate transferases, were reduced in their activity resulting in a more homogeneous glycopattern on the surface of recombinantly produced HRP from *PpFWK3<sup>HRP</sup>* (Table 3).

Enzymatic characterizations of HRP revealed an increase in the affinity to the substrate ABTS, but a decrease of  $V_{max}$  for HRP with a more homogeneous glycopattern. Also, a decreased stability at 60°C for the homogeneously glycosylated HRP compared to the heterogeneously hyperglycosylated glycovariant was observed.

In conclusion, we irreversibly eliminated the *OCH1* encoded  $\alpha$ -1,6-mannosyltransferase activity of *P. pastoris*. The phenotype of the generated *och1* knockout platform strain resembled the phenotype described for the same knockout in *S. cerevisiae*. Nevertheless, the strain was successfully employed for the production of recombinant HRP as a reporter enzyme. Strain specific parameters were determined in comparative bioreactor cultivations. Recombinant HRP from either an unaltered *P. pastoris* strain or the *och1* knockout strain was purified and characterized. The main findings of this study can be summarized as:

- The *och1* knockout strains were characterized by slow growth, increased temperature sensitivity and formation of cell clusters. The altered N-glycosylation pathway and resultant structural impacts in the *PpFWK3* strain appears to have triggered the dynamic reorganization of surface mannose residues and other glycan structures. The cellular response seemed to be more diverse than just a simple lack of an outer chain hypermannan structure, and may also involve secondary counter-regulatory mechanisms on the metabolic or structural level<sup>20,38</sup>. Our results in this regard are in direct agreement with previous work on *och1* deletion strains of *S. cerevisiae*<sup>19,39</sup>. Lectin based glycoprofiling represented a rapid and reliable method to provide functional proof for the successful deletion of Och1p activity in *P. pastoris*.
- In the course of consecutive methanol pulses, the *och1* knockout strains lost their metabolic activity due to the formation of cell clusters, thus making the adaption of current production processes necessary.
- As shown by detailed LC-MS data, the produced recombinant enzyme exhibited a more homogeneous surface glycosylation, which is beneficial for subsequent downstream processing and applications.
- $V_{max}$  with ABTS as substrate and the thermal stability at 60°C were reduced for the homogeneously glycosylated HRP, whereas its affinity for ABTS was increased, rendering the enzyme suitable for most applications.

Here, we report the thorough biotechnological characterization of a *P. pastoris* platform strain that allows the production of recombinant proteins with considerably increased homogeneity in their



glycosylation pattern due to an irreversible knockout of the *OCH1* gene. Currently, efforts are driven forward to elucidate the potential benefits of the cell morphological changes in glycoengineered *P. pastoris* strains for the expression of recombinant proteins<sup>40</sup>. Also, future studies will focus on rescuing the growth impaired phenotype to generate a strain that shares the favorable growth phenotype of a wildtype strain but still allows the production of homogeneously glycosylated secreted proteins.

## Methods

**Chemicals.** Enzymes and deoxynucleotide triphosphates were obtained from Thermo Scientific (formerly Fermentas, Germany). Phusion™ High-Fidelity DNA-polymerase was from Finnzymes (Finland). 2,2'-azino-bis(3-ethylbenzthiazoline-6-sulfonic acid) diammonium salt (ABTS) was purchased from Sigma-Aldrich (Austria). Difco™ yeast nitrogen base w/o amino acids (YNB), Difco™ yeast nitrogen base w/o amino acids and ammonia sulfate (YNB2), Bacto™ tryptone and Bacto™ yeast extract were purchased from Becton Dickinson (Austria). Zeocin™ was purchased from InvivoGen (France) via Eubio (Austria). Fluorescein isothiocyanate (FITC) labeled lectins for microscopic analysis were obtained from Vector Laboratories (USA), comprising wheat germ agglutinin (WGA) from *Triticum vulgare*, *Lens culinaris* agglutinin (LCA), *Galanthus nivalis* lectin (GNL) and *Solanum tuberosum* lectin (STL). FM® 4–64 membrane stain and Hoechst 33342 or 4',6-diamidino-2-phenylindole (DAPI) nucleic acid stains were purchased from Life Technologies (USA). Other chemicals were obtained from Carl Roth (Germany).

**Microorganisms.** DNA manipulations were performed in accordance to standard protocols<sup>41</sup> in *E. coli* Top10F<sup>2</sup> (Life Technologies, formerly Invitrogen, Austria). All *P. pastoris* strains in this study were based on the wildtype strain CBS 7435 (identical to NRRL Y-11430 or ATCC 76273). Initial *OCH1* knockout studies were performed in a *ku70* deletion strain, previously described by Näätäsaari *et al.*<sup>18</sup>, hereafter called *Ppku70*-. Since *P. pastoris* strains with *Mut<sup>s</sup>* phenotype have been repeatedly shown to be superior over strains with *Mut<sup>r</sup>* phenotype for the production of recombinant proteins (e.g.<sup>26</sup>), the ultimate *och1* knockout strain was based on a *Mut<sup>s</sup>* strain described in<sup>18</sup>, hereafter called *PpMutS*.

**Deletion of the *OCH1* gene.** Based on the genome sequence of the *P. pastoris* wildtype strain CBS 7435<sup>42</sup>, the primers *OCH1*-5int-fw1 and *OCH1*-5int-rv1 were designed to amplify a DNA fragment upstream the *OCH1* open reading frame from genomic DNA isolated according to<sup>43</sup>. Primers *OCH1*-3int-fw1b and *OCH1*-3int-rv1b were designed to amplify a fragment downstream of the *OCH1* ORF. *OCH1*-5int-rv1 and *OCH1*-3int-fw1b were designed to add sequences that overlap with the *FRT* flanked inner part of a flipper cassette. All primer sequences are listed in Table 5.

The two *OCH1* targeting fragments of approximately 1.5 kb each were used to assemble a flipper cassette via overlap extension PCR<sup>18</sup>. Transformation of 100 ng of the assembled flipper cassette into either *Ppku70*- or *PpMutS* was performed as described by Lin-Cereghino *et al.*<sup>44</sup>. Transformants were identified on yeast extract-peptone-dextrose (YPD) agar plates containing 100 mg·L<sup>-1</sup> Zeocin™. Double homologous recombination of the flipper cassette in the *OCH1* locus was verified by PCR using the primers *OCH1*check-fw1 and *OCH1*check-rv2 (Table 5) and Sanger sequencing, using isolated genomic DNA as template. Expression of the FLP recombinase gene was induced by growing positive transformants on minimal methanol agar plates. The FLP recombinase mediated excision of the *FRT* flanked inner part of the flipper cassette was shown by restored sensitivity of the cells towards Zeocin™ and again by PCR and Sanger sequencing. The resulting *Ppku70*- *och1* knockout strain was designated *PpFWK1*, the *PpMutS* *och1* knockout strain was designated *PpFWK3*.

Complementation of the observed phenotype of the *PpFWK3* strain was performed by transforming a plasmid that was constructed by assembly<sup>45</sup> of two fragments, which were generated by PCR using the primers *OCH1*rescue-fw1 and *OCH1*rescue-rv1 using genomic DNA from *PpMutS* as template, and *OCH1*rescue\_T4fw and *OCH1*rescue\_T4rv using the plasmid pPpT4\_S<sup>18</sup> as template (Table 5). The resulting plasmid contained the wildtype *OCH1* ORF plus 698 bp of upstream sequence, putatively harboring the natural *OCH1* promoter, and was designated pPpT4\_BamHI\_*OCH1*rescue. Approximately 500 ng of *BamHI* linearized plasmid were transformed to *PpFWK3*, aliquots were plated on YPD Zeocin™ agar plates and incubated at 28 °C for two days. PCR with the primers *OCH1*check-fw1 and *OCH1*check-rv2 from isolated genomic DNA of transformant strains was performed to confirm the unaltered replacement of the former *OCH1* ORF by a single *FRT* site. A second PCR with the primers *OCH1*-ORF-fw and *OCH1*-ORF-rv from the same genomic DNA was performed to confirm the presence of a plasmid transmitted *OCH1* ORF somewhere else in the genome. A resulting strain with restored wildtype phenotype was designated *PpFWK3<sup>R</sup>*.

**Phenotypic strain characterization.** *Lectin based glycoprofiling via fluorescence microscopy.* Qualitative analysis of lectin binding was performed by incubating 500 µL of *PpMutS* or *PpFWK3* cell suspensions in 20 mM HEPES buffer, pH 7.4, at an OD<sub>600</sub> of 0.3 with 500 µL of the respective lectin solution (250 pmol·mL<sup>-1</sup> in 20 mM HEPES, pH 7.4) for 30 min at 4 °C. If appropriate, 5 µg·mL<sup>-1</sup> HOECHST 33342 nucleic acid stain or 0.5 µg·mL<sup>-1</sup> FM® 4–64 membrane stain were included in the incubation mix. After thorough washing by repeated centrifugation (1700 × g, 5 min) and resuspension, cells were diluted in 1.0 mL of particle free phosphate buffered saline (PBS; 50 mM, pH 7.4) and mounted in FlexiPERM® coverslip 12-well plates for microscopic analysis. Images were acquired on a Zeiss Epifluorescence Axio Observer.Z1 deconvolution microscopy system (Carl Zeiss, Germany) equipped with LD Plan-Neofluar objectives and the LED illumination system Colibri®. Exposure wavelengths and filter sets of the individual channels were chosen according to the respective fluorophore(s) (DAPI/Hoechst 33342: ex/em 365/450 nm; FITC: ex/em 485/525 nm; FM® 4–64 ex/em 485/>620 nm), and combined with differential interference contrast (DIC) images for ease of orientation. Exposure time and illumination parameters were adjusted individually for optimal visibility. For bud scar visualization, Z-stack image series of representative spots were recorded and processed via moderate iterative deconvolution. Lectin cytoadhesion was quantified by incubating the cells with the respective lectin solutions and FM® 4–64 as described above (4 °C, 30 min), followed by extensive washing. Cells were then lysed by treatment with Triton X-100/SDS (1.0/1.0%) for 24 h under vivid agitation. The FITC fluorescence intensity in the lysis buffer was assessed in a microplate reader (TECAN, Austria) at ex/em 485/525 nm and normalized to the content of FM® 4–64 for direct comparison between the individual samples. Lectin solutions without cells were subjected to the same treatment and analyzed in order to exclude potential degradation of the fluorophore. Control experiments via fluorescence-activated cell sorting (FACS) were performed to verify similar uptake of the membrane stain in both strains.

*Membrane permeabilization experiments.* To gain information on the steric accessibility of cell wall-embedded chitin and other carbohydrates, cell permeability was enhanced by treatment with concentrated methanol at -20 °C for 20 min, followed by lectin staining. The cells contained in 1.0 mL of precooled suspension (OD<sub>600</sub> of 0.3) were harvested by centrifugation, resuspended in 100 µL PBS buffer and added dropwise to 1.0 mL of icecold methanol under vivid agitation. After 20 min, cells were pelleted again and excessive solvent was removed via repeated washing and centrifugation with fresh PBS buffer. After rehydration in 1.0 mL of 20 mM HEPES buffer, pH 7.4, cells were subjected to the same lectin staining protocol as described above and analyzed via fluorescence microscopy. Efficient membrane permeabilization was verified via successful counterstaining of the nuclear DNA with a normally non-membrane permeable DAPI dye.

**Table 5 | Oligonucleotide primer list.** Primers used for the amplification of upstream and downstream sequences of the *OCH1* locus from genomic DNA, for amplification of the whole *OCH1* locus for Sanger sequencing, for amplification of fragments to assemble pPpT4\_BamHI\_*OCH1*rescue and to amplify the *OCH1* ORF

primer name	sequence (5' - 3')
<i>OCH1</i> -5int-fw1	GAAGTGTGTAACCTTTTAAATGACGGGATCTAAATACGTCATG
<i>OCH1</i> -5int-rv1	CTAITCTCTAGAAAGTATAGGAACCTCGGCTGATGATAITTTGCTACGAACACTG
<i>OCH1</i> -3int-fw1b	GTTCTATACTTTCTAGAGAATAGGAACCTCGGAGATTAGAGAATGAATACCTTCTTAAAGCGATCG
<i>OCH1</i> -3int-rv1b	GAAGTATTAGGAGCTGAAGAAGCAGAGGCAGAG
<i>OCH1</i> check-fw1	CACACATATAAAGGCAATCTACG
<i>OCH1</i> check-rv2	CAATAACTTCTGCAATAGACTGC
<i>OCH1</i> rescue-fw1	TTCATAGGCTTGGGGTAATAG
<i>OCH1</i> rescue-rv1	CTTGAGCGGCCGCTTAGTCCTTCCAACCTTCCCTTC
<i>OCH1</i> rescue_T4fw	GCATACATTTGAAGGAAGTTGGAAGGACTAAGCGGCCGCTCAAGAGGAT
<i>OCH1</i> rescue_T4rv	CTAITTTCTCTGTCATCTATTACCCCAAGCCTATGAAGGATCTGGGTACCCGACAG
<i>OCH1</i> -ORF-fw	ATGGCGAAGGCAGATGGC
<i>OCH1</i> -ORF-rv	TTAGTCCTTCCAACCTTCTTCAAATG



### Production of the reporter enzyme horseradish peroxidase in shake flask

**experiments.** Aliquots of approximately 2  $\mu\text{g}$  of *SmlI* linearized plasmid pPpT4-S<sup>18</sup>, harboring a HRP gene containing nine potential N-glycosylation sites were transformed into either *PpMutS* or *PpFWK3*. The transformed HRP gene encodes for a new acidic HRP isoenzyme. A detailed description on the identification of new HRP isoenzymes will be given elsewhere (Näätsaari *et al.*, manuscript in preparation). The HRP gene was codon optimized for expression in *P. pastoris* based on a codon table described in<sup>46</sup>. Expression of the gene was regulated by the *AOX1* promoter. Efficient secretion of HRP to the supernatant was facilitated by fusion of the prepro signal sequence of the *S. cerevisiae* mating factor alpha to the N-terminus of the mature HRP. Transformations were performed according to<sup>44</sup> with the following modification: Whereas an overnight culture of *PpMutS* was diluted to an OD<sub>600</sub> of 0.2 to grow to an OD<sub>600</sub> of 0.8–1.0 in approximately 5 h prior to preparation of the cells for electroporation, an overnight culture of *PpFWK3* was diluted to a starting OD<sub>600</sub> of 0.7 to account for its decreased growth rate. Transformants were grown on YPD Zeocin™ agar plates and randomly chosen for screening in micro scale cultivations in 96-deep well plates, similarly to<sup>47</sup>. The cells were cultivated in 250  $\mu\text{L}$  iron-supplemented BMD1% (11  $\text{g}\cdot\text{L}^{-1}$   $\alpha\text{-D}(+)\text{-glucose}$  monohydrate, 13.4  $\text{g}\cdot\text{L}^{-1}$  YNB, 0.4  $\text{mg}\cdot\text{L}^{-1}$  D(+)-biotin, 278  $\text{mg}\cdot\text{L}^{-1}$   $\text{FeSO}_4\cdot 7\text{H}_2\text{O}$ , 0.1 M potassium phosphate buffer, pH 6.0) for approximately 60 h, then induced once with 250  $\mu\text{L}$  BMM2 (1% (v/v) methanol, 13.4  $\text{g}\cdot\text{L}^{-1}$  YNB, 0.4  $\text{mg}\cdot\text{L}^{-1}$  D(+)-biotin, 0.1 M potassium phosphate buffer, pH 6.0) and three times with 50  $\mu\text{L}$  BMM10 (5% (v/v) methanol, 13.4  $\text{g}\cdot\text{L}^{-1}$  YNB, 0.4  $\text{mg}\cdot\text{L}^{-1}$  D(+)-biotin, 0.1 M potassium phosphate buffer, pH 6.0) per well 12 h, 24 h and 36 h after the first addition of BMM2. Induction with the methanol containing media BMM2 and BMM10 induced the production of HRP which was under control of the *AOX1* promoter. The respective HRP production strains were designated *PpMutS*<sup>HRP</sup> and *PpFWK3*<sup>HRP</sup>.

Small scale cultivations were performed in 0.5 L Ultra Yield Flasks (BioSilta, Finland) in 45 mL iron-supplemented BMD1%. After approximately 60 h, 5 mL BMM10 were added. Twelve hours and 36 h after the first induction pulse, 0.5 mL pure methanol were added. Twenty-four hours and 48 h after the first induction pulse, 0.25 mL pure methanol were added. HRP activity in the supernatant was determined by mixing 15  $\mu\text{L}$  of culture supernatant with 140  $\mu\text{L}$  of assay solution (1 mM ABTS, 0.8 mM H<sub>2</sub>O<sub>2</sub>, 50 mM NaOAc buffer, pH 4.5) and following the increase in absorbance at 405 nm in a Spectramax Plus 384 plater reader (Molecular Devices, Germany) at room temperature for 3 min. Promising clones were streaked to single colonies and cultivated again in quadruplicates for rescreening. The copy number of the HRP gene in selected *PpMutS* and *PpFWK3* transformant strains was determined via quantitative real-time PCR according to a protocol of Abad *et al.*<sup>48</sup> and as described previously in<sup>26</sup>.

**Bioreactor cultivations.** Four different *P. pastoris* strains (Table 6) were characterized in terms of physiology, biomass growth and productivity by a novel, dynamic strategy of conducting methanol pulses during batch cultivations in the controlled environment of a bioreactor, which we have described recently<sup>16,24,26</sup>.

**Culture media.** Yeast nitrogen base medium (YNBM): 20  $\text{g}\cdot\text{L}^{-1}$   $\alpha\text{-D}(+)\text{-glucose}$  monohydrate, 3.4  $\text{g}\cdot\text{L}^{-1}$  YNB2, 10  $\text{g}\cdot\text{L}^{-1}$  (NH<sub>4</sub>)<sub>2</sub>SO<sub>4</sub>, 0.4  $\text{g}\cdot\text{L}^{-1}$  D(+)-biotin, 0.1 M potassium phosphate buffer, pH 6.0.

Trace element solution (PTM1): 6  $\text{g}\cdot\text{L}^{-1}$  CuSO<sub>4</sub>·5H<sub>2</sub>O, 0.08  $\text{g}\cdot\text{L}^{-1}$  NaI, 3  $\text{g}\cdot\text{L}^{-1}$  MnSO<sub>4</sub>·H<sub>2</sub>O, 0.2  $\text{g}\cdot\text{L}^{-1}$  Na<sub>2</sub>MoO<sub>4</sub>·2H<sub>2</sub>O, 0.02  $\text{g}\cdot\text{L}^{-1}$  H<sub>3</sub>BO<sub>3</sub>, 0.5  $\text{g}\cdot\text{L}^{-1}$  CoCl<sub>2</sub>, 20  $\text{g}\cdot\text{L}^{-1}$  ZnCl<sub>2</sub>, 65  $\text{g}\cdot\text{L}^{-1}$  FeSO<sub>4</sub>·7H<sub>2</sub>O, 0.2  $\text{g}\cdot\text{L}^{-1}$  D(+)-biotin, 5  $\text{mL}\cdot\text{L}^{-1}$  95–98% H<sub>2</sub>SO<sub>4</sub>.

Basal salt medium (BSM): 44  $\text{g}\cdot\text{L}^{-1}$   $\alpha\text{-D}(+)\text{-glucose}$  monohydrate, 1.17  $\text{g}\cdot\text{L}^{-1}$  CaSO<sub>4</sub>·2H<sub>2</sub>O, 18.2  $\text{g}\cdot\text{L}^{-1}$  K<sub>2</sub>SO<sub>4</sub>, 14.9  $\text{g}\cdot\text{L}^{-1}$  MgSO<sub>4</sub>·7H<sub>2</sub>O, 4.13  $\text{g}\cdot\text{L}^{-1}$  KOH, 26.7  $\text{mL}\cdot\text{L}^{-1}$  85% (v/v) o-phosphoric acid, 0.2  $\text{mL}\cdot\text{L}^{-1}$  Antifoam Struktol J650, 4.35  $\text{mL}\cdot\text{L}^{-1}$  PTM1, NH<sub>4</sub>OH as N-source (see experimental procedure).

Base: NH<sub>4</sub>OH, concentration was determined by titration with 0.25 M potassium hydrogen phthalate.

**Preculture.** Frozen stocks (−80°C) of either *PpMutS*<sup>HRP</sup> and *PpFWK3*<sup>HRP</sup> were pre-cultivated in 100 mL of YNBM in 1 L shake flasks at 30°C and 230 rpm for max. 24 h. The preculture was transferred aseptically to the respective culture vessel. The inoculation volume was 10% of the final starting volume.

**Batch cultivation.** Batch cultivations were carried out in a 3 L working volume Labfors glass bioreactor (Infors, Switzerland). BSM was sterilized in the bioreactor and pH was adjusted to pH 5.0 by using concentrated ammonia solution after autoclaving. Sterile filtered PTM1 was transferred to the reactor aseptically. Dissolved oxygen (dO<sub>2</sub>) was measured with a sterilizable polarographic dissolved oxygen electrode (Mettler Toledo, Switzerland). The pH was measured with a sterilizable electrode (Mettler Toledo, Switzerland) and maintained constant with a step controller using 2.5 M ammonia solution. Base consumption was determined gravimetrically. Cultivation temperature was set to 30°C and agitation was fixed to 1495 rpm. The culture was aerated with 2.0 vvm dried air and offgas of the culture was measured by using an infrared cell for CO<sub>2</sub> and a paramagnetic cell for O<sub>2</sub> concentration (Servomax, Switzerland). Temperature, pH, dO<sub>2</sub>, agitation as well as CO<sub>2</sub> and O<sub>2</sub> in the offgas were measured online and logged in a process information management system (PIMS Lucullus; Biospectra, Switzerland).

**Table 6 | *P. pastoris* strains used for biotechnological characterisation during bioreactor cultivations**

strain	name
<i>P. pastoris</i> Mut <sup>S</sup>	<i>PpMutS</i>
<i>P. pastoris</i> Mut <sup>S</sup> HRP	<i>PpMutS</i> <sup>HRP</sup>
<i>P. pastoris</i> Mut <sup>S</sup> och1	<i>PpFWK3</i>
<i>P. pastoris</i> Mut <sup>S</sup> och1 HRP	<i>PpFWK3</i> <sup>HRP</sup>

After the complete consumption of the substrate glucose, which was indicated by an increase of dO<sub>2</sub> and a drop in offgas activity, the first methanol pulse (adaptation pulse) of a final concentration of 0.5% (v/v) was conducted with methanol supplemented with PTM1 (12 mL PTM1 per 1 L of methanol). Subsequently, between five and seven pulses were performed with 1% or 2% (v/v) methanol for each strain. For each pulse, at least two samples were taken to determine the concentrations of the substrate methanol and product as well as dry cell weight (DCW) and OD<sub>600</sub> to calculate the strain specific parameters. The induction period for *PpMutS*<sup>HRP</sup> and *PpFWK3*<sup>HRP</sup> was carried out in the presence of 1 mM of the heme precursor  $\delta$ -aminolevulinic acid.

**Analysis of growth- and expression-parameters.** DCW was determined by centrifugation of 5 mL culture broth (4,000  $\times$  g, 10 min, 4°C), washing the pellet with 5 mL deionized water and subsequent drying at 105°C to a constant weight in an oven. OD<sub>600</sub> of the culture broth was measured using a spectrophotometer (Genesys 20; Thermo Scientific, Austria). The activity of HRP was determined using a CuBiAn XC enzymatic robot (Innovatis, Germany). Cell free samples (10  $\mu\text{L}$ ) were added to 140  $\mu\text{L}$  of 1 mM ABTS in 50 mM potassium phosphate buffer, pH 6.5. The reaction mixture was incubated at 37°C and was started by the addition of 20  $\mu\text{L}$  of 0.075% H<sub>2</sub>O<sub>2</sub>. Changes of absorbance at 415 nm were measured for 80 s and rates were calculated. Calibration was done using commercially available horseradish peroxidase (Type VI-A, Sigma-Aldrich, Austria, P6782, Lot# 118K76734) as standard at six different concentrations (0.02; 0.05; 0.1; 0.25; 0.5 and 1.0 U·mL<sup>-1</sup>). Protein concentrations were determined at 595 nm using the Bradford Protein Assay Kit (Bio-Rad Laboratories GmbH, Austria) with bovine serum albumin as standard.

**Substrate concentrations.** Concentration of methanol was determined in cell free samples by HPLC (Agilent Technologies, USA) equipped with a Supelcoguard column, a Supelcogel C-610H ion-exchange column (Sigma-Aldrich, Austria) and a refractive index detector (Agilent Technologies, USA). The mobile phase was 0.1% H<sub>3</sub>PO<sub>4</sub> with a constant flow rate of 0.5 mL·min<sup>-1</sup> and the system was run isocratically. Calibration was done by measuring standard points in the range of 0.1 to 10  $\text{g}\cdot\text{L}^{-1}$  methanol.

**Data analysis.** Strain characteristic parameters were determined at a carbon dioxide evolution rate (CER) above 2.5 mmol·L<sup>-1</sup>·h<sup>-1</sup> during each methanol pulse. Measurements of biomass, product and substrate concentration were executed in duplicates. Along the observed standard deviation for the single measurement, the error was propagated to the specific rates  $q_s$  and  $q_p$  as well as to the yield coefficients. The error of determination of the specific rates and the yields was therefore set to 10% and 5%, respectively<sup>16,24</sup>.

**Enzyme purification.** *Size exclusion chromatography.* The supernatants from *PpMutS*<sup>HRP</sup> and *PpFWK3*<sup>HRP</sup> produced in small scale cultures in 0.5 L Ultra Yield Flasks were concentrated to approximately 500  $\mu\text{L}$  each using Vivaspin 20 tubes (Sartorius Stedim Biotech, Germany) with 10 kDa MWCO and recovered from the tubes resulting in a volume of max. 1500  $\mu\text{L}$ , prior to size exclusion chromatography (SEC) on a HiLoad™ 16/60 Superdex 200 prep grade column (GE Healthcare Europe, Austria). SEC was performed at a flow rate of approximately 9 cm·h<sup>-1</sup>, fractions of 1.2 mL were collected and assayed for HRP activity using ABTS as substrate.

*2-step purification protocol.* To purify the secreted HRP produced in bioreactor cultivations, the fermentation broths were harvested and centrifuged (4,000  $\times$  g, 20 min) and the cell free supernatants were subjected to diafiltration with buffer (500 mM NaCl, 20 mM NaOAc, pH 6.0) for a subsequent purification step via a mixed mode resin (hydrophobic charge induction chromatography, HCIC) followed by a size exclusion step (SEC). We have recently described this 2-step flowthrough based strategy for the HRP isoenzyme ClA<sup>27</sup>. The catalytic activity and the protein content in all fractions were determined, active fractions were pooled and concentrated via ultrafiltration to approximately 3  $\text{mg}\cdot\text{mL}^{-1}$  for HRP produced in *PpMutS*<sup>HRP</sup> and 0.3  $\text{mg}\cdot\text{mL}^{-1}$  for HRP produced in *PpFWK3*<sup>HRP</sup> for subsequent enzyme characterization.

**Enzyme characterization.** The two HRP preparations produced in either *PpMutS*<sup>HRP</sup> or in *PpFWK3*<sup>HRP</sup> were characterized to determine differences between the hypermannosylated HRP from *PpMutS*<sup>HRP</sup> and its glycovariant produced in *PpFWK3*<sup>HRP</sup>.



**Liquid chromatography-mass spectrometry (LC-MS) analysis.** Protein N-glycosylation was analyzed by releasing the N-glycans with peptide:N-glycosidase F (Roche, Mannheim). The released N-glycans were desalted and analyzed using a porous graphitic carbon capillary column (ThermoScientific) coupled to a mass spectrometer (Maxis 4 G, Bruker, Bremen). Deviating from previous work<sup>49</sup>, glycans were not reduced and a steep gradient was applied leading to the elution of all glycans within approximately 2 min.

**Kinetic constants with ABTS.** Protein concentrations of the HRP preparations were determined at 595 nm using the Bradford Protein Assay Kit (Bio-Rad Laboratories GmbH, Austria) with bovine serum albumin as standard. The kinetic constants for ABTS were determined for both HRP glycovariants. The reaction was started by adding 10  $\mu$ L enzyme solution (3 mg mL<sup>-1</sup> HRP from PpMut<sup>SHRP</sup> and 0.3 mg mL<sup>-1</sup> HRP from PpFWK3<sup>HRP</sup>) to 990  $\mu$ L reaction buffer containing ABTS in varying concentrations (0.01–10 mM), 1 mM H<sub>2</sub>O<sub>2</sub> and 50 mM potassium phosphate, pH 6.5. The change in absorbance at 420 nm was recorded in a spectrophotometer UV-1601 (Shimadzu, Japan) at 30°C controlled with a temperature controller (CPS controller 240 A; Shimadzu, Japan). Absorption curves were recorded with a software program (UVPC Optional Kinetics; Shimadzu, Japan). Measurements were performed in triplicates.

**Thermal stability.** Both enzyme solutions were incubated at 60°C for 1 h. At different time points, aliquots were withdrawn, the solutions were immediately cooled and centrifuged (20,000  $\times$  g, 15 min) to pellet precipitated proteins and the remaining catalytic activity in the supernatants was measured<sup>28</sup>.

- Hasslacher, M. *et al.* High-level intracellular expression of hydroxynitrile lyase from the tropical rubber tree *Hevea brasiliensis* in microbial hosts. *Protein Expr. Purif.* **11**, 61–71 (1997).
- Werten, M. W., van den Bosch, T. J., Wind, R. D., Mooibroek, H. & de Wolf, F. A. High-yield secretion of recombinant gelatins by *Pichia pastoris*. *Yeast* **15**, 1087–1096 (1999).
- Jahic, M., Rotticci-Mulder, J. C., Martinelle, M., Hult, K. & Enfors, S.-O. Modeling of growth and energy metabolism of *Pichia pastoris* producing a fusion protein. *Bioprocess Biosyst. Eng.* **24**, 385–393 (2002).
- Lin-Cereghino, G. P., Lin-Cereghino, J., Ilgen, C. & Cregg, J. M. Production of recombinant proteins in fermenter cultures of the yeast *Pichia pastoris*. *Curr. Opin. Biotechnol.* **13**, 329–332 (2002).
- Parekh, R. B. Effects of glycosylation on protein function. *Curr. Opin. Struct. Biol.* **1**, 750–754 (1991).
- Ryckaert, S., Martens, V., De Vusser, K. & Contreras, R. Development of a *S. cerevisiae* whole cell biocatalyst for in vitro sialylation of oligosaccharides. *J. Biotechnol.* **119**, 379–388 (2005).
- Wildt, S. & Gerngross, T. U. The humanization of N-glycosylation pathways in yeast. *Nat. Rev. Microbiol.* **3**, 119–128 (2005).
- Hamilton, S. R. & Gerngross, T. U. Glycosylation engineering in yeast: the advent of fully humanized yeast. *Curr. Opin. Biotechnol.* **18**, 387–392 (2007).
- De Pourcq, K., De Schutter, K. & Callewaert, N. Engineering of glycosylation in yeast and other fungi: current state and perspectives. *Appl. Microbiol. Biotechnol.* **87**, 1617–1631 (2010).
- Vervecken, W. *et al.* In vivo synthesis of mammalian-like, hybrid-type N-glycans in *Pichia pastoris*. *Appl. Environ. Microbiol.* **70**, 2639–2646 (2004).
- Nagasu, T. *et al.* Isolation of new temperature-sensitive mutants of *Saccharomyces cerevisiae* deficient in mannose outer chain elongation. *Yeast* **8**, 535–547 (1992).
- Nakayama, K., Nagasu, T., Shimma, Y., Kuromitsu, J. & Jigami, Y. OCH1 encodes a novel membrane bound mannosyltransferase: outer chain elongation of asparagine-linked oligosaccharides. *EMBO J.* **11**, 2511–2519 (1992).
- Choi, B.-K. *et al.* Use of combinatorial genetic libraries to humanize N-linked glycosylation in the yeast *Pichia pastoris*. *Proc. Natl. Acad. Sci. U.S.A.* **100**, 5022–5027 (2003).
- Mille, C. *et al.* Identification of a new family of genes involved in beta-1,2-mannosylation of glycans in *Pichia pastoris* and *Candida albicans*. *J. Biol. Chem.* **283**, 9724–9736 (2008).
- Veitch, N. C. Horseradish peroxidase: a modern view of a classic enzyme. *Phytochemistry* **65**, 249–259 (2004).
- Dietzsch, C., Spadiut, O. & Herwig, C. A dynamic method based on the specific substrate uptake rate to set up a feeding strategy for *Pichia pastoris*. *Microb. Cell Fact.* **10**, 14–22 (2011).
- Morawski, B. *et al.* Functional expression of horseradish peroxidase in *Saccharomyces cerevisiae* and *Pichia pastoris*. *Protein Eng.* **13**, 377–384 (2000).
- Näätsaari, L. *et al.* Deletion of the *Pichia pastoris* KU70 homologue facilitates platform strain generation for gene expression and synthetic biology. *PLoS ONE* **7**, e39720 (2012).
- Zhou, J., Zhang, H., Liu, X., Wang, P. G. & Qi, Q. Influence of N-glycosylation on *Saccharomyces cerevisiae* morphology: a golgi glycosylation mutant shows cell division defects. *Curr. Microbiol.* **55**, 198–204 (2007).
- Lee, B. N. & Elion, E. A. The MAPKKK Ste11 regulates vegetative growth through a kinase cascade of shared signaling components. *Proc. Natl. Acad. Sci. U.S.A.* **96**, 12679–12684 (1999).
- Non-Conventional Yeasts In Genetics, Biochemistry And Biotechnology*. (Springer Berlin Heidelberg, 2003). doi:10.1007/978-3-642-55758-3.
- Shibuya, N., Goldstein, I. J., Van Damme, E. J. & Peumans, W. J. Binding properties of a mannose-specific lectin from the snowdrop (*Galanthus nivalis*) bulb. *J. Biol. Chem.* **263**, 728–734 (1988).
- Fouquaert, E. *et al.* Related lectins from snowdrop and maize differ in their carbohydrate-binding specificity. *Biochem. Biophys. Res. Commun.* **380**, 260–265 (2009).
- Dietzsch, C., Spadiut, O. & Herwig, C. A fast approach to determine a fed batch feeding profile for recombinant *Pichia pastoris* strains. *Microb. Cell Fact.* **10**, 85–94 (2011).
- Zalai, D., Dietzsch, C., Herwig, C. & Spadiut, O. A dynamic fed batch strategy for a *Pichia pastoris* mixed feed system to increase process understanding. *Biotechnol. Prog.* **28**, 878–886 (2012).
- Krainer, F. W. *et al.* Recombinant protein expression in *Pichia pastoris* strains with an engineered methanol utilization pathway. *Microb. Cell Fact.* **11**, 22–35 (2012).
- Spadiut, O., Rossetti, L., Dietzsch, C. & Herwig, C. Purification of a recombinant plant peroxidase produced in *Pichia pastoris* by a simple 2-step strategy. *Protein Expr. Purif.* **86**, 89–97 (2012).
- Spadiut, O. *et al.* Improving thermostability and catalytic activity of pyranose 2-oxidase from *Trametes multicolor* by rational and semi-rational design. *FEBS J.* **276**, 776–792 (2009).
- Chen, Z. *et al.* Enhancement of the gene targeting efficiency of non-conventional yeasts by increasing genetic redundancy. *PLoS ONE* **8**, e57952 (2013).
- Cabib, E. & Bowers, B. Chitin and yeast budding. Localization of chitin in yeast bud scars. *J. Biol. Chem.* **246**, 152–159 (1971).
- Chen, C. *et al.* A high-throughput screening system for genes extending life-span. *Exp. Gerontol.* **38**, 1051–1063 (2003).
- Chaudhari, R. D., Stenson, J. D., Overton, T. W. & Thomas, C. R. Effect of bud scars on the mechanical properties of *Saccharomyces cerevisiae* cell walls. *Chem. Eng. Sci.* **84**, 188–196 (2012).
- Lesage, G. & Bussey, H. Cell wall assembly in *Saccharomyces cerevisiae*. *Microbiol. Mol. Biol. Rev.* **70**, 317–343 (2006).
- De Groot, P. W. J., Ram, A. F. & Klis, F. M. Features and functions of covalently linked proteins in fungal cell walls. *Fungal Genet. Biol.* **42**, 657–675 (2005).
- Klis, F. M., Boersma, A. & De Groot, P. W. J. Cell wall construction in *Saccharomyces cerevisiae*. *Yeast* **23**, 185–202 (2006).
- Kapteyn, J. C. *et al.* Altered extent of cross-linking of beta1,6-glycosylated mannoproteins to chitin in *Saccharomyces cerevisiae* mutants with reduced cell wall beta1,3-glucan content. *J. Bacteriol.* **179**, 6279–6284 (1997).
- Maupin, K. A., Liden, D. & Haab, B. B. The fine specificity of mannose-binding and galactose-binding lectins revealed using outlier motif analysis of glycan array data. *Glycobiology* **22**, 160–169 (2012).
- Hirayama, H. & Suzuki, T. Metabolism of free oligosaccharides is facilitated in the och1D mutant of *Saccharomyces cerevisiae*. *Glycobiology* **21**, 1341–1348 (2011).
- Nakanishi-Shindo, Y., Nakayama, K., Tanaka, A., Toda, Y. & Jigami, Y. Structure of the N-linked oligosaccharides that show the complete loss of alpha-1,6-polymannose outer chain from och1, och1 mnn1, and och1 mnn1 alg3 mutants of *Saccharomyces cerevisiae*. *J. Biol. Chem.* **268**, 26338–26345 (1993).
- Jacobs, P. P. *et al.* *Pichia* surface display: display of proteins on the surface of glycoengineered *Pichia pastoris* strains. *Biotechnol. Lett.* **30**, 2173–2181 (2008).
- Current Protocols In Molecular Biology*. (John Wiley & Sons, Inc., 2001). doi:10.1002/0471142727.
- Küberl, A. *et al.* High-quality genome sequence of *Pichia pastoris* CBS7435. *J. Biotechnol.* **154**, 312–320 (2011).
- Harju, S., Fedosyuk, H. & Peterson, K. R. Rapid isolation of yeast genomic DNA: Bust n' Grab. *BMC Biotechnol.* **4**, 8–13 (2004).
- Lin-Cereghino, J. *et al.* Condensed protocol for competent cell preparation and transformation of the methylotrophic yeast *Pichia pastoris*. *BioTechniques* **38**, 44–48 (2005).
- Gibson, D. G. *et al.* Enzymatic assembly of DNA molecules up to several hundred kilobases. *Nat. Methods* **6**, 343–345 (2009).
- Abad, S. *et al.* Stepwise engineering of a *Pichia pastoris* D-amino acid oxidase whole cell catalyst. *Microb. Cell Fact.* **9**, 24–35 (2010).
- Weis, R. *et al.* Reliable high-throughput screening with *Pichia pastoris* by limiting yeast cell death phenomena. *FEMS Yeast Res.* **5**, 179–89 (2004).
- Abad, S. *et al.* Real-time PCR-based determination of gene copy numbers in *Pichia pastoris*. *Biotechnol. J.* **5**, 413–420 (2010).
- Pabst, M. *et al.* Isomeric analysis of oligomannosidic N-glycans and their dolichol-linked precursors. *Glycobiology* **22**, 389–399 (2012).
- Nett, J. H. *et al.* A combinatorial genetic library approach to target heterologous glycosylation enzymes to the endoplasmic reticulum or the Golgi apparatus of *Pichia pastoris*. *Yeast* **28**, 237–252 (2011).
- Hamilton, S. R. *et al.* Production of complex human glycoproteins in yeast. *Science* **301**, 1244–1246 (2003).
- Jacobs, P. P., Geysens, S., Vervecken, W., Contreras, R. & Callewaert, N. Engineering complex-type N-glycosylation in *Pichia pastoris* using GlycoSwitch technology. *Nat. Protoc.* **4**, 58–70 (2009).
- Hamilton, S. R. *et al.* Humanization of yeast to produce complex terminally sialylated glycoproteins. *Science* **313**, 1441–1443 (2006).



54. Hopkins, D. *et al.* Elimination of  $\beta$ -mannose glycan structures in *Pichia pastoris*. *Glycobiology* **21**, 1616–1626 (2011).

### Acknowledgments

The authors are very grateful to the Austrian Science Fund (FWF): project P24861-B19 and FWF W901 DK Molecular Enzymology for financial support. We would also like to thank Michaela Gerstmann, Astrid Weninger and Karl Metzger for excellent technical assistance in the lab and Daniel Maresch for excellent assistance with LC-MS.

### Author contributions

F.W.K. and O.S. conceived of and planned the study. F.W.K., C.G., L.N., M.W., R.P. and O.S. conducted the different experiments. C.H., A.G. and F.A. supervised parts of the research. F.W.K. and O.S. wrote the paper.

### Additional information

**Supplementary information** accompanies this paper at <http://www.nature.com/scientificreports>

**Competing financial interests:** The authors declare no competing financial interests.

**How to cite this article:** Krainer, F.W. *et al.* Knockout of an endogenous mannosyltransferase increases the homogeneity of glycoproteins produced in *Pichia pastoris*. *Sci. Rep.* **3**, 3279; DOI:10.1038/srep03279 (2013).



This work is licensed under a Creative Commons Attribution 3.0 Unported license. To view a copy of this license, visit <http://creativecommons.org/licenses/by/3.0>